Mathematical Modeling and Simulation of the Female Menstrual Cycle

Dissertation von
Isabel Reinecke

eingereicht am
Fachbereich Mathematik und Informatik
der Freien Universität Berlin

im September 2008

Betreuer: Prof. Dr. Dr. h.c. Peter Deuflhard

Gutachter: Prof. Dr. Dr. h.c. Peter Deuflhard
Prof. Dr. Dr. h.c. Hans Georg Bock

Datum der Disputation: 27. März 2009

Contents

Eidesstattliche Versicherung

Hiermit erkläre ich, dass die vorliegende Dissertation von mir selbständig verfasst wurde und alle von mir genutzten Hilfsmittel und Hilfen angegeben wurden.

Introduction

Roughly half of the world's population is female and there are more than 100 million women worldwide regularly using hormonal contraceptives such as the birth control pill. Nevertheless, the menstrual cycle has so far received comparatively little attention in the field of mathematical modeling. In this context, the term "menstrual cycle" refers to the processes of the control system in the female body drafted in Fig. 1.

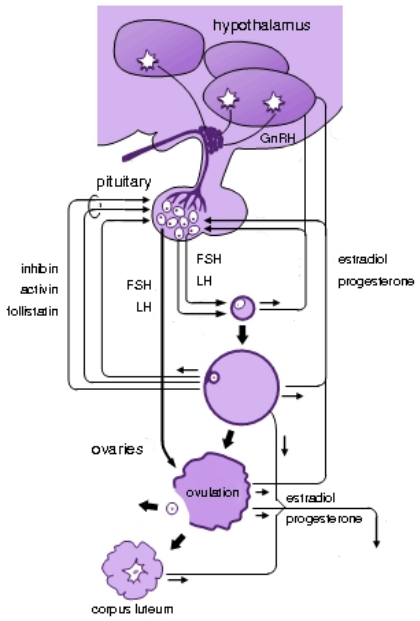

Figure 1: Control system of the female menstrual cycle, modified from [56].

In fact, there are only few models describing the dynamics of the female menstrual cycle. Up to now, the focus has mainly been on coarse interactions like feedback mechanisms among the most important hormones [33, 76, 81] and follicular masses [6, 7, 37] or, explicitly, on follicular dynamics [11, 12, 13, 51]. Modeling of biochemical processes like receptor binding [5, 14, 41, 85] which are part of this control system can be found as well. The model derived in [37] is able to reproduce quite well the given experimental data estimated from [58] for some of the essential elements of the control system. However, the dynamics of progesterone and estradiol belonging to these essential elements and the dynamics in the hypothalamus are not included.

Nonetheless, since the model in [37] offers a suitable approach for LH and FSH as well as for the follicular development, it is chosen as basis in the subsequent modeling process.

In order to be able to cover a vast range of external manipulations, the mathematical model that is developed here must comprise the main components where the processes belonging to the menstrual cycle occur, as well as their interconnections. This rather elaborate mathematical model is the basis for a detailed analysis and could be helpful for possible drug design. Testing medical or pharmaceutical therapies is cost-intensive since clinical studies must be conducted. The integration of a detailed mathematical model in this process could be advantageous.

Outline. Some modeling fundamentals that can be used for mathematical modeling in physiology in general and that are applied here to the modeling of the female menstrual cycle are introduced in Chapter 1. Here, the human body, even if it is an entity, is not regarded as a single homogenous system, but as decomposed into compartments. The mathematical basis for the model, a system of differential equations, is introduced. Since the processes take place in different parts of the body and influence each other with a certain delay, passing over to delay differential equations is deemed a reasonable step.

Next, the compartment model, as developed in [37], is recalled. Based on this model and with the aid of the above modeling fundamentals, a model for the female menstrual cycle is developed step by step in Chapter 2. The pulsatile release of the gonadotropin-releasing hormone (GnRH) is controlled by a complex neural network. Here it is chosen to model the pulse time points of this GnRH pulse generator by a stochastic process. The final model, named GynCycle, describes the dynamics of hormones, enzymes, receptors (partly at different states and in different compartments), follicular phases, and the GnRH pulse generator.

When modeling complex physiological processes and control systems in the human body such as the female menstrual cycle, a large number of parameters arises naturally. Their values are not known for the most part, thus making parameter estimation necessary. In order to simplify this often high-dimensional problem, a method is developed in Chapter 3 for the decomposition of the mathematical model into several smaller model parts. This method is carried out for GynCycle.

By model decomposition, the problem can be reduced. In the next step, the parameters that can probably be estimated simultaneously are computationally estimated. The full model consists of stiff delay differential equations including a stochastic approach for the pulse generator. Finally in Chapter 4, the results are shown by comparing simulations of GynCycle with experimental data.

In order to show possible applications, the model is extended for the intake of hormonal contraceptives. The corresponding simulations are performed in Chapter 5. Moreover, the effects of continuous administration of GnRH are treated.

Chapter 1

Basic Modeling Concepts

First, some principle modeling concepts are introduced that could be useful in the modeling of physiological processes and that are used to construct the complex mathematical model of the human menstrual cycle. The concept of compartmentalization of the considered body parts and how the connections between the compartments can be modeled, for example, via receptor binding and feedback mechanisms, is described. If the biochemical mechanisms are known, simple reaction kinetics can be used and if enzymes catalyze the reaction, simple enzyme kinetics are applied. Taking into account the fact that the different elements of the system influence each other with a certain delay, delay differential equations instead of ordinary differential equations are used.

1.1 Compartmentalization of the human body

The human body is not a closed homogeneous system; it consists of organs and tissues etc. in which different processes take place. In order to reduce the biological complexity, the body parts that are essential in the processes are extracted and divided into discrete body elements, referred to as *compartments* [1] that are interconnected via the shared blood system [53], here called *transport compartment*. The characteristics of compartments are that isolated processes take place, but at the same time they can interact with each other. The model formulating the relations between these compartments is called *compartmental model* [83] and this process of organizing the human body in compartments is referred to as *compartmentalization* which is the concept of pharmacokinetic modeling [1]. More precisely, *physiologically based compartments* are used in this context since the compartments are based on the actual anatomy and physiology [1].

1.2 Interfaces between the compartments

The compartments are non-closed systems and can influence each other. The question arises, how exactly the exchange takes place and what possibilities there are for interrelations between compartments.

On the one hand, it is possible that only coarse interrelations such as inhibiting or stimulating effects are known. Then these feedback mechanisms can be modeled by Hill functions. On the other hand, it is possible in some cases to model on a biochemical basis via e.g. receptor binding.

1.2.1 Receptor binding and recycling

It is often the case that the hormone that is synthesized in one compartment reaches another compartment through the blood circulation and binds to its corresponding receptor. They form a complex and thereby the receptor becomes activated:

$$\mathrm{R}_{activatable} + \mathrm{H} \quad \rightarrow \quad (\mathrm{H\text{-}R}_{activated}).$$

Usually, the receptor does not return directly to the activatable state after dissociating from the hormone, but becomes first desensitized or inactivatable:

$$\mathrm{R}_{activatable} \quad \rightarrow \quad \mathrm{R}_{activated} \quad \rightarrow \quad \mathrm{R}_{inactivatable} \quad \rightarrow \quad \mathrm{R}_{activatable}.$$

1.2.2 Feedback regulation

If the biochemical details are not established and only a stimulatory or inhibitory effect of one hormone on another is known, modeling can be done by use of feedback functions originating from enzyme kinetics. Positive feedback can be described by applying Michaelis-Menten kinetics, negative feedback by mechanisms for inhibitory enzymes [72].

If a substrate S stimulates another substrate P, it holds

$$\begin{aligned} S &\text{ increases} \quad \Rightarrow \quad P \text{ increases} \\ S &\text{ decreases} \quad \Rightarrow \quad P \text{ decreases,} \end{aligned}$$

where the italics denote the corresponding concentrations now and in the following. The inhibition of S on P can be described by

$$\begin{aligned} S &\text{ increases} \quad \Rightarrow \quad P \text{ decreases} \\ S &\text{ decreases} \quad \Rightarrow \quad P \text{ increases.} \end{aligned}$$

A simple method to model these observations mathematically, is the appliance of *Hill functions* that are commonly used to model feedback in physiology. They have values between 0 and 1, thus they are bounded. Additionally, the Hill functions provide a kind of switch, enabling to model the event that the concentration has to exceed a certain threshold value in order to be effective. At this switch the values of the Hill function change from values near 0 to values near 1 or the other way around.

Definition 1.1. The *Hill function for positive feedback (stimulation)* is defined by

$$h^+(S;T,n) := \frac{\left(\frac{S}{T}\right)^n}{1+\left(\frac{S}{T}\right)^n} = \frac{S^n}{T^n+S^n}$$

and the *Hill function for negative feedback (inhibition)* by

$$h^-(S;T,n) := \frac{1}{1+\left(\frac{S}{T}\right)^n} = \frac{T^n}{T^n+S^n},$$

where S denotes the concentration of the hormone ($S \geq 0$) that acts with a positive and negative feedback, respectively, $T \in \mathbb{R}_+$ the *threshold value*, and $n \geq 1$ the *Hill coefficient*.

It is $h^+ \equiv 1 - h^-$, where $h^+(\cdot;T,n) : [0,\infty) \to [0,1)$ is strictly monotonically increasing and $h^-(\cdot;T,n) : [0,\infty) \to (0,1]$ strictly monotonically decreasing. The switch is the more distinctive, the higher the Hill coefficient n is chosen. The threshold value T denotes the value at which the Hill function has the value $\frac{1}{2}$, i.e. where it changes from values near 0 to values near 1.

The resulting dynamics of P if S is stimulatory is given by

$$\frac{d}{dt}P = p^+ \cdot h^+(S;T,n), \quad p^+ \in \mathbb{R}_+,$$

and the resulting dynamics of P if S is inhibitory by

$$\frac{d}{dt}P = p^- \cdot h^-(S;T,n), \quad p^- \in \mathbb{R}_+.$$

It is possible that the effect of S is not constant, i.e. that there are at least two effects responsible for the result.

Definition 1.2. The *biphasic Hill function* [66] is defined by

$$h^{-,+}(S) := h^-(S;T^-,T^+,n) := h^-(S;T^-,n) + h^+(S;T^+,n),$$

where $T^- < T^+$ and S denotes the concentration of the hormone ($S \geq 0$) that exerts an inhibitory effect at low concentration and a stimulatory effect at high concentration.

Lemma 1.1. *The unique minimum of $h^{-,+}(\cdot)$ on $[0,\infty)$ is given by $T_S^{-,+} := (T^- \cdot T^+)^{\frac{1}{2}}$. Furthermore it is $h^{-,+}(S) \in [h^{-,+}(T_S^{-,+}),1]$ for all $S \in [0,\infty)$.*

Proof. It is $h^{-,+}(S) > 0$ for all $S \geq 0$ and since $T^+ > T^-$ it holds for $S > 0$

$$\begin{aligned} h^{-,+}(S) &= \frac{T^{-,n}}{T^{-,n}+S^n} + \frac{S^n}{T^{+,n}+S^n} \\ &= 1 - \frac{S^n \cdot (T^{+,n} - T^{-,n})}{(T^{-,n}+S^n)\cdot(T^{+,n}+S^n)} < 1. \end{aligned}$$

The derivation of $h^{-,+}(\cdot)$ is given by

$$\frac{d}{dS}h^{-,+}(S) = -\frac{n \cdot T^{-,n} \cdot S^{n-1}}{(T^{-,n}+S^n)^2} + \frac{n \cdot T^{+,n} \cdot S^{n-1}}{(T^{+,n}+S^n)^2}. \tag{1.1}$$

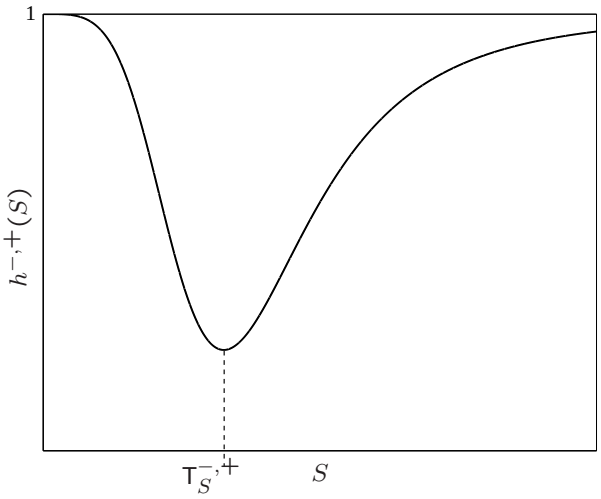

Figure 1.1: Biphasic Hill function $h^{-,+}(\cdot)$ with the threshold value $T_S^{-,+}$ $(n > 1)$.

If $\frac{d}{dS}h^{-,+}(S) = 0$, it follows $S = 0$ or $S = (T^- \cdot T^+)^{\frac{1}{2}} =: T_S^{-,+}$. The first term of the right side of Eq. (1.1) is negative and the second term is positive for all $S > 0$. It is for $S > 0$

$$\begin{aligned}\frac{d}{dS}h^{-,+}(S) < 0 &\Leftrightarrow \frac{d}{dS}h^{-}(S;T^-,n) > \frac{d}{dS}h^{+}(S;T^+,n)\\ &\Leftrightarrow \frac{n\cdot T^{-,n}\cdot S^{n-1}}{(T^{-,n}+S^n)^2} > \frac{n\cdot T^{+,n}\cdot S^{n-1}}{(T^{+,n}+S^n)^2}\\ &\Leftrightarrow S^{2\cdot n} < T^{-,n}\cdot T^{+,n}\\ &\Leftrightarrow S < (T^-\cdot T^+)^{\frac{1}{2}}\end{aligned}$$

and analogously

$$\frac{d}{dS}h^{-,+}(S) > 0 \Leftrightarrow S > (T^-\cdot T^+)^{\frac{1}{2}}.$$

It follows that $h^{-,+}(\cdot)$ is decreasing on $[0, T_S^{-,+})$ and increasing on $(T_S^{-,+}, \infty)$. That proves that $S = (T^- \cdot T^+)^{\frac{1}{2}}$ is the unique minimum. The maximum is given for $S = 0$ since it is $h^{-,+}(S) = 1$. Moreover it is $\lim_{S\to\infty} h^{-,+}(S) = 1$. It follows $h^{-,+}(S) \in [h^{-,+}(T_s^{-,+}), 1]$ for $S \geq 0$. □

Thus $T_S^{-,+}$ is the threshold value for the switch from inhibition to stimulation [66]. Note that $T_S^{-,+}$ is independent of n. An example for the biphasic function is shown in Figure 1.1.

The dynamics of P is then given by

$$\frac{d}{dt}P = p^{-,+}\cdot h^{-,+}(S;T^-,T^+,n), \quad p^{-,+}\in\mathbb{R}_+.$$

1.3 Metabolic processes

Many processes in the human body are only partly explored and this limits the modeling possibilities. In this context, neither molecular processes, nor genetic, nor spatial effects in cells are incorporated. Here it is considered in detail if the biochemical reaction mechanisms are known to a certain extent.

1.3.1 Reaction kinetics

If reaction mechanisms are given, they can be modeled by simple reaction kinetics if no enzymes are involved.

Considering the irreversible reaction

$$\mathrm{S} \quad \overset{k}{\rightarrow} \quad \mathrm{P},$$

simple reaction kinetics for the concentrations of the product P and of the substrate S can be assumed:

$$\frac{d}{dt}P = k \cdot S, \quad \frac{d}{dt}S = -\frac{d}{dt}P, \quad k \in \mathbb{R}_+.$$

If the reversible reaction is considered

$$\mathrm{S} \quad \underset{k_{-1}}{\overset{k_1}{\rightleftharpoons}} \quad \mathrm{P},$$

simple reaction kinetics lead to the product and substrate rates

$$\frac{d}{dt}P = k_1 \cdot S - k_{-1} \cdot P, \quad \frac{d}{dt}S = -\frac{d}{dt}P, \quad k_1, k_{-1} \in \mathbb{R}_+.$$

1.3.2 Enzyme kinetics

Since many reactions in the human body are catalyzed by enzymes and since it is not appropriate to assume first-order reaction kinetics in these cases, the mechanism called Michaelis-Menten is chosen to model the dynamics. It is the simplest and most common approach for enzyme catalyzed reactions.

Modeling the irreversible enzyme catalyzed overall reaction

$$\mathrm{S} \quad \rightarrow \quad \mathrm{P},$$

by introducing the enzyme E, the *Michaelis-Menten mechanism* has the form [72]

$$\mathrm{E} + \mathrm{S} \quad \underset{k_{-1}}{\overset{k_1}{\rightleftharpoons}} \quad (\mathrm{E\text{-}S}) \quad \overset{k_2}{\rightarrow} \quad \mathrm{P} + \mathrm{E},$$

where k_{-1}, k_1, $k_2 \in \mathbb{R}_+$ denote the reaction constants, E the enzyme, and (E-S) the complex. Assuming constant total enzyme concentration $E_{total} = E + (E\text{-}S)$ and the quasi-stationary state for the enzyme complex concentration $\frac{d}{dt}(E\text{-}S) = 0$ yields

$$\begin{aligned}\frac{d}{dt}(E\text{-}S) &= k_1 \cdot E \cdot S - k_{-1} \cdot (E\text{-}S) - k_2 \cdot (E\text{-}S) \\ &= k_1 \cdot (E_{total} - (E\text{-}S)) \cdot S - (k_{-1} + k_2) \cdot (E\text{-}S) = 0\end{aligned}$$

which leads to

$$(E\text{-}S) = \frac{k_1 \cdot E_{total} \cdot S}{k_1 \cdot S + k_{-1} + k_2}.$$

Since it is $\frac{d}{dt}P = k_2 \cdot (E\text{-}S)$, the reaction rate for the product can be modeled by

$$\frac{d}{dt}P = k_2 \cdot E_{total} \cdot \frac{S}{K_M + S},$$

where P denotes the product concentration and S the substrate concentration, with the *Michaelis-Menten constant*

$$K_M := \frac{k_{-1} + k_2}{k_1}.$$

For the reaction rate of the substrate S, it is

$$\frac{d}{dt}S = -k_2 \cdot E_{total} \cdot \frac{S}{K_M + S}.$$

Obviously, assuming Michaelis-Menten kinetics instead of first-order reaction kinetics leads to a product formation rate that is not linearly but sigmoidally dependent on the substrate concentration and bounded by the maximal rate

$$V_{max} := k_2 \cdot E_{total}.$$

The situation is more complicated in the case of reversible reactions such as

$$\mathrm{S} \quad \leftrightharpoons \quad \mathrm{P},$$

where the Michaelis-Menten mechanism is described by [72]

$$\mathrm{E} + \mathrm{S} \quad \underset{k_{-1}}{\overset{k_1}{\leftrightharpoons}} \quad (\mathrm{E\text{-}S}) \quad \underset{k_{-2}}{\overset{k_2}{\leftrightharpoons}} \quad \mathrm{P} + \mathrm{E}, \quad k_{-2} \in \mathbb{R}_+.$$

Assuming again constant total enzyme concentration and the quasi-stationary state for the enzyme complex concentration yields

$$\begin{aligned}\frac{d}{dt}(E\text{-}S) &= k_1 \cdot S \cdot E - k_{-1} \cdot (E\text{-}S) - k_2 \cdot (E\text{-}S) + k_{-2} \cdot P \cdot E \\ &= (k_1 \cdot S + k_{-2} \cdot P) \cdot (E_{total} - (E\text{-S})) - (k_{-1} + k_2) \cdot (E\text{-}S) = 0\end{aligned}$$

which leads to

$$(E\text{-}S) = \frac{(k_1 \cdot S + k_{-2} \cdot P) \cdot E_{total}}{k_1 \cdot S + k_{-2} \cdot P + k_{-1} + k_2}.$$

Since it is $\frac{d}{dt}P = k_2 \cdot (E\text{-}S) - k_{-2} \cdot P \cdot E$, the reaction rate for the product does no longer depend only on the substrate concentration, but also on the product concentration:

$$\frac{d}{dt}P = E_{total} \cdot \frac{k_2 \cdot S - \frac{k_{-1} \cdot k_{-2}}{k_1} \cdot P}{K_M + S + \frac{k_{-2}}{k_1} \cdot P}.$$

For the substrate S, the reaction rate is

$$\frac{d}{dt}S = -E_{total} \cdot \frac{k_2 \cdot S - \frac{k_{-1} \cdot k_{-2}}{k_1} \cdot P}{K_M + S + \frac{k_{-2}}{k_1} \cdot P}.$$

For the purpose of simplification the following notations are introduced:

Definition 1.3. Dependence by Michaelis-Menten kinetics in the case of an irreversible reaction is expressed by the *irreversible Michaelis-Menten function*

$$f^{irrev}(S, E; p^{irrev}) := p_1^{irrev} \cdot E \cdot \frac{S}{p_2^{irrev} + S},$$

where $p^{irrev} := (p_1^{irrev}, p_2^{irrev})^T$, $p^{irrev} \in \mathbb{R}_+^2$, denotes the parameter vector, S the substrate concentration, and E the total enzyme concentration. In the case of a reversible reaction, the *reversible Michaelis-Menten function* is defined by

$$f^{rev}(P, S, E; p^{rev}) := E \cdot \frac{p_1^{rev} \cdot S - p_2^{rev} \cdot P}{p_3^{rev} + S + p_4^{rev} \cdot P},$$

where $p^{rev} := (p_1^{rev}, p_2^{rev}, p_3^{rev}, p_4^{rev})^T$, $p^{rev} \in \mathbb{R}_+^4$, denotes the parameter vector and P the product concentration.

It holds for the irreversible case $p_1^{irrev} = k_2$ and $p_2^{irrev} = K_M$ and for the reversible case $p_1^{rev} := k_2$, $p_2^{rev} := \frac{k_{-1} \cdot k_{-2}}{k_1}$, $p_3^{rev} := K_M$, and $p_4^{rev} := \frac{k_{-2}}{k_1}$ [66].

Normally, the reactions in the human body are reversible. But in order to simplify the modeling of this mechanism, it is possible to neglect the reverse reaction if the rate constant of the reverse reaction is very small compared to the rate constant of the forward reaction: $k_1 \gg k_{-1}$. The advantage is a lower number of parameters.

1.4 Delay differential equations

By the compartmentalization, essential spatial effects are incorporated. Usually the dynamics of the concentrations are well described by ordinary differential equations.

If there are body parts where only few molecules participate in the processes as e.g. in the cell, the modeling by ordinary differential equations is not adequate. Cells play a certain role here in the modeling of the human menstrual cycle, e.g. in the follicular development. However, a high number of cells is involved in this case and it is the total effect that is interesting, rather than the processes within a single cell.

Even if a division into compartments is accomplished, it is possible that there are spatial effects within one compartment that can be neglected at the cost of the model's quality. To improve the model, this compartment, in turn, could be divided into several compartments, or modeling by partial differential equations could be done.

The model that is developed in the next chapter is based upon a deterministic modeling approach by using a (non-autonomous) system of differential equations

$$\frac{d}{dt}y(t) = f(t, y(t)),$$

where $y : \mathbb{R} \to \mathbb{R}^n$, $f : \mathbb{R} \times \mathbb{R}^n \to \mathbb{R}^n$, $n \in \mathbb{N}$. As aforementioned, since the processes take place in different parts of the body and influence each other with a certain delay, not ordinary but delay differential equations are chosen. In order to consider the time delays, e.g. due to transport effects, they can be incorporated into the differential equations by using dependency of $t - \tau$ instead of t with the delay $\tau \in \mathbb{R}_+$. The (non-autonomous) system of delay differential equations (DDEs) is given by

$$\frac{d}{dt}y(t) = f(t; y(t); y(t-\tau_1), \ldots, y(t-\tau_m)),$$

where $y : \mathbb{R} \to \mathbb{R}^n$, $f : \mathbb{R} \times \mathbb{R}^{n\times(m+1)} \to \mathbb{R}^n$, $n, m \in \mathbb{N}$, and $\tau_i \in \mathbb{R}_+$, $i = 1, \ldots, m$, denote the discrete, state-independent delays.

To describe the biological variety in an adequate manner, the application of integro-differential equations with distributed lags (see e.g. [54]) instead of delay differential equations with discrete delays is more accurate, but, concomitantly, more expensive which is why here it is restricted to constant delays. The equations would be of the form

$$\frac{d}{dt}y(t) = f\left(t; y(t); \tilde{y}_1(t), \ldots, \tilde{y}_m(t)\right),$$

where for $l = 1, \ldots, m$

$$\tilde{y}_l(t) := \int_{\tau_{l,min}}^{\infty} y(t-\theta) \cdot g_l(\theta)\, d\theta, \quad t \geq t_0,$$

$g_l(\cdot)$, $l = 1, \ldots, m$, denote probability densities

$$\int_{\tau_{l,min}}^{\infty} g_l(\theta)\, d\theta = 1,$$

and $\tau_{l,min}$ the minimal delay $\tau_{l,min}$ for each delayed process, $l = 1, \ldots, m$.

As approach for the discrete delay, the mean value of the density shifted by the minimal delay can be chosen (see e.g. [40]):

$$\tau_l := \tau_{l,min} + \int_0^{\infty} (\tau - \tau_{l,min}) \cdot g_l(\tau)\, d\tau.$$

A particularity of DDEs compared to ODEs is that an initial function instead of an initial value $y(t_0) = y_0$ must be given to solve the system for $t \geq t_0$:

$$y(t_0 - \theta) = \phi(\theta), \quad 0 \leq \theta \leq \tau_{max},$$

where $\tau_{max} := \max_{l\in\{1,\ldots,m\}} \tau_l$. Thus it is an infinite dimensional problem. In the case of integro-differential equations the initial function

$$y(t_0 - \theta) = \phi(\theta), \quad 0 \leq \theta \leq \infty,$$

must be provided.

In the following it is assumed that a solution exists.

Chapter 2

Model Development - GynCycle

This chapter presents how a complex mathematical model for the human menstrual cycle is developed. Using model fundamentals for feedback mechanisms, reaction and enzyme kinetics, differential equations are obtained that describe the dynamics of the involved elements as, for example, hormones, enzymes, receptors, and follicular masses. Moreover, a special feature of the menstrual cycle is presented. From the hypothalamus, the hormone GnRH is released in pulses that cannot simply be modeled by use of differential equations but by use of a stochastic approach.

Despite the relevance of this topic, few mathematical models exist dealing with the human menstrual cycle or parts of it [5, 11, 14, 37, 51, 85]. One of these models [37] provides the basis for the further modeling since it is the most elaborate of the models for the human menstrual so far. It comprises the dynamics in the pituitary and in the ovaries and calculates progesterone, estradiol, and inhibin concentrations, essential components of the control system, as linear combinations of follicular masses. Unfortunately, it offers no modeling approach for the GnRH pulse generator in the hypothalamus.

Basically the processes take place in three different areas, the hypothalamus, the pituitary, and the ovaries (compartments), that are interconnected through the blood circulation (transport compartment). A very important element in this control system is the GnRH pulse generator. From the hypothalamus, the hormone GnRH is released in pulses into the pituitary portal system with the aid of a mechanism, the GnRH pulse generator. One part binds to the GnRH receptors in the pituitary and the remaining part reaches the blood system where the GnRH is rapidly cleared. By binding of GnRH to its receptor, the receptor becomes activated and thus stimulates the release of the gonadotropins FSH and LH into the blood system. In this way, the gonadotropins reach the ovaries where they bind to their respective receptor and thereby activate them. Thus, the enzymes get activated and promote the biosynthesis of the gestagens, androgens, and estrogens in the follicles. The follicular development, in turn, is regulated by the gonadotropins. Progesterone, estradiol, and inhibin reach the blood system and thus the hypothalamus and pituitary where they can regulate the processes by means of positive and negative feedback. In Fig. 2.1, an overview over the compartmental model of this control system is shown.

In the following, the control system is described in detail and modeling approaches

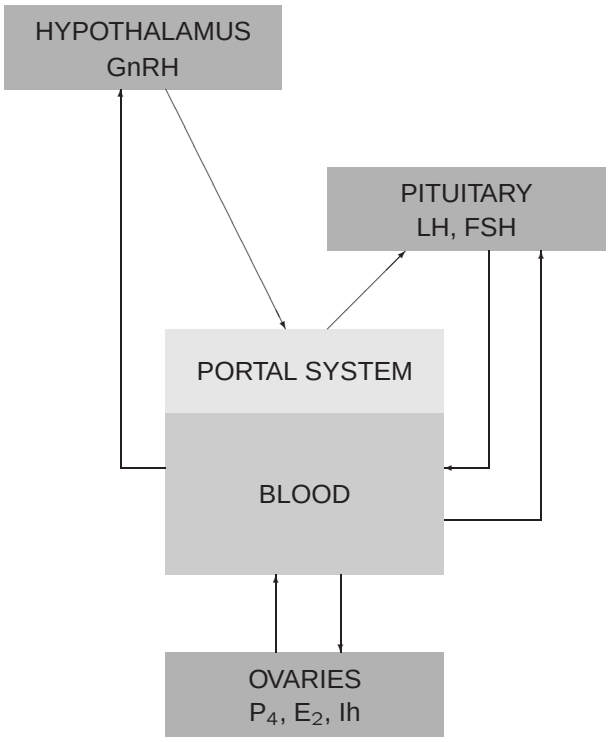

Figure 2.1: Compartmental model of the human menstrual cycle. The three main compartments hypothalamus, pituitary, and ovaries (dark grey) are connected through the blood system. It is distinguished between the pituitary portal system (hypophysic blood system) and the remaining blood system both represented by transport compartments (lighter grey). In the hypothalamus the hormone GnRH, in the pituitary the gonadotropins LH and FSH, and in the ovaries the steroids progesterone (P_4) and estradiol (E_2) as well as the hormone inhibin (Ih) are synthesized.

for the different parts are presented and discussed. On the basis of Fig. 2.1, the model is developed bit by bit by replacing the compartments and the connections between compartments by a detailed modeling approach. The final model is presented in a figure at the end of this chapter.

In Section 2.1 the basic compartment model from [37] is presented. In Sections 2.2 and 2.3, the pulse generator for the GnRH release in the hypothalamus and the model equations for the GnRH concentration in the pituitary portal system being important for the dynamics in the pituitary are derived. The receptor binding of GnRH in the pituitary as well as the dynamics of the LH and FSH synthesis and release are presented in Sections 2.4 and 2.5. In Sections 2.6 and 2.7, modeling approaches for the follicular development, receptor, and enzyme concentrations, and the biosynthesis of steroids as well their blood concentrations are discussed. Finally in Section 2.8, the results are summarized and a model scheme with all components of the complex model is shown. Moreover, all model equations and parameters are listed.

2.1 Basic compartment model

The model presented in [37] is composed of 13 delay differential equations where four of them describe the dynamics in the pituitary and the resulting concentrations of the gonadotropins LH and FSH in the blood and the remaining nine describe the dynamics of the follicular masses. Comparison with experimental data shows that this model is capable of describing the dynamics of the human menstrual cycle in a sound way. That is why it is here referred to as the *basic compartment model* in the following. However, the dynamics of the progesterone, estradiol, and inhibin concentrations in the blood, essential components of the regulatory system, arise as linear combinations of follicular masses and are not part of the dynamical system. The activities in the hypothalamus, especially the GnRH pulse generator and the resulting pulsatile secretion of GnRH into the blood circulation, are not included. An overview of the control system considered in the basic compartment model is given in Fig. 2.2.

In [37], the following assumptions regarding the influence of progesterone, estradiol, and inhibin on the LH and FSH dynamics are made:

- High blood levels of estradiol promote rapid LH synthesis, whereas progesterone inhibits the LH synthesis in the luteal phase [74].
- Inhibin inhibits the FSH synthesis [34, 39, 58, 73].
- Progesterone stimulates the release of FSH and LH when estradiol blood levels are in a normal range during the late follicular phase [10].
- Estradiol inhibits the release of FSH and LH into the blood circulation and it has a greater inhibitory effect on FSH release than on LH release [84, 71, 75].
- The release rate of LH and FSH is assumed to be proportional to the amount of LH and FSH on reserve in the pituitary, respectively.
- Finally, the clearance rates of LH and FSH are assumed to be proportional to the blood levels of LH and FSH, respectively.

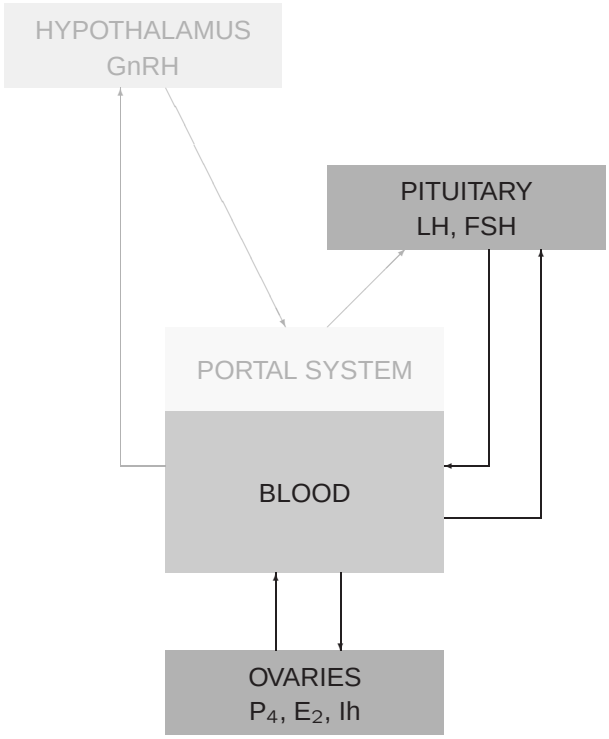

Figure 2.2: Control system considered in [37]. The compartments of the human menstrual cycle that are included in the model are shaded dark grey.

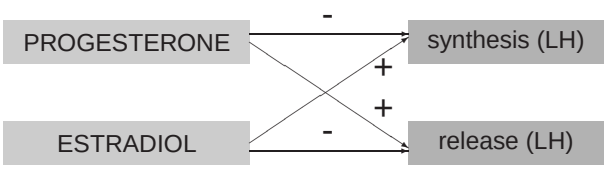

Figure 2.3: Model scheme for LH synthesis and release in [37]. +: stimulatory, −: inhibitory.

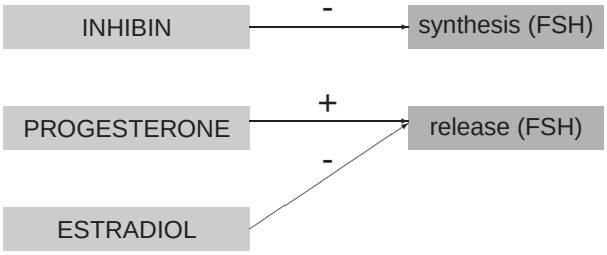

Figure 2.4: Model scheme for FSH synthesis and release in [37]. +: stimulatory, −: inhibitory.

- The period of time between changes in the blood concentrations of P_4, E_2, and Ih and changes in the synthesis of LH and FSH are captured by a time delay [71].

Based upon these assumptions, the model schemes shown in Figs. 2.3 and 2.4 are developed. The stored gonadotropin mass is determined by synthesis (syn) and release (rel). Once released into the blood circulation, it is distributed in the blood volume V_B where it is eliminated proportionally to the present concentration ($clear$).

In the following, E_2 denotes the estradiol concentration, P_4 the progesterone concentration, and Ih the inhibin concentration in the blood. For the dynamics of the LH synthesis and release and, finally, the LH concentration in the blood, the following equations are chosen in the basic compartment model:

$$\frac{d}{dt}P_{LH}(t) = syn_{LH}(E_2(t-\tau_{E_2}), P_4(t-\tau_{P_4})) - rel_{LH}(E_2(t), P_4(t), P_{LH}(t)) \tag{2.1}$$

$$\frac{d}{dt}LH(t) = \frac{1}{V_B} \cdot rel_{LH}(E_2(t), P_4(t), P_{LH}(t)) - clear_{LH}(LH(t)), \tag{2.2}$$

where

$$syn_{LH}(E_2, P_4) = \frac{a_1 \cdot \frac{a_2 \cdot E_2^{a_3}}{a_4^{a_3} + E_2^{a_3}}}{1 + \frac{P_4}{a_5}} \tag{2.3}$$

$$rel_{LH}(E_2, P_4, P_{LH}) = \frac{a_6 \cdot (1 + a_7 \cdot P_4)}{1 + a_8 \cdot E_2} \cdot P_{LH} \tag{2.4}$$

$$clear_{LH}(LH) = a_9 \cdot LH \tag{2.5}$$

and P_{LH} denotes the mass of stored LH in the pituitary, LH the LH concentration in the blood and τ_{P_4}, τ_{E_2} the delays for the progesterone and estradiol concentration, respectively.

The model equations for FSH are of the form

$$\frac{d}{dt}P_{FSH}(t) = syn_{FSH}(Ih(t-\tau_{Ih})) - rel_{FSH}(E_2(t), P_4(t), P_{FSH}(t)) \tag{2.6}$$

$$\frac{d}{dt}FSH(t) = \frac{1}{V_B} \cdot rel_{FSH}(E_2(t), P_4(t), P_{FSH}(t)) - clear_{FSH}(FSH(t)), \tag{2.7}$$

where

$$syn_{FSH}(Ih) = \frac{a_{10}}{1+\frac{Ih}{a_{11}}} \tag{2.8}$$

$$rel_{FSH}(E_2, P_4, P_{FSH}) = \frac{a_{12} \cdot (1 + a_{13} \cdot P_4)}{1 + a_{14} \cdot E_2^2} \cdot P_{FSH} \tag{2.9}$$

$$clear_{FSH}(FSH) = a_{15} \cdot FSH \tag{2.10}$$

and P_{FSH} denotes the mass of stored FSH in the pituitary, FSH the FSH concentration in the blood and τ_{Ih} the delay for the inhibin concentration. The coefficients $a_i \in \mathbb{R}_+$, $i = 1, \ldots, 15$, are the parameters of the pituitary compartment.

The follicular dynamics are described by modeling active follicular masses at different stages where active mass is defined as mass that is growing and secreting hormones [37]. The following partition into follicular stages is done:

- Menstrual Follicular Stage (MsF): mass of immature follicles
- Secondary Follicular Stage (SeF): mass of secondary follicles
- Preovulatory Follicular Stage (PrF): mass of the dominant follicle
- Ovulatory Scar 1 (Sc_1): mass during ovulation
- Ovulatory Scar 1 (Sc_2): mass during luteinization
- Luteal Stage i (Lut_i): mass of the corpus luteum at stage i, $i = 1, \ldots, 4$.

In the basic compartment model, the differential equations for the follicular phase are given by

$$\frac{d}{dt}MsF(t) = b_1 \cdot FSH(t) + \left(b_2 \cdot FSH(t) - b_3 \cdot \left(\frac{LH(t)}{LH_0}\right)^{b_4}\right) \cdot MsF(t) \tag{2.11}$$

$$\frac{d}{dt}SeF(t) = b_3 \cdot \left(\frac{LH(t)}{LH_0}\right)^{b_4} \cdot MsF(t) + \left(b_5 \cdot \left(\frac{LH(t)}{LH_0}\right)^{b_6} - b_7 \cdot \frac{LH(t)}{LH_0}\right) \cdot SeF(t) \tag{2.12}$$

$$\frac{d}{dt}PrF(t) = b_7 \cdot \frac{LH(t)}{LH_0} \cdot SeF(t) - b_8 \cdot \left(\frac{LH(t)}{LH_0}\right)^{b_9} \cdot PrF(t), \tag{2.13}$$

where LH_0 represents the unit of measurement of LH. For the mass dynamics during ovulation and luteinization, the equations are

$$\frac{d}{dt}Sc_1(t) = b_8 \cdot \left(\frac{LH(t)}{LH_0}\right)^{b_9} \cdot PrF(t) - b_{10} \cdot Sc_1(t) \tag{2.14}$$

$$\frac{d}{dt}Sc_2(t) = b_{10} \cdot Sc_1(t) - b_{11} \cdot Sc_2(t), \tag{2.15}$$

and finally for the luteal phase:

$$\frac{d}{dt}Lut_1(t) = b_{11} \cdot Sc_2(t) - b_{12} \cdot Lut_1(t) \tag{2.16}$$

$$\frac{d}{dt}Lut_2(t) = b_{12} \cdot Lut_1(t) - b_{13} \cdot Lut_2(t) \tag{2.17}$$

$$\frac{d}{dt}Lut_3(t) = b_{13} \cdot Lut_2(t) - b_{14} \cdot Lut_3(t) \tag{2.18}$$

$$\frac{d}{dt}Lut_4(t) = b_{14} \cdot Lut_3(t) - b_{15} \cdot Lut_4(t), \tag{2.19}$$

where $b_i \in \mathbb{R}_+$, $i = 1, \ldots, 15$, denote the parameters of the ovarian compartment.

The ovarian hormones estradiol, progesterone, and inhibin are released at the rate γ_i from the follicles at stage F_i into the blood, $i = 1, \ldots, 9$, where they are eliminated at the constant rate δ. The following differential equations describe the changes of the hormone's blood concentration C:

$$\frac{d}{dt}C = \frac{1}{V_B} \cdot \sum_{i=1}^{n} \gamma_i \cdot F_i - \delta \cdot C,$$

where F_i denotes the corresponding active mass, $i = 1, \ldots, 9$ [37]. It is assumed that the clearance from the blood occurs on a faster time scale than the follicular and luteal development, hence, δ is large. Dividing by δ and defining $\varepsilon := \frac{1}{\delta}$ where ε is small yields:

$$\varepsilon \cdot \frac{d}{dt}C = \frac{1}{V_B} \cdot \sum_{i=1}^{n} \frac{\gamma_i}{\delta} \cdot F_i - C.$$

Since ε is small, the quasi-stationary state $\varepsilon \cdot \frac{d}{dt}C \approx 0$ can be assumed which leads to

$$C(t) = \sum_{i=1}^{n} C_i \cdot F_i,$$

where $C_i := \frac{\gamma_i}{\delta \cdot V_B}$.

Estradiol is secreted mainly by the secondary follicles and the preovulatory follicle and partially by the corpus luteum. Therefore, the concentration $E_2(\cdot)$ may be written as a linear combination of SeF, PrF, and Lut_4 (including a basal concentration):

$$E_2(t) = c_1 + c_2 \cdot SeF(t) + c_3 \cdot PrF(t) + c_4 \cdot Lut_4(t). \tag{2.20}$$

Progesterone and inhibin are secreted mainly in the luteal phase by the corpus luteum, however, inhibin is also secreted by the preovulatory follicle. Thus, the concentrations of $P_4(\cdot)$ and $Ih(\cdot)$ (including a basal concentration) can be written as:

$$P_4(t) = c_5 \cdot Lut_3(t) + c_6 \cdot Lut_4(t) \tag{2.21}$$

$$Ih(t) = c_7 + c_8 \cdot PrF(t) + c_9 \cdot Lut_3(t) + c_{10} \cdot Lut_4(t), \tag{2.22}$$

where $c_i \in \mathbb{R}_+$, $i = 1, \ldots, 10$, denote the parameters for these auxiliary equations [37].

2.2 GnRH pulse generator in the hypothalamus

It is possible that the substrates are not released at a constant rate into the blood system, but in pulses. Such a mechanism is presented in this section. The question arises whether the deterministic modeling approach by differential equations is able to reproduce this effect. Modeling by a stochastic approach seems to be more suitable in this case.

In the hypothalamus, the processes are determined by a mechanism called *GnRH pulse generator* resulting in pulsatile release of GnRH into the pituitary portal system.

There are about 1000 [68] up to 1500 [52] GnRH neurons producing GnRH in the hypothalamus. They represent the final output neurons of an integrated neural network [42]. Regulation of the pulse frequency and pulse mass is mainly affected by estrogens and progesterone. Estrogens act on many components of the GnRH network including the brainstem A2 neurons. It binds to the estrogen receptors leading to an increased noradrenaline secretion in the case of A2 neurons and, thereby, facilitating the activity within the GnRH neural network. Thus, the expression of GnRH-mRNA is enhanced resulting eventually in an increased GnRH secretion [42]. In contrast, progesterone inhibits the GnRH pulses via progesterone receptors [77]. Summarized, GnRH is stored in the GnRH neurons and released when the neurons become stimulated.

The GnRH pulse generator is an essential component of the reproductive control system. If it fails, it may have serious consequences for the entire cycle. The GnRH release in pulses, the frequency, and the amplitude are critical for a normal menstrual cycle [86]. Continuous GnRH administration, for example, leads to desensitization of the GnRH receptors in the pituitary. That, in turn, results in a decrease of LH and FSH release into the blood circulation, wherefore a normal follicular development is no longer possible. Hence, the question of developing therapy methods with aid of a mathematical model in the case of dysfunction of the pulse generator could be of great interest.

There have been some approaches for modeling the neural network explicitly, e.g. [30]. The main reason for avoiding this is the uncertainty of the exact processes in the hypothalamus concerning the regulation of the human menstrual cycle [42, 77]. Another reason is the immense effort required for modeling the neural network in a decent manner. Instead, a stochastic approach is chosen to model the overall effect of the pulsatile release of GnRH [47].

Basically there are two components of this mechanism that are modeled:

- GnRH pulse frequency (pulse time points)

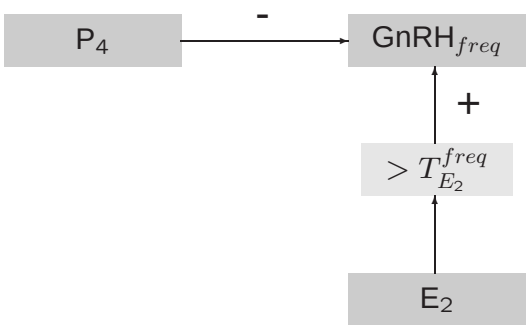

Figure 2.5: Model scheme for the regulation of the pulse frequency. $T_{E_2}^{freq}$: threshold value for the estradiol concentration in the case of frequency regulation. $+$: stimulatory, $-$: inhibitory.

- GnRH pulse mass (the amount of GnRH that is stored between two pulse time points and that is released per pulse).

The modeling of these two components is presented in the following.

2.2.1 Pulse frequency

The GnRH pulse frequency is not constant during the menstrual cycle. In the follicular phase, GnRH is released at approximately constant intervals: the length of interval between two pulses is about 80 or 90 minutes. At mid-cycle, the gaps between the pulses shorten [45, 86]. As a result of the higher pulse frequency at mid-cycle, it is assumed that estradiol because of its rising levels at mid-cycle, at least at high concentrations stimulates the GnRH pulse frequency. In the luteal phase, the interval between the pulses is prolonged to several hours [45]. Progesterone is the main factor of this reduction of pulse frequency [32, 45]. In the early luteal phase, the pulse frequency diminishes to one pulse every 2 to 4 hours, in the mid-luteal phase to every 4 to 6 hours and in the late luteal phase to every 8 to 12 hours [9]. The model scheme for the regulation of the GnRH pulse frequency is presented in Fig. 2.5.

To model the pulsatility in an adequate manner, a stochastic approach is chosen. A similar approach for a pulse generator has been presented in [47], in the context of modeling the male reproductive hormone system. The idea is to model the pulse time points by a renewal process. Let $\{S_j\}_{j\in\mathbb{N}}$ be a sequence of independent and identically distributed random variables with the distribution function F (and density function f). The pulse time points $\{T_j\}_{j\in\mathbb{N}_0}$ are then modeled by

$$T_0 := 0, \quad T_{j+1} := T_j + S_{j+1}, \quad j \in \mathbb{N}_0.$$

It is required that the pulse time points are feedback-regulated by delayed progesterone and estradiol concentrations. Moreover, regulation of the pulse pattern is desired. The most natural choice, the Poisson process, is not suitable in this case since it does not offer this kind of flexibility as opposed to the Weibull density that is chosen here for

the survival time between two pulses:

$$\begin{aligned} f(s) &= P[s|\lambda(\cdot)] \\ &= \gamma \cdot (\lambda(s) \cdot s)^{\gamma-1} \cdot \exp\left(-(\lambda(s) \cdot s)^{\gamma}\right). \end{aligned}$$

where $\gamma \in \mathbb{R}_+$. A sort of stochastic time transformation of a Weibull renewal process is exerted, i.e. transformation of the deterministic term $\lambda(s)$ into the stochastic term

$$\int_{T_{j-1}}^{s} \lambda(r)\, dr.$$

Thus the following is obtained:

$$\begin{aligned} f(s) &= P[s|T_{j-1}, \lambda(\cdot)] \\ &= \gamma \cdot \lambda(s) \cdot \left(\int_{T_{j-1}}^{s} \lambda(r)\, dr\right)^{\gamma-1} \cdot \exp\left(-\left(\int_{T_{j-1}}^{s} \lambda(r)\, dr\right)^{\gamma}\right). \end{aligned}$$

By the stochastic time transformation dependency of the pulse time points is achieved.

The delayed feedback can be included in the pulse intensity function $\lambda(\cdot)$ and in addition, due to the parameter γ it is possible to regulate the pulse pattern. Suppose that the survival time is S_j, starting at the pulse time point T_{j-1}, $j \in \mathbb{N}$. Then it is:

$$F(S_j) = \int_{T_{j-1}}^{T_{j-1}+S_j} f(s)\, ds = P[T_{j-1} < s \leq T_j | T_{j-1}, \lambda(\cdot)] \tag{2.23}$$

$$= 1 - \exp\left(-\left(\int_{T_{j-1}}^{T_j} \lambda(r)\, dr\right)^{\gamma}\right). \tag{2.24}$$

Feedback regulation of the GnRH pulse frequency and mass by progesterone and estradiol represents the interface from the ovaries to the pituitary. The steroids are released into the blood and reach the hypothalamus through the blood circulation. They influence the work of the neural network in a complicated and not fully known way. Only inhibitory, stimulatory or a combined influence can be observed. These feedback mechanisms are modeled by the Hill functions.

The function $\lambda(\cdot)$ describes the pulse intensity and allows the feedback regulation of the pulse time points. Progesterone has a negative effect and estradiol a positive effect (at high concentration) on the GnRH pulse frequency [32, 45]:

$$\lambda(t) = h^{-}\left(P_4(t-\tau_{P_4}); T_{P_4}^{freq}, n_{P_4}^{freq}\right) \cdot \left(1 + h^{+}\left(E_2(t-\tau_{E_2}); T_{E_2}^{freq}, n_{E_2}^{freq}\right)\right) \cdot \lambda_{max}, \tag{2.25}$$

where P_4 and E_2 denote the progesterone and estradiol concentrations in the blood, respectively, τ_{P_4}, τ_{E_2} the delays, $T_{P_4}^{freq}$, $T_{E_2}^{freq}$ the threshold values, $n_{P_4}^{freq}$, $n_{E_2}^{freq}$ the Hill coefficients, and $\lambda_{max} \in \mathbb{R}_+$. Written as differential equation, the first model equation (Eq. 1 in Table 3.6 at the end of this chapter) is given:

$$\begin{aligned} \frac{d}{dt}\Lambda(t) &= \lambda(t) \\ &= h^{-}\left(P_4(t-\tau_{P_4}); T_{P_4}^{freq}, n_{P_4}^{freq}\right) \cdot \left(1 + h^{+}\left(E_2(t-\tau_{E_2}); T_{E_2}^{freq}, n_{E_2}^{freq}\right)\right) \cdot \lambda_{max}, \end{aligned}$$

where $\Lambda(s) := \int_0^s \lambda(r)\, dr$ denotes the cumulative pulse intensity function.

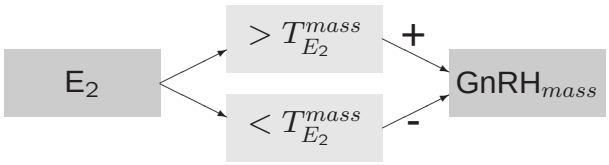

Figure 2.6: Model scheme for the regulation of the GnRH pulse mass. $T_{E_2}^{mass}$: threshold value for the estradiol concentration in the case of mass regulation. +: stimulatory, −: inhibitory.

Lemma 2.1. *The pulse intensity $\lambda(\cdot)$ is bounded: $\lambda(t) \in (0, 2\cdot\lambda_{max})$ for all $t \geq 0$.*

Proof. Since $h^-(\cdot) \in (0,1]$ and $h^+(\cdot) \in [0,1)$, it follows $\lambda(t) > 0$ and $\lambda(t) < 2 \cdot \lambda_{max}$ for all $t \geq 0$. □

2.2.2 Pulse mass

The amount of GnRH pulse mass, denoted by $M_{GnRH,j}$, that is stored between two pulses T_{j-1} and T_j is affected by estradiol as well. Estradiol inhibits the GnRH amplitude [65], whereas progesterone has no significant effect [77]. The GnRH surge, in turn, is triggered by rising estradiol upon the hypothalamus [9]. Hence, it is reasonable to assume that estradiol is inhibitory at low concentrations and stimulatory at high concentrations [9, 82, 86]. The model scheme for the regulation of the GnRH pulse mass is presented in Fig. 2.6. Since estradiol acts differently on the GnRH pulse mass, it is assumed here that there are at least two effects responsible for the regulation of the GnRH pulse mass: One mechanism leads to a negative feedback, the other one to a positive feedback. One model approach for this case is presented in Chapter 1. These two effects are modeled with aid of the biphasic Hill function, the sum of the Hill functions h^- and h^+.

The mass $M_{GnRH,j}$ can be calculated by introducing the accummulated mass M_{GnRH} (Eq. 2 in Table 3.6):

$$\frac{d}{dt}M_{GnRH}(t) = \left(h^-(E_2(t-\tau_{E_2}); T_{E_2,1}, n_{E_2,1}) + h^+(E_2(t-\tau_{E_2}); T_{E_2,2}, n_{E_2,2})\right) \cdot M_{max}, \tag{2.26}$$

where $T_{E_2,1}, n_{E_2,1}, T_{E_2,2}, n_{E_2,2}, M_{max} \in \mathbb{R}_+$ denote the parameters.

Define $h^{-,+}(E_2) := h^-(E_2; T_{E_2,1}, n_{E_2,1}) + h^+(E_2; T_{E_2,2}, n_{E_2,2})$. Assume that $T_{E_2,1} < T_{E_2,2}$ and $n_{E_2,1} = n_{E_2,2}$. Then the unique minimum of $h^{-,+}$ on $\mathbb{R}_+$ is given by (see Lemma 1.1)

$$T_{E_2}^{mass} := (T_{E_2,1} \cdot T_{E_2,2})^{\frac{1}{2}}.$$

Furthermore, it is $h^{-,+}(E_2) \in [h^{-,+}\left(T_{E_2}^{mass}\right), 1]$ for all $E_2 \in [0, \infty)$.

The pulse mass $M_{GnRH,j}$ is stored between the two pulse time points T_{j-1} and T_j

and is completely released at the next pulse time point T_j, $j \in \mathbb{N}$:

$$\begin{aligned} M_{GnRH,j} &= M_{GnRH}(T_j) - M_{GnRH}(T_{j-1}) \\ &= \int_{T_{j-1}}^{T_j} (h^-(E_2(t-\tau_{E_2}); T_{E_2,1}, n_{E_2,1}) + h^+(E_2(t-\tau_{E_2}); T_{E_2,2}, n_{E_2,2})) \cdot M_{max}\, dt. \end{aligned} \tag{2.27}$$

2.3 GnRH concentration in the pituitary portal system

Except for the pituitary portal system, the GnRH concentration does not play a major role in the blood system: the GnRH concentration in the blood circulation is not detectable [59]. That is why it is neglected in the remaining blood system in the further modeling. Additionally to the release of GnRH in pulses, a basal GnRH secretion at the constant rate b_{FSH} can be assumed. This basal secretion is independent of feedback mechanisms since even at high GnRH pulse frequency the GnRH concentration declines not to zero values but to a baseline level [59]. Moreover, the GnRH pulse mass is not released at once, but distributed into the pituitary portal system with the blood volume V_{PPS}. It is assumed that the distribution does not occur at a constant rate but attains a peak with short delay after the start of the release that is the last pulse time point and which can be modeled by use of a Gamma density. Binding of GnRH to its receptor located in the pituitary is proportional to the present GnRH concentration in the pituitary portal system and to the unbound GnRH receptor concentration with the rate constant β_{GnRH}. The clearance of GnRH is assumed to be proportional to the present GnRH concentration in the pituitary portal system where the clearance rate is denoted by α_{GnRH}.

In order to be accurate, the pulse masses of the foregoing pulses must be considered as well, see [47] and [46]. In this case the dynamics of the GnRH concentration can be described by

$$\begin{aligned} \frac{d}{dt}GnRH(t) = \frac{b_{GnRH}}{V_{PPS}} &+ \sum_{i=1}^{j} \frac{M_{GnRH,i}}{V_{PPS}} \cdot \psi(t - T_i) \\ &- \beta_{GnRH} \cdot GnRH(t) \cdot R_{GnRH}(t) - \alpha_{GnRH} \cdot GnRH(t). \end{aligned} \tag{2.28}$$

Here, the masses of the foregoing pulses are not considered since it is assumed that

$$\sum_{i=1}^{j-1} \frac{M_{GnRH,i}}{V_{PPS}} \cdot \psi(t - T_i) \ll \frac{M_{GnRH,j}}{V_{PPS}} \cdot \psi(t - T_j), \quad t \in (T_j, T_{j+1}).$$

It follows for the GnRH concentration in the pituitary portal system:

$$\begin{aligned} \frac{d}{dt}GnRH(t) = \frac{b_{GnRH}}{V_{PPS}} &+ \frac{M_{GnRH,j}}{V_{PPS}} \cdot \psi(t - T_j) \\ &- \beta_{GnRH} \cdot GnRH(t) \cdot R_{GnRH}(t) - \alpha_{GnRH} \cdot GnRH(t), \end{aligned} \tag{2.29}$$

where $t \in [T_j, T_{j+1})$ for all $j \in \mathbb{N}$, $GnRH$ and R_{GnRH} denote the GnRH and GnRH receptor concentration, respectively, and ψ the normalized density function for the GnRH mass distribution.

In [47], a generalized Gamma family of densities has been chosen

$$\psi(t) := \begin{cases} \frac{\beta_3}{\Gamma(\beta_1)\cdot\beta_2^{\beta_1\cdot\beta_3}} \cdot t^{\beta_1\cdot\beta_3-1} \cdot \exp\left(-\left(\frac{t}{\beta_2}\right)^{\beta_3}\right) & \text{if } t \geq 0, \\ 0 & \text{if } t < 0, \end{cases}$$

where $\beta_1 > 1$, $\beta_2 > 0$, and $\beta_3 > 0$. The standard Gamma density

$$\psi(t) := \begin{cases} \frac{a^m}{\Gamma(m)} \cdot t^{m-1} \cdot \exp(-a \cdot t) & \text{if } t \geq 0, \\ 0 & \text{if } t < 0, \end{cases}$$

where $a, m \in \mathbb{R}_+$, $m \geq 1$, which is obtained for $\beta_1 = m$, $\beta_2 = \frac{1}{a}$, and $\beta_3 = 1$ in the generalized case, is sufficient here since the exact shape of the GnRH pulses is not known. More precisely, it is $\psi(t) := \frac{a^m}{\Gamma(m)} \cdot \left(\frac{t}{[t]}\right)^{m-1} \cdot \exp(-\frac{a}{[t]} \cdot t)$ for $t \geq 0$, for simplicity, the first notation is used in the following. The Gamma distribution is selected here since it is more realistic than simple exponential decline since the maximum is not reached at the pulse time point but it is delayed. The parameters can be chosen so that the distribution is asymmetric, reaching the maximum relatively quickly and declining slowly.

Note that in the first case (Eq. (2.28)), it holds

$$\lim_{t\uparrow T_j} \frac{d}{dt} GnRH(t) = \lim_{t\downarrow T_j} \frac{d}{dt} GnRH(t) = \frac{d}{dt} GnRH(T_j)$$

but in the second case (Eq. (2.29)), it is

$$\lim_{t\uparrow T_j} \frac{d}{dt} GnRH(t) \neq \lim_{t\downarrow T_j} \frac{d}{dt} GnRH(t) = \frac{d}{dt} GnRH(T_j).$$

If a and m are chosen appropriately, the difference is negligible (see Chapter 4).

The GnRH dynamics are summarized in Fig. 2.7.

2.4 Mechanisms in the pituitary

The hormone GnRH is transported over the pituitary portal system into the pituitary where it binds to its receptor and activates it which stimulates the release of the gonadotropins LH and FSH that are both synthesized in the pituitary. Moreover, the synthesis of LH and FSH in the pituitary as well as the secretion from this pool are regulated by the steroids produced in the ovaries.

2.4.1 Receptor binding of GnRH

GnRH stimulates the release of LH and FSH, but it has no effect on other pituitary hormones [32]. Within a few seconds after binding of this peptide to its receptor, a massive calcium entrance into the cell occurs [62]. This leads after a couple of minutes to the release of stored LH and FSH. The amplitude of the GnRH pulses (amplitude

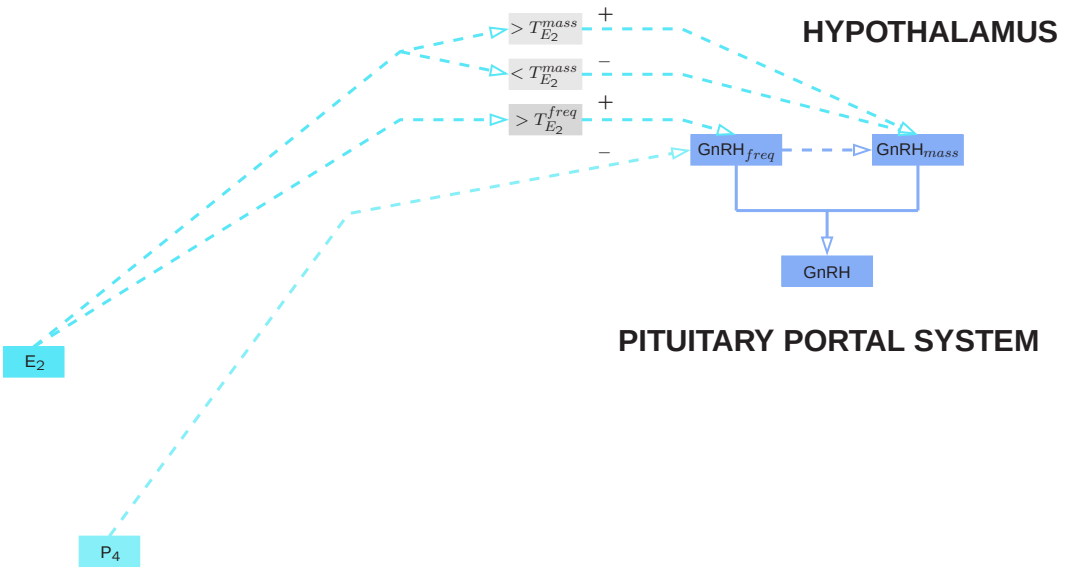

Figure 2.7: Model scheme for the GnRH dynamics.

modulation) and, as fine regulation, the frequency of GnRH pulses (frequency modulation) regulate the LH and FSH concentrations over the cycle [62]. LH responds to GnRH more quickly and more distinctive than FSH [32].

The pulsatility of GnRH secretion is necessary since continuous administration of GnRH leads to decreasing LH and FSH concentrations [57]. This phenomenon can be explained by the negative feedback of GnRH on its receptor [32]. Declining response of the GnRH receptors on GnRH is called *desensitization* [16].

In [41], a mathematical model for the GnRH receptor binding including the receptor recycling which leads to the release of LH is developed. Unfortunately, the model is not designed for the human but for the ovine case, which is why the results must be handled with care when using it for the human case. The model scheme for the receptor binding in the pituitary is adopted from [41], shown in Fig. 2.8. After binding of GnRH to its receptor at the rate r_1, the complex stimulates the release of LH from the LH pool. The activated receptor becomes at first desensitized at the rate r_2 and returns to the unbound state at the rate r_3. The resulting model equations for the receptor recycling are [41]:

$$\frac{d}{dt} R_{GnRH} = r_3 \cdot R_{GnRH}\text{-}d - r_1 \cdot GnRH \cdot R_{GnRH} \tag{2.30}$$

$$\frac{d}{dt} (GnRH\text{-}R_{GnRH}) = r_1 \cdot GnRH \cdot R_{GnRH} - r_2 \cdot (GnRH\text{-}R_{GnRH}) \tag{2.31}$$

$$\frac{d}{dt} R_{GnRH}\text{-}d = r_2 \cdot (GnRH\text{-}R_{GnRH}) - r_3 \cdot R_{GnRH}\text{-}d, \tag{2.32}$$

where $(GnRH\text{-}R_{GnRH})$ denotes the complex concentration in the pituitary and $R_{GnRH}\text{-}d$ the concentration of the desensitized receptors.

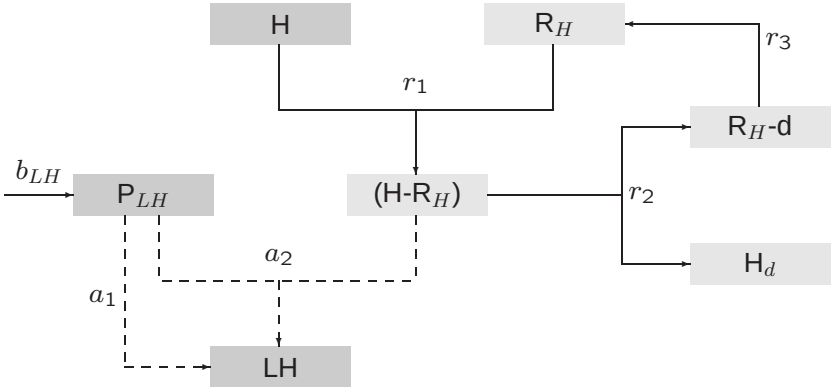

Figure 2.8: Model scheme for the receptor binding in the pituitary [41]. H: GnRH, R_H: GnRH receptor, (H-R_H): hormone-receptor complex, R_H-d: desensitized receptor, H_d: degraded hormone.

Note that the sum of R_{GnRH}, $(GnRH\text{-}R_{GnRH})$, and $R_{GnRH}\text{-}d$ is constant since

$$\frac{d}{dt}R_{GnRH} + \frac{d}{dt}(GnRH\text{-}R_{GnRH}) + \frac{d}{dt}R_{GnRH}\text{-}d = 0.$$

Here it is stated that if the GnRH concentration increases, the number of free receptors decreases, but it has no influence on the total number of receptors. However, the total number of GnRH receptors is not constant [16] and here it is assumed that GnRH exerts a negative feedback not only on the number of free receptors but also on the total number of receptors. In order to make the total number of receptors more dynamic, another term is added. If there is a high GnRH concentration, it is assumed that the free receptors are cleared at a rate near r_4. If the GnRH concentration is low, it is assumed that the free receptors are produced at a rate near r_4. One possibility to incorporate the negative feedback of GnRH on its receptor is to write the differential equation for the free receptor concentration as

$$\begin{aligned}\frac{d}{dt}R_{GnRH} = {} & r_4 \cdot f_{GnRH}(GnRH; T_{GnRH}) + r_3 \cdot R_{GnRH}\text{-}d \\ & - r_1 \cdot GnRH \cdot R_{GnRH},\end{aligned} \tag{2.33}$$

where $T_{GnRH} \in \mathbb{R}_+$ and

$$f_{GnRH}(GnRH; T_{GnRH}) := \frac{1 - \frac{GnRH}{T_{GnRH}}}{1 + \frac{GnRH}{T_{GnRH}}}$$

since it holds

$$\begin{aligned} f_{GnRH}(0; T_{GnRH}) &= 1 \\ f_{GnRH}(T_{GnRH}; T_{GnRH}) &= 0 \\ \lim_{GnRH \to \infty} f_{GnRH}(GnRH; T_{GnRH}) &= -1 \end{aligned}$$

so that this approach is equivalent to the one above (Eq. (2.30)) if $GnRH = T_{GnRH}$. LH is synthesized at the constant basal rate b_{LH} and its release from the pituitary into the blood circulation is dependent on the stored LH mass in the pituitary and on the concentration of the GnRH receptor complex. For the LH dynamics, it is, slightly changed from [41]:

$$\frac{d}{dt}P_{LH} = b_{LH} - a_1 \cdot P_{LH} - a_2 \cdot P_{LH} \cdot (GnRH\text{-}R_{GnRH}) \tag{2.34}$$

$$\frac{d}{dt}LH \ = \frac{1}{V_B} \cdot (a_1 \cdot P_{LH} + a_2 \cdot P_{LH} \cdot (GnRH\text{-}R_{GnRH}))\,, \tag{2.35}$$

where P_{LH} denotes the LH mass in the pituitary, LH the LH concentration in the blood, and a_1, a_2 the rate constants.

Additionally, the calcium dynamics are included in the model presented in [5] and [85]. It is described in the form of model schemes in Figs. 2.9 and 2.10 whereby the model equations are taken from [85]. Again, it is assumed that initially GnRH bounds to its receptor

$$\mathrm{GnRH} + \mathrm{R}_{GnRH} \quad \underset{k_{-1}}{\overset{k_1}{\rightleftharpoons}} \quad (\mathrm{GnRH\text{-}R}_{GnRH}),$$

where k_1 and k_{-1} denote the rate constants for the forward and reverse reactions, respectively. The bound complex in turn can form dimers

$$2\,(\mathrm{GnRH\text{-}R}_{GnRH}) \quad \underset{k_{-2}}{\overset{k_2}{\rightleftharpoons}} \quad (\mathrm{GnRH\text{-}R}_{GnRH})_2,$$

where k_2 and k_{-2} denote the rate constants. Formation of larger aggregates is possible. It is assumed that the average number of monomers forming a macroaggregate is n. Then the aggregates move into the cell which is called internalization. The internalized hormones are completely degraded. Parts of the receptors are also degraded, the remaining receptors, the fraction $\theta \in (0, 1)$, return to the membrane at the rate k_{11} and with the delay τ. A simple reaction mechanism is assumed for this process:

$$n\,(\mathrm{GnRH\text{-}R}_{GnRH}) \quad \xrightarrow{(1-\theta)\cdot k_{11}} \quad n\,\mathrm{GnRH}_d + n\,\mathrm{R}_{GnRH,d}$$

and

$$n\,(\mathrm{GnRH\text{-}R}_{GnRH}) \quad \xrightarrow{\theta\cdot k_{11}} \quad n\,\mathrm{GnRH}_d + n\,\mathrm{R}_{GnRH},$$

where GnRH_d denotes the degraded hormone and $\mathrm{R}_{GnRH,d}$ the degraded receptor. There is a low basal rate of receptor synthesis, P_0, and free receptors are degraded at the rate γ. By the reaction of a G protein (GQ) with the dimer an effector (E) is produced

$$(\mathrm{GnRH\text{-}R}_{GnRH})_2 + GQ \quad \underset{k_{-3}}{\overset{k_3}{\rightleftharpoons}} \quad E,$$

where k_3 and k_{-3} denote the rate constants. Additionally, another dependence of GQ on the dimer concentration is mentioned in [85], but not presented here, since it is

not used for the complex model. These reflections lead to the following differential equations for the free receptor, the complex, and the dimer concentrations:

$$\begin{aligned}\frac{d}{dt}R_{GnRH} &= -k_1 \cdot GnRH \cdot R_{GnRH} + k_{-1} \cdot (GnRH\text{-}R_{GnRH}) \\ &\quad + \theta \cdot k_{11} \cdot n \cdot (GnRH\text{-}R_{GnRH})_\tau + P_0 - \gamma \cdot R_{GnRH} \qquad (2.36)\\ \frac{d}{dt}(GnRH\text{-}R_{GnRH}) &= k_1 \cdot GnRH \cdot R_{GnRH} - k_{-1} \cdot (GnRH\text{-}R_{GnRH}) \\ &\quad + 2 \cdot k_{-2} \cdot (GnRH\text{-}R_{GnRH})_2 - 2 \cdot k_2 \cdot (GnRH\text{-}R_{GnRH})^2 \\ &\quad - k_{11} \cdot n \cdot (GnRH\text{-}R_{GnRH}) \qquad (2.37)\\ \frac{d}{dt}(GnRH\text{-}R_{GnRH})_2 &= -k_{-2} \cdot (GnRH\text{-}R_{GnRH})_2 + k_2 \cdot (GnRH\text{-}R_{GnRH})^2 \\ &\quad - k_3 \cdot GQ \cdot (GnRH\text{-}R_{GnRH})_2 + k_{-3} \cdot E \qquad (2.38)\end{aligned}$$

and for the G protein and the effector concentrations:

$$\begin{aligned}\frac{d}{dt}GQ &= -k_3 \cdot GQ \cdot (GnRH\text{-}R_{GnRH})_2 + k_{-3} \cdot E \\ &\quad + k_{33} \cdot \exp\left(-\frac{t - T_j}{k_{333}}\right) \cdot (GnRH\text{-}R_{GnRH})_2 \qquad (2.39)\\ \frac{d}{dt}E &= k_3 \cdot GQ \cdot (GnRH\text{-}R_{GnRH})_2 - k_{-3} \cdot E, \qquad (2.40)\end{aligned}$$

where

$$\begin{aligned}&(GnRH\text{-}R_{GnRH})_\tau := (GnRH\text{-}R_{GnRH})(t-\tau) \cdot \chi(t-\tau),\\ &\chi(t) := \begin{cases} 1 & \text{if } t \geq 0 \\ 0 & \text{if } t < 0. \end{cases}\end{aligned}$$

The remaining part of the model presented in [85] is only coarsely presented since it is not included in the model at this point. It is further assumed that the production of inositol 1,4,5-triphosphate (IP_3) is proportional to the concentration of E, with the constant rate k_5 and that it is eliminated at the constant rate k_{-5} proportional to its concentration:

$$\frac{d}{dt}IP_3 = k_5 \cdot E - k_{-5} \cdot IP_3. \qquad (2.41)$$

When IP_3 binds to receptors on the membrane of the endoplasmic reticulum (ER), the Ca^{2+} that is stored in the ER is released. It is assumed that the fraction of open channels, CHO, depends on IP_3 through Michaelis-Menten kinetics:

$$CHO(t) = \frac{\alpha \cdot IP_3(t)}{1 + \alpha \cdot IP_3(t)} \cdot (\theta_1 + \theta_1 \cdot \beta \cdot (t - T_j) \cdot \exp(1 - \beta \cdot (t - T_j))), \qquad (2.42)$$

where T_j, $j \in \mathbb{N}$, denote the GnRH pulse time points and $\alpha, \beta, \theta_1 \in \mathbb{R}_+$ the parameters. The Ca^{2+} concentration dynamics in the endoplasmic reticulum, CA_{ER}, and the

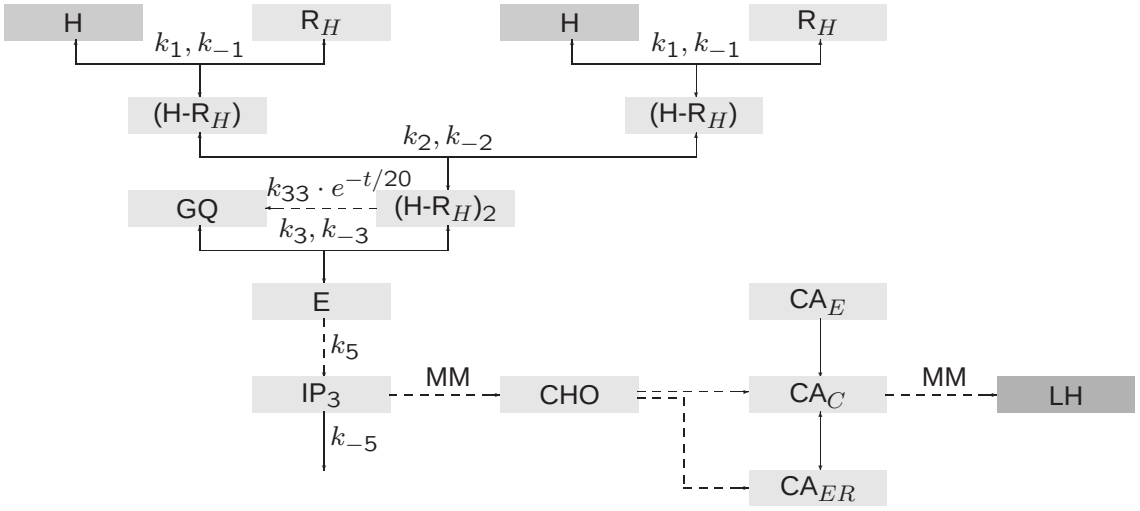

Figure 2.9: Model scheme for the receptor binding in the pituitary including calcium dynamics in the cell [85]. H: GnRH, R_H: free GnRH receptor, (H-R_H): hormone-receptor complex, (H-R_H)$_2$: hormone-receptor dimer, GQ: G protein, E: effector, IP_3: Inositol 1, 4, 5-triphosphate, CA_E: external Ca^{2+}, CA_C: cytosolic Ca^{2+}, CA_{ER}: endoplasmic reticulum (ER) Ca^{2+}, CHO: fraction of open ER Ca^{2+} channels, MM: Michaelis-Menten kinetics.

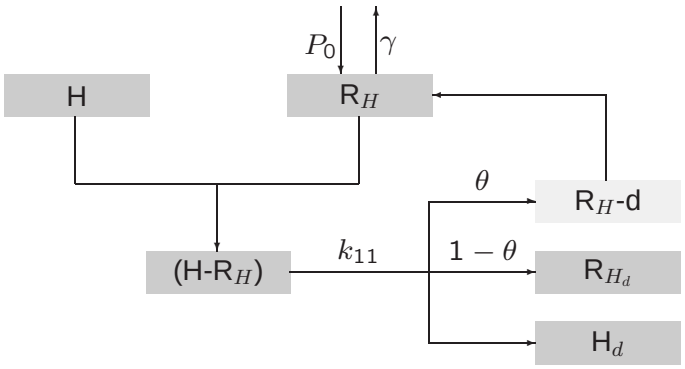

Figure 2.10: Model scheme for the receptor recycling in the pituitary [85], slightly modified by ignoring macroaggregation and including the state of the desensitized receptor R_H-d. H: GnRH, R_H: free GnRH receptor, (H-R_H): hormone-receptor complex, H_d: degraded GnRH, R_{H_d}: degraded receptor.

concentration of the cytosolic Ca^{2+} dynamics, CA_C, are described by the differential equations [85]

$$\begin{aligned}\frac{d}{dt}CA_{ER} = & -CHO \cdot ERR \cdot (CA_{ER} - CA_C) \\ & + k_{-6} \cdot \frac{CA_C^2}{T_{CA,1}^2 + CA_C^2} \cdot (ERUL - CA_{ER}) \qquad (2.43)\\ \frac{d}{dt}CA_C = & \theta_2 \cdot CHO \cdot ERR \cdot (CA_{ER} - CA_C) \\ & - \theta_2 \cdot k_{-6} \cdot \frac{CA_C^2}{T_{CA,1}^2 + CA_C^2} \cdot (ERUL - CA_{ER}) \\ & + VSR \cdot (CA_E - CA_C) - k_7 \cdot \frac{CA_C^2}{T_{CA,2}^2 + CA_C^2} + k_9 \cdot CA_E \qquad (2.44)\end{aligned}$$

where

$$ERR = k_6 + k_{66} \cdot CA_C - k_{666} \cdot CA_C^2 \qquad (2.45)$$

denote the rate constant for calcium that is released from the ER into the cytoplasm,

$$VSR = k_8 \cdot E + k_{88} \cdot CA_C - k_{888} \cdot CA_C^2 \cdot VSRO \qquad (2.46)$$

the rate of calcium influx from extracellular calcium into the cytosol, *VSRO* the fraction of open calcium channels in the outer membrane decreasing in the presence of hormone and increasing in the absence of hormone,

$$\frac{d}{dt}VSRO = \begin{cases} -v_1 & \text{if } GnRH > 0, \\ v_2 & \text{if } GnRH = 0, \end{cases} \qquad (2.47)$$

and k_6, k_{-6}, k_{66}, k_{666}, k_7, k_8, k_{88}, k_{888}, k_9, $ERUL$, θ_2, $T_{CA,1}$, $T_{CA,2}$, v_1, $v_2 \in \mathbb{R}_+$ the parameters. The external Ca^{2+} concentration, CA_E, remains constant. Finally, it is assumed that the release of LH depends on CA_C through Michaelis-Menten kinetics [85]:

$$\frac{d}{dt}LH = k_{10} \cdot \frac{CA_C^2}{T_{CA,3}^2 + CA_C^2}, \quad k_{10}, T_{CA,3} \in \mathbb{R}_+. \qquad (2.48)$$

This model [85] focus on the GnRH-induced secretion of LH, since GnRH has effect only on gonadotropin release and not on synthesis. The release stimulation is described in more detail which is why it could offer a suitable alternative. At this stage, the calcium dynamics presented in this model will not be incorporated in the complex model since it goes beyond the limits for this modeling process.

The research focus on the case of LH, since it is a key element at mid-cycle. Therefore, it can only be assumed that the release of FSH mediated by GnRH is comparable to the LH release, see [86].

In Fig. 2.10, the receptor recycling process, as it is derived in [85], slightly modified, is presented. Additionally to [5] that is constrained to the receptor binding leading to

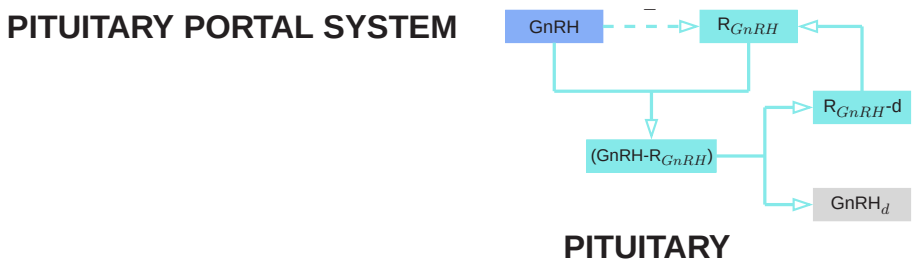

Figure 2.11: Model scheme for the GnRH receptor binding and recycling.

calcium dynamics and, finally, to the LH dynamics, the recycling process is included in [85]. Thus, assuming a receptor recycling mechanism similar to the one in [41], though derived for the ovine case, seems to be reasonable even for women.

The GnRH receptor binding can be summarized in the following way: The GnRH molecule binds to its receptor and forms a complex. The complex is the active form of the receptor. The bound receptor does not return instantly to the unbound state, but arrives first at a desensitized state where it cannot be activated.

The receptor binding can be modeled as presented in Chapter 1. Finally, in order to model the GnRH receptor binding, Eqs. (2.31), (2.32), and (2.33) are taken. In order to make the total receptor concentration more dynamic, it is assumed that GnRH exerts a negative feedback not only on the number of free receptors but also on the total number of receptors [66]. The dynamics are then described by (Eqs. 4 to 6 in Table 3.6):

$$\begin{aligned}
\frac{d}{dt}R_{GnRH} &= r_4 \cdot \frac{T_{GnRH} - GnRH}{T_{GnRH} + GnRH} + r_3 \cdot R_{GnRH}\text{-}d - r_1 \cdot GnRH \cdot R_{GnRH} \\
\frac{d}{dt}(GnRH\text{-}R_{GnRH}) &= r_1 \cdot GnRH \cdot R_{GnRH} - r_2 \cdot (GnRH\text{-}R_{GnRH}) \\
\frac{d}{dt}R_{GnRH}\text{-}d &= r_2 \cdot (GnRH\text{-}R_{GnRH}) - r_3 \cdot R_{GnRH}\text{-}d, \quad r_1, \ldots, r_4, T_{GnRH} \in \mathbb{R}_+,
\end{aligned}$$

where the first term in the equation for R_{GnRH} has values in $(-r_4, r_4)$, $GnRH \in \mathbb{R}_+$, depending on the GnRH concentration. The GnRH receptor dynamics are visualized in Fig. 2.11.

2.4.2 Synthesis and release of FSH and LH

The changes in the stored gonadotropin depend on two effects: the synthesis and the release. The synthesis as well as the release of the gonadotropins is regulated by progesterone, estradiol, and inhibin serving as interface from the ovaries to the pituitary. Inhibitory, stimulatory, and a combination of these effects can be observed that are modeled here by Hill functions.

In addition to the definitions and assumptions presented in Section 2.1 (see Figs. 2.3 and 2.4),

- *syn* denotes the synthesis in the pituitary, *rel* the release from the pituitary into the blood, and *clear* the clearance in the blood
- progesterone inhibits and estradiol stimulates the synthesis of LH
- estradiol inhibits and progesterone stimulates the release of LH
- inhibin inhibits the synthesis of FSH
- estradiol inhibits and progesterone stimulates the release of FSH
- the release rate of LH and FSH is proportional to the amount of LH and FSH stored in the pituitary, respectively
- the gonadotropin mass is distributed in the blood volume V_B
- the clearance rates of LH and FSH, denoted by α_{LH} and α_{FSH}, are proportional to the blood levels of LH and FSH, respectively,

the additional assumptions that are presented in the following are made.

It is assumed that there is a basal production of LH as in [41] at the constant rate b_{LH}. Analogously, a basal rate b_{FSH} in the case of FSH is defined. The release of both, LH and FSH, is assumed to be proportional to the GnRH receptor complex concentration and to their stored mass P_{LH} and P_{FSH}, respectively. Probably, the inhibitory effect of estradiol does not remain during the entire cycle. Actually, it has the ability to exert both negative and positive feedback on the secretion of the gonadotropins [2, 65, 82, 86]. Since the initiation of the LH and FSH surge is the consequence of the stimulation by estradiol [86], it is assumed that estradiol is inhibitory at low concentrations and stimulatory at high concentrations. This biphasic feedback is also part of the regulation of the GnRH pulse generator (see Chapter 1 and Section 2.2). The biphasic effect of estradiol is modeled analogously to the case of the GnRH mass with T_{LH}^{pit} and T_{FSH}^{pit} as threshold values between inhibition and stimulation for LH and FSH, respectively. The stimulatory effect of estradiol is amplified by progesterone [32, 82].

In contrast to the assumed stimulatory effect of progesterone, it is possible that estradiol can inhibit FSH synthesis [2] and progesterone can, in combination with estradiol, exert a negative feedback on the FSH secretion [86]. Inhibin inhibits the FSH synthesis [32, 58] and, moreover, the FSH release [45, 55]. These feedback mechanisms are mediated by receptor binding for which the mechanism is not completely clarified.

Summarized, the following assumptions for the synthesis and release of LH and FSH can be made [66]:

- Progesterone inhibits the LH synthesis and stimulates the LH release [37].
- Estradiol stimulates the LH synthesis and inhibits the LH release at low concentration and stimulates it at high concentration [2, 65, 82, 86].

and:

- Progesterone stimulates the FSH release [37].

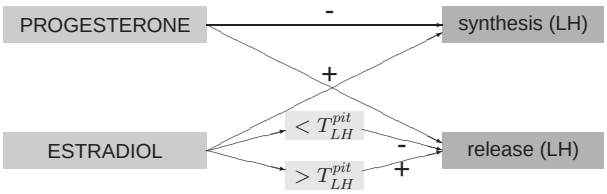

Figure 2.12: Regulation of LH synthesis and release by progesterone and estradiol. +: stimulatory, −: inhibitory, T_{LH}^{pit}: threshold value for the switch from inhibitory to stimulatory effect.

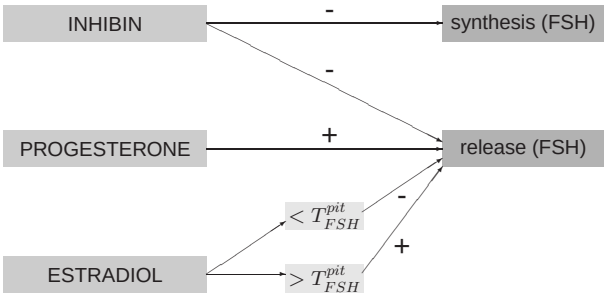

Figure 2.13: Regulation of FSH synthesis and release by progesterone, estradiol, and inhibin. +: stimulatory, −: inhibitory, T_{FSH}^{pit}: threshold value for the switch from inhibitory to stimulatory effect.

- Estradiol inhibits the FSH release at low concentration and stimulates it at high concentration [2, 65, 82, 86].
- Inhibin inhibits the FSH synthesis and release [37, 45, 55].

The assumptions are visualized in the Figs. 2.12 and 2.13.

From this it follows for the stored LH in the pituitary (Eq. 7 in Table 3.6):

$$\frac{d}{dt}P_{LH} = syn_{LH}(P_{4,\tau_{P_4}}, E_{2,\tau_{E_2}}) - rel_{LH}(P_{4,\tau_{P_4}}, E_{2,\tau_{E_2}}, (GnRH\text{-}R_{GnRH}), P_{LH}),$$

where

$$\begin{aligned} syn_{LH} &= b_{LH} + h_1^-(P_4) \cdot h_1^+(E_2) \cdot syn_{LH,max} \\ rel_{LH} &= h_3^+(P_4) \cdot \left(h_2^-(E_2) + h_2^+(E_2)\right) \cdot rel_{LH,max} \cdot (GnRH\text{-}R_{GnRH}) \cdot P_{LH} \end{aligned}$$

and $syn_{LH,max}, rel_{LH,max} \in \mathbb{R}_+$ denote the parameters.

For the FSH pool, the dynamics can be described by (Eq. 9 in Table 3.6):

$$\frac{d}{dt}P_{FSH} = syn_{FSH}(Ih_{\tau_{Ih}}) - rel_{FSH}(P_{4,\tau_{P_4}}, E_{2,\tau_{E_2}}, Ih_{\tau_{Ih}}, (GnRH\text{-}R_{GnRH}), P_{FSH}),$$

where

$$\begin{aligned} syn_{FSH} &= b_{FSH} + h_3^-(Ih) \cdot syn_{FSH,max} \\ rel_{FSH} &= h_5^+(P_4) \cdot \left(h_4^-(E_2) + h_4^+(E_2)\right) \cdot h_5^-(Ih) \cdot rel_{FSH,max} \cdot (GnRH\text{-}R_{GnRH}) \cdot P_{FSH} \end{aligned}$$

and $syn_{FSH,max}, rel_{FSH,max} \in \mathbb{R}_+$ denote the parameters.

2.5 FSH and LH concentrations in the blood

The gonadotropins FSH and LH leave the pituitary and enter the blood circulation. To obtain their concentrations, their masses are divided by the volume of distribution. In the blood, the gonadotropins are metabolized proportionally to their concentrations.

If the additional assumptions are considered (see Fig. 2.12), the model equations for the LH dynamics have the following modified form in comparison to the basic compartment model (Eq. 8 in Table 3.6):

$$\begin{aligned}\frac{d}{dt}LH = \frac{1}{V_B} \cdot rel_{LH}(E_{2,\tau_{E_2}+\tau_{LH,1}}, P_{4,\tau_{P_4}+\tau_{LH,1}}, (GnRH\text{-}R_{GnRH})_{\tau_{LH,1}}, P_{LH,\tau_{LH,1}}) \\ - clear_{LH}(LH),\end{aligned}$$

where

$$clear_{LH} = \alpha_{LH} \cdot LH$$

and $\alpha_{LH} \in \mathbb{R}_+$ denote the parameter. Note that the constant parameter a_2 in Eqs. (2.34) and (2.35) is replaced by the non-constant term

$$\big(h_2^-(E_2) + h_2^+(E_2)\big) \cdot h_3^+(P_4) \cdot rel_{LH,max}.$$

In the case of FSH (see Fig. 2.13), the model equations for the LH dynamics have the following modified form in comparison to the basic compartment model (Eq. 10 in Table 3.6):

$$\begin{aligned}\frac{d}{dt}FSH = \frac{1}{V_B} \cdot rel_{FSH}\big(E_{2,\tau_{E_2}+\tau_{FSH,1}}, P_{4,\tau_{P_4}+\tau_{FSH,1}}, Ih_{\tau_{Ih}+\tau_{FSH,1}}, \\ (GnRH\text{-}R_{GnRH})_{\tau_{FSH,1}}, P_{FSH,\tau_{FSH,1}}\big) - clear_{FSH}(FSH),\end{aligned}$$

where

$$clear_{FSH} = \alpha_{FSH} \cdot FSH$$

and $\alpha_{FSH} \in \mathbb{R}_+$ denote the parameter.

It is $h_i^+(H) := h_i^+(H; T_i^+, n_i^+)$ and $h_i^-(H) := h_i^-(H; T_i^-, n_i^-)$, $i = 1, \ldots, 5$, and $H_\tau := H(t-\tau)$, for the concentrations $H = E_2, P_4, Ih, (GnRH\text{-}R_{GnRH}), P_{LH}$, P_{FSH} and the delays $\tau = \tau_{E_2}, \tau_{P_4}, \tau_{E_2} + \tau_{LH,1}, \tau_{Ih}, \tau_{E_2} + \tau_{FSH,1}, \tau_{P_4} + \tau_{FSH,1}$, $\tau_{Ih} + \tau_{FSH,1}$ where $\tau_{LH,1}, \tau_{FSH,1}$ arise due to the mean time period between the hormone's synthesis in the pituitary and its maximal distribution in the blood.

The dynamics of LH and FSH are visualized in Fig. 2.14.

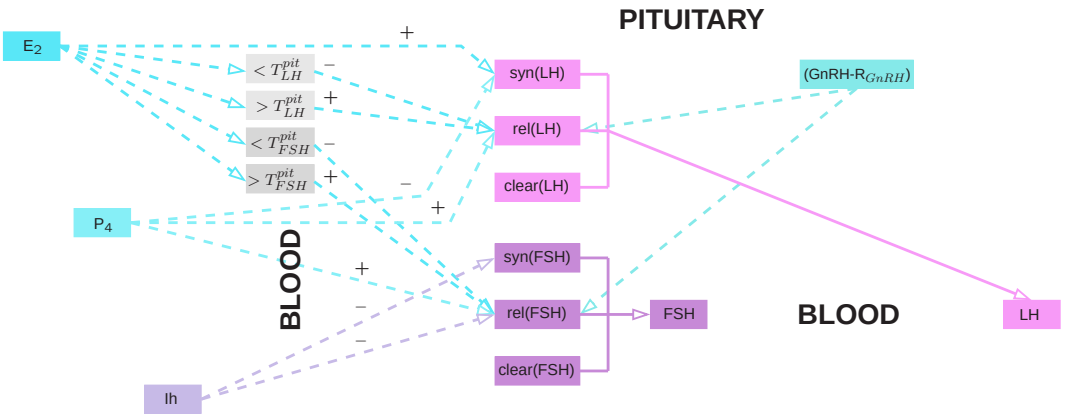

Figure 2.14: Model scheme for the dynamics of LH and FSH.

2.6 Dynamics in the ovaries

The follicular development is primarily controlled by LH and FSH where FSH plays an important role especially at the beginning while LH promotes follicular growth up to ovulation and maintains the activities of the corpus luteum in the second half of the cycle. The process of development can be divided into several stages characterized by the LH and FSH receptor concentrations, the enzyme production, and the biosynthesis of steroids, hormones deriving from cholesterol.

For simplicity, it is assumed that the total receptor concentration is constant. The enzyme concentrations in the follicles depend on the LH and FSH blood concentrations and on the concentrations of activated LH and FSH receptors. By assuming simple Michaelis-Menten kinetics, model equations for the steroidogenesis can be developed, the steroid biosynthesis in the ovaries, from which the steroid concentrations in the blood arise. In the following, there are three main questions to be clarified: which parts of the steroidogenesis occurs in which cells and at which stage.

A couple of immature follicles start the follicular development in every menstrual cycle normally resulting in ovulation at mid-cycle which enables reproduction. The processes mainly take place in two cell types of the follicles, the granulosa and the theca cells. These cells express different receptors and enzymes [9, 15, 32, 79, 80]. In these follicles, progesterone and estradiol as well as other steroids are synthesized.

2.6.1 Follicular development

The whole purpose of regulation carried out by reproductive hormones is eventually the follicular development in the ovaries which is shown in Fig. 2.15. Out of the pool of immature follicles in the ovaries, a couple of them enter the menstrual cycle and run through the single follicular stages, unless they undergo atresia. The production of steroids depends largely upon the follicles' growth and maturation.

There are mainly two cell types that are important in the pathway of follicular development, the granulosa and the theca cells. They differ in, for instance, receptor

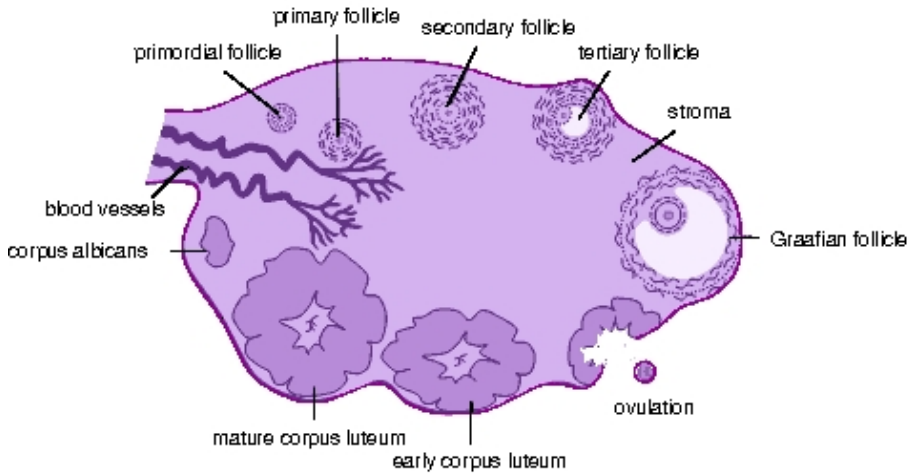

Figure 2.15: Follicular development, modified from [56]. The shapes of the various follicular stages within one ovary are visualized.

expression and enzyme production. The androgen synthesis in the theca cells is mainly mediated by the enzymes cholesterol side-chain cleavage (P450scc), 17α-hydroxylase ($P450_{17\text{-}OH}$), and 3β-hydroxysteroid dehydrogenase (3β-HSD) [9]. In granulosa cells, the enzyme 17β-hydroxysteroid dehydrogenase (17β-HSD) transforms androstenedione into testosterone, and aromatase (P450arom) catalyzes the reaction from testosterone to estradiol [9]. The enzymes P450scc and 3β-HSD are produced in the granulosa cells as well.

The following approaches are conceivable and have been developed to some extent in the past:

1. *Modeling the dynamics of single follicles.* The time points where follicles enter the maturing process are generated by a stochastic process. This is done in [51] and [11] where the dynamics in the follicles are represented by the estradiol concentrations. The dynamics are described by a system of differential equations. This model is able to characterize ovulatory as well as anovulatory cycles [51]. In [11], the model is modified in order to model PCOS.

2. *Modeling on a cellular level.* There are mainly two different cell types in the follicles: theca and granulosa cells. By modeling the cell growth and maturation process as well as the receptor complex concentration, the steroid synthesis and release dynamics can be determined. The case of growth kinetics of the granulosa cell population has been treated in [12] and [13].

3. *Modeling follicular masses in discrete stages.* The number of follicles in every single stage is not important, only its mass. Every stage has its characteristic enzyme and steroid production. This approach is used in [37], [38], [71], and [75].

4. *Two-cell theory.* The idea of modeling follicular masses could be combined with the two-cell theory. That means that the total follicular masses are not considered, but a granulosa cell mass and a theca cell mass since granulosa and theca cells are the locations where steroidogenesis takes place.

The third approach, that is used in the complex model, is chosen in [37], the basic compartment model. By including additional information, the model for the follicular development from the basic compartment model will be modified. In the following, the influence of the gonadotropins FSH and LH is studied.

The ovaries contain a pool of immature *primordial follicles* consisting of approximately 400,000 follicles at puberty [32, 45]. They possess an oocyte, an immature egg-cell, that is surrounded by a single layer of flattened, poorly differentiated cells called granulosa cells [32, 45, 80]. Out of this pool, 1 to 15 [9] or even 30 [45] enter the follicular growth and maturation process of the menstrual cycle. It is assumed that this first step of the so-called initial recruitment [80] is independent of the gonadotropins FSH and LH [9, 45, 69, 87], but regulated by intra-ovarian factors [80].

When the primordial follicle has left the pool of resting follicles, the size of the oocyte begins to increase, the zona pellucida, a membrane that will eventually surround the oocyte, begins to form, and the granulosa cells assume a cuboidal shape. The follicle at this stage is called *primary follicle* [32, 80]. It is assumed that the follicular growth is still independent of FSH and LH [87].

As the so-called *secondary follicle* or preantral follicle [32, 80] is being formed, the granulosa cells express FSH receptors [45, 80]. But to start the gonadotropin-dependent follicular development and to ensure the further development, a certain, individually varying threshold value T_{FSH}^{foll} for FSH has to be exceeded [45, 80]. Henceforth, the follicles are gonadotropin-sensitive [32, 45]. The growth of F_s is assumed to be proportional to its own mass and to a function of the FSH concentration. The transition from the secondary follicle to the next stage is promoted by FSH [80] and is also proportional to its mass:

$$\begin{aligned}\frac{d}{dt}F_s(t) = {} & d_1 \cdot h^+(FSH_{\tau_{FSH,2}}; T_{FSH}^{foll}, n_{FSH}^{foll}) \\ & + d_2 \cdot f_1(FSH_{\tau_{FSH,2}}) \cdot F_s(t) - d_3 \cdot f_1(FSH_{\tau_{FSH,2}}) \cdot F_s(t), \end{aligned} \tag{2.49}$$

where F_p is assumed to be constant and is included in the parameter d_1, $\tau_{FSH,2}$ denotes the delay for *FSH*, n_{FSH} the Hill coefficient, and $d_i \in \mathbb{R}_+$, $i = 1, \ldots, 3$, the remaining parameters.

The follicle is now called the *tertiary follicle* or antral follicle [32]. The granulosa cells rapidly proliferate and the follicle continues to enlarge [32, 80]. The production of IGF-2 starts and it diffuses into the surrounding ovarian stroma inducing the differentiation of the theca cells [45]. These express LH receptors and become LH-sensitive [45, 80]. Since the thecal layer is formed, LH can also have a stimulating effect on the follicular development. Within the granulosa layer, fluid is accumulating leading to the formation of the so-called antrum. The follicles are no longer only FSH responsive but FSH dependent [69, 80]. The growth of F_t as well as the transition of F_t to the

next stage are proportional to its own mass and a function of LH and FSH

$$\frac{d}{dt}F_t(t) = d_3 \cdot f_1(FSH_{\tau_{FSH,2}}) \cdot F_s(t) + d_4 \cdot f_2(FSH_{\tau_{FSH,2}}, LH_{\tau_{LH,2}}) \cdot F_t(t) - d_5 \cdot f_2(FSH_{\tau_{FSH,2}}, LH_{\tau_{LH,2}}) \cdot F_t(t), \tag{2.50}$$

where $\tau_{LH,2}$ denotes the delay for LH and $d_i \in \mathbb{R}_+$, $i = 4, 5$, the parameters.

Among the recruited follicles, selection of normally one dominant follicle takes place and the subordinate follicles undergo atresia [45, 80]. The mechanism leading to this selection is still unknown [45]. Upon the completion of this growth phase, the follicle, now referred to as *Graafian follicle* or preovulatory follicle, is prepared for ovulation [32, 80]. FSH induces LH receptors in the granulosa cells and, consequently, LH as well as FSH promote follicular maturation [45, 80]. The growth as well as the transition to the next stage are LH dependent:

$$\frac{d}{dt}F_g(t) = d_5 \cdot f_2(FSH_{\tau_{FSH,2}}, LH_{\tau_{LH,2}}) \cdot F_t(t) + d_6 \cdot f_1(LH_{\tau_{LH,2}}) \cdot F_g(t) - d_7 \cdot f_1(LH_{\tau_{LH,2}}) \cdot F_g(t), \tag{2.51}$$

where $d_i \in \mathbb{R}_+$, $i = 6, 7$, denote the parameters.

The growth and maturation process is completed and the follicle is ready for ovulation when speaking of the *ovulatory follicle*. LH stimulates this process where the follicle ruptures and releases the ovum. Then, the cells of the ruptured follicle change morphologically, which is called luteinization [80]. The follicle at this stage is referred to as *luteinizing follicle* [80]. The correct term from now on is corpus luteum when speaking of the follicle [45]. LH has no influence on these changes, the corpus luteum is establishing autonomously [45]:

$$\frac{d}{dt}M_o(t) = d_7 \cdot f_1(LH_{\tau_{LH,2}}) \cdot F_g(t) - d_8 \cdot M_o(t) \tag{2.52}$$

$$\frac{d}{dt}M_l(t) = d_8 \cdot M_o(t) - d_9 \cdot M_l(t), \tag{2.53}$$

where $d_i \in \mathbb{R}_+$, $i = 8, 9$, denote the rate constants.

It runs through the stages *early corpus luteum*, *mature corpus luteum*, and *late corpus luteum*. At the beginning of this phase, it is referred to as *early corpus luteum*. In the *mature corpus luteum* as well as in the *late corpus luteum*, LH becomes more and more indispensable in the maintenance of corpus luteum activities [80]. LH promotes the transition from the early to the mature and from the mature to the late corpus luteum

$$\frac{d}{dt}L_e(t) = d_9 \cdot M_l(t) - d_{10} \cdot f_1(LH_{\tau_{LH,2}}) \cdot L_e(t) \tag{2.54}$$

$$\frac{d}{dt}L_m(t) = d_{10} \cdot f_1(LH_{\tau_{LH,2}}) \cdot L_e(t) - d_{11} \cdot f_1(LH_{\tau_{LH,2}}) \cdot L_m(t) \tag{2.55}$$

$$\frac{d}{dt}L_l(t) = d_{11} \cdot f_1(LH_{\tau_{LH,2}}) \cdot L_m(t) - d_{12} \cdot L_l(t). \tag{2.56}$$

where $d_i \in \mathbb{R}_+$, $i = 10, 11, 12$, denote the parameters.

The regression of the corpus luteum ends, unless pregnancy occurs, as an avascular scar, the *corpus albicans* [80]

$$\frac{d}{dt}L_a(t) = d_{12} \cdot L_l(t) - d_{13} \cdot L_a(t), \tag{2.57}$$

where $d_{13} \in \mathbb{R}_+$ denotes the rate constant.

The functions $f_1(\cdot)$ and $f_2(\cdot, \cdot)$ could be defined by

$$f_1(H) := H^\alpha, \quad \alpha \in \mathbb{R}_+$$

and

$$f_2(H_1, H_2) := H_1^{\alpha_1} \cdot H_2^{\alpha_2}, \quad \alpha_1, \alpha_2 \in \mathbb{R}_+.$$

H, H_1, and H_2 stand for the dimensionless FSH or LH concentrations, $\frac{FSH}{FSH_0}$ or $\frac{LH}{LH_0}$, where FSH_0 and LH_0 denote the units of FSH and LH, respectively. This possibility is based on the basic compartment model [37]. It could be assumed that the growth within on stage and the transition from one stage to the next is, if it is dependent on *FSH* or *LH*, proportional to *FSH* or *LH*. With the expansion of the equations by the additional exponents it is aimed at refining the model.

Two essential processes, that have to be distinguished, can be identified: the maturation of the follicles or, understood in a discrete manner, the transition of a follicular stage to the next one, and the growth, the proliferation of cells within one stage. The exact assignment of the influence of FSH and LH on the transition between stages and on the growth at the stages is difficult since the specifications in the literature vary. Simulation of the different possibilities could help to decide which approach is to be chosen. The assumed influence of the gonadotropins at the different stages is shown in Fig. 2.16 schematically. The physiological classification can be used as basis for the determination of the mathematical partitioning. To improve the quality, each stage could be divided into several steps as it was done in the basic compartment model for the luteal phase. These model equations could be written separately for the cases of granulosa and theca cells if desired as proposed in the fourth approach. There are other factors influencing follicular development that have been neglected at this state of modeling since FSH and LH are the main hormones regulating the follicular growth and maturation.

Summarized it can be said: The growth and maturation of the follicles in the ovaries are not modeled via receptor binding but directly. It is assumed that the follicular development divided into nine stages is only influenced by FSH and LH and by their own masses. In the follicular phase (secondary to Graafian follicle), the follicles mature and grow resulting normally in one dominant follicle. During ovulation (ovulatory and luteinizing follicle), the ovum is released and in the luteal phase, the follicle becomes a corpus luteum and finally a corpus albicans. Growth is assumed for the first three phases F_s, F_t, and F_g [66]:

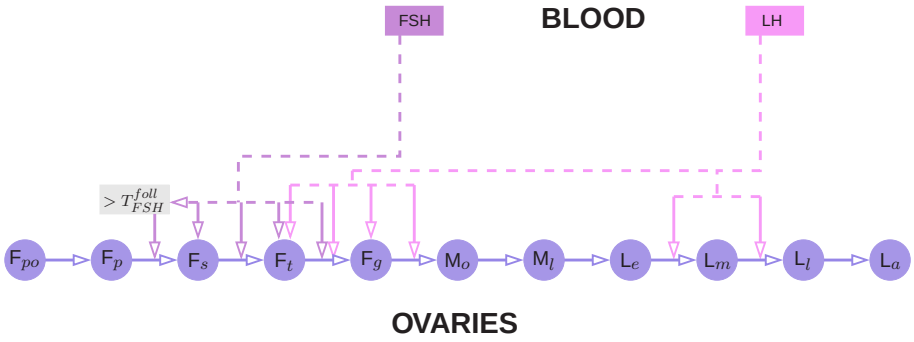

Figure 2.16: Model scheme for the gonadotropin-dependence during the follicular development. The gonadotropins FSH and LH influence the growth and maturation at certain stages, growth stimulation is expressed by an arrow towards the circle, maturation (transition) stimulation by an arrow to the transition arrow. FSH stimulates the transition from F_p to F_s if its concentration is higher than the threshold value T_{FSH}^{foll}. F_{po}: primordial follicle, F_p: primary follicle, F_s: secondary follicle, F_t: tertiary follicle, F_g: Graafian follicle, M_o: ovulatory follicle, M_l: luteinizing follicle, L_e: early corpus luteum, L_m: mature corpus luteum, L_l: late corpus luteum, L_a: corpus albicans.

- Secondary follicle (Eq. 11 in Table 3.6):

$$\frac{d}{dt}F_s(t) = d_1 \cdot h^+\left(FSH_{\tau_{FSH,2}}; T_{FSH}^{foll}, n_{FSH}^{foll}\right) + \left(d_2 \cdot FSH_{\tau_{FSH,2}}^{\alpha_1} - d_3 \cdot FSH_{\tau_{FSH,2}}^{\alpha_2}\right) \cdot F_s(t)$$

- Tertiary follicle (Eq. 12 in Table 3.6):

$$\frac{d}{dt}F_t(t) = d_3 \cdot FSH_{\tau_{FSH,2}}^{\alpha_2} \cdot F_s(t) + \left(d_4 \cdot FSH_{\tau_{FSH,2}}^{\alpha_3} \cdot LH_{\tau_{LH,2}}^{\alpha_4} - d_5 \cdot FSH_{\tau_{FSH,2}}^{\alpha_5} \cdot LH_{\tau_{LH,2}}^{\alpha_6}\right) \cdot F_t(t)$$

- Graafian follicle (Eq. 13 in Table 3.6):

$$\frac{d}{dt}F_g(t) = d_5 \cdot FSH_{\tau_{FSH,2}}^{\alpha_5} \cdot LH_{\tau_{LH,2}}^{\alpha_6} + \left(d_6 \cdot LH_{\tau_{LH,2}}^{\alpha_7} - d_7 \cdot LH_{\tau_{LH,2}}^{\alpha_8}\right) \cdot F_g(t)$$

- Ovulatory and luteinizing follicle (Eqs. 14 and 15 in Table 3.6):

$$\frac{d}{dt}M_o(t) = d_7 \cdot LH_{\tau_{LH,2}}^{\alpha_8} \cdot F_g(t) - d_8 \cdot M_o(t)$$
$$\frac{d}{dt}M_l(t) = d_8 \cdot M_o(t) - d_9 \cdot M_l(t).$$

- Corpus luteum (Eqs. 16 to 18 in Table 3.6):

$$\begin{aligned}\frac{d}{dt}L_e(t) &= d_9 \cdot M_l(t) - d_{10} \cdot LH^{\alpha_9}_{\tau_{LH,2}} \cdot L_e(t)\\ \frac{d}{dt}L_m(t) &= d_{10} \cdot LH^{\alpha_9}_{\tau_{LH,2}} \cdot L_e(t) - d_{11} \cdot LH^{\alpha_{10}}_{\tau_{LH,2}} \cdot L_m(t)\\ \frac{d}{dt}L_l(t) &= d_{11} \cdot LH^{\alpha_{10}}_{\tau_{LH,2}} \cdot L_m(t) - d_{12} \cdot L_l(t)\end{aligned}$$

- Corpus albicans (Eq. 19 in Table 3.6):

$$\frac{d}{dt}L_a(t) = d_{12} \cdot L_l(t) - d_{13} \cdot L_a(t).$$

The parameters α_i, $i = 1, \ldots, 9$, can reduce or increase the influence of the gonadotropins LH and FSH at the different follicular stages.

2.6.2 Receptor binding of LH and FSH

In order to find out more about the effects of the gonadotropins on the events in the ovary, it is necessary to identify the interface between the two compartments pituitary and ovaries. The gonadotropins FSH and LH are released into the blood and reach the ovaries. Stimulation of follicular growth and maturation and, therewith, biosynthesis of the steroids is enhanced mainly by gonadotropin coupling to its receptor which activates a cascade of reactions. FSH and LH bind to their receptors and form a complex. By interacting with the G protein and transforming of GDP to GTP, the enzyme adenylate cyclase (or adenylyl cyclase, AC) gets activated. The activated AC reacts with ATP, forming cAMP. By influence of cAMP, protein kinase A (PKA) gets activated leading to higher enzyme synthesis and therefore to stimulation of the steroidogenesis [80].

In [14], a model for the FSH-induced cAMP production in ovarian follicles is derived. An overview of the reaction scheme is given in Fig. 2.17. FSH binds to its receptor, R_{FSH}, at the constant rate k_+. This results in the formation of an active complex, (FSH-R_{FSH}), that dissociates at the constant rate k_-:

$$\mathrm{FSH} + \mathrm{R}_{FSH} \quad \underset{k_-}{\overset{k_+}{\rightleftharpoons}} \quad (\mathrm{FSH\text{-}R}_{FSH}).$$

The bound receptor is phosphorylated and therefore inactivated which is mediated by cAMP

$$(\mathrm{FSH\text{-}R}_{FSH}) \quad \xrightarrow{\rho} \quad (\mathrm{FSH\text{-}R}_{FSH}\text{-p}),$$

where ρ is defined in form of a Hill function of cAMP

$$\rho(cAMP) = \frac{\alpha \cdot cAMP^{\gamma}}{\delta^{\gamma} + cAMP^{\gamma}},$$

where δ denotes the threshold parameter, γ the Hill coefficient, and $\alpha \in \mathbb{R}_+$ a rate constant. Then the receptor complex is internalized and FSH dissociates

$$(\text{FSH-R}_{FSH}\text{-p}) \quad \stackrel{k_i}{\rightarrow} \quad \text{R}_i + \text{FSH},$$

and, finally, FSH is hydrolyzed and the receptor returns to the cell membrane

$$\text{R}_i \quad \stackrel{k_r}{\rightarrow} \quad \text{R}_{FSH}.$$

The following equations for the receptor recycling are obtained, slightly modified from [14] by including the delay $\tau_{FSH,2}$:

$$\begin{aligned}
\frac{d}{dt}R_{FSH} &= k_- \cdot (FSH\text{-}R_{FSH}) + k_r \cdot R_i && (2.58)\\
&\quad - k_+ \cdot FSH_{\tau_{FSH,2}} \cdot R_{FSH} && (2.59)\\
\frac{d}{dt}(FSH\text{-}R_{FSH}) &= k_+ \cdot FSH_{\tau_{FSH,2}} \cdot R_{FSH} - (\rho + k_-) \cdot (FSH\text{-}R_{FSH}) && (2.60)\\
\frac{d}{dt}(FSH\text{-}R_{FSH}\text{-}p) &= \rho \cdot (FSH\text{-}R_{FSH}) - k_i \cdot (FSH\text{-}R_{FSH}\text{-}p) && (2.61)\\
\frac{d}{dt}R_i &= k_i \cdot (FSH\text{-}R_{FSH}\text{-}p) - k_r \cdot R_i. && (2.62)
\end{aligned}$$

The bound receptors activate the inactive adenylate cyclase, AC_i. The activation depends on the complex concentration that is multiplied by the amplification parameter σ representing the average number of adenylate cyclase activated by one bound receptor. The concentration of the activated adenylate cyclase (AC_a) is FSH-sensitive. If $\sigma \cdot (FSH - R_{FSH}) > AC_a$, the differential equation is increasing, else if $\sigma \cdot (FSH - R_{FSH}) < AC_a$, it is decreasing. A factor $\beta \in \mathbb{R}_+$ acts as time scale parameter. Since this process is autoamplified, the term $\sigma \cdot (FSH - R_{FSH}) - AC_a$ is multiplied with AC_a. This leads to the differential equation

$$\frac{d}{dt}AC_a = \beta \cdot (\sigma \cdot (FSH\text{-}R_{FSH}) - AC_a) \cdot AC_a. \tag{2.63}$$

By reaction of AC_a with ATP, cAMP is synthesized at the rate ω activating the PKA

$$\text{ATP} + \text{AC}_a \quad \stackrel{\omega}{\rightarrow} \quad \text{cAMP}.$$

Finally, cAMP is hydrolyzed at the rate k_{PDE}. This leads to the following equations

$$\begin{aligned}
\frac{d}{dt}AC_a &= \beta \cdot (\sigma \cdot (FSH\text{-}R_{FSH}) - AC_a) \cdot AC_a && (2.64)\\
\frac{d}{dt}cAMP &= \omega \cdot AC_a - k_{PDE} \cdot cAMP. && (2.65)
\end{aligned}$$

In the model presented in [14], the cycle of G protein activation/deactivation is not included. Moreover, it is assumed that the total number of FSH receptors (free, active, phosphorylated, and internalized) remains constant and that the amount of FSH is sufficiently large to be unaffected by binding to receptors.

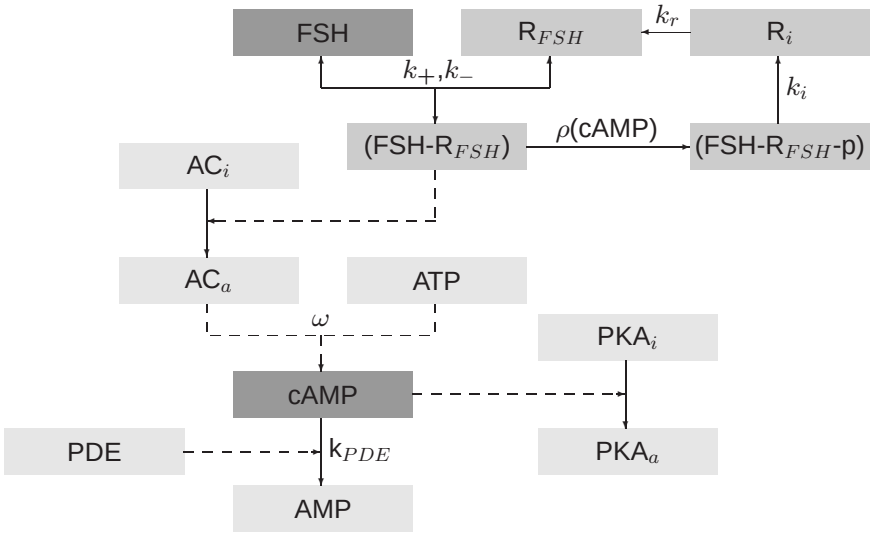

Figure 2.17: Model scheme for the FSH-induced cAMP production ([14]). R_{FSH}: free FSH receptor, (FSH-R_{FSH}): hormone-receptor complex, (FSH-R_{FSH}-p): phosphorylated receptor, R_i: internalized receptor, AC_i: inactive adenylate cyclase, AC_a: active adenylate cyclase, ATP: adenosine triphosphate, cAMP: cyclic adenosine monophosphate, AMP: adenosine monophosphate, PDE: phosphodiesterase, PKA_i: inactive protein kinase A, PKA_a: active protein kinase A.

For simplicity, only the receptor recycling is incorporated into the model and assume that ρ is constant. The receptor binding and recycling is described in Chapter 1. In this case, there are two inactivatable states: phosphorylated denoted by (FSH-R_{FSH}-p) and internalized denoted by R_i [14]. Thus, the receptor recycling for the FSH receptors in the ovaries can be modeled by (Eqs. 20 to 23 in Table 3.6):

$$\frac{d}{dt}R_{FSH} = k_-^{FSH} \cdot (FSH\text{-}R_{FSH}) + k_r^{FSH} \cdot R_i^{FSH} \tag{2.66}$$

$$- k_+^{FSH} \cdot FSH_{\tau_{FSH,2}} \cdot R_{FSH} \tag{2.67}$$

$$\frac{d}{dt}(FSH\text{-}R_{FSH}) = k_+^{FSH} \cdot FSH_{\tau_{FSH,2}} \cdot R_{FSH} - (\rho^{FSH} + k_-^{FSH}) \cdot (FSH\text{-}R_{FSH}) \tag{2.68}$$

$$\frac{d}{dt}(FSH\text{-}R_{FSH}\text{-}p) = \rho^{FSH} \cdot (FSH\text{-}R_{FSH}) - k_i^{FSH} \cdot (FSH\text{-}R_{FSH}\text{-}p) \tag{2.69}$$

$$\frac{d}{dt}R_i^{FSH} = k_i^{FSH} \cdot (FSH\text{-}R_{FSH}\text{-}p) - k_r^{FSH} \cdot R_i^{FSH}, \tag{2.70}$$

where $k_-^{FSH}, k_+^{FSH}, k_r^{FSH}, k_i^{FSH}, \rho^{FSH}, \tau_{FSH,2} \in \mathbb{R}_+$ denote the parameters. It is feasible to model the LH receptor dynamics in a similar manner as in the case of FSH [14] since its primary signaling intermediary is cAMP as well, but other signal transduction pathways are also possible [80]. Analogously for the LH receptors the model equations

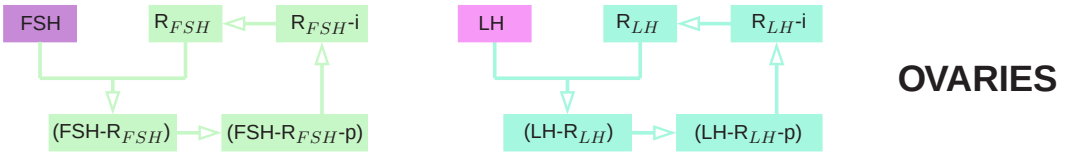

Figure 2.18: Model scheme for the dynamics of the LH and FSH receptors in the ovaries including receptor recycling.

are given by, Eqs. 24 to 27 in Table 3.6, [66]:

$$\frac{d}{dt}R_{LH} = k_-^{LH} \cdot (LH\text{-}R_{LH}) + k_r^{LH} \cdot R_i^{LH} - k_+^{LH} \cdot LH_{\tau_{LH,2}} \cdot R_{LH} \tag{2.71}$$

$$\frac{d}{dt}(LH\text{-}R_{LH}) = k_+^{LH} \cdot LH_{\tau_{LH,2}} \cdot R_{LH} - (\rho^{LH} + k_-^{LH}) \cdot (LH\text{-}R_{LH}) \tag{2.72}$$

$$\frac{d}{dt}(LH\text{-}R_{LH}\text{-}p) = \rho^{LH} \cdot (LH\text{-}R_{LH}) - k_i^{LH} \cdot (LH\text{-}R_{LH}\text{-}p) \tag{2.73}$$

$$\frac{d}{dt}R_i^{LH} = k_i^{LH} \cdot (LH\text{-}R_{LH}\text{-}p) - k_r^{LH} \cdot R_i^{LH}, \tag{2.74}$$

where $k_-^{LH}, k_+^{LH}, k_r^{LH}, k_i^{LH}, \rho^{LH}, \tau_{LH,2} \in \mathbb{R}_+$ denote the parameters. In both cases, simple reaction kinetics is used as presented in Chapter 1 where the reaction from the activatable receptor to the activated receptor (complex) is assumed to be reversible as opposed to the remaining reactions that are assumed to be irreversible [14]. The model scheme for the receptor binding of LH and FSH including receptor recycling are shown in Fig. 2.18.

The total receptor concentration in the case of FSH is given by

$$R_{FSH,total} = R_{FSH} + (FSH\text{-}R_{FSH}) + (FSH\text{-}R_{FSH}\text{-}p) + R_i. \tag{2.75}$$

FSH receptors are only expressed in the granulosa cells [16] while LH receptors are expressed in the theca cells and, at a later stage, in the granulosa cells as well [9, 32]. There is evidence that the total concentration for both, FSH and LH receptors, depend on the follicular stage [16] and in the granulosa cells on FSH and estradiol concentrations. Coarsely, the dynamics can be described by:

$$\frac{d}{dt}R_{LH,total} = f(F_t^{theca}, \dots, L_a^{theca}) + f(F_g^{gran}, \dots, L_a^{gran}; FSH, E_2) \tag{2.76}$$

$$\frac{d}{dt}R_{FSH,total} = f(F_s^{gran}, \dots, L_a^{gran}; FSH, E_2), \tag{2.77}$$

where f is not further specified. $F_{po}^{gran}, \dots, L_a^{gran}$ denote the granulosa cell masses, $F_{po}^{theca}, \dots, L_a^{theca}$ the theca cell masses at the different follicular stages. For simplicity, it can be assumed that the total receptor concentration is constant during the cycle as it is done in [14].

2.6.3 Total enzyme concentrations and enzyme activation

The enzymes P450scc, $P450_{17\text{-}OH}$, P450arom, 3β-HSD, and 17β-HSD are important catalyzers in the steroidogenesis. Their concentrations depend on the follicular stage [9, 79]. Moreover, the production of the steroids is controlled by LH and FSH and by LH and FSH receptors. The LH and the FSH molecules bind to their respective receptor and activate a cascade of reactions. This results in the synthesis of cAMP and thus in an enhanced mRNA concentration activating the enzyme synthesis [16, 80].

Primary follicles consist mainly of granulosa cells exhibiting FSH receptors. The follicular mass is still small, that is why no detectable enzyme amount is produced. The enzymes P450arom and 17β-HSD are produced in the granulosa cells [9, 80] via the FSH receptor binding from the secondary follicle. In the tertiary follicle, there are also theca cells expressing LH receptors. Thus, the enzymes P450scc, $P450_{17\text{-}OH}$, and 3β-HSD are produced [9] via the LH receptor binding [80]. In the Graafian follicle, the granulosa cells exhibit also LH receptors leading to the expression of P450scc and 3β-HSD via the LH receptor binding. In the corpus luteum, the processes are similar to the ones in the Graafian follicle. The cells, then, are called luteinized theca and luteinized granulosa cells, respectively [80].

As first modeling approach, it is assumed that the total enzyme concentrations are proportional to the follicular masses from the secondary or tertiary follicular stage to the late luteal stage [66]. For this reason, the total concentrations are written as a linear combination of the respective follicular masses:

$$
\begin{aligned}
3\beta\text{-}HSD_{total} &= f_{lincom}(F_t, \ldots, L_l; e_1) && (2.78)\\
17\beta\text{-}HSD_{total} &= f_{lincom}(F_s, \ldots, L_l; e_2) && (2.79)\\
P450scc_{total} &= f_{lincom}(F_t, \ldots, L_l; e_3) && (2.80)\\
P450_{17\text{-}OH,total} &= f_{lincom}(F_t, \ldots, L_l; e_4) && (2.81)\\
P450arom_{total} &= f_{lincom}(F_s, \ldots, L_l; e_5), && (2.82)
\end{aligned}
$$

where $3\beta\text{-}HSD_{total}, 17\beta\text{-}HSD_{total}, P450scc_{total}, P450_{17\text{-}OH,total}, P450arom_{total}$ denote the total enzyme concentrations, $e_1 =: (e_{11}, \ldots, e_{17})^T, e_3 =: (e_{31}, \ldots, e_{37})^T, e_4 =: (e_{41}, \ldots, e_{47})^T \in \mathbb{R}_+^7$, $e_2 =: (e_{21}, \ldots, e_{28})^T, e_5 =: (e_{51}, \ldots, e_{58})^T \in \mathbb{R}_+^8$ the parameters and the function $f_{lincom}(\cdot;\cdot)$ defines the linear combination of follicular masses:

$$
f_{lincom}(A; p) := \sum_{i=1}^{n} p_i \cdot A_i, \quad p \in \mathbb{R}_+^n, \quad A \in \mathbb{R}_+^n, \quad n \in \mathbb{N}.
$$

The total enzyme concentrations depend on F_s only if they are expressed in the granulosa cells. The model scheme for the enzymes is shown in Fig. 2.19.

The enzymes are activated by the receptor binding. Once they have accomplished their objective, that is the activation of the steroid synthesis, they will be inactivated. If it is assumed here that the enzymes are activated proportionally to the receptor complex concentration as well as to the total enzyme concentration and are deactivated proportionally to its concentration, the following system of differential equations for

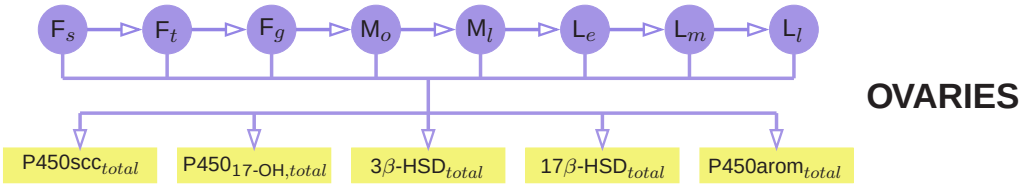

Figure 2.19: Model scheme for the total enzyme concentrations (general dependency on the follicular masses is shown).

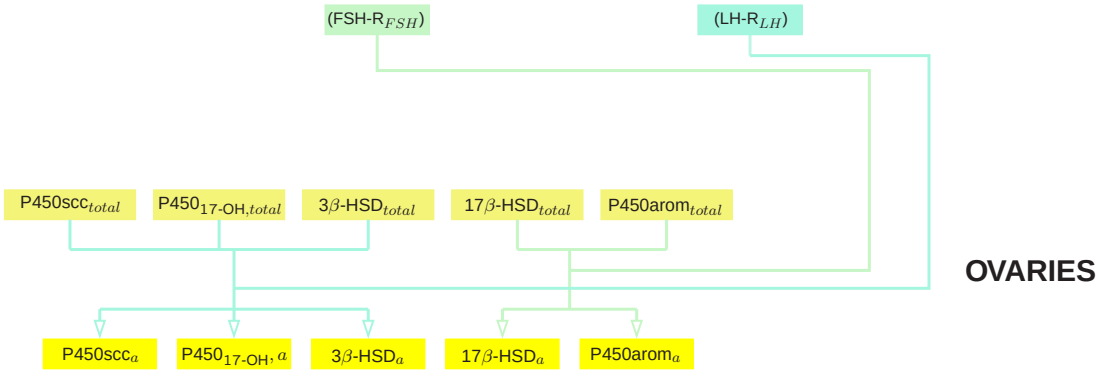

Figure 2.20: Model scheme for the activation of the enzymes.

the activated enzyme concentrations is obtained (Eqs. 28 to 32 in Table 3.6):

$$\frac{d}{dt}3\beta\text{-}HSD_a = a_1 \cdot 3\beta\text{-}HSD_{total} \cdot (LH\text{-}R_{LH}) - a_2 \cdot 3\beta\text{-}HSD_a \tag{2.83}$$

$$\frac{d}{dt}17\beta\text{-}HSD_a = a_3 \cdot 17\beta\text{-}HSD_{total} \cdot (FSH\text{-}R_{FSH}) - a_4 \cdot 17\beta\text{-}HSD_a \tag{2.84}$$

$$\frac{d}{dt}P450scc_a = a_5 \cdot P450scc_{total} \cdot (LH\text{-}R_{LH}) - a_6 \cdot P450scc_a \tag{2.85}$$

$$\frac{d}{dt}P450_{17\text{-}OH,a} = a_7 \cdot P450_{17\text{-}OH,total} \cdot (LH\text{-}R_{LH}) - a_8 \cdot P450_{17\text{-}OH,a} \tag{2.86}$$

$$\frac{d}{dt}P450arom_a = a_9 \cdot P450arom_{total} \cdot (FSH\text{-}R_{FSH}) - a_{10} \cdot P450arom_a, \tag{2.87}$$

where $3\beta\text{-}HSD_a, 17\beta\text{-}HSD_a, P450scc_a, P450_{17\text{-}OH,a}, P450arom_a$ denote the concentrations of the active enzymes and a_i, $i = 1, \ldots, 10$, the rate constants. The model scheme for the activation of the enzymes is shown in Fig. 2.20.

2.6.4 Biosynthesis of the steroids

The steroids are produced in the follicular and luteal cells, whereupon they, to a certain extent, are released into the blood circulation. Since the steroids bind to plasma proteins, transport effects must be considered.

Cholesterol reacts to pregnenolone via the enzyme P450scc, pregnenolone to progesterone via 3β-HSD, and progesterone to 17α-hydroxyprogesterone via $P450_{17\text{-OH}}$ [32]. Whereas this metabolic route is referred to as $\Delta 4$ pathway, there is an alternative route, the $\Delta 5$ pathway, including the reactions of pregnenolone to 17α-hydroxypregnenolone via $P450_{17\text{-OH}}$, 17α-hydroxypregnenolone to DHEA via $P450_{17\text{-OH}}$, and DHEA to androstenedione via 3β-HSD which is preferred in humans [15]. The reaction of androstenedione to testosterone is catalyzed by the enzyme 17β-HSD from the secondary stage and testosterone to estradiol via P450arom in mature follicles [9]. A good source for the steroidogenesis (biosynthesis of the steroids) is the KEGG PATHWAY Database [17]. The reactions and their catalyzing factors are available in more detail.

It is assumed that the cholesterol concentration is constant. For the enzyme catalyzed reactions, the simple Michaelis-Menten mechanism (irreversible and reversible) presented in the Chapter 1 is applied. Moreover, it is assumed that one molecule substrate reacts to one molecule product. The fact that an enzyme can catalyze several reactions is ignored. The steroids are released proportionally to their concentration.

The following equations describe an extract of the steroidogenesis, found in the KEGG PATHWAY Database [17], that is shown in the Figs. 2.21 and 2.22. Even if the reactions often involve other substrates as well, it is justifiable to simplify the mechanism: since it is not enough known about the dynamics of the other substrates, here it is started with assuming that their concentrations are constant. Moreover, if the reaction mechanism is considered in more detail, the model is getting cumbersome.

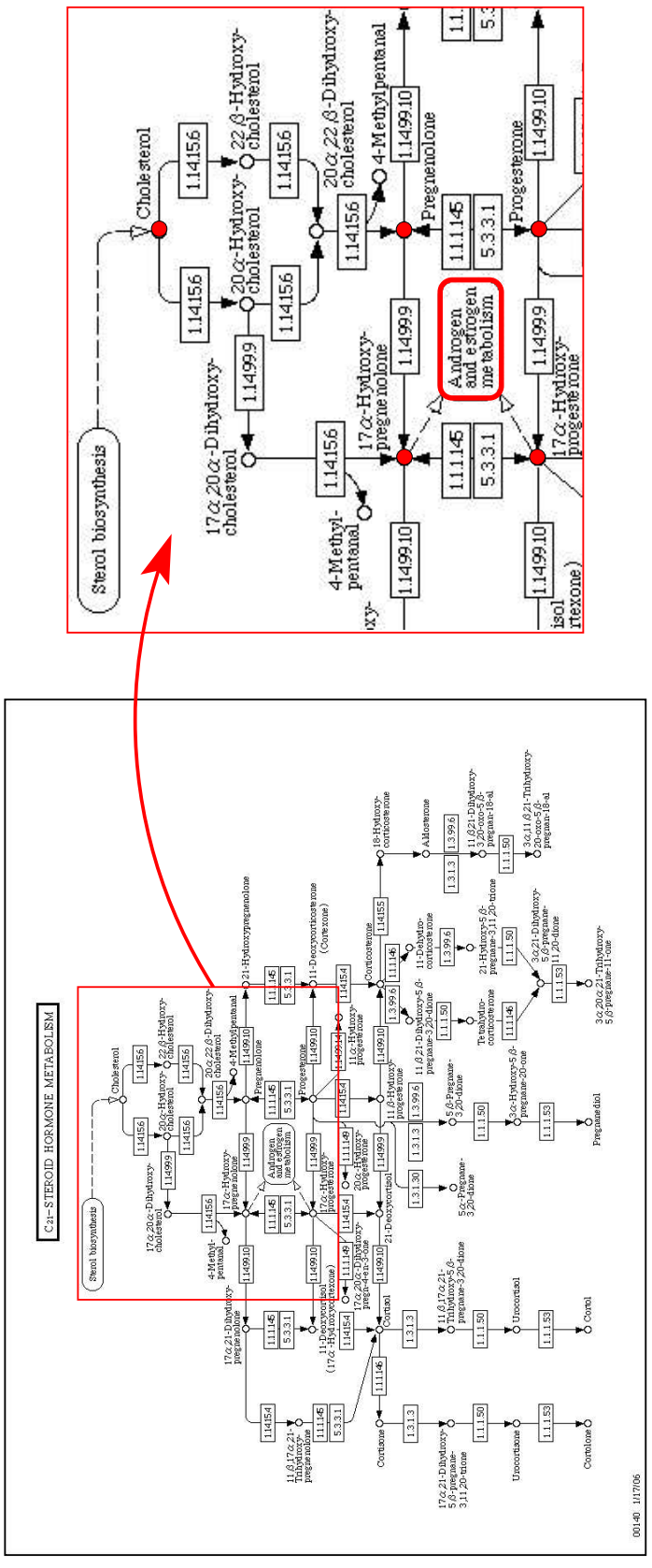

Figure 2.21: C_{21}-steroid hormone metabolism (modified from [17]).

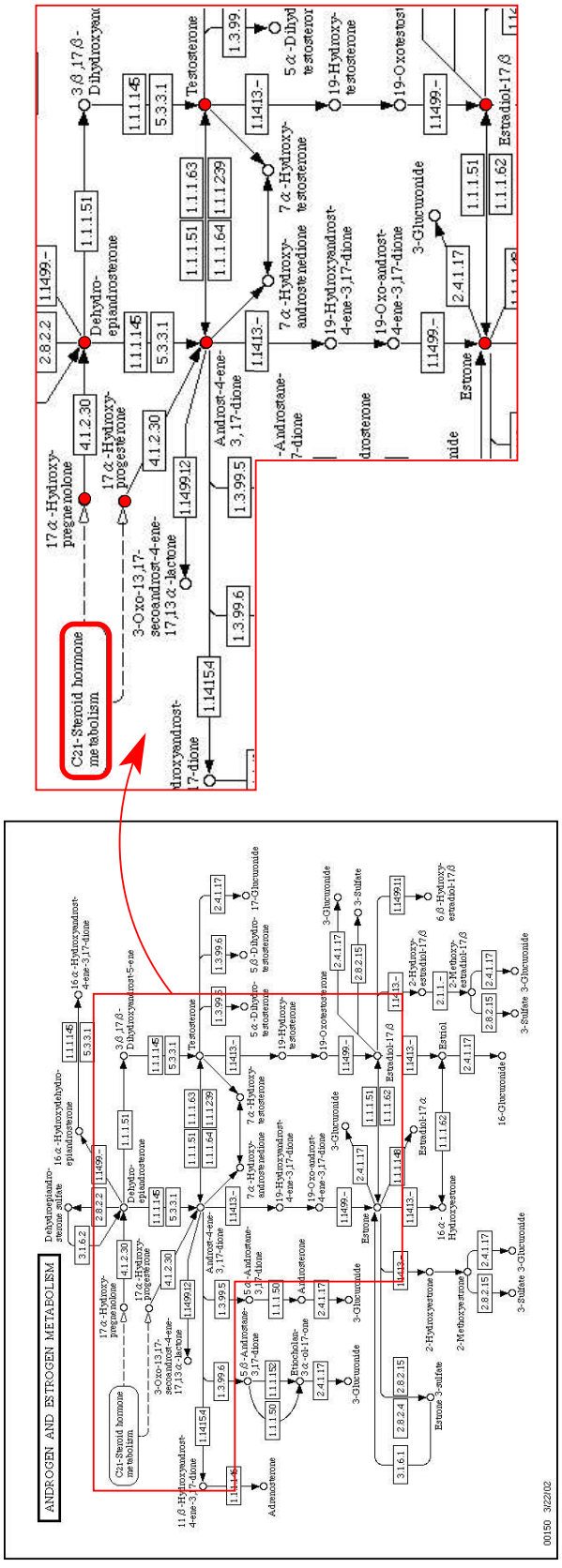

Figure 2.22: Androgen and estrogen metabolism (modified from [17]).

The dynamics of the gestagens pregnenolone and progesterone occurring in the theca and granulosa cells according to the model scheme presented in Fig. 2.23 are modeled by (Eqs. 33 and 34 in Table 3.6):

$$\begin{aligned}\frac{d}{dt}preg_O &= c_1 \cdot P450scc_a \cdot chol_O - f^{rev}(prog_O, preg_O, 3\beta\text{-}HSD_a; p_1) \\ &\quad - f^{irrev}(preg_O, P450_{17\text{-}OH,a}; k_1) - c_2 \cdot preg_O \qquad (2.88)\\ \frac{d}{dt}prog_O &= f^{rev}(prog_O, preg_O, 3\beta\text{-}HSD_a; p_1) \\ &\quad - f^{irrev}(prog_O, P450_{17\text{-}OH,a}; k_2) - c_3 \cdot prog_O, \qquad (2.89)\end{aligned}$$

where $chol_O$ denotes the cholesterol concentration that is assumed to be constant, $preg_O$ the pregnenolone concentration, and $prog_O$ the progesterone concentration. In the theca cells, the steroids that are without exception produced in the theca cells, the dynamics of the gestagens 17α-hydroxypregnenolone and 17α-hydroxyprogesterone and of the androgens DHEA, androstenedione, and testosterone, are given by (Eqs. 35 to 39 in Table 3.6):

$$\begin{aligned}\frac{d}{dt}17\text{-}preg_O &= f^{irrev}(preg_O, P450_{17\text{-}OH,a}; k_1) \\ &\quad - f^{rev}(17\text{-}prog_O, 17\text{-}preg_O, 3\beta\text{-}HSD_a; p_2) \\ &\quad - f^{irrev}(17\text{-}preg_O, P450_{17\text{-}OH,a}; k_3) - c_4 \cdot 17\text{-}preg_O \qquad (2.90)\\ \frac{d}{dt}17\text{-}prog_O &= f^{irrev}(prog_O, P450_{17\text{-}OH,a}; k_2) \\ &\quad + f^{rev}(17\text{-}prog_O, 17\text{-}preg_O, 3\beta\text{-}HSD_a; p_2) \\ &\quad - f^{irrev}(17\text{-}prog_O, P450_{17\text{-}OH,a}; k_4) - c_5 \cdot 17\text{-}prog_O \qquad (2.91)\\ \frac{d}{dt}DHEA_O &= f^{irrev}(17\text{-}preg_O, P450_{17\text{-}OH,a}; k_3) \\ &\quad - f^{irrev}(DHEA_O, 3\beta\text{-}HSD_a; k_5) - c_6 \cdot DHEA_O \qquad (2.92)\\ \frac{d}{dt}andro_O &= f^{irrev}(17\text{-}prog_O, P450_{17\text{-}OH,a}; k_4) + f^{irrev}(DHEA_O, 3\beta\text{-}HSD_a; k_5) \\ &\quad - f^{rev}(test_O, andro_O, 17\beta\text{-}HSD_a; p_3) \\ &\quad - f^{irrev}(andro_O, P450arom_a; k_6) - c_7 \cdot andro_O \qquad (2.93)\\ \frac{d}{dt}test_O &= f^{rev}(test_O, andro_O, 17\beta\text{-}HSD_a; p_3) \\ &\quad - f^{irrev}(test_O, P450arom_a; k_7) - c_8 \cdot test_O, \qquad (2.94)\end{aligned}$$

where 17-$preg_O$ denotes the 17α-hydroxypregnenolone concentration, 17-$prog_O$ the 17α-hydroxyprogesterone concentration, $DHEA_O$ the dehydroepiandrosterone concentration, $andro_O$ the androstenedione concentration, and $test_O$ the testosterone concentration. Finally, the dynamics of the estrogens estrone and estradiol occurring only in

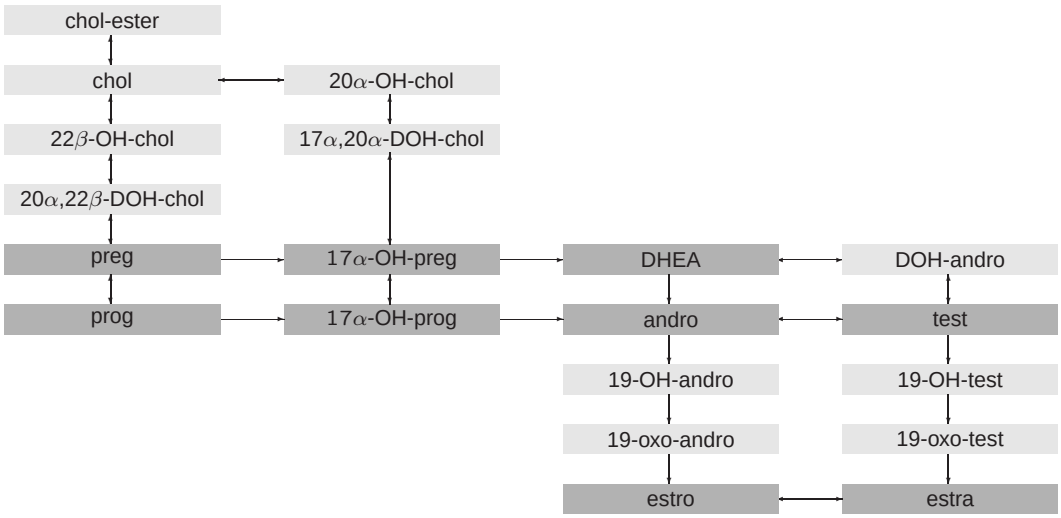

Figure 2.23: Model scheme for the steroidogenesis (summary of the Figs. 2.21 and 2.22). The steroids that are colored dark grey are incorporated into the model since being the most important ones. chol-ester: Cholesterol ester, chol: Cholesterol, 20α-OH-chol: 20α-Hydroxycholesterol, 22β-OH-chol: 22β-Hydroxycholesterol, 17α,20α-DOH-chol: 17α,20α-Dihydroxycholesterol, 20α,22β-DOH-chol: 20α,22β-Dihydroxycholesterol, preg: Pregnenolone, 17α-OH-preg: 17α-Hydroxypregnenolone, prog: Progesterone, 17α-OH-prog: 17α-Hydroxyprogesterone, DHEA: Dehydroepiandrosterone, DOH-andro: 3β,17β-Dihydroxyandrost-5-ene, andro: Androstenedione (Androst-4-ene-3,17-dione), test: Testosterone, 19-OH-andro: 19-Hydroxyandrostenedione (19-Hydroxyandrost-4-ene-3,17-dione), 19-OH-test: 19-Hydroxytestosterone, 19-oxo-andro: 19-Oxo-androstenedione (19-Oxo-androst-4-ene-3,17-dione), 19-oxo-test: 19-Oxotestosterone, estro: Estrone, estra: Estradiol (Estradiol-17β).

the granulosa cells are described by (Eqs. 40 and 41 in Table 3.6):

$$\begin{aligned}\frac{d}{dt}estro_O &= f^{irrev}(andro_O, P450arom_a; k_6)\\ &\quad - f^{rev}(estra_O, estro_O, 17\beta\text{-}HSD_a; p_4) - c_9 \cdot estro_O \qquad (2.95)\\ \frac{d}{dt}estra_O &= f^{irrev}(test_O, P450arom_a; k_7)\\ &\quad + f^{rev}(estra_O, estro_O, 17\beta\text{-}HSD_a; p_4) - c_{10} \cdot estra_O, \qquad (2.96)\end{aligned}$$

where $estro_O$ denotes the estrone concentration and $estra_O$ the estradiol concentration. The parameters are given by $c_i \in \mathbb{R}_+$, $i = 1, \ldots, 10$, $k_i \in \mathbb{R}_+^2$, $i = 1, \ldots, 7$, and $p_i \in \mathbb{R}_+^4$, $i = 1, \ldots, 4$.

2.7 Steroid and inhibin concentrations in the blood

The steroids are synthesized in the cells of the follicles, the theca and granulosa cells. At first, they enter the follicular fluid in the ovary. A part of this steroid mass reaches the blood system, where it is distributed in the blood volume V_B. Taking into account that changes in the steroid mass affect the steroid concentration in the blood after a certain time, delay terms $\tau_{prog}, \tau_{estra}$ for progesterone and estradiol, respectively, are included. The steroids are cleared proportionally to its concentration in the blood (Eqs. 42 to 49 in Table 3.6):

$$\frac{d}{dt} steroid_B(t) = \frac{s_{steroid}}{V_B} \cdot steroid_O(t - \tau_{steroid}) - \alpha_{steroid} \cdot steroid_B(t),$$

where $s_{steroid}, \alpha_{steroid} \in \mathbb{R}_+$ denote the rate constants, $steroid_O$ the steroid concentration in the ovaries, $steroid_B$ the steroid concentration in the blood, and $\tau_{steroid}$ the delay where *steroid* stands for concentrations of progesterone, 17α-hydroxypregnenolone, 17α-hydroxyprogesterone, DHEA, androstenedione, testosterone, estrone, and estradiol. In particular, the following equations for the two most important steroids are obtained:

$$\frac{d}{dt} P_4(t) = \frac{s_{P_4}}{V_B} \cdot prog_O(t - \tau_{prog}) - \alpha_{P_4} \cdot P_4(t) \tag{2.97}$$

$$\frac{d}{dt} E_2(t) = \frac{s_{E_2}}{V_B} \cdot estra_O(t - \tau_{estra}) - \alpha_{E_2} \cdot E_2(t), \tag{2.98}$$

where P_4 denotes the serum progesterone concentration, E_2 the serum estradiol concentration, and $s_{P_4}, s_{E_2}, \alpha_{P_4}, \alpha_{E_2} \in \mathbb{R}_+$ the rate constants. The biosynthesis together with the two-cell-theory is visualized in Fig. 2.24.

The effective steroid concentrations in the blood is diminished by binding to certain plasma proteins. Estradiol and testosterone bind preferably to sex hormone-binding globulin (SHBG) and to albumin [79], progesterone to cortico-steroid-binding globulin (CBG) and also to albumin [32]. The concentration of these proteins is increased by estrogens and decreased by androgens and progestins [32, 79]. However, the proportions of free and bound estradiol, for example, do not vary significantly during the menstrual cycle [32]. Therefore, it is assumed for simplicity that the binding protein concentrations are constant. In order to model transport effects in a decent manner, s_{P_4} and s_{E_2} are no longer constants, but depend on estrogens, androgens, and progestins.

There are other factors originating from the ovaries that are important for the regulation of the control system as, for example, inhibin, activin, and follistatin. There are two forms of inhibin composed of a α-subunit coupled with one of two β-subunits: inhibin A ($\alpha\beta_A$) and inhibin B ($\alpha\beta_B$) [55]. Activins consist of two β-subunits and can be found in three forms: activin A ($\beta_A\beta_A$), activin B ($\beta_B\beta_B$), and activin AB ($\beta_A\beta_B$). Both inhibins and activins modulate the FSH secretion in the pituitary. Moreover, they play a role in the follicular differentiation and steroidogenesis [55]. They are produced in the follicles where they are regulated by FSH, LH, androgens, and by local factors [9, 32, 55]. Follistatin is an activin binding protein that can reverse the activities of activin. It is part of the complete inhibin, activin, and follistatin regulatory system

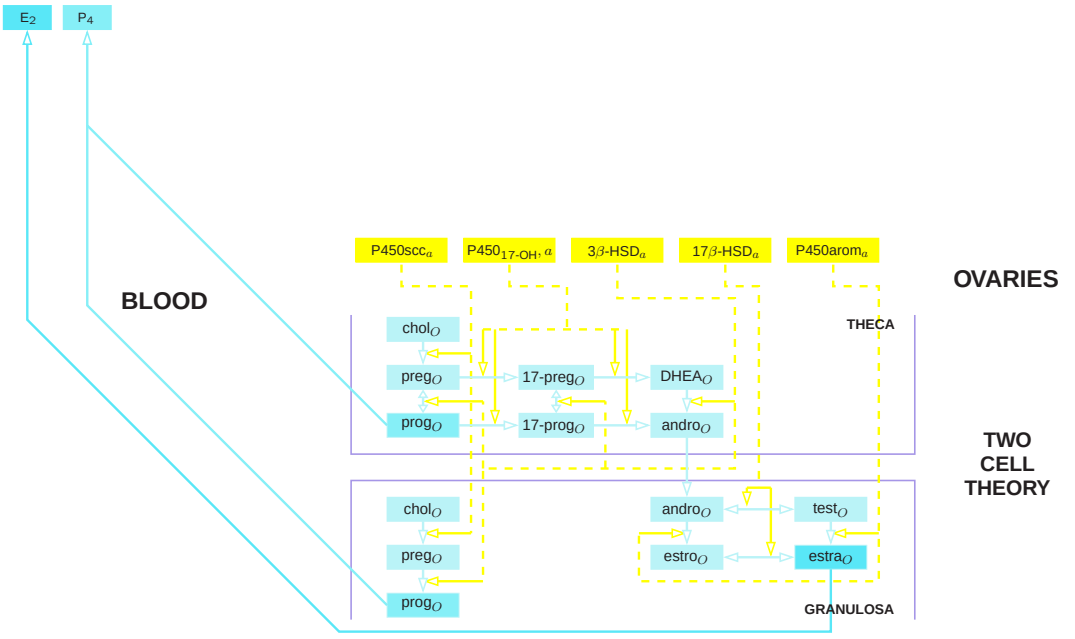

Figure 2.24: Model scheme for the biosynthesis of the steroids including the two-cell-theory.

[9]. But as a first approach, the inhibin concentration is modeled similarly to the basic compartment model, as linear combination of follicular masses analogously to [37] (Eq. 50 in Table 3.6):

$$Ih(t) = ih_1 + ih_2 \cdot F_t(t) + ih_3 \cdot L_m(t) + ih_4 \cdot L_l(t), \tag{2.99}$$

where Ih denotes the serum inhibin concentration and $ih_i \in \mathbb{R}_+$, $i = 1, \ldots, 4$, the parameters. This is visualized in Fig. 2.25. For simplicity, the regulation and the effects of activin and follistatin are not incorporated into the model at this stage.

2.8 Summary

Although being of great interest for half of the population, the menstrual cycle has received relatively little attention in the field of mathematical modeling in the past. Up to now, there are some models that, coarsely summarized, either are able to describe the dynamics of some of the most important hormones and the follicular development or deal with the biochemical background of receptor binding as part of the control system. One of these models for the entire cycle presented in [37] is used as starting point for the further modeling. Since here the intention is not to simply match data but to study mechanisms, it is not aimed at developing a model that is as simple as possible. Instead, it is the purpose here to incorporate as many processes as possible, within reasonable limits.

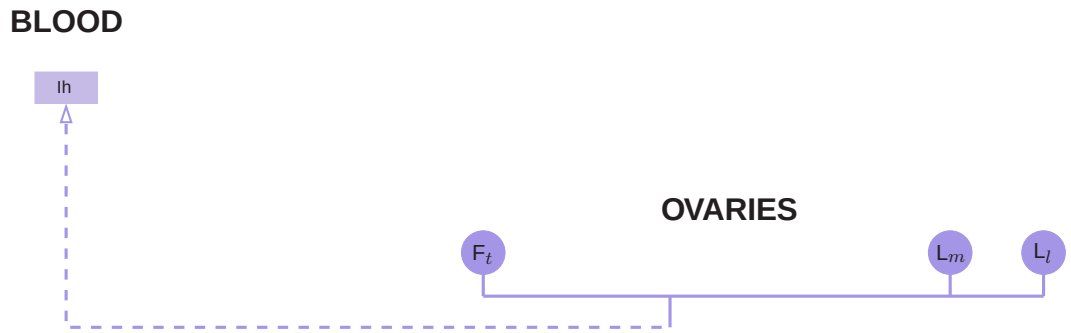

Figure 2.25: Model scheme for inhibin.

The hope is that the resulting complex model offers an expanded field of applications in comparison with smaller models. Below, the different components of the model and some of their possible applications are presented showing why this high level of complexity in the model could be useful:

- *GnRH pulse generator.* The modeling of the GnRH pulse generator is necessary to simulate the dysfunction of the GnRH pulse generator. If the hypothalamus fails, the amount of GnRH secretion is insufficient, whereupon the pituitary releases too little FSH and LH.

- *Pituitary dynamics.* In case of pituitary failure (hypopituitarism), the FSH and LH concentrations in the blood are low which is why the ovaries produce too little hormone. In contrast, GnRH is released in higher amounts.

- *Enzymes in the ovaries.* With this level of complexity, simulating enzyme deficiency is possible. For example, in patients with $P450_{17\text{-}OH}$ deficiency, elevated levels of gonadotropin can be found. This results in an impaired conversion of pregnenolone and progesterone to androgens and, finally, to estrogens [32].

- *Steroidogenesis in the ovaries and steroid concentrations in the blood.* One example is ovarian failure. Since there is little hormonal output from the ovaries in this case, GnRH, FSH, and LH are increasingly released from the hypothalamus and the pituitary because of the feedback regulation. Moreover, if there is interest in serum steroid concentrations other than progesterone and estradiol, the quite elaborate modeling of the steroidogenesis in the follicles is necessary.

- *Follicular development.* The modeling of the follicular development is helpful if one aims at simulating the action of contraceptives. Then, it should be possible to see that the follicular masses of the phases F_g and M_o are approximately zero or at least not sufficient to lead to ovulation. In this way, possible drugs could be tested helping to design suitable treatments. Another possible application is PCOS, where a complex of varying symptoms is meant. One definition is that the ovaries are continuously stimulated by high levels of LH which leads to increased ovarian androgen secretion and commonly enlarged follicles [32].

Hence, it can be seen that the present, rather complex model offers numerous possibilities to simulate disorders and therapies. In order to cover various application fields, the model must comprise the essential components and interrelations of the regulatory system. Simulations of this model could help to predict the activity and regulation of components that cannot be measured in the human as, for example, the GnRH concentration in the pituitary portal system. Moreover, simulations could help deciding which experiments could be done next in order to clarify mechanisms in the control system. Above all, if a detailed model is available, there are more possibilities to treat individual cases, or at least to simulate groups of patients.

The first step in this model development was the determination of the essential processes and interactions belonging to the hormonal regulation of the follicular development. Basically, the three compartments hypothalamus, pituitary, and ovaries connected through the blood circulation are involved. In this control system, the GnRH pulse generator plays an important role. The frequency and the amplitude of the GnRH pulses are regulated mainly by the ovarian hormones progesterone and estradiol. The released GnRH reaches from the pituitary portal system into the pituitary where it binds to its receptor. By this activation of the receptor, the secretion of the gonadotropins LH and FSH is stimulated. Both the synthesis and the release are regulated primarily by progesterone, estradiol, and inhibin via feedback mechanisms. The gonadotropins are released into the blood circulation and transported to the ovaries. They bind to their receptors and initiate signal transduction leading to the synthesis of enzymes that are necessary for the steroidogenesis. In addition, LH and FSH are essential components in the regulation of follicular growth and maturation. Enzyme concentrations and, thus, steroidogenesis depend on the follicle's stage.

Existing and new modeling approaches are presented and discussed. The dynamics are modeled deterministically by use of delay differential equations in order to consider the fact that the processes do not take place in one single compartment and that the effect of one compartment's hormone on another compartment's hormone is retarded due to the spatial separation and other effects. The GnRH pulse generator has a special position in this system. For the pulse time points and the associated release of the stored GnRH pulse mass, a stochastic approach was chosen. Enzyme catalyzed reactions are modeled by assuming Michaelis-Menten kinetics. If the biochemical actions are not known in detail, but feedback mechanisms among hormones can be assumed, the Hill functions are applied.

The model development resulting in a complex model for the control system of the human menstrual cycle is presented here. The following features were added to the basic compartment model:

- the GnRH pulse generator
- the receptor binding in the pituitary and in the ovaries being regarded as interface between the compartments
- the steroidogenesis including enzymes dynamics was treated in more detail than hitherto by applying the two cell theory

The model scheme for this complex model, including all components that have been discussed in Chapter 2, is shown in Fig. 2.26 [66].

A large number of model equations and parameters arise in this model. To give an overview, the equations are listed in Table 2.1 and the parameters in Table 2.2.

The final model consists of 49 delay differential equations describing the dynamics of the GnRH pulse generator, hormones, receptors, active enzymes, and follicular masses. Additionally, 6 auxiliary equations model the total enzymes and inhibin concentrations. In the following this model is called GynCycle.

Table 2.1: Model equations. The 49 delay differential equations, the 6 functions for the total enzyme concentrations in the ovaries, the inhibin concentration in the blood, and the auxiliary functions are listed. In the first column, the delay differential equations are consecutively numbered. All components and their corresponding equation are given in the second and third column.

no	component	equation
1	GnRH pulse frequency	$\frac{d}{dt}\Lambda(t) = h^-\left(P_4(t-\tau_{P_4}); T_{P_4}^{freq}, n_{P_4}^{freq}\right)$ $\cdot \left(1 + h^+\left(E_2(t-\tau_{E_2}); T_{E_2}^{freq}, n_{E_2}^{freq}\right)\right) \cdot \lambda_{max}$
		$\Lambda(t) = \int_0^t \lambda(r)\, dr$
2	GnRH pulse mass	$\frac{d}{dt}M_{GnRH}(t) = \left(h^-(E_2(t-\tau_{E_2}); T_{E_2,1}, n_{E_2,1})\right.$ $\left. + h^+(E_2(t-\tau_{E_2}); T_{E_2,2}, n_{E_2,2})\right) \cdot M_{max}$
		$M_{GnRH,j} = M_{GnRH}(T_j) - M_{GnRH}(T_{j-1})$
3	GnRH	$\frac{d}{dt}GnRH(t) = \frac{b_{GnRH}}{V_{PPS}} + \frac{M_{GnRH,j}}{V_{PPS}} \cdot \psi(t-T_j) - \beta_{GnRH} \cdot GnRH(t) \cdot R_{GnRH}(t)$
	(pituitary portal system)	$- \alpha_{GnRH} \cdot GnRH(t), \quad t \in [T_j, T_{j+1}), \quad \forall j \in \mathbb{N}$
	ψ	$\psi(t) = \frac{a^m}{\Gamma(m)} \cdot t^{m-1} \cdot \exp(-a \cdot t), \quad t \geq 0, \quad \psi(t) = 0, \quad t < 0$
4	free GnRH receptor	$\frac{d}{dt}R_{GnRH} = r_4 \cdot f_{GnRH}(GnRH; T_{GnRH}) + r_3 \cdot R_{GnRH}\text{-}d - r_1 \cdot GnRH \cdot R_{GnRH}$
	$f_{GnRH}(GnRH; T_{GnRH})$	$f_{GnRH}(GnRH; T_{GnRH}) = \frac{1-\frac{GnRH}{T_{GnRH}}}{1+\frac{GnRH}{T_{GnRH}}}$
5	bound GnRH receptor	$\frac{d}{dt}(GnRH\text{-}R_{GnRH}) = r_1 \cdot GnRH \cdot R_{GnRH} - r_2 \cdot (GnRH\text{-}R_{GnRH})$
6	desens. GnRH receptor	$\frac{d}{dt}R_{GnRH}\text{-}d = r_2 \cdot (GnRH\text{-}R_{GnRH}) - r_3 \cdot R_{GnRH}\text{-}d$
7	LH (pituitary)	$\frac{d}{dt}P_{LH} = syn_{LH}(E_{2,\tau_{E_2}}, P_{4,\tau_{P_4}})$ $- rel_{LH}(E_{2,\tau_{E_2}}, P_{4,\tau_{P_4}}, (GnRH\text{-}R_{GnRH}), P_{LH})$
8	LH (blood)	$\frac{d}{dt}LH = \frac{1}{V_B} \cdot rel_{LH}(E_{2,\tau_{E_2}+\tau_{LH,1}}, P_{4,\tau_{P_4}+\tau_{LH,1}},$ $(GnRH\text{-}R_{GnRH})_{\tau_{LH,1}}, P_{LH,\tau_{LH,1}}) - clear_{LH}(LH)$
	syn(LH)	$syn_{LH} = b_{LH} + h_1^-(P_4) \cdot h_1^+(E_2) \cdot syn_{LH,max}$
	rel(LH)	$rel_{LH} = \left(h_2^-(E_2) + h_2^+(E_2)\right) \cdot h_3^+(P_4) \cdot rel_{LH,max} \cdot (GnRH\text{-}R_{GnRH}) \cdot P_{LH}$
	clear(LH)	$clear_{LH} = \alpha_{LH} \cdot LH$
9	FSH (pituitary)	$\frac{d}{dt}P_{FSH} = syn_{FSH}(Ih_{\tau_{Ih}})$ $- rel_{FSH}(E_{2,\tau_{E_2}}, P_{4,\tau_{P_4}}, Ih_{\tau_{Ih}}, (GnRH\text{-}R_{GnRH}), P_{FSH})$
10	FSH (blood)	$\frac{d}{dt}FSH = \frac{1}{V_B} \cdot rel_{FSH}(E_{2,\tau_{E_2}+\tau_{FSH,1}}, P_{4,\tau_{P_4}+\tau_{FSH,1}}, Ih_{\tau_{Ih}+\tau_{FSH,1}},$ $(GnRH\text{-}R_{GnRH})_{\tau_{FSH,1}}, P_{FSH,\tau_{FSH,1}}) - clear_{FSH}(FSH)$
	syn(FSH)	$syn_{FSH} = b_{FSH} + h_3^-(Ih) \cdot syn_{FSH,max}$
	rel(FSH)	$rel_{FSH} = \left(h_4^-(E_2) + h_4^+(E_2)\right) \cdot h_5^+(P_4) \cdot h_5^-(Ih) \cdot rel_{FSH,max}$ $\cdot (GnRH\text{-}R_{GnRH}) \cdot P_{FSH}$
	clear(FSH)	$clear_{FSH} = \alpha_{FSH} \cdot FSH$
11	secondary follicle	$\frac{d}{dt}F_s(t) = d_1 \cdot h^+(FSH_{\tau_{FSH,2}}; T_{FSH}^{foll}, n_{FSH}^{foll}) + d_2 \cdot f_1(FSH_{\tau_{FSH,2}}) \cdot F_s(t)$ $- d_3 \cdot f_1(FSH_{\tau_{FSH,2}}) \cdot F_s(t)$
12	tertiary follicle	$\frac{d}{dt}F_t(t) = d_3 \cdot f_1(FSH_{\tau_{FSH,2}}) \cdot F_s(t) + d_4 \cdot f_2(FSH_{\tau_{FSH,2}}, LH_{\tau_{LH,2}}) \cdot F_t(t)$

Table 2.1: Model equations. The 49 delay differential equations, the 6 functions for the total enzyme concentrations in the ovaries, the inhibin concentration in the blood, and the auxiliary functions are listed. In the first column, the delay differential equations are consecutively numbered. All components and their corresponding equation are given in the second and third column.

no	component	equation
		$- d_5 \cdot f_2(FSH_{\tau_{FSH,2}}, LH_{\tau_{LH,2}}) \cdot F_t(t)$
13	Graafian follicle	$\frac{d}{dt}F_g(t) = d_5 \cdot f_2(FSH_{\tau_{FSH,2}}, LH_{\tau_{LH,2}}) \cdot F_t(t) + d_6 \cdot f_1(LH_{\tau_{LH,2}}) \cdot F_g(t)$ $- d_7 \cdot f_1(LH_{\tau_{LH,2}}) \cdot F_g(t)$
14	ovulatory follicle	$\frac{d}{dt}M_o(t) = d_7 \cdot f_1(LH_{\tau_{LH,2}}) \cdot F_g(t) - d_8 \cdot M_o(t)$
15	luteinizing follicle	$\frac{d}{dt}M_l(t) = d_8 \cdot M_o(t) - d_9 \cdot M_l(t)$
16	early corpus luteum	$\frac{d}{dt}L_e(t) = d_9 \cdot M_l(t) - d_{10} \cdot f_1(LH_{\tau_{LH,2}}) \cdot L_e(t)$
17	mature corpus luteum	$\frac{d}{dt}L_m(t) = d_{10} \cdot f_1(LH_{\tau_{LH,2}}) \cdot L_e(t) - d_{11} \cdot f_1(LH_{\tau_{LH,2}}) \cdot L_m(t)$
18	late corpus luteum	$\frac{d}{dt}L_l(t) = d_{11} \cdot f_1(LH_{\tau_{LH,2}}) \cdot L_m(t) - d_{12} \cdot L_l(t)$
19	corpus albicans	$\frac{d}{dt}L_a(t) = d_{12} \cdot L_l(t) - d_{13} \cdot L_a(t)$
	f_1, f_2	$f_1(H) = H^\alpha, \quad f_2(H_1, H_2) = H_1^{\alpha_1} \cdot H_2^{\alpha_2}$
	h^+, h^-	$h^+(H;T,n) = \frac{(\frac{H}{T})^n}{1+(\frac{H}{T})^n}, \quad h^-(H;T,n) = \frac{1}{1+(\frac{H}{T})^n}$
	inhibin (blood)	$Ih(t) = ih_1 + ih_2 \cdot F_t(t) + ih_3 \cdot L_m(t) + ih_4 \cdot L_l(t)$
20	free FSH receptors	$\frac{d}{dt}R_{FSH} = k_-^{FSH} \cdot (FSH\text{-}R_{FSH}) + k_r^{FSH} \cdot R_i^{FSH}$ $- k_+^{FSH} \cdot FSH_{\tau_{FSH,2}} \cdot R_{FSH}$
21	bound FSH receptors	$\frac{d}{dt}(FSH\text{-}R_{FSH}) = k_+^{FSH} \cdot FSH_{\tau_{FSH,2}} \cdot R_{FSH}$ $- (\rho^{FSH} + k_-^{FSH}) \cdot (FSH\text{-}R_{FSH})$
22	phos. FSH receptors	$\frac{d}{dt}(FSH\text{-}R_{FSH}\text{-}p) = \rho^{FSH} \cdot (FSH\text{-}R_{FSH}) - k_i^{FSH} \cdot (FSH\text{-}R_{FSH}\text{-}p)$
23	int. FSH receptors	$\frac{d}{dt}R_i^{FSH} = k_i^{FSH} \cdot (FSH\text{-}R_{FSH}\text{-}p) - k_r^{FSH} \cdot R_i^{FSH}$
24	free LH receptors	$\frac{d}{dt}R_{LH} = k_-^{LH} \cdot (LH\text{-}R_{LH}) + k_r^{LH} \cdot R_i^{LH} - k_+^{LH} \cdot LH_{\tau_{LH,2}} \cdot R_{LH}$
25	bound LH receptors	$\frac{d}{dt}(LH\text{-}R_{LH}) = k_+^{LH} \cdot LH_{\tau_{LH,2}} \cdot R_{LH} - (\rho^{LH} + k_-^{LH}) \cdot (LH\text{-}R_{LH})$
26	phos. LH receptors	$\frac{d}{dt}(LH\text{-}R_{LH}\text{-}p) = \rho^{LH} \cdot (LH\text{-}R_{LH}) - k_i^{LH} \cdot (LH\text{-}R_{LH}\text{-}p)$
27	int. LH receptors	$\frac{d}{dt}R_i^{LH} = k_i^{LH} \cdot (LH\text{-}R_{LH}\text{-}p) - k_r^{LH} \cdot R_i^{LH}$
28	active 3β-HSD	$\frac{d}{dt}3\beta\text{-}HSD_a = a_1 \cdot 3\beta\text{-}HSD_{total} \cdot (LH\text{-}R_{LH}) - a_2 \cdot 3\beta\text{-}HSD_a$
29	active 17β-HSD	$\frac{d}{dt}17\beta\text{-}HSD_a = a_3 \cdot 17\beta\text{-}HSD_{total} \cdot (FSH\text{-}R_{FSH}) - a_4 \cdot 17\beta\text{-}HSD_a$
30	active P450scc	$\frac{d}{dt}P450scc_a = a_5 \cdot P450scc_{total} \cdot (LH\text{-}R_{LH}) - a_6 \cdot P450scc_a$
31	active $P450_{17\text{-}OH}$	$\frac{d}{dt}P450_{17\text{-}OH,a} = a_7 \cdot P450_{17\text{-}OH,total} \cdot (LH\text{-}R_{LH}) - a_8 \cdot P450_{17\text{-}OH,a}$
32	active P450arom	$\frac{d}{dt}P450arom_a = a_9 \cdot P450arom_{total} \cdot (FSH\text{-}R_{FSH}) - a_{10} \cdot P450arom_a$
	total 3β-HSD	$3\beta\text{-}HSD_{total} = f_{lincom}(F_t, \ldots, L_l; e_1)$
	total 17β-HSD	$17\beta\text{-}HSD_{total} = f_{lincom}(F_s, \ldots, L_l; e_2)$
	total P450scc	$P450scc_{total} = f_{lincom}(F_t, \ldots, L_l; e_3)$
	total $P450_{17\text{-}OH}$	$P450_{17\text{-}OH,total} = f_{lincom}(F_t, \ldots, L_l; e_4)$
	total P450arom	$P450arom_{total} = f_{lincom}(F_s, \ldots, L_l; e_5)$
	f_{lincom}	$f_{lincom}(A;p) = \sum_{i=1}^{n} p_i \cdot A_i$
33	pregnenolone (ovaries)	$\frac{d}{dt}preg_0 = c_1 \cdot P450scc_a \cdot chol - f^{rev}(prog_0, preg_0, 3\beta\text{-}HSD_a; p_1)$ $- f^{irrev}(preg_0, P450_{17\text{-}OH,a}; k_1) - c_2 \cdot preg_0$
34	progesterone (ovaries)	$\frac{d}{dt}prog_0 = f^{rev}(prog_0, preg_0, 3\beta\text{-}HSD_a; p_1) - f^{irrev}(prog_0, P450_{17\text{-}OH,a}; k_2)$ $- c_3 \cdot prog_0$
35	17α-OH-preg. (ovaries)	$\frac{d}{dt}17\text{-}preg_0 = f^{irrev}(preg_0, P450_{17\text{-}OH,a}; k_1)$ $- f^{rev}(17\text{-}prog_0, 17\text{-}preg_0, 3\beta\text{-}HSD_a; p_2)$ $- f^{irrev}(17\text{-}preg_0, P450_{17\text{-}OH,a}; k_3) - c_4 \cdot 17\text{-}preg_0$
36	17α-OH-prog. (ovaries)	$\frac{d}{dt}17\text{-}prog_0 = f^{irrev}(prog_0, P450_{17\text{-}OH,a}; k_2)$ $+ f^{rev}(17\text{-}prog_0, 17\text{-}preg_0, 3\beta\text{-}HSD_a; p_2)$ $- f^{irrev}(17\text{-}prog_0, P450_{17\text{-}OH,a}; k_4) - c_5 \cdot 17\text{-}prog_0$
37	DHEA (ovaries)	$\frac{d}{dt}DHEA_0 = f^{irrev}(17\text{-}preg_0, P450_{17\text{-}OH,a}; k_3) - f^{irrev}(DHEA_0, 3\beta\text{-}HSD_a; k_5)$ $- c_6 \cdot DHEA_0$
38	androstenedione (ovaries)	$\frac{d}{dt}andro_0 = f^{irrev}(17\text{-}prog_0, P450_{17\text{-}OH,a}; k_4) + f^{irrev}(DHEA_0, 3\beta\text{-}HSD_a; k_5)$ $- f^{rev}(test_0, andro_0, 17\beta\text{-}HSD_a; p_3) - f^{irrev}(andro_0, P450arom_a; k_6)$ $- c_7 \cdot andro_0$
39	testosterone (ovaries)	$\frac{d}{dt}test_0 = f^{rev}(test_0, andro_0, 17\beta\text{-}HSD_a; p_3) - f^{irrev}(test_0, P450arom_a; k_7)$ $- c_8 \cdot test_0$
40	estrone (ovaries)	$\frac{d}{dt}estro_0 = f^{irrev}(andro_0, P450arom_a; k_6) - f^{rev}(estra_0, estro_0, 17\beta\text{-}HSD_a; p_4)$

Table 2.1: Model equations. The 49 delay differential equations, the 6 functions for the total enzyme concentrations in the ovaries, the inhibin concentration in the blood, and the auxiliary functions are listed. In the first column, the delay differential equations are consecutively numbered. All components and their corresponding equation are given in the second and third column.

no	component	equation
41	estradiol (ovaries)	$\begin{aligned}&- c_9 \cdot estro_0\\ \frac{d}{dt}estra_0 = {}& f^{irrev}(test_0, P450arom_a; k_7) + f^{rev}(estra_0, estro_0, 17\beta\text{-}HSD_a; p_4)\\ &- c_{10} \cdot estra_0\end{aligned}$
	f^{irrev}	$f^{irrev}(S, E; p) = p_1 \cdot E \cdot \frac{S}{p_2+S}, \quad p \in \mathbb{R}^2_+$
	f^{rev}	$f^{rev}(P, S, E; p) = \frac{E\cdot(p_1\cdot S - p_2\cdot P)}{p_3+S+p_4\cdot P}, \quad p \in \mathbb{R}^4_+$
42	progesterone (blood)	$\frac{d}{dt}P_4(t) = \frac{s_{P_4}}{V_B} \cdot prog(t-\tau_{prog}) - \alpha_{P_4} \cdot P_4(t)$
43	estradiol (blood)	$\frac{d}{dt}E_2(t) = \frac{s_{E_2}}{V_B} \cdot estra(t-\tau_{estra}) - \alpha_{E_2} \cdot E_2(t)$
44	17α-OH-preg. (blood)	$\frac{d}{dt}17\text{-}preg_B = \frac{s_{17\text{-}preg}}{V_B} \cdot 17\text{-}preg_0(t-\tau_{17\text{-}preg}) - \alpha_{17\text{-}preg} \cdot 17\text{-}preg_B(t)$
45	17α-OH-prog. (blood)	$\frac{d}{dt}17\text{-}prog_B = \frac{s_{17\text{-}prog}}{V_B} \cdot 17\text{-}prog_0(t-\tau_{17\text{-}prog}) - \alpha_{17\text{-}prog} \cdot 17\text{-}prog_B(t)$
46	DHEA (blood)	$\frac{d}{dt}DHEA_B = \frac{s_{DHEA}}{V_B} \cdot DHEA_0(t-\tau_{DHEA}) - \alpha_{DHEA} \cdot DHEA_B(t)$
47	androstenedione (blood)	$\frac{d}{dt}andro_B = \frac{s_{andro}}{V_B} \cdot andro_0(t-\tau_{andro}) - \alpha_{andro} \cdot andro_B(t)$
48	testosterone (blood)	$\frac{d}{dt}test_B = \frac{s_{test}}{V_B} \cdot test_0(t-\tau_{test}) - \alpha_{test} \cdot test_B(t)$
49	estrone (blood)	$\frac{d}{dt}estro_B = \frac{s_{estro}}{V_B} \cdot estro_0(t-\tau_{estro}) - \alpha_{estro} \cdot estro_B(t)$

Table 2.2: Parameters. The parameters are assigned to their component. A short remark about the type of parameter is given in the third column. In the fourth column, the number of parameters arising in the respective component is noted. Altogether, there are 208 parameters.

component	parameters	explanation	#
GnRH pulse frequency	γ	Weibull density parameter	
	λ_{max}	intensity parameter	
	$T^{freq}_{P_4}$, $n^{freq}_{P_4}$, $T^{freq}_{E_2}$, $n^{freq}_{E_2}$	Hill function parameter	6
GnRH pulse mass	M_{max}	mass parameter	
	$T_{E_2,1}$, $n_{E_2,1}$, $T_{E_2,2}$, $n_{E_2,2}$	Hill function parameter	5
GnRH (pituitary portal system)	α_{GnRH}, β_{GnRH}	rate constants	
	b_{GnRH}	basal release rate	
	V_{PPS}	blood volume	
	a, m	Gamma density parameter	6
GnRH receptors	r_i, $i = 1, \dots, 4$	rate constants	
	T_{GnRH}	threshold	5
LH	T_i^-, n_i^-, $i = 1, 2$, T_i^+, n_i^+, $i = 1, \dots, 3$	Hill function parameter	
	b_{LH}	basal synthesis rate	
	α_{LH}	rate constant	
	$syn_{LH,max}$, $rel_{LH,max}$	synthesis/release parameter	14
FSH	T_i^-, n_i^-, $i = 3, 4, 5$, T_i^+, n_i^+, $i = 4, 5$	Hill function parameter	
	b_{FSH}	basal synthesis rate	
	α_{FSH}	rate constant	
	$syn_{FSH,max}$, $rel_{FSH,max}$	synthesis/release parameter	14
follicles	d_i, $i = 1, \dots, 13$	rate constants	
	T^{foll}_{FSH}, n^{foll}_{FSH}	Hill function parameter	
	α_i, $i = 1, \dots, 10$	exponents	25
inhibin	ih_i, $i = 1, \dots, 4$	lin. com. parameter	4

Table 2.2: Parameters. The parameters are assigned to their component. A short remark about the type of parameter is given in the third column. In the fourth column, the number of parameters arising in the respective component is noted. Altogether, there are 208 parameters.

component	parameters	explanation	#
LH receptors	k_-^{LH}, k_r^{LH}, k_+^{LH}, k_i^{LH}, ρ^{LH}	rate constants	5
FSH receptors	k_-^{FSH}, k_r^{FSH}, k_+^{FSH}, k_i^{FSH}, ρ^{FSH}	rate constants	5
total enzymes	$e_{1,j}$, $j = 1, \dots, 7$ (3β-HSD),	lin. com. parameter	
	$e_{2,j}$, $j = 1, \dots, 8$ (17β-HSD),	lin. com. parameter	
	$e_{3,j}$, $j = 1, \dots, 7$ (P450scc),	lin. com. parameter	
	$e_{4,j}$, $j = 1, \dots, 7$ (P450$_{17-OH}$),	lin. com. parameter	
	$e_{5,j}$, $j = 1, \dots, 8$ (P450arom)	lin. com. parameter	37
active enzymes	a_1, a_2 (3β-HSD), a_3, a_4 (17β-HSD),	rate constants	
	a_5, a_6 (P450scc), a_7, a_8 (P450$_{17-OH}$),	rate constants	
	a_9, a_{10} (P450arom)	rate constants	10
steroids (ovaries)	*chol*	const. cholesterol conc.	
	c_i, $i = 1, \dots, 10$	rate constants	
	$k_{i,j}$, $i = 1, \dots, 7$, $j = 1, 2$	irrev. MM parameter	
	$p_{i,j}$, $i = 1, \dots, 4$, $j = 1, \dots, 4$	rev. MM parameter	40
steroids (blood)	s_{P_4}, s_{E_2}, $s_{17\text{-}preg}$, $s_{17\text{-}preg}$,	rate constants	
	s_{DHEA}, s_{andro}, s_{test}, s_{estro}	rate constants	
	α_{P_4}, α_{E_2}, $\alpha_{17\text{-}preg}$, $\alpha_{17\text{-}preg}$,	rate constants	
	$\alpha_{17\text{-}preg}$, α_{DHEA}, α_{andro}, α_{test}, α_{estro}	rate constants	
	V_B	blood volume	17
delays	τ_{P_4}, τ_{E_2}, τ_{Ih},		
	$\tau_{FSH,1}$, $\tau_{LH,1}$, $\tau_{FSH,2}$, $\tau_{LH,2}$,		
	τ_{prog}, τ_{estra}, $\tau_{17\text{-}preg}$, $\tau_{17\text{-}prog}$,		
	τ_{DHEA}, τ_{andro}, τ_{test}, τ_{estro}		15

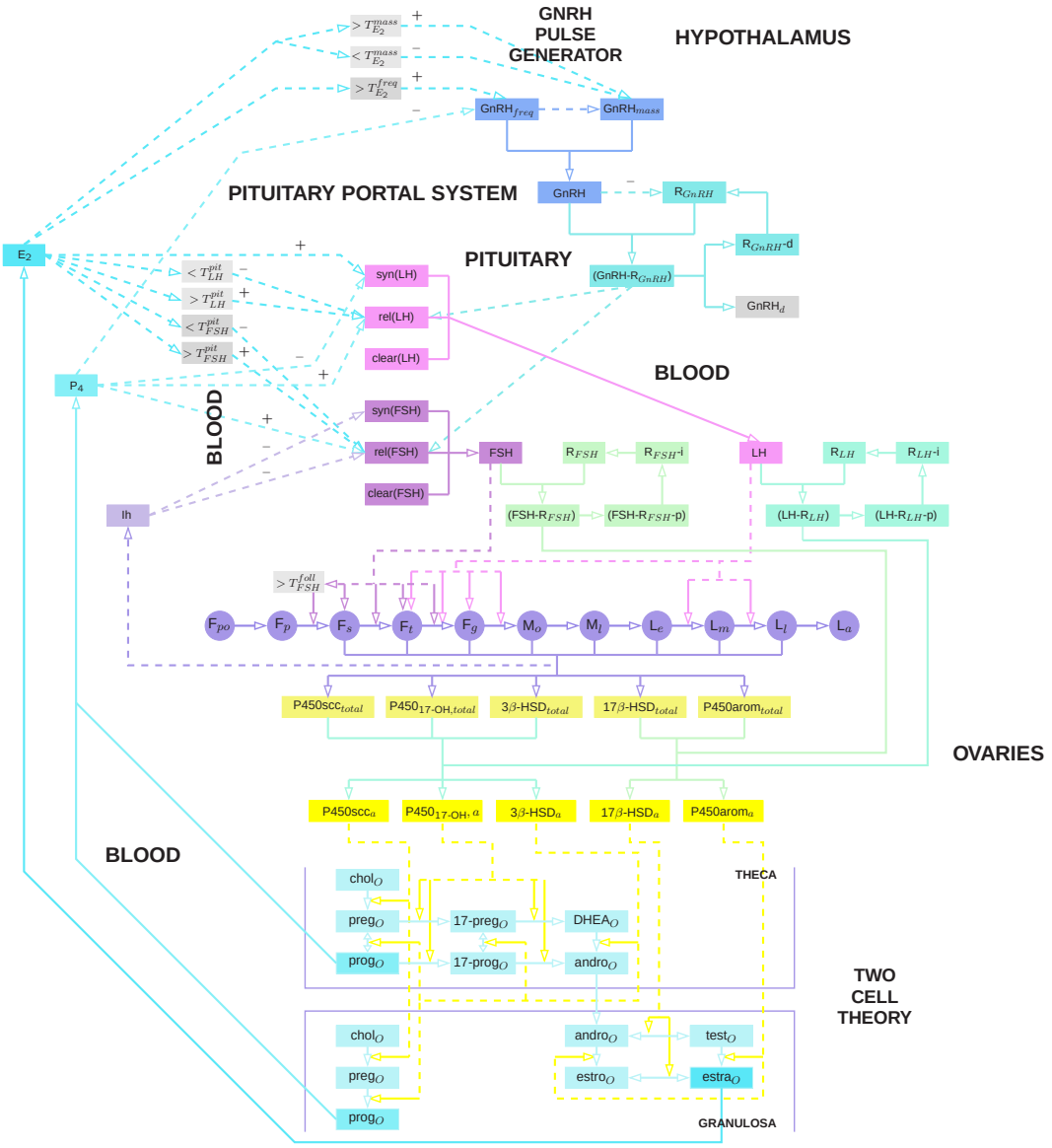

Figure 2.26: Detailed model scheme for the control system of the human menstrual cycle (the Figs. 2.7, 2.11, 2.14, 2.16, 2.18, 2.19, 2.20, 2.24, and 2.25 are merged). The different parts of the complex model (without the steroids in the blood except for P_4 and E_2) presented in this chapter are summarized in one single model scheme. The abbreviations are as introduced before.

Chapter 3

Model Decomposition

When modeling complex physiological processes and control systems in the human body such as the human menstrual cycle, a large number of parameters can arise. Often their values are not known, which is why parameter estimation is necessary, albeit expensive and possibly not successful. That is why it could be useful to consider possibilities to simplify the problem of parameter estimation.

Suppose that the mathematical model consists of a system of (delay) differential equations (see Section 1.4)

$$\frac{d}{dt}y = f(y, y_{\tau_1}, \ldots, y_{\tau_m}; p), \tag{3.1}$$

where $y : \mathbb{R} \to \mathbb{R}^n$, $y =: (y_1, \ldots, y_n)^T$, $f : \mathbb{R} \times \mathbb{R}^{n\times(m+1)} \to \mathbb{R}^n$, $f =: (f_1, \ldots, f_n)^T$, $n \in \mathbb{N}$, $m \in \mathbb{N}_0$, and $\tau_i \in \mathbb{R}_+$, $i = 1, \ldots, m$, denote the constant delays if $m \geq 1$, and $p \in \mathbb{R}_+^{n_p}$, $n_p \in \mathbb{N}$, the vector of parameters.

Definition 3.1. In the mathematical model defined in Eq. (3.1), $y_1, \ldots, y_n$ are called the *elements*.

In the following a method is developed that uses the availability of experimental data for the decomposition of the complex mathematical model (published in [67]). This method is applied implicitly in [37] where the mathematical model consisting of 13 differential equations is divided into two disjoint model parts. Parameter estimation is performed separately for the two parts using approximations of experimental data as input and afterwards they are recomposed to a dynamic model. In order to simplify parameter estimation or even to make it possible, decomposition of the complex model could be helpful. Instead of a high-dimensional problem, several smaller models are obtained that can be treated more easily and successfully.

The procedure for the parameter estimation can be summarized in the following way:

1. model decomposition into disjoint model parts

2. parameter estimation for a selection of parameters by using experimental data as input

3. recomposition of the model parts to the original model with the estimated parameter values

A graph theoretical approach can help identifying these model parts. Graphs are frequently used to model a binary relationship between objects [29]. Here the definition of a graph is based on the direct dependency of the right hand side of the system on its elements. If the model parts are determined, the corresponding differential equations belonging to the elements of these model parts can be solved separately if the required input is available.

At first, the definition and method of the model decomposition are presented in Section 3.1. This procedure is shown for the model of the human menstrual cycle presented in Section 3.2 and the results are visualized. Finally, the results of this chapter are summarized in Section 3.3.

3.1 Definition and method of the model decomposition

At first the graph representing the mathematical model and the requirements for the model decomposition are defined in Section 3.1.1. In Sections 3.1.2, 3.1.3, and 3.1.4 the different steps to obtain the model decomposition are presented.

3.1.1 Representation of the mathematical model by a graph

First some terms that are used to describe the graph theoretical approach are introduced [4, 23, 29]:

Definition 3.2. A *graph* is a pair $G = (V, E)$ of disjoint sets with $E \subseteq V^2$, where V^2 denotes the set of all subsets of V that consists of two elements. The elements of V are called the *vertices* of the graph G and the elements of E its *edges*, where an edge is an unordered pair of distinct vertices. An edge $e = \{v_i v_j\} \in E$ (short $e = v_i v_j$ or $e = v_j v_i$) *connects* the two vertices $v_i, v_j \in V$.

A *directed graph* is a graph $G = (V, E)$ together with the two maps $init : E \to V$ and $ter : E \to V$. To every edge e, an *initial vertex* $init(e)$ and a *terminal vertex* $ter(e)$ are assigned. A directed edge is also called *arc*. If $init(e) = ter(e)$, then e is called a *loop*.

The system of differential equations is represented here by the directed graph $G = (V, E)$. The vertices are then given by $V := \{v_1, \ldots, v_n\}$, the *set of elements*, where $v_i := \arg(y_i)$, $i = 1, \ldots, n$, correspond with the elements of the system y_i, $i = 1, \ldots, n$, respectively. An arc from one vertex to a second vertex is given if the right hand side of the element represented by the second vertex is directly dependent on the element represented by the first vertex:

$$E = \left\{ v_i v_j \in V^2 \middle| \frac{\partial f_j}{\partial y_i} + \sum_{k=1}^{m} \frac{\partial f_j}{\partial y_{\tau_k, i}} \neq 0 \right\}.$$

Define the set of parameters by $P := \{p_1, \ldots, p_{n_p}\}$.

The definition of the adjacency matrix is needed in the following [4, 23, 29].

Definition 3.3. Two vertices $v_i, v_j \in V$ of the graph G are called *adjacent* if $v_i v_j \in E$. The *adjacency matrix* $A := (a_{ij})_{n\times n}$ of G is defined by

$$a_{ij} := \begin{cases} 1 & \text{if } v_i v_j \in E \\ 0 & \text{else.} \end{cases}$$

In the definition of G given here, loops are possible, but they are not important in the following, which is why they are neglected. The following definition is needed [23]:

Definition 3.4. If $V' \subseteq V$ and $E' \subseteq E$, then $G' := (V', E')$ is a *subgraph* of G, written $G' \subseteq G$.

That means that here the graph G is reduced to the subgraph $G' = (V, E') \subseteq G$ where $E' := E \backslash \{e \in E | init(e) = ter(e)\}$. The corresponding adjacency matrix is then given by $A' := (a'_{ij})_{n\times n}$ where $a'_{ij} := a_{ij}$ for all $i, j = 1, \ldots, n$, $i \neq j$, and $a'_{ii} := 0$, $i = 1, \ldots, n$, i.e. the diagonal of A is set to zero.

In order to perform parameter estimation, experimental data are necessary for fitting the parameters. As in the case of the human menstrual cycle [66], experimental data describing the data over the cycle are not given for all elements of the system. The following definition is useful and simplifies the formulations. From now on the elements and their corresponding vertices are used equivalently.

Definition 3.5. An element $v \in V$ of the system in Eq. (3.1) is called an *exp-element* if usable experimental data are given for this element over the considered time span. Otherwise it is called a *non-exp-element*.

Suppose that N exp-elements $v_1^{exp}, \ldots, v_N^{exp} \in V$ are given where $v_j^{exp} = v_{i_j}$, $j = 1, \ldots, N$, with $1 \leq i_1 < \cdots < i_N \leq n$ and $N \in \mathbb{N}$, $N \leq n$. Then $V^{exp} := \{v_1^{exp}, \ldots, v_N^{exp}\}$ is called the *set of exp-elements*.

Based on these exp-elements the set of elements is decomposed. It is essential that experimental data for at least two elements from $\{y_1, \ldots, y_n\}$ are available, i.e. $N \geq 2$, in order to be able to obtain at least two model parts.

Summarized, from the model parts that emerge through the model decomposition, the following properties are required:

- The model parts, denoted by V_i^{part}, $i = 1, \ldots, N'$, and the parts of the corresponding parameters, denoted by P_i^{part}, $i = 1, \ldots, N'$, where $N' \leq N$, should be disjoint in order to avoid double parameter estimation.

- Every model part V_i^{part}, $i = 1, \ldots, N'$, should contain at least one exp-element in order to be able to perform parameter estimation.

- Moreover, there should be at least one model part V_i^{part}, $i \in \{1, \ldots, N'\}$, that needs, if at all, input from exp-elements, i.e. $V_i^{inp} = V^{inp,exp}$, and no approximations of elements from other model parts that are non-exp-elements, i.e. $V_i^{inp,app} = \emptyset$, and that furthermore does not need parameter input, i.e. $P_i^{part} = \emptyset$, in order to have a model part to start the parameter estimation.

It is possible that not all elements can be assigned to a model part. These elements form the rest set V^{rest} and the corresponding parameters the parameter rest set P^{rest}.

Definition 3.6. The *model decomposition* is defined by the partition of the set of elements V into the *model parts* $V_1^{part}, \ldots, V_{N'}^{part} \subset V$ and the *rest set* $V^{rest} \subset V$, and the partition of the parameters into the *parameter parts* $P_1^{part}, \ldots, P_{N'}^{part} \subset P$ and the *parameter rest set* $P^{rest} \subset P$, where $N' \leq N$, $N \geq 2$, if

$$
\begin{aligned}
&(i) \quad V = \bigcup_{i=1}^{N'} V_i^{part} \cup V^{rest} \\
&(ii) \quad V_i^{part} \cap V_j^{part} = \emptyset \quad \forall i, j = 1, \ldots, N' \wedge i \neq j \\
&(iii) \quad V_i^{part} \cap V^{rest} = \emptyset \quad \forall i = 1, \ldots, N' \\
&(iv) \quad P_i^{part} \cap P_j^{part} = \emptyset \quad \forall i, j = 1, \ldots, N' \wedge i \neq j \\
&(v) \quad P_i^{part} \cap P^{rest} = \emptyset \quad \forall i = 1, \ldots, N' \\
&(vi) \quad V_i^{part} \cap V^{exp} \neq \emptyset \quad \forall i = 1, \ldots, N' \\
&(vii) \quad V^{rest} \cap V^{exp} = \emptyset \\
&(viii) \exists i \in \{1, \ldots, N'\} : V_i^{inp,app} = \emptyset \quad \wedge \quad P_i^{inp} = \emptyset.
\end{aligned}
$$

The different sets are introduced and defined more concisely in the subsequent sections. It is shown that such a model decomposition exist for a model under the conditions described above.

3.1.2 Determination of sets of predecessors and groupings

Interpolations of the experimental data for the exp-elements can replace the exp-elements in the simulation of the mathematical model. That is why the connections between these exp-elements and the remaining elements can be eliminated in the following proceeding. Then all predecessors of the exp-elements, the *sets of predecessors*, V_j^{pre}, $j = 1, \ldots, N$, are determined in order to obtain a first, not necessarily unique, assignment of the elements to the exp-elements.

The elimination of arcs leads to a further reduction of the graph G'. Define $G'' := (V, E'') \subseteq G'$, where

$$E'' = E' \setminus \left\{ e \in E' \middle| init(e) \in V^{exp} \right\}.$$

The corresponding values of the adjacency matrix are set to zero in order to obtain the adjacency matrix of the subgraph G'': $A'' := (a''_{ij})_{n \times n}$ where $a''_{ij} := a'_{ij}$ for $i \notin V^{exp}$ and $a''_{ij} := 0$ for $i \in V^{exp}$, $j = 1, \ldots, n$.

Sets of predecessors

Another definition for the relation of two vertices is needed in order to assign the elements to exp-elements [4, 23, 29].

Definition 3.7. A *walk* (of length $k \in \mathbb{N}$) is a non-empty directed graph $P = (V, E)$ of the form

$$V = \{v_0, v_1, \ldots, v_k\}, \quad E = \{v_0v_1, v_1v_2, \ldots, v_{k-1}v_k\}.$$

It is called a v_iv_j-*walk* if the first vertex in the walk is given by v_i and the last by v_j. A walk is called a *path* if the vertices are pairwise distinct.

Definition 3.8. The vertex $v_i \in V$ is called a *predecessor* (*of order* $k \in \mathbb{N}$) of $v_j \in V$, if there is a v_iv_j-walk (of length k) in G''.

Then all predecessors of an exp-element form a set:

Definition 3.9. The sets of predecessors for $v_j^{exp} \in V^{exp}$, $j = 1, \ldots, N$, are given by

$$V_j^{pre} := \{v \in V | (v = v_j^{exp}) \vee (\exists v v_j^{exp}\text{-path} \in G'')\}.$$

The set of parameters belonging to the element v_i denoted by P_i, $i = 1, \ldots, n$, is defined by:

$$P_i := \left\{ p_j \in P \middle| \frac{\partial f_i}{\partial p_j} \neq 0 \right\}.$$

Definition 3.10. The set of parameters belonging to the set of predecessors V_j^{pre}, $j = 1, \ldots, N$, is given by

$$P_j^{pre} := \bigcup_{l=1}^{n_j^{pre}} P_{V_j^{pre}(l)}, \quad n_j^{pre} := |V_j^{pre}|,$$

where V_j^{pre} is understood as tuple and $V_j^{pre}(l)$ denotes the l-th component if the elements of V_j^{pre} are ordered by ascending index for all $l = 1, \ldots, N$.

The elements that cannot be assigned to a set of predecessors form a separate set.

Definition 3.11. The elements that do not belong to a set of predecessors form the *rest set* V^{rest}:

$$V^{rest} := V \setminus \bigcup_{j=1}^{N} V_j^{pre}$$

and the corresponding parameters the *parameter rest set*:

$$P^{rest} := P \setminus \bigcup_{j=1}^{N} P_j^{pre}.$$

The vertex v_l, $l \in \{1,\dots,n\}$, is a predecessor of order 1 of the exp-element $v_j^{exp} = v_{i_j}$, $j \in \{1,\dots,N\}$, if $a_{l,j}^{pre,1} := a''_{l,i_j} = 1$, i.e. if there is an arc from v_l to v_{i_j}. Predecessors of order ≤ 2 of the exp-elements are given by

$$a_{l,j}^{pre,2} := \max\left\{a_{l,j}^{pre,1}, a''_{l,1}\cdot a_{1,j}^{pre,1},\dots,a''_{l,n}\cdot a_{n,j}^{pre,1}\right\},\quad l=1,\dots,n,\quad j=1,\dots,N,$$

since if $a_{l,j}^{pre,2}=1$ there is an arc from v_l to v_{i_j} or a path $\{v_lv_{l'}, v_{l'}v_{i_j}\}\subseteq E$ of length 2 for a $l'\in\{1,\dots,n\}$.

Generally, the following lemma is true.

Lemma 3.1. *The vertex v_l is a predecessor of order $\leq k$, $k\geq 2$, of $v_{i_j}\in V^{exp}$ if $a_{l,j}^{pre,k}=1$, where*

$$a_{l,j}^{pre,k} := \max\left\{a_{l,j}^{pre,k-1}, a''_{l,1}\cdot a_{1,j}^{pre,k-1},\dots,a''_{l,n}\cdot a_{n,j}^{pre,k-1}\right\},\quad l=1,\dots,n,\quad j=1,\dots,N.$$

Proof. The case for $k=2$ is given above and it follows that if $a_{l,j}^{pre,2}=1$ then v_l is a predecessor of v_{i_j}. Suppose that the proposition holds for a $k\geq 2$. For $k+1$, it is

$$a_{l,j}^{pre,k+1} := \max\left\{a_{l,j}^{pre,k}, a''_{l,1}\cdot a_{1,j}^{pre,k},\dots,a''_{l,n}\cdot a_{n,j}^{pre,k}\right\},\quad l=1,\dots,n,\quad j=1,\dots,N.$$

If the maximum is equal $a_{l,j}^{pre,k}$, then the proposition is true for $k+1$ as well since v_l is a predecessor of order $\leq k < k+1$ if $a_{l,j}^{pre,k}=1$. Otherwise there is a $l'\in\{1,\dots,n\}$ such that the maximum is given by $a''_{l,l'}\cdot a_{l',j}^{pre,k}$. Then $v_{l'}$ is a predecessor of order $\leq k$ of v_{i_j} if $a_{l',j}^{pre,k}=1$ and v_l is a predecessor of order 1 of $v_{l'}$ if $a''_{l,l'}=1$. Hence there is a $v_lv_{i_j}$-path of length $\leq k+1$, if $a_{l',j}^{pre,k}=1$ and $a''_{l,l'}=1$ and thus if $a_{l',j}^{pre,k}\cdot a''_{l,l'}=1$. If follows that if $a_{l,j}^{pre,k+1}=1$, then v_l is a predecessor of order $\leq k+1$ of v_{i_j}. □

Define

$$A^{pre,k} := (a_{l,j}^{pre,k})_{l=1,\dots,n,j=1,\dots,N}\in\mathbb{R}^{n\times N}\quad \forall k=1,\dots,n-1,$$
$$A^{pre} := A^{pre,n-1},\quad A^{pre} =: (a_{l,j}^{pre})_{l=1,\dots,n,j=1,\dots,N}.$$

It follows:

Corollary 3.1. *The vertex v_l, $l\in\{1,\dots,n\}$, is a predecessor of $v_{i_j}\in V^{exp}$, $j\in\{1,\dots,N\}$, if $a_{l,j}^{pre}=1$.*

Thus the sets of predecessors can be determined by

$$V_j^{pre} = V^{exp}\cup\left\{v_l\in V\mid a_{l,j}^{pre}=1\right\},\quad j=1,\dots,N.$$

The algorithmic calculation of A^{pre} and V_j^{pre}, $j=1,\dots,N$, is shown in Algorithm 1.

It can be proved that each set of predecessors contains one and only one exp-element.

for $j = 1, \ldots, N$ **do**
  for $l = 1, \ldots, n$ **do**
    $a^{pre}_{l,j} = a''_{l,i_j}$;
  end
  for $k = 2, \ldots, n-1$ **do**
    for $l_1 = 1, \ldots, n$ **do**
      for $l_2 = 1, \ldots, n$ **do**
        $a^{pre}_{l_1,j} = \max(a^{pre}_{l_1,j}, a''_{l_1,l_2} \cdot a^{pre}_{l_2,j})$;
      end
    end
  end
  $V^{pre}_j = v^{exp}_j$;
  for $l = 1, \ldots, n$ **do**
    if $a^{pre}_{l,j} = 1$ **then**
      $V^{pre}_j = V^{pre}_j \cup \{l\}$;
    end
  end
end

Algorithm 1: Algorithm for the determination of A^{pre} and of the sets of predecessors V^{pre}_j, $j = 1, \ldots, N$.

Lemma 3.2. *It is* $V^{pre}_j \cap V^{exp} \neq \emptyset$ *for all* $j = 1, \ldots, N$. *In particular,* $|V^{pre}_j \cap V^{exp}| = 1$ *for all* $j = 1, \ldots, N$.

Proof. Per definition is $v^{exp}_j \in V^{pre}_j$, where $v^{exp}_j \in V^{exp}$. For all $e \in E''$ it is $init(e) \notin V^{exp}$ if $init(e) \in V^{pre}_j$, thus it follows $(V^{pre}_j \backslash \{v^{exp}_j\}) \cap V^{exp} = \emptyset$ (because of the definition of V^{pre}_j, see Def. 3.9). □

The rest set contains no exp-elements. It holds $V^{rest} \cap V^{exp} = \emptyset$ since $V^{exp} \subseteq \bigcup_{j=1}^{N} V^{pre}_j$ (condition (vii) in Def. 3.6).

Groupings

Under certain conditions it can be useful to merge sets of predecessors which is presented in this section.

Consider the case that two sets of predecessors match except for the exp-elements:

$$V^{pre}_j \backslash V^{exp} = V^{pre}_{j'} \backslash V^{exp}, \quad j, j' \in \{1, \ldots, N\}, j \neq j'.$$

By the concept of grouping that is presented here, it can be avoided for the time being that the emerging disjoint model parts consist in V^{pre}_j and $\{v^{exp}_{j'}\}$, i.e. that one of these model parts only consists of the exp-element.

Definition 3.12. The sets of predecessors $V^{pre}_{j_1}, \ldots, V^{pre}_{j_l}$, where $j_1, \ldots, j_l \in \{1, \ldots, N\}$

and $l \in \{1, \ldots, N\}$, form a *grouping*

$$V_j^{group} := \bigcup_{k=1}^{l} V_{j_k}^{pre}$$

if they match except for the exp-elements:

$$V_{j_k}^{pre} \backslash V^{exp} = V_{j_{k'}}^{pre} \backslash V^{exp}, \quad \forall k, k' \in \{1, \ldots, l\}, k \neq k'.$$

If $l = 1$ then $V_j^{group} = V_{j_1}^{pre}$.

There are $N' \leq N$ groupings V_j^{group}. The assignment of the sets of predecessors to groupings is unique.

Lemma 3.3. *It holds*

$$\forall i \in \{1, \ldots, N\} \exists! j \in \{1, \ldots, N'\} : V_i^{pre} \subseteq V_j^{group}.$$

Proof. The groupings are defined such that every set of predecessors is assigned to at least one grouping. In order to show uniqueness, suppose that there is a set of predecessors that belongs to two groupings:

$$V_i^{pre} \subseteq V_j^{group} \quad \wedge \quad V_i^{pre} \subseteq V_{j'}^{group}, \quad i \in \{1, \ldots, N\},$$

where $V_j^{group} := \bigcup_{k=1}^{l} V_{j_k}^{pre}$ and $V_{j'}^{group} := \bigcup_{k'=1}^{l'} V_{j'_{k'}}^{pre}$. Then it is $V_i^{pre} \backslash V^{exp} = V_{j_k}^{pre} \backslash V^{exp}$ for all $k = 1, \ldots, l$ and $V_i^{pre} \backslash V^{exp} = V_{j'_{k'}}^{pre} \backslash V^{exp}$ for all $k' = 1, \ldots, l'$. Thus it follows

$$V_{j_k}^{pre} \backslash V^{exp} = V_{j'_{k'}}^{pre} \backslash V^{exp}, \quad \forall k = 1, \ldots, l \quad \forall k' = 1, \ldots, l'$$

and finally $V_j^{group} = V_{j'}^{group}$. □

The calculation of the groupings V_j^{group}, $j = 1, \ldots, N'$, is presented in the Algorithm 2.

Each grouping contains at least one exp-element.

Lemma 3.4. *It holds* $V_j^{group} \cap V^{exp} \neq \emptyset, \quad \forall j = 1, \ldots, N'.$

Proof. It is

$$V_j^{group} \cap V^{exp} = \left(\bigcup_{k=1}^{l} V_{j_k}^{pre} \right) \cap V^{exp} = \bigcup_{k=1}^{l} \left(V_{j_k}^{pre} \cap V^{exp} \right) \neq \emptyset$$

since $V_j^{pre} \cap V^{exp} \neq \emptyset$ for all $j = 1, \ldots, N$ (Lemma 3.2). □

If the groupings are not disjoint, it is necessary to remove the elements that appear in more than one set in all sets except for one. This leads to the concept of determination of model parts which is presented in the next section.

for $j = 1, \ldots, N$ **do**
  $V_j^{length} = |V_j^{pre}|$;
  $V_j^{temp} = V_j^{pre}$;
end
$N' = 0$;
for $j = 1, \ldots, N$ **do**
  if $|V_j^{temp}| > 0$ **then**
    $N' = N' + 1$;
    $V_{N'}^{group} = V_j^{pre}$;
    for $l = j + 1, \ldots, N$ **do**
      if $|V_l^{temp}| > 0$ **then**
        if $V_j^{pre} \backslash V_j^{exp} = V_l^{pre} \backslash V_l^{exp}$ **then**
          $V_{N'}^{group} = V_{N'}^{group} \cup V_l^{exp}$;
          $V_l^{temp} = \emptyset$;
        end
      end
    end
  end
end

Algorithm 2: Algorithm for the determination of the groupings V_j^{group}, $j = 1, \ldots, N'$.

3.1.3 Determination of disjoint model parts

The objective of this chapter is a disjoint partition of the model. First of all, it is necessary to define the criteria for a reasonable partition of the model. For example, it could be desired that the maximal dimension of the model parts is not too large or that the maximal number of parameters to be estimated is rather small.

The first criterion here is to determine the grouping with minimal number of parameters. If the minimum is not unique, then the second criterion is applied, to find the grouping with minimal number of elements in the set of groupings with minimal number of parameters. If the minimum is still not unique, the element with the smallest index of these groupings is chosen since in this case the choices are considered to be equivalent.

In order to apply the first criterion it is necessary to define the set of parameters belonging to one grouping:

$$P_j^{group} := \bigcup_{l=1}^{n_j^{group}} P_{V_j^{group}(l)}, \quad n_j^{group} := |V_j^{group}|,$$

where $V_j^{group}(l)$ is defined as the l-th component if the elements of V_j^{group} are ordered by ascending index.

The idea consists in removing the elements of the first chosen grouping from the other groupings. Then the next grouping is chosen according to the criteria men-

tioned above and again, the elements of this grouping are removed from the remaining groupings. This procedure is continued until there is only one grouping left.

That means that first

$$j_{min}^1 := \arg\left(\min_j |P_j^{group}|\right)$$

is calculated. If $|j_{min}^1| > 1$, then

$$j_{min}^{'1} := \arg\left(\min_{j \in j_{min}^1} |V_j^{group}|\right)$$

is determined. If still $|j_{min}^{'1}| > 1$, the element with the smallest index is taken: $j_{min}^{''1} := j_{min}^{'1}(1)$ (i.e. the first component if $j_{min}^{'1}$ is ordered by ascending index). For simplicity denote $j_{min}^{'1}$ and $j_{min}^{''1}$ also by j_{min}^1 in the following. Define as the model and parameter part for j_{min}^1

$$V_{j_{min}^1}^{part} := V_{j_{min}^1}^{group}$$
$$P_{j_{min}^1}^{part} := P_{j_{min}^1}^{group}.$$

Then the other groupings of both the elements and the parameters are reduced:

$$V_j^{group} \backslash V_{j_{min}^1}^{group}, \quad \forall j \neq j_{min}^1$$
$$P_j^{group} \backslash P_{j_{min}^1}^{group}, \quad \forall j \neq j_{min}^1.$$

In the second step the same procedure as above must be conducted. Assume for simplicity that j_{min}^2 is unique. Then it is

$$j_{min}^2 = \arg\left(\min_{j \neq j_{min}^1} |P_j^{group} \backslash P_{j_{min}^1}^{group}|\right)$$

and the emerging model and parameter parts are given by

$$V_{j_{min}^2}^{part} := V_{j_{min}^2}^{group} \backslash V_{j_{min}^1}^{group}$$
$$P_{j_{min}^2}^{part} := P_{j_{min}^2}^{group} \backslash P_{j_{min}^1}^{group}.$$

Again, the remaining groupings of elements and parameters are reduced:

$$\left(V_j^{group} \backslash V_{j_{min}^1}^{group}\right) \backslash V_{j_{min}^2}^{group} = V_j^{group} \backslash \left(\bigcup_{l=1}^{2} V_{j_{min}^l}^{group}\right), \quad \forall j \neq j_{min}^1 \wedge j \neq j_{min}^2$$
$$\left(P_j^{group} \backslash P_{j_{min}^1}^{group}\right) \backslash P_{j_{min}^2}^{group} = P_j^{group} \backslash \left(\bigcup_{l=1}^{2} P_{j_{min}^l}^{group}\right), \quad \forall j \neq j_{min}^1 \wedge j \neq j_{min}^2.$$

This procedure can be continued until there is only one element grouping and one parameter grouping left which form the last model and parameter part (after reduction).

Definition 3.13. Generally, the model parts and the parameter parts are defined by:

$$V_{j_{min}^1}^{part} := V_{j_{min}^1}^{group}$$
$$P_{j_{min}^1}^{part} := P_{j_{min}^1}^{group}$$

where

$$j_{min}^1 := \arg\left(\min_{j \in \arg(\min_k |P_k^{group}|)} |V_j^{group}|\right)(1),$$

and for $l' = 2, \ldots, N'$:

$$V_{j_{min}^{l'}}^{part} := V_{j_{min}^{l'}}^{group} \setminus \left(\bigcup_{l=1}^{l'-1} V_{j_{min}^l}^{group}\right)$$
$$P_{j_{min}^{l'}}^{part} := P_{j_{min}^{l'}}^{group} \setminus \left(\bigcup_{l=1}^{l'-1} P_{j_{min}^l}^{group}\right),$$

where

$$j_{min}^{l'} = \arg\left(\min_{j \in \arg(\min_{k \neq j_{min}^l \forall l < l'} \left|P_k^{group} \setminus \left(\bigcup_{l=1}^{l'-1} P_{j_{min}^l}^{group}\right)\right|)} \left|V_j^{group} \setminus \left(\bigcup_{l=1}^{l'-1} V_{j_{min}^l}^{group}\right)\right|\right)(1),$$

where the notation (1) means the first component if the set is ordered by ascending index.

The algorithm for the determination of the model parts is presented in Algorithm 3.

It follows from their construction that the emerging model parts and the parameter parts are disjoint:

Lemma 3.5. *The model parts and the parameter parts are each pairwise disjoint:*

$$V_i^{part} \cap V_j^{part} = \emptyset, \quad \forall i, j = 1, \ldots, N', i \neq j \quad \textit{(condition (ii) in Def. 3.6)},$$
$$P_i^{part} \cap P_j^{part} = \emptyset, \quad \forall i, j = 1, \ldots, N', i \neq j \quad \textit{(condition (iv) in Def. 3.6)}.$$

Proof. Choose $l_1, l_2 \in \{1, \ldots, N'\}$ arbitrarily. W.l.o.g. it is assumed that $l_1 < l_2$. Then it is

$$\begin{aligned} V_{j_{min}^{l_1}}^{part} \cap V_{j_{min}^{l_2}}^{part} &= \left(V_{j_{min}^{l_1}}^{group} \setminus (\bigcup_{l=1}^{l_1-1} V_{j_{min}^l}^{group})\right) \cap \left(V_{j_{min}^{l_2}}^{group} \setminus (\bigcup_{l=1}^{l_2-1} V_{j_{min}^l}^{group})\right) \\ &= \left(V_{j_{min}^{l_1}}^{group} \cap (\bigcap_{l=1}^{l_1-1} \neg V_{j_{min}^l}^{group})\right) \cap \left(V_{j_{min}^{l_2}}^{group} \cap (\bigcap_{l=1}^{l_2-1} \neg V_{j_{min}^l}^{group})\right). \end{aligned}$$

for $j = 1, \ldots, N'$ **do**
  $V_j^{part} = V_j^{group}$;
  $P_j^{part} = \bigcup_{l=1}^{|V_j^{group}|} P_{V_j^{group}(l)}$;
end
$N'_{min} = \{1, \ldots, N'\}$;
while $N'_{min} \neq \emptyset$ **do**
  % first criterion:
  $j_{min} = \arg\left(\min_{j=1,\ldots,|N'_{min}|} |P^{part}_{N'_{min}(j)}|\right)$;
  if $|j_{min}| > 1$ **then**
    % second criterion:
    $j_{min} = j_{min}\left(\arg\left(\min_{j=1,\ldots,|j_{min}|} |V^{part}_{N'_{min}(j_{min}(j))}|\right)\right)$;
    if $|j_{min}| > 1$ **then**
      $j_{min} = j_{min}(1)$;
    end
  end
  for $l = 1, \ldots, |N'_{min}|$ **do**
    if $l \neq j_{min}$ **then**
      $V^{part}_{N'_{min}(l)} = V^{part}_{N'_{min}(l)} \backslash V^{part}_{N'_{min}(j_{min})}$;
      $P^{part}_{N'_{min}(l)} = P^{part}_{N'_{min}(l)} \backslash P^{part}_{N'_{min}(j_{min})}$;
    end
  end
  $N'_{min} = N'_{min} \backslash j_{min}$;
end

Algorithm 3: Algorithm for the determination of the model parts V_j^{part} and of the parameter parts P_j^{part}, $j = 1, \ldots, N'$.

Since it is $l_1 \in \{1, \ldots, l_2 - 1\}$, it follows

$$V_{j_{min}^{l_1}}^{group} \cap \left(\bigcap_{l=1}^{l_2-1} \neg V_{j_{min}^{l}}^{group} \right) = V_{j_{min}^{l_1}}^{group} \cap \neg V_{j_{min}^{l_1}}^{group} \cap \left(\bigcap_{l=1, l \neq l_1}^{l_2-1} \neg V_{j_{min}^{l}}^{group} \right) = \emptyset,$$

that means $V_{j_{min}^{l_1}}^{part} \cap V_{j_{min}^{l_2}}^{part} = \emptyset$. It can be proved analogously that the parameter parts are disjoint. □

The rest set is disjoint to the model parts.

Lemma 3.6. *The conditions*

$$(iii) V^{rest} \cap V_j^{part} = \emptyset \quad \forall j = 1, \ldots, N$$
$$(v) \; P^{rest} \cap P_j^{part} = \emptyset \quad \forall j = 1, \ldots, N$$

in Def. 3.6 are satisfied.

Proof. It holds $V = V^{rest} \cup \left(\bigcup_{j=1}^{N} V_j^{pre} \right)$ because of Def. 3.11 and $\bigcup_{j=1}^{N} V_j^{pre} \subset V$. Moreover it is

$$V^{rest} \cap \left(\bigcup_{j=1,\ldots,N} V_j^{pre} \right) = \emptyset$$

and

$$\bigcup_{j=1,\ldots,N} V_j^{pre} = \bigcup_{j=1,\ldots,N'} V_j^{group} = \bigcup_{j=1,\ldots,N'} V_j^{part}.$$

□

The decomposition of the model is complete.

Lemma 3.7. *It is*

$$\sum_{j=1}^{N'} n_j^{part} + n^{rest} = n,$$

where $n^{rest} := |V^{rest}|$ *and* $n_j^{part} := |V_j^{part}|$ *for all* $j = 1, \ldots, N'$.

Proof. Since the model parts are disjoint, it is

$$\left| \bigcup_{j=1}^{N'} V_j^{part} \right| = \sum_{j=1}^{N'} |V_j^{part}|.$$

Hence it follows

$$n = |V| = |V^{rest}| + \left| \bigcup_{j=1}^{N'} V_j^{part} \right| = n^{rest} + \sum_{j=1}^{N'} n_j^{part},$$

since the rest set is disjoint with all model parts. □

Analogously to the groupings, each model part contains at least one exp-element.

Lemma 3.8. *It holds* $V_j^{part} \cap V^{exp} \neq \emptyset \quad \forall j \in \{1, \dots, N'\}$.

Proof. For $l' = 1$, see Lemma 3.4 and Def. 3.13. It holds for $j_{min}^{l'} \in \{1, \dots, N'\}$, $l' = 2, \dots, N'$,

$$V_{j_{min}^{l'}}^{part} = V_{j_{min}^{l'}}^{group} \cap \left(\neg \left(\bigcup_{l=1}^{l'-1} V_{j_{min}^{l}}^{group} \right) \right)$$

which yields

$$\begin{aligned} V_{j_{min}^{l'}}^{part} \cap V^{exp} &= \left(V_{j_{min}^{l'}}^{group} \cap \left(\neg \left(\bigcup_{l=1}^{l'-1} V_{j_{min}^{l}}^{group} \right) \right) \right) \cap V^{exp} \\ &= \left(V_{j_{min}^{l'}}^{group} \cap V^{exp} \right) \cap \left(\neg \left(\bigcup_{l=1}^{l'-1} V_{j_{min}^{l}}^{group} \right) \right). \end{aligned}$$

Since $V_i^{pre} \cap V^{exp} = \{v_i^{exp}\}$, it is

$$(V_j^{pre} \cap V^{exp}) \cap V_i^{pre} = \{v_j^{exp}\} \cap V_i^{pre} = \emptyset \quad \forall i, j = 1, \dots, N, i \neq j.$$

It follows, since the assignment of the sets of predecessors to groupings is unique,

$$(V_j^{group} \cap V^{exp}) \cap V_i^{group} = \emptyset \quad \forall i, j = 1, \dots, N', i \neq j$$

which for all $l' = 2, \dots, N'$ leads to

$$\bigcup_{l=1}^{l'-1} \left((V_{j_{min}^{l'}}^{group} \cap V^{exp}) \cap V_{j_{min}^{l}}^{group} \right) = (V_{j_{min}^{l'}}^{group} \cap V^{exp}) \cap \left(\bigcup_{l=1}^{l'-1} V_{j_{min}^{l}}^{group} \right) = \emptyset.$$

Since $V_{j_{min}^{l'}}^{group} \cap V^{exp} \neq \emptyset$, it follows

$$\left(V_{j_{min}^{l'}}^{group} \cap V^{exp} \right) \cap \left(\neg \left(\bigcup_{l=1}^{l'-1} V_{j_{min}^{l}}^{group} \right) \right) \neq \emptyset$$

and finally $V_{j_{min}^{l'}}^{part} \cap V^{exp} \neq \emptyset$. □

Corollary 3.2. *It holds* $V_j^{part} \neq \emptyset \quad \forall j \in \{1, \dots, N'\}$.

The model parts can be regarded as subgraphs of G': Define

$$E_j^{part} := \{vv' \in E' | v, v' \in V_j^{part}\}$$

and $G_j^{part} := (V_j^{part}, E_j^{part})$ for all $j = 1, \dots N'$.

3.1.4 Determination of input

Finally, it is necessary to determine which input is necessary in order to solve the model parts separately.

Definition 3.14. The *sets of element input* for the model part V_j^{part}, $j = 1, \ldots, N'$, are defined by

$$\begin{aligned} V_j^{inp} &:= \left\{ v \in V \backslash V_j^{part} | \exists v' \in V_j^{part} : vv' \in E \right\} \\ &= \left\{ v_l \in V \backslash V_j^{part} | \exists v_{l'} \in V_j^{part} : a'_{ll'} = 1 \right\} \end{aligned}$$

and the *sets of parameter input* by

$$P_j^{inp} := \left(\bigcup_{l=1}^{n_j^{part}} P_{V_j^{part}(l)} \right) \backslash P_j^{part}.$$

Two types of element input can be distinguished: $V_j^{inp,app}$, $j = 1, \ldots, N'$, for the input by approximations of non-exp-elements from other model parts and $V_j^{inp,exp}$, $j = 1, \ldots, N'$, for the input by approximations of experimental data. It is

$$V_j^{inp} = V_j^{inp,exp} \cup V_j^{inp,app} \quad \wedge \quad V_j^{inp,exp} \cap V_j^{inp,app} = \emptyset, \quad \forall j \in \{1, \ldots, N'\}.$$

The sets $V_j^{inp,app}$ and $V_j^{inp,exp}$, $j = 1, \ldots N'$, are given by

$$\begin{aligned} V_j^{inp,app} &:= V_j^{inp} \backslash V^{exp} \\ V_j^{inp,exp} &:= V_j^{inp} \backslash V_j^{inp,app}. \end{aligned}$$

Due to the construction of the model parts, there is a $j \in \{1, \ldots, N'\}$ such that $V_j^{inp,app} = \emptyset$ and $P_j^{inp} = \emptyset$, i.e. that the condition $(viii)$ of Def. 3.6 is satisfied which is proved in the next lemma:

Lemma 3.9. *There is a* $j \in \{1, \ldots, N'\}$ *such that* $V_j^{inp,app} = \emptyset \quad \wedge \quad P_j^{inp} = \emptyset$.

Proof. It is $V_{j_{min}^1}^{part} = V_{j_{min}^1}^{group}$, thus it follows $V_{j_{min}^1}^{inp} = \emptyset$ and finally $V_{j_{min}^1}^{inp,app} = \emptyset$. Moreover it holds $P_{j_{min}^1}^{part} = P_{j_{min}^1}^{group}$ which yields

$$P_{j_{min}^1}^{inp} = \left(\bigcup_{l=1}^{n_{j_{min}^1}^{part}} P_{V_{j_{min}^1}^{part}(l)} \right) \backslash P_{j_{min}^1}^{part}$$

and since

$$\bigcup_{l=1}^{n_{j_{min}^1}^{part}} P_{V_{j_{min}^1}^{part}(l)} = \bigcup_{l=1}^{n_{j_{min}^1}^{group}} P_{V_{j_{min}^1}^{group}(l)} = P_{j_{min}^1}^{group} = P_{j_{min}^1}^{part},$$

it follows $P_{j_{min}^1}^{inp} = \emptyset$. □

Thus the parameter estimation can be started with the model part $V^{part}_{j^1_{min}}$, as it does not need any input from other model parts (if at all input of approximations of experimental data). After parameter estimation of this model part, approximations of its elements can be generated that can serve as input for the remaining model parts in the further parameter estimation. If there are several model parts that do not require input (except for exp-elements), then parameter estimation can be performed parallelly.

3.2 Decomposition of GynCycle

In this section, the model decomposition is performed for GynCycle which is derived in Chapter 2 (originally in [67]) and the results are visualized.

3.2.1 Graph representation

The model presented in the preceding chapter consists of 49 elements. Experimental data are available for the elements (see appendix)

- y_1 (GnRH pulse frequency),
- y_8 (LH),
- y_{10} (FSH),
- y_{42} (progesterone),
- y_{43} (estradiol),
- y_{44} (17α-hydroxypregnenolone),
- y_{45} (17α-hydroxyprogesterone),
- y_{46} (DHEA),
- y_{47} (androstenedione),
- y_{48} (testosterone), and
- y_{49} (estrone).

Since the dynamics of inhibin, for which experimental data are also available, is not described by a differential equation (it is calculated as a linear combination of the follicular masses y_{12}, y_{17}, and y_{18}), it is represented by the element y_{50}. The additional arcs e for y_{50} are given if

$$\begin{aligned} \frac{\partial f_i}{\partial y_{50}} \neq 0 \quad &\Rightarrow \quad init(e) = 50 \quad \wedge \quad ter(e) = i, \\ \frac{\partial y_{50}}{\partial y_i} \neq 0 \quad &\Rightarrow \quad init(e) = i \quad \wedge \quad ter(e) = 50. \end{aligned}$$

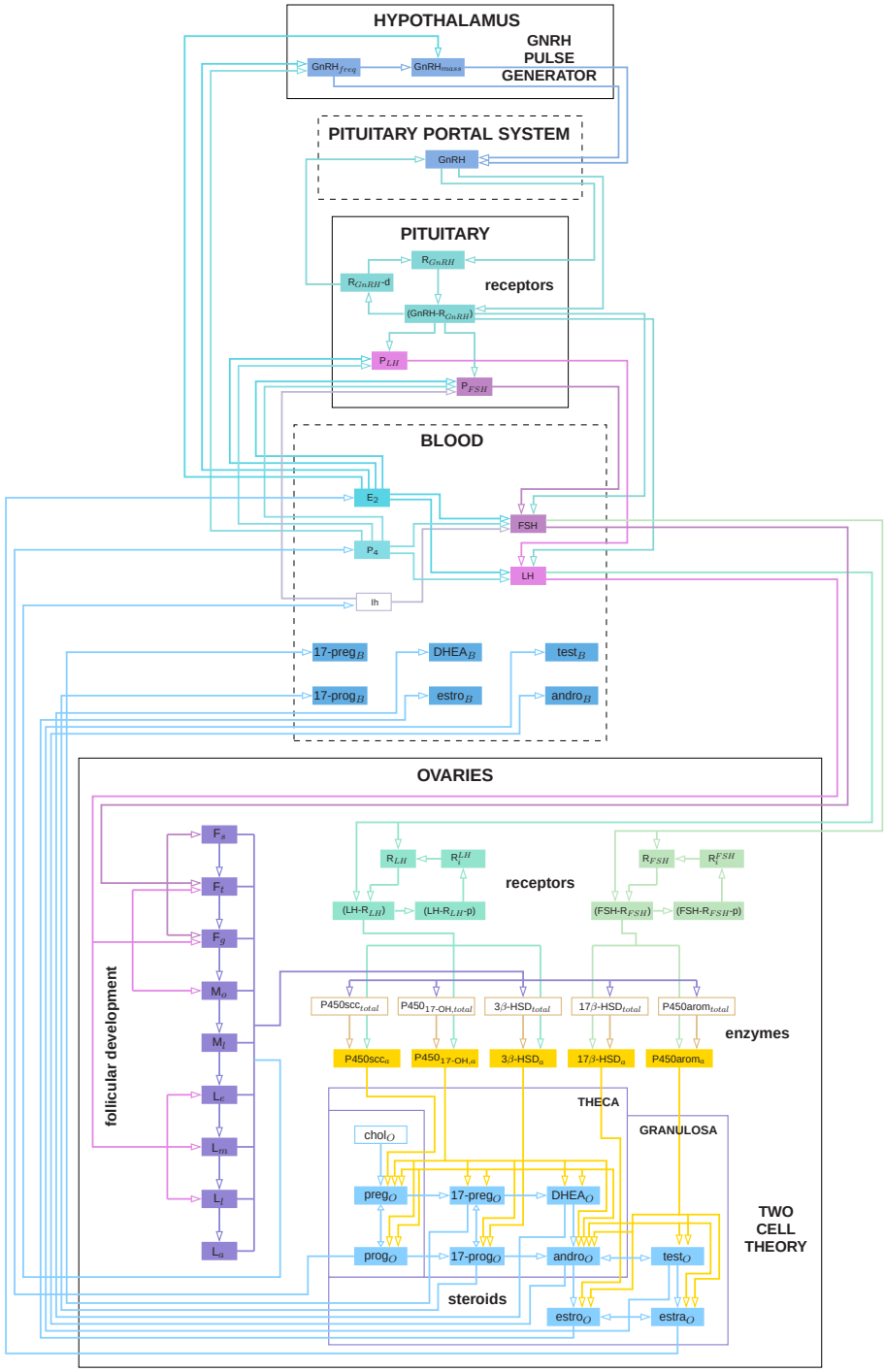

Figure 3.1: The dependencies within the complex model of the human menstrual cycle. An arrow is given if the dynamics of the element where the arrow ends is directly dependent on the element where the arrow starts (without loops).

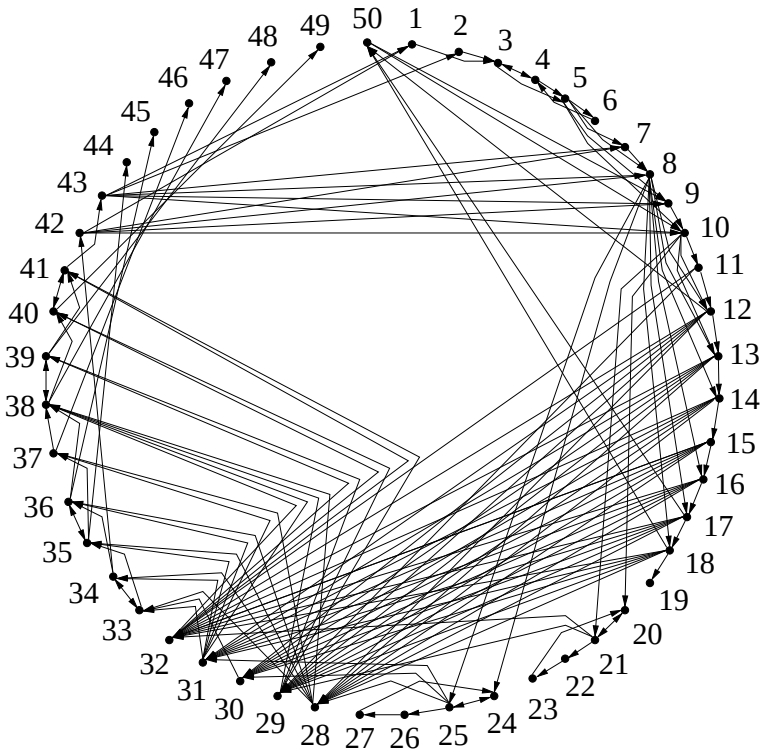

Figure 3.2: Visualization of the graph for the model given in Table 3.6 (without loops).

Hence there is a total of $n = 50$ elements (see Table 3.6 and Fig. 3.1). The graph for this model is visualized in Figure 3.2.

Furthermore, there are $n_p = 208$ parameters and $N = 12$ exp-elements:

$$V^{exp} = \{1, 8, 10, 42, 43, 44, 45, 46, 47, 48, 49, 50\}.$$

3.2.2 Sets of predecessors and groupings

By executing Algorithm 1 for the model in Table 3.6, the following sets of predecessors are obtained:

j	V_j^{pre}
1	1
2	2, 3, 4, 5, 6, 7, 8
3	2, 3, 4, 5, 6, 9, 10
4	11, 12, 13, 14, 15, 16, 17, 18, 24, 25, 26, 27, 28, 30, 31, 33, 34, 42
5	11, 12, 13, 14, 15, 16, 17, 18, 20, 21, 22, 23, 24, 25, 26, 27, 28, 29, 30, 31, 32, 33, 34, 35, 36, 37, 38, 39, 40, 41, 43
6	11, 12, 13, 14, 15, 16, 17, 18, 24, 25, 26, 27, 28, 30, 31, 33, 34, 35, 36, 44
7	11, 12, 13, 14, 15, 16, 17, 18, 24, 25, 26, 27, 28, 30, 31, 33, 34, 35, 36, 45
8	11, 12, 13, 14, 15, 16, 17, 18, 24, 25, 26, 27, 28, 30, 31, 33, 34, 35, 36, 37, 46

j	V_j^{pre}
9	11, 12, 13, 14, 15, 16, 17, 18, 20, 21, 22, 23, 24, 25, 26, 27, 28, 29, 30, 31, 32, 33, 34, 35, 36, 37, 38, 39, 47
10	11, 12, 13, 14, 15, 16, 17, 18, 20, 21, 22, 23, 24, 25, 26, 27, 28, 29, 30, 31, 32, 33, 34, 35, 36, 37, 38, 39, 48
11	11, 12, 13, 14, 15, 16, 17, 18, 20, 21, 22, 23, 24, 25, 26, 27, 28, 29, 30, 31, 32, 33, 34, 35, 36, 37, 38, 39, 40, 41, 49
12	11, 12, 13, 14, 15, 16, 17, 18, 50

Only the vertex v_{19} is not a predecessor of an element of V^{exp} thus the rest set consists of this element:

$$V^{rest} = \{19\}.$$

By executing Algorithm 2 for the model in Table 3.6, the following groupings are obtained:

j	V_j^{group}
1	1
2	2, 3, 4, 5, 6, 7, 8
3	2, 3, 4, 5, 6, 9, 10
4	11, 12, 13, 14, 15, 16, 17, 18, 24, 25, 26, 27, 28, 30, 31, 33, 34, 42
5	11, 12, 13, 14, 15, 16, 17, 18, 20, 21, 22, 23, 24, 25, 26, 27, 28, 29, 30, 31, 32, 33, 34, 35, 36, 37, 38, 39, 40, 41, 43, 49
6	11, 12, 13, 14, 15, 16, 17, 18, 24, 25, 26, 27, 28, 30, 31, 33, 34, 35, 36, 44, 45
7	11, 12, 13, 14, 15, 16, 17, 18, 24, 25, 26, 27, 28, 30, 31, 33, 34, 35, 36, 37, 46
8	11, 12, 13, 14, 15, 16, 17, 18, 20, 21, 22, 23, 24, 25, 26, 27, 28, 29, 30, 31, 32, 33, 34, 35, 36, 37, 38, 39, 47, 48
9	11, 12, 13, 14, 15, 16, 17, 18, 50

The number of sets is reduced from $N = 12$ to $N' = 9$. It is $V_i^{group} = V_i^{pre}$ for $j = 1, \ldots, 4$, $V_5^{group} = V_5^{pre} \cup V_{11}^{pre}$, $V_6^{group} = V_6^{pre} \cup V_7^{pre}$, $V_7^{pre} = V_8^{pre}$, $V_8^{group} = V_9^{pre} \cup V_{10}^{pre}$, and $V_9^{group} = V_{12}^{pre}$.

3.2.3 Model parts

By executing Algorithm 3 for the model in Table 3.6, the following disjoint model parts are obtained:

j	V_j^{part}
1	1
2	2, 3, 4, 5, 6, 7, 8
3	9, 10
4	24, 25, 26, 27, 28, 30, 31, 33, 34, 42
5	40, 41, 43, 49
6	35, 36, 44, 45

j	V_j^{part}
7	$37, 46$
8	$20, 21, 22, 23, 29, 32, 38, 39, 47, 48$
9	$11, 12, 13, 14, 15, 16, 17, 18, 50$

3.2.4 Input

The following required input for the model parts of the model in Table 3.6 is obtained:

j	$V_j^{inp,exp}$	$V_j^{inp,app}$	P_j^{inp}
1	$42,\ 43$	$-$	$-$
2	$1, 42, 43$	$-$	$7, 8$
3	$42, 43, 50$	5	$7, 8, 38$
4	8	$12, 13, 14, 15, 16, 17, 18$	$38, 70$
5	$-$	$29, 32, 38, 39$	$38, 173, 174, 176, 177$
6	$-$	$28, 31, 33, 34$	$38, 150, 151, 153, 154$
7	$-$	$28, 31, 35$	$38, 160, 161$
8	10	$11, 12, 13, 14, 15, 16, 17, 18, 28, 31, 36, 37$	$38, 163, 164, 166, 167$
9	$8, 10$	$-$	$-$

Hence it is possible to start parameter estimation with the two model parts V_1^{part} and V_9^{part} since $V_1^{inp,app} = \emptyset \wedge P_1^{inp} = \emptyset$ and $V_9^{inp,app} = \emptyset \wedge P_9^{inp} = \emptyset$.

3.2.5 Result

As result, the different disjoint model parts as well as the arcs between the model parts are obtained. There is an arc from a first model part to a second model part, if there is an arc of one vertex of the first model part to a vertex of the second model part. The result is presented in Table 3.2.5 as well as visualized in Figure 3.3.

Table 3.5: The results of the model decomposition for the mathematical model with 49 differential equations and an equation for inhibin ($n = 50$) as well as of the $n_p = 208$ parameters (Table 3.6).

j	Name	V_j^{part}/V^{rest}	$V^{exp} \cap V_j^{part}$	P_j^{part}/P^{rest}	$V_j^{inp,exp}$	$V_j^{inp,app}$	P_j^{inp}	$\lvert V_j^{part}\rvert$	$\lvert P_j^{part}\rvert$
1	GnRH	1	1	$1,\dots,8$	$42,43$	–	–	1	8
2	LH	$2,\dots,8$	8	$9,\dots,40$	$1,42,43$	–	7, 8 (GnRH)	7	32
3	FSH	$9,10$	10	$41,\dots,54$, $59,60$	$42,43,50$	5	7, 8 (GnRH), 38 (LH)	2	16
4	P_4	$24,\dots,28$, $30,31,33$, $34,42$	42	$93,\dots,106$, $117,\dots,134$, $145,\dots,155$, $185,186,187$	8	$12,\dots,18$	38 (LH), 70 (Ih)	10	46
5	estro, E_2	$40,41,43$, 49	$43,49$	$179,\dots,184$, $188,189,190$, $206,207,208$	–	$29,32,38$, 39	38 (LH), $173,174$, $176,177$ (andro, test)	4	12
6	17preg, 17prog	$35,36,44$, 45	$44,45$	$156,\dots,165$, $191,\dots,196$	–	$28,31,33$, 34	38 (LH), $150,151$, $153,154$ (P_4)	4	16
7	DHEA	$37,46$	46	$166,167,168$, $197,198,199$	–	$28,31,35$	38 (LH), $160,161$ (17preg, 17prog)	2	6
8	andro, test	$20,\dots,23$, $29,32,38$, $39,47,48$	$47,48$	$88,\dots,92$, $107,\dots,116$, $135,\dots,144$, $169,\dots,178$, $200,\dots,205$	10	$11,\dots,18$, $28,31,36$, 37	38 (LH), 64 (Ih), $163,164$ (17preg, 17prog), $166,167$ (DHEA)	10	41
9	Ih	$11,\dots,18$, 50	50	$55,\dots,58$, $61,\dots,86$	$8,10$	–	–	9	30
	rest set	19	–	87	–	18	86 (Ih)	1	1
								$\sum = 50$	$\sum = 208$

The dependencies among the model parts and parameter parts forcing a certain order of parameter estimation are visualized in Figs. 3.4 and 3.5.

The model parts can be classified in three groups of model parts that could be treated parallelly in parameter estimation:

$$\begin{array}{lllllllllll} V_1^{part} & & & & & & & & & & \\ V_2^{part} & \rightarrow & V_3^{part} & & & & & & & & \\ V_9^{part} & \rightarrow & V_4^{part} & \rightarrow & V_6^{part} & \rightarrow & V_7^{part} & \rightarrow & V_8^{part} & \rightarrow & V_5^{part}. \end{array}$$

Since the order for the parameter parts is more restrictive:

$$\left((P_1^{part} \rightarrow P_2^{part} \rightarrow P_3^{part}),\ P_9^{part}\right) \rightarrow P_4^{part} \rightarrow P_6^{part} \rightarrow P_7^{part} \rightarrow P_8^{part} \rightarrow P_5^{part},$$

where $P_1^{part} \rightarrow P_2^{part} \rightarrow P_3^{part}$ and P_9^{part} can be treated parallelly, the model parts must be determined in this order, too. Thus the order of parameter estimation is given by

$$\left(((P_1^{part}, V_1^{part}) \rightarrow (P_2^{part}, V_2^{part}) \rightarrow (P_3^{part}, V_3^{part})),\ (P_9^{part}, V_9^{part})\right) \rightarrow (P_4^{part}, V_4^{part})$$
$$\rightarrow (P_6^{part}, V_6^{part}) \rightarrow (P_7^{part}, V_7^{part}) \rightarrow (P_8^{part}, V_8^{part}) \rightarrow (P_5^{part}, V_5^{part}).$$

where $(P_1^{part}, V_1^{part}) \rightarrow (P_2^{part}, V_2^{part}) \rightarrow (P_3^{part}, V_3^{part})$ and (P_9^{part}, V_9^{part}) can be treated parallelly.

3.3 Summary

A method for simplifying the parameter estimation in the case of a large model in physiology is developed here. In order to be able to apply this procedure, it is necessary that experimental data are provided for at least two of the elements. The more experimental data is available, the smaller the model parts become on average. The mathematical basis is, for example, a system of differential equations. With the help of these model parts, it is possible to perform parameter estimation for smaller dimensions. At the end, the model parts can be recomposed replacing the input of approximations of experimental data by the corresponding elements of other model parts resulting in a dynamic model.

The detailed procedure for the determination of the model parts can be summarized as follows:

1. transformation of the mathematical model into the corresponding graph
2. calculation of the adjacency matrix
3. defining the set of exp-elements
4. reducing the graph by removing the arcs starting in exp-elements
5. determining the sets of predecessors, the elements whereupon the exp-elements depend

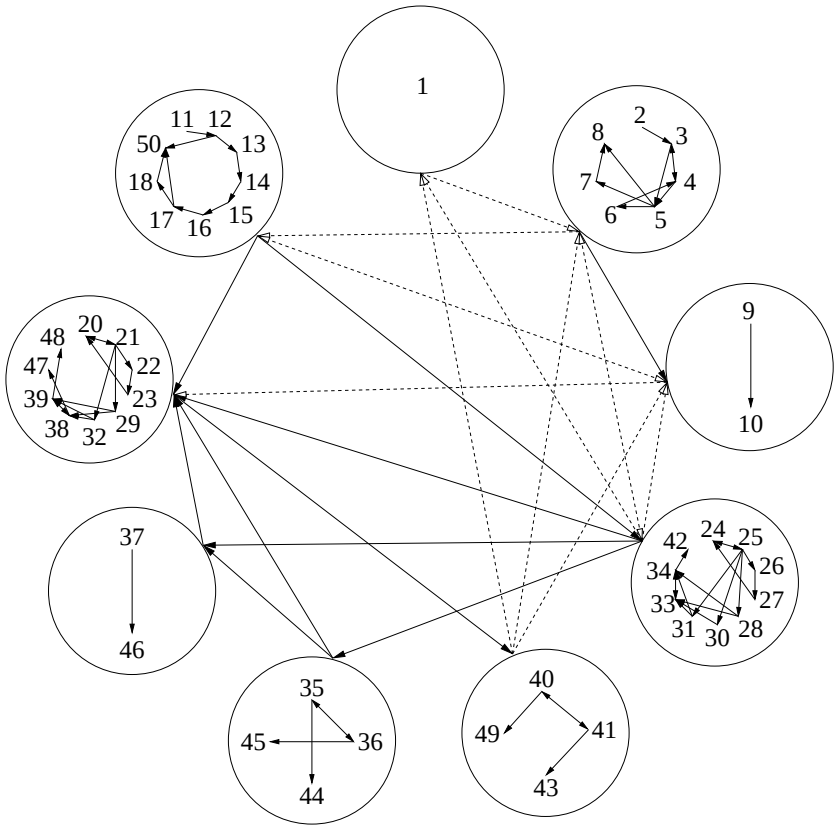

Figure 3.3: Visualization of the subgraphs G_j^{part}, $j = 1, \ldots, N'$, representing the model parts without the rest set V^{rest}. The arc from G_i^{part} to G_j^{part} is given if $V_i^{part} \cap V_j^{inp} \neq \emptyset$. If $V_i^{part} \cap V_j^{inp,app} = \emptyset$, the arc is dotted, otherwise it is solid.

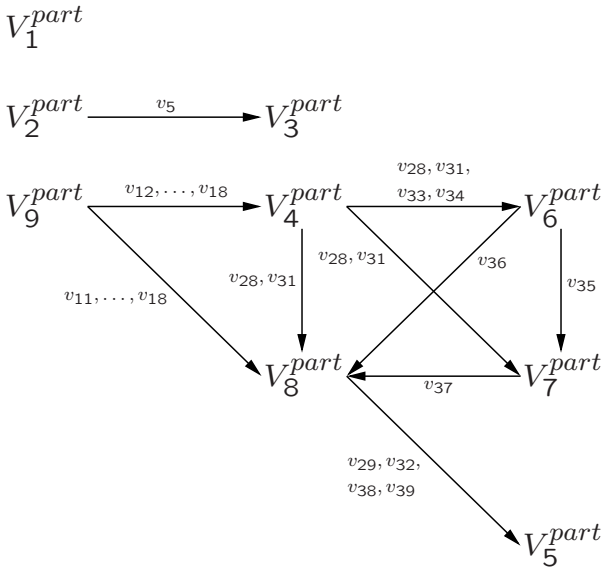

Figure 3.4: Dependency of the model parts (only input of approximations is considered).

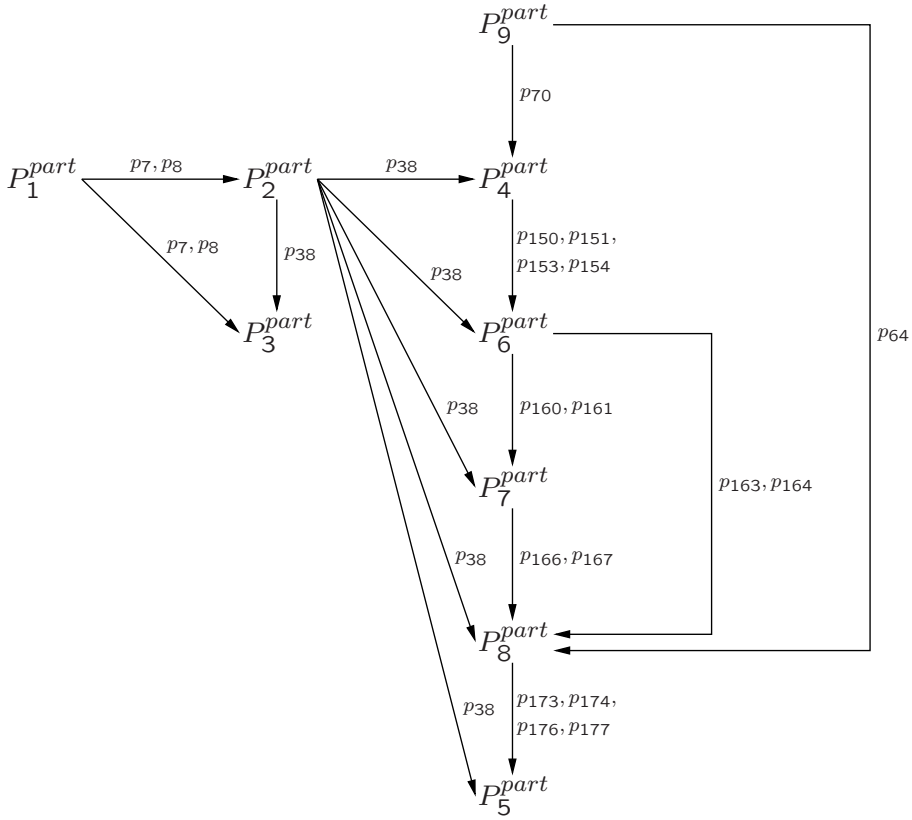

Figure 3.5: Dependency of the parameter parts.

6. merging sets of predecessors to groupings if they match except for the exp-element
7. subsequently finding the grouping with the smallest number of parameters (if unique) and remove the elements of this grouping from the other groupings in order to obtain disjoint model parts
8. determining the direct predecessors of the elements of the model parts and distinguish between exp-elements and elements that need to be approximated (non-exp-elements).

Finally, a decomposition of the model into disjoint model parts is obtained. This decomposition is not necessarily complete. It is possible that there are elements that do not belong to one of the model parts forming the rest set. These elements cannot be estimated.

An example of the functionality is presented showing that it is possible to reduce the dimension of the problem $n = 50$ to $N' = 10$ problems with a dimension of order in the range of 1 to 10. The number of parameters of each parameter part is between 6 and 46 instead of $n_p = 208$. And it is partly possible to perform parameter estimation parallelly which reduces the total time for solving this optimization problem.

This occurs if there is more than one model part that, if at all, needs input from approximations of experimental data. That means that in this case parameter estimation can be performed independently from the other model parts. If there is more than one part with these conditions, it is possible to start parameter estimation with all of these model parts simultaneously. This could reduce the time that is needed to perform parameter estimation for all model parts and for the entire model in the end.

Table 3.6: Model equations for the human menstrual cycle. The 49 delay differential equations and one equation for the exp-element y_{50} are listed. In the first column, the delay differential equations are consecutively numbered. The corresponding elements are given in the second and the equations in the third column.

no	element	equation
1	GnRH_{freq}	$\frac{d}{dt}y_1(t) = \frac{p_3^{p_4}}{p_3^{p_4}+y_{42}(t-p_7)^{p_4}} \cdot \left(1 + \frac{y_{43}(t-p_8)^{p_6}}{p_5^{p_6}+y_{43}(t-p_8)^{p_6}}\right) \cdot p_2$ $y_1(T_j) - y_1(T_{j-1}) = (-\ln(1-U_j))^{\frac{1}{p_1}}, U_j \sim U[0,1], \forall j \in \mathbb{N}$
2	GnRH_{mass}	$\frac{d}{dt}y_2(t) = \left(\frac{p_{10}^{p_{11}}}{p_{10}^{p_{11}}+y_{43}(t-p_8)^{p_{11}}} + \frac{y_{43}(t-p_8)^{p_{13}}}{p_{12}^{p_{13}}+y_{43}(t-p_8)^{p_{13}}}\right) \cdot p_9$
3	GnRH	$\frac{d}{dt}y_3(t) = \frac{p_{16}}{p_{17}} + \frac{y_2(T_j)-y_2(T_{j-1})}{p_{17}} \cdot \frac{p_{18}^{p_{19}}}{\Gamma(p_{19})} \cdot (t-T_j)^{p_{19}-1} \cdot \exp(-p_{18} \cdot (t-T_j))$ $- p_{14} \cdot y_3(t) - p_{15} \cdot y_3(t) \cdot y_4(t), \quad t \in [T_j, T_{j+1}), \quad \forall j \in \mathbb{N}$
4	R_{GnRH}	$\frac{d}{dt}y_4(t) = p_{22} \cdot \frac{p_{23}-y_3(t)}{p_{23}+y_3(t)} + p_{21} \cdot y_6(t) - p_{20} \cdot y_3(t) \cdot y_4(t)$
5	($\mathrm{GnRH\text{-}R}_{GnRH}$)	$\frac{d}{dt}y_5(t) = p_{20} \cdot y_3(t) \cdot y_4(t) - p_{24} \cdot y_5(t)$
6	R_{GnRH}-d	$\frac{d}{dt}y_6(t) = p_{24} \cdot y_5(t) - p_{21} \cdot y_6(t)$
7	P_{LH}	$\frac{d}{dt}y_7(t) = p_{25} + \frac{p_{26}^{p_{27}}}{p_{26}^{p_{27}}+y_{42}(t-p_7)^{p_{27}}} \cdot \frac{y_{43}(t-p_8)^{p_{29}}}{p_{28}^{p_{29}}+y_{43}(t-p_8)^{p_{29}}} \cdot p_{30} - \frac{y_{42}(t-p_7)^{p_{36}}}{p_{35}^{p_{36}}+y_{42}(t-p_7)^{p_{36}}}$ $\cdot \left(\frac{p_{31}^{p_{32}}}{p_{31}^{p_{32}}+y_{43}(t-p_8)^{p_{32}}} + \frac{y_{43}(t-p_8)^{p_{34}}}{p_{33}^{p_{34}}+y_{43}(t-p_8)^{p_{34}}}\right) \cdot p_{37} \cdot y_5(t) \cdot y_7(t)$
8	LH	$\frac{d}{dt}y_8(t) = \frac{p_{37}}{p_{38}} \cdot \left(\frac{p_{31}^{p_{32}}}{p_{31}^{p_{32}}+y_{43}(t-p_8-p_{39})^{p_{32}}} + \frac{y_{43}(t-p_8-p_{39})^{p_{34}}}{p_{33}^{p_{34}}+y_{43}(t-p_8-p_{39})^{p_{34}}}\right)$ $\cdot \frac{y_{42}(t-p_7-p_{39})^{p_{36}}}{p_{35}^{p_{36}}+y_{42}(t-p_7-p_{39})^{p_{36}}} \cdot y_5(t-p_{39}) \cdot y_7(t-p_{39}) - p_{40} \cdot y_8(t)$

Table 3.6: Model equations for the human menstrual cycle. The 49 delay differential equations and one equation for the exp-element y_{50} are listed. In the first column, the delay differential equations are consecutively numbered. The corresponding elements are given in the second and the equations in the third column.

no	element	equation
9	P_{FSH}	$\frac{d}{dt}y_9(t) = p_{41} + \frac{p_{42}^{p_{43}}}{p_{42}^{p_{43}}+y_{50}(t-p_{45})^{p_{43}}} \cdot p_{44}$ $- \frac{y_{42}(t-p_7)^{p_{51}}}{p_{50}^{p_{51}}+y_{42}(t-p_7)^{p_{51}}} \cdot \frac{p_{52}^{p_{53}}}{p_{52}^{p_{53}}+y_{50}(t-p_{45})^{p_{53}}}$ $\cdot \left(\frac{p_{46}^{p_{47}}}{p_{46}^{p_{47}}+y_{43}(t-p_8)^{p_{47}}} + \frac{y_{43}(t-p_8)^{p_{49}}}{p_{48}^{p_{49}}+y_{43}(t-p_8)^{p_{49}}}\right) \cdot p_{54} \cdot y_5(t) \cdot y_9(t)$
10	FSH	$\frac{d}{dt}y_{10} = \frac{p_{54}}{p_{38}} \cdot \left(\frac{p_{46}^{p_{47}}}{p_{46}^{p_{47}}+y_{43}(t-p_8-p_{59})^{p_{47}}} + \frac{y_{43}(t-p_8-p_{59})^{p_{49}}}{p_{48}^{p_{49}}+y_{43}(t-p_8-p_{59})^{p_{49}}}\right)$ $\cdot \frac{y_{42}(t-p_7-p_{59})^{p_{51}}}{p_{50}^{p_{51}}+y_{42}(t-p_7-p_{59})^{p_{51}}} \cdot \frac{p_{52}^{p_{53}}}{p_{52}^{p_{53}}+y_{50}(t-p_{45}-p_{59})^{p_{53}}}$ $\cdot y_5(t-p_{59}) \cdot y_9(t-p_{59}) - p_{60} \cdot y_{10}(t)$
11	F_s	$\frac{d}{dt}y_{11}(t) = p_{61} \cdot \frac{y_{10}(t-p_{64})^{p_{63}}}{p_{62}^{p_{63}}+y_{10}(t-p_{64})^{p_{63}}} + \big(p_{65} \cdot y_{10}(t-p_{64})^{p_{67}}$ $- p_{66} \cdot y_{10}(t-p_{64})^{p_{68}}\big) \cdot y_{11}(t)$
12	F_t	$\frac{d}{dt}y_{12}(t) = p_{66} \cdot y_{10}(t-p_{64})^{p_{68}} \cdot y_{11}(t) + \big(p_{69} \cdot y_{10}(t-p_{64})^{p_{72}} \cdot y_8(t-p_{70})^{p_{73}}$ $- p_{71} \cdot y_{10}(t-p_{64})^{p_{74}} \cdot y_8(t-p_{70})^{p_{75}}\big) \cdot y_{12}(t)$
13	F_g	$\frac{d}{dt}y_{13}(t) = p_{71} \cdot y_{10}(t-p_{64})^{p_{74}} \cdot y_8(t-p_{70})^{p_{75}} \cdot y_{12}(t)$ $+ p_{76} \cdot y_8(t-p_{70})^{p_{78}} \cdot y_{13}(t) - p_{77} \cdot y_8(t-p_{70})^{p_{79}} \cdot y_{13}(t)$
14	M_o	$\frac{d}{dt}y_{14}(t) = p_{77} \cdot y_8(t-p_{70})^{p_{79}} \cdot y_{13}(t) - p_{80} \cdot y_{14}(t)$
15	M_l	$\frac{d}{dt}y_{15}(t) = p_{80} \cdot y_{14}(t) - p_{81} \cdot y_{15}(t)$
16	L_e	$\frac{d}{dt}y_{16}(t) = p_{81} \cdot y_{15}(t) - p_{82} \cdot y_8(t-p_{70})^{p_{83}} \cdot y_{16}(t)$
17	L_m	$\frac{d}{dt}y_{17}(t) = p_{82} \cdot y_8(t-p_{70})^{p_{83}} \cdot y_{16}(t) - p_{84} \cdot y_8(t-p_{70})^{p_{85}} \cdot y_{17}(t)$
18	L_l	$\frac{d}{dt}y_{18}(t) = p_{84} \cdot y_8(t-p_{70})^{p_{85}} \cdot y_{17}(t) - p_{86} \cdot y_{18}(t)$
19	L_a	$\frac{d}{dt}y_{19}(t) = p_{86} \cdot y_{18}(t) - p_{87} \cdot y_{19}(t)$
20	R_{FSH}	$\frac{d}{dt}y_{20}(t) = p_{88} \cdot y_{21}(t) + p_{89} \cdot y_{23}(t) - p_{90} \cdot y_{10}(t-p_{64}) \cdot y_{20}(t)$
21	(FSH-R_{FSH})	$\frac{d}{dt}y_{21}(t) = p_{90} \cdot y_{10}(t-p_{64}) \cdot y_{20}(t) - (p_{91}+p_{88}) \cdot y_{21}(t)$
22	(FSH-R_{FSH}-p)	$\frac{d}{dt}y_{22}(t) = p_{91} \cdot y_{21}(t) - p_{92} \cdot y_{22}(t)$
23	R_i^{FSH}	$\frac{d}{dt}y_{23}(t) = p_{92} \cdot y_{22}(t) - p_{89} \cdot y_{23}(t)$
24	R_{LH}	$\frac{d}{dt}y_{24}(t) = p_{93} \cdot y_{25}(t) + p_{94} \cdot y_{27}(t) - p_{95} \cdot y_8(t-p_{70}) \cdot y_{24}(t)$
25	(LH-R_{LH})	$\frac{d}{dt}y_{25}(t) = p_{95} \cdot y_8(t-p_{70}) \cdot y_{24}(t) - (p_{96}+p_{93}) \cdot y_{25}(t)$
26	(LH-R_{LH}-p)	$\frac{d}{dt}y_{26}(t) = p_{96} \cdot y_{25}(t) - p_{97} \cdot y_{26}(t)$
27	R_i^{LH}	$\frac{d}{dt}y_{27}(t) = p_{97} \cdot y_{26}(t) - p_{94} \cdot y_{27}(t)$
28	3β-HSD_a	$\frac{d}{dt}y_{28}(t) = p_{98} \cdot \left(\sum_{i=1}^{7} p_{99+i} \cdot y_{11+i}(t)\right) \cdot y_{25}(t) - p_{99} \cdot y_{28}(t)$
29	17β-HSD_a	$\frac{d}{dt}y_{29}(t) = p_{107} \cdot \left(\sum_{i=1}^{8} p_{108+i} \cdot y_{10+i}(t)\right) \cdot y_{21}(t) - p_{108} \cdot y_{29}(t)$
30	P450scc$_a$	$\frac{d}{dt}y_{30}(t) = p_{117} \cdot \left(\sum_{i=1}^{7} p_{118+i} \cdot y_{11+i}(t)\right) \cdot y_{25}(t) - p_{118} \cdot y_{30}(t)$
31	$P450_{17\text{-}OH,a}$	$\frac{d}{dt}y_{31}(t) = p_{126} \cdot \left(\sum_{i=1}^{7} p_{127+i} \cdot y_{11+i}(t)\right) \cdot y_{25}(t) - p_{127} \cdot y_{31}(t)$
32	P450arom$_a$	$\frac{d}{dt}y_{32}(t) = p_{135} \cdot \left(\sum_{i=1}^{8} p_{136+i} \cdot y_{10+i}(t)\right) \cdot y_{21}(t) - p_{136} \cdot y_{32}(t)$
33	preg$_O$	$\frac{d}{dt}y_{33}(t) = p_{145} \cdot y_{30}(t) - y_{28}(t) \cdot \frac{p_{146} \cdot y_{33}(t) - p_{147} \cdot y_{34}(t)}{p_{148}+y_{33}(t)+p_{149} \cdot y_{34}(t)}$ $- p_{150} \cdot y_{31}(t) \cdot \frac{y_{33}(t)}{p_{151}+y_{33}(t)} - p_{152} \cdot y_{33}(t)$
34	prog$_O$	$\frac{d}{dt}y_{34}(t) = y_{28}(t) \cdot \frac{p_{146} \cdot y_{33}(t) - p_{147} \cdot y_{34}(t)}{p_{148}+y_{33}(t)+p_{149} \cdot y_{34}(t)} - p_{153} \cdot y_{31}(t) \cdot \frac{y_{34}(t)}{p_{154}+y_{34}(t)}$ $- p_{155} \cdot y_{34}(t)$
35	17-preg$_O$	$\frac{d}{dt}y_{35}(t) = p_{150} \cdot y_{31}(t) \cdot \frac{y_{33}(t)}{p_{151}+y_{33}(t)} - y_{28}(t) \cdot \frac{p_{156} \cdot y_{35}(t) - p_{157} \cdot y_{36}(t)}{p_{158}+y_{35}(t)+p_{159} \cdot y_{36}(t)}$ $- p_{160} \cdot y_{31}(t) \cdot \frac{y_{35}(t)}{p_{161}+y_{35}(t)} - p_{162} \cdot y_{35}(t)$

Table 3.6: Model equations for the human menstrual cycle. The 49 delay differential equations and one equation for the exp-element y_{50} are listed. In the first column, the delay differential equations are consecutively numbered. The corresponding elements are given in the second and the equations in the third column.

no	element	equation
36	17-prog$_O$	$\frac{d}{dt}y_{36}(t) = p_{153}\cdot y_{31}(t)\cdot\frac{y_{34}(t)}{p_{154}+y_{34}(t)} + y_{28}(t)\cdot\frac{p_{156}\cdot y_{35}(t)-p_{157}\cdot y_{36}(t)}{p_{158}+y_{35}(t)+p_{159}\cdot y_{36}(t)}$ $- p_{163}\cdot y_{31}(t)\cdot\frac{y_{36}(t)}{p_{164}+y_{36}(t)} - p_{165}\cdot y_{36}(t)$
37	DHEA$_O$	$\frac{d}{dt}y_{37}(t) = p_{160}\cdot y_{31}(t)\cdot\frac{y_{35}(t)}{p_{161}+y_{35}(t)} - p_{166}\cdot y_{28}(t)\cdot\frac{y_{37}(t)}{p_{167}+y_{37}(t)}$ $- p_{168}\cdot y_{37}(t)$
38	andro$_O$	$\frac{d}{dt}y_{38}(t) = p_{163}\cdot y_{31}(t)\cdot\frac{y_{36}(t)}{p_{164}+y_{36}(t)} + p_{166}\cdot y_{28}(t)\cdot\frac{y_{37}(t)}{p_{167}+y_{37}(t)}$ $- y_{29}(t)\cdot\frac{p_{169}\cdot y_{38}(t)-p_{170}\cdot y_{39}(t)}{p_{171}+y_{38}(t)+p_{172}\cdot y_{39}(t)} - p_{173}\cdot y_{32}(t)\cdot\frac{y_{38}(t)}{p_{174}+y_{38}(t)}$ $- p_{175}\cdot y_{38}(t)$
39	test$_O$	$\frac{d}{dt}y_{39}(t) = y_{29}(t)\cdot\frac{p_{169}\cdot y_{38}(t)-p_{170}\cdot y_{39}(t)}{p_{171}+y_{38}(t)+p_{172}\cdot y_{39}(t)} - p_{176}\cdot y_{32}(t)\cdot\frac{y_{39}(t)}{p_{177}+y_{39}(t)}$ $- p_{178}\cdot y_{39}(t)$
40	estro$_O$	$\frac{d}{dt}y_{40}(t) = p_{173}\cdot y_{32}(t)\cdot\frac{y_{38}(t)}{p_{174}+y_{38}(t)} - y_{29}(t)\cdot\frac{p_{179}\cdot y_{40}(t)-p_{180}\cdot y_{41}(t)}{p_{181}+y_{40}(t)+p_{182}\cdot y_{41}(t)}$ $- p_{183}\cdot y_{40}(t)$
41	estra$_O$	$\frac{d}{dt}y_{41}(t) = p_{176}\cdot y_{32}(t)\cdot\frac{y_{39}(t)}{p_{177}+y_{39}(t)} + y_{29}(t)\cdot\frac{p_{179}\cdot y_{40}(t)-p_{180}\cdot y_{41}(t)}{p_{181}+y_{40}(t)+p_{182}\cdot y_{41}(t)}$ $- p_{184}\cdot y_{41}(t)$
42	P_4	$\frac{d}{dt}y_{42}(t) = \frac{p_{185}}{p_{38}}\cdot y_{34}(t-p_{186}) - p_{187}\cdot y_{42}(t)$
43	E_2	$\frac{d}{dt}y_{43}(t) = \frac{p_{188}}{p_{38}}\cdot y_{41}(t-p_{189}) - p_{190}\cdot y_{43}(t)$
44	17-preg$_B$	$\frac{d}{dt}y_{44}(t) = \frac{p_{191}}{p_{38}}\cdot y_{35}(t-p_{192}) - p_{193}\cdot y_{44}(t)$
45	17-prog$_B$	$\frac{d}{dt}y_{45}(t) = \frac{p_{194}}{p_{38}}\cdot y_{36}(t-p_{195}) - p_{196}\cdot y_{45}(t)$
46	DHEA$_B$	$\frac{d}{dt}y_{46}(t) = \frac{p_{197}}{p_{38}}\cdot y_{37}(t-p_{198}) - p_{199}\cdot y_{46}(t)$
47	andro$_B$	$\frac{d}{dt}y_{47}(t) = \frac{p_{200}}{p_{38}}\cdot y_{38}(t-p_{201}) - p_{202}\cdot y_{47}(t)$
48	test$_B$	$\frac{d}{dt}y_{48}(t) = \frac{p_{203}}{p_{38}}\cdot y_{39}(t-p_{204}) - p_{205}\cdot y_{48}(t)$
49	estro$_B$	$\frac{d}{dt}y_{49}(t) = \frac{p_{206}}{p_{38}}\cdot y_{40}(t-p_{207}) - p_{208}\cdot y_{49}(t)$
50	Ih	$y_{50}(t) = p_{55} + p_{56}\cdot y_{12}(t) + p_{57}\cdot y_{17}(t) + p_{58}\cdot y_{18}(t)$

Chapter 4

Simulation of GynCycle

A model for the female menstrual cycle, called GynCycle, is developed in Chapter 2 and decomposed into model parts in Chapter 3. The next step is to choose adequate numerical tools for the numerical integration of GynCycle and to determine suitable parameter values for performing simulations that are in accordance with the given experimental data (see appendix).

In this chapter the different steps that lead to the simulation of GynCycle are shown. With the model decomposition presented in Chapter 3, the first step is done. Here important approaches and auxiliary means are presented that are used for obtaining the parameter values.

First the numerical integration of GynCycle, i.e. the solver and the integration of the pulse generator into this solver, is presented in Section 4.1. Then it is shown how the parameter values are obtained. Not all parameters are suited for use in the parameter estimation. Those which are suitable can be determined via sensitivity analysis (even if the result only holds for the current state) which is presented in Section 4.2. Then in Section 4.3, after some remarks concerning the parameter estimation for GynCycle are made, the most sensitive parameters are identified and the parameter values are listed in the appendix. Finally the simulations of GynCycle are shown in Section 4.4.

4.1 Numerical integration

In the following set w.l.o.g. $t_0 := 0$. The mathematical model GynCycle is a non-autonomous system of DDEs (see Section 1.4)

$$\begin{aligned} y'(t) &= f(t; y(t); y(t-\tau_1), \ldots, y(t-\tau_m)), \quad t \geq 0, \\ y(t) &= \phi(t), \qquad\qquad\qquad\qquad\qquad\quad t \leq 0, \end{aligned} \tag{4.1}$$

where $y : \mathbb{R} \to \mathbb{R}^n$, $f : \mathbb{R} \times \mathbb{R}^{n\times(m+1)} \to \mathbb{R}^n$, $n, m \in \mathbb{N}$, and $\tau_i \in \mathbb{R}_+$, $i = 1, \ldots, m$, denote multiple, constant, thus state-independent delays and $\phi : \mathbb{R} \to \mathbb{R}^n$ the initial function.

In this section first some comments concerning the choice of the solver are made. Then the solver that is used here, RADAR5, is presented in more detail. Since the

deterministic system of delay differential equations is coupled with a stochastic model for the pulse generator in GynCycle, the solver must be expanded.

4.1.1 Choice of the solver

The problem of solving GynCycle is stiff. There are various definitions for *stiffness*. Roughly said, if implicit solvers are successful as opposed to explicit solvers, the system is stiff [19]. Here the assumption is allowed that GynCycle is stiff, since the explicit DDE solver dde23 (Matlab) takes much more time in comparison to the implicit DDE solver RADAR5 (Fortran90) even for relatively small time periods (comparing the computing time for the interval $[0, 2]$, the RADAR5 solver is faster than the dde23 solver with a factor of approximately 70; with increasing interval, the factor increases as well).

Here RADAR5, developed and implemented by Guglielmi and Hairer (Version 2.1, Fortran90, 2005), is chosen since it is concipated for a large class of stiff delay differential equations and can handle multiple, possibly small delays. Moreover RADAR5 provides good results for GynCycle. According to [35] there is no other code available that can solve general differential-algebraic delay equations with multiple, state-dependent delays.

There are some other, older programs for stiff delay differential equations with multiple delays, e.g. DDE-STRIDE (Fortran77) by Baker, Butcher and Paul (1992) and DIFSUB-DDE (Fortran77) by Bocharov, Marchuk and Romanyukha (1996). DDE-STRIDE is an adaption of the code STRIDE to delay differential equations and neutral problems. This code can solve stiff problems with several state-dependent delays (including vanishing delays). DIFSUB-DDE is an extension of the code DIFSUB by GEAR (based on BDF) to delay differential equations with constant delays. Both are not concipated for general differential-algebraic delay equations. In [35], RADAR5 and DIFSUB-DDE are compared (even though most codes for stiff delay equations (including RADAR5) are still in an experimental stage [35]).

4.1.2 Numerical integration with RADAR5

For the numerical integration of GynCycle, the solver RADAR5 is used which is designed for solving stiff delay differential equations (see above). Collocation methods based on Radau nodes have been successfully applied to stiff ordinary differential equations (e.g. in RADAU5) and they have excellent stability properties also for delay equations [35]. Thus RADAR5 has been developed based on RADAU5.

In this section the numerical method of the integrator RADAR5 is presented.

Problem formulation

RADAR5 is concipated for initial value problems of a general class of (stiff) delay differential equations:

$$\begin{aligned} &M \cdot y'(t) = f(t; y(t); y(\alpha_1(t, y(t))), \ldots, y(\alpha_m(t, y(t)))) \,, \\ &y(t_0) = y_0, \\ &y(t) = \phi(t), \quad t < t_0, \end{aligned}$$

where M is a constant $(n \times n)$-matrix and $\alpha_l(t, y(t)) \leq t$ for all $t \geq t_0$ and for all $l = 1, \ldots, m$. A discontinuity at t_0, i.e. $\phi(t_0) \neq y_0$, is allowed.

In the case of GynCycle, the system is explicit, i.e. it is $M := I$, the delays are constant, i.e. $\alpha_l(t, y(t)) := t - \tau_l$, $l = 1, \ldots, m$, and the initial function is given by $\phi(t) := y_0$ for $t \leq t_0$, i.e. there is no discontinuity at $t_0 = 0$.

Numerical method

Denote the discretization grid by $(t_k)_{k \in \mathbb{N}_0}$, where $t_{k-1} < t_k$ for all $k \in \mathbb{N}$, and the step size by $h_k := t_{k+1} - t_k$, $k \in \mathbb{N}_0$.

As mentioned, a collocation method is used in RADAR5. Generally, a collocation method corresponding to the vector $c := (c_1, \ldots, c_s)^T$ is equivalent to the implicit Runge-Kutta method (b, c, A), where $b := (b_1, \ldots, b_s)^T$ and $A := (a_{ij})_{i,j=1,\ldots,s}$ (see e.g. Theorem 6.36, [19]).

Assume $0 \leq c_1 < \cdots < c_s \leq 1$. The collocation polynomial $u_k(\cdot) \in \mathbb{P}_s^n$, where $\mathbb{P}_s^n$ denotes the polynomial space (of order s and dimension n), must satisfy the $s + 1$ conditions on the interval $[t_k, t_{k+1}]$, $k \in \mathbb{N}_0$:

$$\begin{aligned} &(i) \quad u_k(t_k) = y_k \\ &(ii) \quad u_k'(t_k + c_i \cdot h_k) = f\Big(t_k + c_i \cdot h_k; Y_i^{(k)}; \tilde{Y}_{1,i}^{(k)}, \ldots, \tilde{Y}_{m,i}^{(k)}\Big), \quad i = 1, \ldots, s, \end{aligned}$$

where $Y_i^{(k)} := u_k(t_k + c_i \cdot h_k)$ for all $i = 1, \ldots, s$ and $\tilde{Y}_{l,i}^{(k)}$, $l = 1, \ldots, m$, $i = 1, \ldots, s$, is given by [35]

$$\tilde{Y}_{l,i}^{(k)} := \begin{cases} \phi\Big(\alpha_{l,i}^{(k)}\Big), & \text{if } \alpha_{l,i}^{(k)} < t_0 \\ u_{k'}\Big(\alpha_{l,i}^{(k)}\Big), & \text{if } \alpha_{l,i}^{(k)} \in [t_{k'}, t_{k'+1}], k' \leq k, k' \in \mathbb{N}_0, \end{cases}$$

where $\alpha_{l,i}^{(k)} := \alpha_l\Big(t_k + c_i \cdot h_k, Y_i^{(k)}\Big)$ for all $l = 1, \ldots, m$ and $i = 1, \ldots, s$. It follows then $y_{k+1} = u_k(t_k + h_k)$.

Let $\{l_1, \ldots, l_s\}$ denote the Lagrange basis of $\mathbb{P}_{s-1}$ with respect to the nodes $c_1, \ldots, c_s$:

$$l_i(\theta) := \prod_{j=1, j \neq i}^{s} \frac{\theta - c_j}{c_i - c_j}, \quad i = 1, \ldots, s.$$

It holds $l_i(c_j) = \delta_{ij}$ for $i, j = 1, \ldots, s$. Using the Lagrange interpolation formula yields

$$u_k'(t_k + \theta \cdot h_k) = \sum_{j=1}^{s} l_j(\theta) \cdot u_k'(t_k + c_j \cdot h_k) = \sum_{j=1}^{s} l_j(\theta) \cdot f\Big(t_k + c_j \cdot h_k; Y_j^{(k)}; \tilde{Y}_{1,j}^{(k)}, \ldots, \tilde{Y}_{m,j}^{(k)}\Big) \,.$$

It follows for the collocation polynomial

$$\begin{aligned} u_k(t_k+\theta\cdot h_k) &= y_k + h_k\cdot\int_0^\theta u_k'(t_k+\theta'\cdot h_k)\,d\theta' \\ &= y_k + h_k\cdot\sum_{j=1}^{s} f\left(t_k+c_j\cdot h_k; Y_j^{(k)}; \tilde{Y}_{1,j}^{(k)},\ldots,\tilde{Y}_{m,j}^{(k)}\right)\cdot\int_0^\theta l_j(\theta')\,d\theta'. \end{aligned}$$

Define

$$a_{ij} := \int_0^{c_i} l_j(\theta)\,d\theta, \quad i,j=1,\ldots,s$$

and

$$b_j := \int_0^1 l_j(\theta)\,d\theta, \quad j=1,\ldots,s.$$

The collocation polynomial $u_k(\cdot)$ at the nodes $c_1,\ldots,c_s$ is then given by

$$\begin{aligned} (i)\quad & u_k(t_k+c_i\cdot h_k) \\ & = y_k + h_k\cdot\sum_{j=1}^{s} a_{ij}\cdot f\left(t_k+c_j\cdot h_k; Y_j^{(k)}; \tilde{Y}_{1,j}^{(k)},\ldots,\tilde{Y}_{m,j}^{(k)}\right), \quad i=1,\ldots,s, \qquad (4.2) \\ (ii)\quad & u_k(t_{k+1}) = u_k(t_k+h_k) \\ & = y_k + h_k\cdot\sum_{j=1}^{s} b_j\cdot f\left(t_k+c_j\cdot h_k; Y_j^{(k)}; \tilde{Y}_{1,j}^{(k)},\ldots,\tilde{Y}_{m,j}^{(k)}\right). \qquad (4.3) \end{aligned}$$

Equivalently, Eqs. (4.2) and (4.3) can be written as s-step implicit Runge-Kutta method for delay differential equation in symmetric form [19]:

$$\begin{aligned} (i)\quad & Y_i^{(k)} = y_k + h_k\cdot\sum_{j=1}^{s} a_{ij}\cdot f\left(t_k+c_j\cdot h_k; Y_j^{(k)}; \tilde{Y}_{1,j}^{(k)},\ldots,\tilde{Y}_{m,j}^{(k)}\right), \quad i=1,\ldots,s \\ (ii)\quad & y_{k+1} = y_k + h_k\cdot\sum_{j=1}^{s} b_j\cdot f\left(t_k+c_j\cdot h_k; Y_j^{(k)}; \tilde{Y}_{1,j}^{(k)},\ldots,\tilde{Y}_{m,j}^{(k)}\right). \end{aligned}$$

Using again the Lagrange interpolation formula by adding $c_0 := 0$ to the nodes $c_1,\ldots,c_s$, where the Lagrange polynomial $L_i(\cdot)\in\mathbb{P}_s$ is given by

$$L_i(\theta) := \prod_{j=0,j\neq i}^{s}\frac{\theta-c_j}{c_i-c_j}, \quad \Rightarrow \quad L_i(c_j)=\delta_{ij}, \quad i,j=0,\ldots,s,$$

$u_k(\cdot)$ is of the form

$$u_k(t_k+\theta\cdot h_k) = L_0(\theta)\cdot y_k + \sum_{i=1}^{s} L_i(\theta)\cdot Y_i^{(k)}.$$

RADAR5, as mentioned at the beginning of this section, is based on a Radau method, i.e. $c_s := 1$ is chosen and therefore it holds $a_{sj} = b_j$, $j = 1, \ldots, s$. For this reason, the s-step Radau method is given by

$$(i) \quad Y_i^{(k)} = y_k + h_k \cdot \sum_{j=1}^{s} a_{ij} \cdot f\left(t_k + c_j \cdot h_k; Y_j^{(k)}; \tilde{Y}_{1,j}^{(k)}, \ldots, \tilde{Y}_{m,j}^{(k)}\right), \quad i = 1, \ldots, s$$

$$(ii) \quad y_{k+1} = Y_s^{(k)}.$$

More precisely, since differential-algebraic equations are considered, the following nonlinear system must be solved:

$$(i) \quad M \cdot \left(Y_i^{(k)} - y_k\right) = h_k \cdot \sum_{j=1}^{s} a_{ij} \cdot f\left(t_k + c_j \cdot h_k; Y_j^{(k)}; \tilde{Y}_{1,j}^{(k)}, \ldots, \tilde{Y}_{m,j}^{(k)}\right), \quad i = 1, \ldots, s, \tag{4.4}$$

$$(ii) \quad y_{k+1} = Y_s^{(k)}.$$

There are different Radau methods. In RADAR5 the Radau IIA method (see [36], p.72) is used for the numerical integration, where $c_1, \ldots, c_s$ are the zeros of

$$\frac{d^{s-1}}{dc^{s-1}} \left(c^{s-1} \cdot (c-1)^s\right).$$

Since $s = 3$ in RADAR5, c_1, c_2, and c_3 are the zeros of

$$\frac{d^{3-1}}{dc^{3-1}} \left(c^{3-1} \cdot (c-1)^3\right) = 2 \cdot (c-1) \cdot (10 \cdot c^2 - 8 \cdot c + 1)$$

and thus $c_1 = \frac{4-\sqrt{6}}{10}$, $c_2 = \frac{4+\sqrt{6}}{10}$, $c_3 = 1$.

In the case of GynCycle it is

$$\alpha_{l,i}^{(k)} := t_k + c_i \cdot h_k - \tau_l$$

for $l = 1, \ldots, m$ and $i = 1, \ldots, s$ as well as

$$\tilde{Y}_{l,i}^{(k)} := \begin{cases} y_{0,i}, & \text{if } t_k + c_i \cdot h_k - \tau_l < t_0 \\ u_{k'}\left(t_k + c_i \cdot h_k - \tau_l\right), & \text{if } t_k + c_i \cdot h_k - \tau_l \in [t_{k'}, t_{k'+1}], k' \leq k, k' \in \mathbb{N}_0. \end{cases}$$

Solving the nonlinear system

The nonlinear equations in Eq. (4.4) must be solved. In order to reduce the influence of round-off errors ([36], for ODEs), define for $i = 1, \ldots, s$

$$Z_i^{(k)} := Y_i^{(k)} - y_k$$
$$\tilde{Z}_{l,i}^{(k)} := \tilde{Y}_{l,i}^{(k)} - y_k, \quad l = 1, \ldots, m.$$

Reformulation of the nonlinear system yields for $i = 1, \ldots, s$

$$(i) \quad M \cdot Z_i^{(k)} = h_k \cdot \sum_{j=1}^{s} a_{ij} \cdot f\Big(t_k + c_j \cdot h_k; y_k + Z_j^{(k)}; y_k + \tilde{Z}_{1,i}^{(k)}, \ldots, y_k + \tilde{Z}_{m,i}^{(k)}\Big).$$

Thus the nonlinear equations

$$F_i(Z^{(k)}) := M \cdot Z_i^{(k)} - h_k \cdot \sum_{j=1}^{s} a_{ij} \cdot f\Big(t_k + c_j \cdot h_k; y_k + Z_j^{(k)}; y_k + \tilde{Z}_{1,j}^{(k)}, \ldots, y_k + \tilde{Z}_{m,j}^{(k)}\Big) = 0$$

must be solved for $i = 1, \ldots, s$, where $Z^{(k)} := ({Z_1^{(k)}}^T, \ldots, {Z_s^{(k)}}^T)^T$. The nonlinear system is then given by

$$\begin{aligned} F^0(Y^{(k)}) &:= (F_1(Y^{(k)})^T, \ldots, F_s(Y^{(k)})^T)^T \\ &= (I_s \otimes M) \cdot Z^{(k)} - h_k \cdot (A \otimes I_n) \cdot f(Z^{(k)}) = 0, \end{aligned}$$

where

$$f(Z^{(k)}) := \begin{pmatrix} f\Big(t_k + c_1 \cdot h_k; y_k + Z_1^{(k)}; y_k + \tilde{Z}_{1,1}^{(k)}, \ldots, y_k + \tilde{Z}_{m,1}^{(k)}\Big) \\ \vdots \\ f\Big(t_k + c_s \cdot h_k; y_k + Z_s^{(k)}; y_k + \tilde{Z}_{1,s}^{(k)}, \ldots, y_k + \tilde{Z}_{m,s}^{(k)}\Big) \end{pmatrix}.$$

In order to solve this system, the (simplified) Newton method is used. First the starting values are set:

$$(i) \quad Z^{(k),(0)}.$$

The Newton iterations are then given by ($i' \in \mathbb{N}_0$)

$$\begin{aligned} &(ii) \quad DF^0(Z^{(k),(i')}) \cdot \Delta Z^{(k),(i')} = -F^0(Z^{(k),(i')}) \\ &(iii) \quad Z^{(k),(i'+1)} = Z^{(k),(i')} + \Delta Z^{(k),(i')}, \end{aligned}$$

where $DF^0(Z^{(k),(i')})$ denotes the Jacobian matrix of the system.

Each Newton step requires s evaluations of f and the solution of a $(n \cdot s \times n \cdot s)$-dimensional linear system. In the case of the simplified Newton method, the matrix $DF^0(Z^{(k),(i')}) := DF^0(Z^{(k),(0)})$ is the same for all iterations. Its LU-decomposition is done only once and is usually very costly [36]. The simplified Newton iterations are then given by, $i' \in \mathbb{N}_0$:

$$(ii) \quad DF^0(Z^{(k),(0)}) \cdot \Delta Z^{(k),(i')} = -F^0(Z^{(k),(i')}) \tag{4.5}$$

where the exact Jacobian is replaced by an approximation:

$$DF^0(Z^{(k),(0)}) := I_s \otimes M - h_k \cdot A \otimes \left(f_z + \sum_{l'=1}^{m} f_{\tilde{z}_{l'}} \cdot u_{k,\alpha_{l'}} \cdot \alpha_{l',z}^{(k)} \right) - h_k \cdot (A \otimes I_n) \cdot \sum_{l'=1}^{m} L^{(l')} \otimes f_{\tilde{z}_{l'}}, \tag{4.6}$$

with

$$f_z := f_z(t_k; y_k; \tilde{y}_{k,1}, \ldots, \tilde{y}_{k,m}),$$

where $\tilde{y}_{k,l'}$ is defined analogously to $\tilde{Y}_{l'}^{(k)}$,

$$f_{\tilde{z}_{l'}} := f_{\tilde{z}_{l'}}(t_k; y_k; \tilde{y}_{k,1}, \ldots, \tilde{y}_{k,m})$$

for $l' = 1, \ldots, m$ and

$$u_{k,\alpha_{l'}} := u_{k,\alpha_{l'}}\left(\alpha_{l',0}^{(k)}\right)$$
$$\alpha_{l',z}^{(k)} := \alpha_{l',z}(t_k, y_k),$$

where $\alpha_{l',0}^{(k)} := \alpha_{l'}(t_k, y_k)$ and

$$u_{k,\alpha_{l'}}\left(\alpha_{l',i}^{(k)}\right) \cdot \alpha_{l',z}\left(t_k + c_i \cdot h_k, y_k + Z_i^{(k)}\right) = L_i(\alpha_{l'}(t_k + c_i \cdot h_k; y_k + Z_i^{(k)})).$$

The last term in Eq. (4.6) considers that it must be distinguished between two cases for the relation of the current step size and delay (see Fig. 4.1 for the case of constant delay).

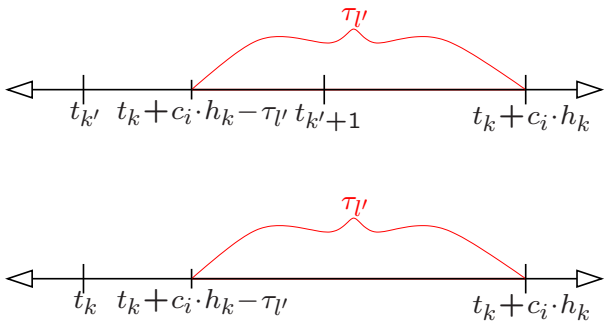

Figure 4.1: On the top: step size (more precisely: $c_i \cdot h_k$) is smaller than delay $\tau_{l'}$. On the bottom: step size (more precisely: $c_i \cdot h_k$) is larger than the delay $\tau_{l'}$.

The matrix $L^{(l')} := (l_{ij}^{(l')})_{i,j=1,\ldots,s}$ is then defined by

$$l_{ij}^{(l')} := \begin{cases} L_j(\sigma_i^{(l')}) & \text{if } \sigma_i^{(l')} > 0 \\ 0 & \text{else} \end{cases}$$

with

$$\sigma_i^{(l')} := \frac{\alpha(t_k + c_i \cdot h_k, y_k + Z_i^{(k)}) - t_k}{h_k}.$$

In the case of GynCycle, the delays are constant and it is $\sigma_i^{(l')} = \frac{c_i \cdot h_k - \tau_{l'}}{h_k}$. If $\sigma_i^{(l')} > 0$, $l' \in \{1, \ldots, m\}$, $i \in \{1, \ldots, s\}$, the current step size h_k is larger than the delay $\tau_{l'}$:

$$h_k \geq c_i \cdot h_k > \tau_{l'}, \quad i = 1, \ldots, s, \quad l' = 1, \ldots, m.$$

If the step size h_k is small compared to all delays $\tau_{l'}$, more precisely $\sigma_i^{(l')} \leq 0$, for all $l' = 1, \ldots, m$, then the Jacobian matrix is similar to the case of the ODEs (if the delays are constant). If h_k is larger than the delay $\tau_{l'}$, more precisely $\sigma_1^{(l')} > 0$, for all $l' = 1, \ldots, m$, it follows $\sigma_i^{(l')} = c_i$ and finally $L^{(l')} = I_s$. In this case it is

$$DF^0(Z^{(k),(0)}) = I_s \otimes M - h_k \cdot A \cdot \left(f_z + \sum_{l'=1}^{m} f_{\tilde{z}_{l'}} + \sum_{l'=1}^{m} f_{\tilde{z}_{l'}} \cdot u_{k,\alpha_{l'}} \cdot \alpha_{l',z} \right).$$

For simplicity of the calculation, $L^{(l')}$ is set to $\mathbf{0_s}$ if $\sigma_i^{(l')} \leq 0$ for at least one i, otherwise it is set to I_s if $\sigma_1^{(l')} > 0$. The correct matrix $L^{(l')}$ is used if problems arise with the convergence of the simplified Newton iteration [35].

Every Radau method is L-stable and thus A invertible [19]. The premultiplication of both sides of Eq. (4.5) with $(h_k \cdot A)^{-1} \otimes I_n$ results in

$$\begin{aligned} F^1(Z^{(k),(i')}) &:= ((h_k \cdot A)^{-1} \otimes I_n) \cdot F^0(Z^{(k),(i')}) \\ &= ((h_k \cdot A)^{-1} \otimes I_n) \cdot ((I_s \otimes M) \cdot Z^{(k),(i')} - h_k \cdot (A \otimes I_n) \cdot f(Z^{(k),(i')})) \\ &= (h_k^{-1} \cdot A^{-1} \otimes M) \cdot Z^{(k),(i')} - f(Z^{(k),(i')}) \end{aligned}$$

and

$$\begin{aligned} DF^1(Z^{(k),(0)}) &:= ((h_k \cdot A)^{-1} \otimes I_n) \cdot DF^0(Z^{(k),(0)}) \\ &= ((h_k \cdot A)^{-1} \otimes I_n) \cdot \left(I_s \otimes M - h_k \cdot A \otimes \left(f_z + \sum_{l'=1}^{m} f_{\tilde{z}_{l'}} \cdot u_{k,\alpha_{l'}} \cdot \alpha_{l',z} \right) \right. \\ &\quad \left. - h_k \cdot (A \otimes I_n) \cdot \sum_{l'=1}^{m} L_{l'} \otimes f_{\tilde{z}_{l'}} \right) \\ &= h_k^{-1} \cdot A^{-1} \otimes M - I_s \otimes \left(f_z + \sum_{l'=1}^{m} f_{\tilde{z}_{l'}} \cdot u_{k,\alpha_{l'}} \cdot \alpha_{l',z} \right) - \sum_{l'=1}^{m} L_{l'} \otimes f_{\tilde{z}_{l'}}. \end{aligned}$$

This transformation leads to a simpler calculation of the iteration step that is replaced by

$$(ii) \quad DF^1(Z^{(k),(0)}) \cdot \Delta Z^{(k),(i')} = -F^1(Z^{(k),(i')}).$$

In the following, only the special case of RADAR5 for GynCycle is considered. If the delays are not state-dependent, as it is the case here, and $M = I$, the terms reduce to

$$F^1(Z^{(k),(i')}) = (h_k^{-1} \cdot A^{-1} \otimes I_n) \cdot Z^{(k),(i')} - f(Z^{(k),(i')})$$

and

$$DF^1(Z^{(k),(0)}) = h_k^{-1} \cdot A^{-1} \otimes I_n - I_s \otimes f_z - \sum_{l'=1}^{m} L_{l'} \otimes f_{\tilde{z}_{l'}}.$$

Further assume for simplicity of notation that $L^{(l')} = 0$ for all $l' = 1, \ldots, m$.

Next A is transformed in order to obtain a "simpler" matrix Λ, in this case a block diagonal form (Chapter IV.8, [36]):

$$T^{-1} \cdot A^{-1} \cdot T = \Lambda,$$

where

$$\Lambda = \begin{pmatrix} \lambda_{11} & 0 & 0 \\ 0 & \lambda_{22} & \lambda_{23} \\ 0 & \lambda_{32} & \lambda_{33} \end{pmatrix}.$$

Premultiplication with $T^{-1} \otimes I_n$ yields

$$\begin{aligned} F^2(Z^{(k),(i')}) &= (T^{-1} \otimes I_n) \cdot F^1(Z^{(k),(i')}) \\ &= (T^{-1} \otimes I_n) \cdot (h_k^{-1} \cdot A^{-1} \otimes I_n) \cdot Z^{(k),(i')} - (T^{-1} \otimes I_n) \cdot f(Z^{(k),(i')}) \\ &= (h_k^{-1} \cdot (\Lambda \cdot T^{-1}) \otimes I_n) \cdot Z^{(k),(i')} - (T^{-1} \otimes I_n) \cdot f(Z^{(k),(i')}) \\ &= h_k^{-1} \cdot (\Lambda \otimes I_n) \cdot (T^{-1} \otimes I_n) \cdot Z^{(k),(i')} - (T^{-1} \otimes I_n) \cdot f(Z^{(k),(i')}) \end{aligned}$$

and

$$\begin{aligned} DF^2(Z^{(k),(0)}) &= (T^{-1} \otimes I_n) \cdot DF^1(Z^{(k),(0)}) \\ &= (T^{-1} \otimes I_n) \cdot (h_k^{-1} \cdot A^{-1} \otimes I_n) - (T^{-1} \otimes I_n) \cdot (I_s \otimes f_z) \\ &= h_k^{-1} \cdot (\Lambda \cdot T^{-1}) \otimes I_n - (I_s \otimes f_z) \cdot (T^{-1} \otimes I_n) \\ &= (h_k^{-1} \cdot \Lambda \otimes I_n - I_s \otimes f_z) \cdot (T^{-1} \otimes I_n). \end{aligned}$$

Again for a simpler calculation, the iteration step is replaced by

$$(ii) \quad DF^2(Z^{(k),(0)}) \cdot \Delta Z^{(k),(i')} = -F^2(Z^{(k),(i')}).$$

Finally the transformation $w^{(k)} := (T^{-1} \otimes I_n) \cdot Z^{(k)}$ is conducted:

$$(ii)(h_k^{-1} \cdot \Lambda \otimes I_n - (I_s \otimes f_y)) \cdot \Delta w^{(k)} = -h_k^{-1} \cdot (\Lambda \otimes I_n) \cdot w^{(k)} + (T^{-1} \otimes I_n) \cdot F((T \otimes I_n) \cdot w^{(k)}).$$

Since $T^{-1} \cdot A^{-1} \cdot T = \Lambda$, the matrices A^{-1} and Λ are similar, i.e. A^{-1} and Λ have the same eigenvalues. In RADAR5, Λ has one real eigenvalue, $\hat{\gamma}$, and one complex pair of eigenvalues, $\hat{\alpha} \pm i\hat{\beta}$, where $\hat{\gamma} := \lambda_{11}$, $\hat{\alpha} := \lambda_{22} = \lambda_{33}$, $\hat{\beta} := \lambda_{23} = -\lambda_{32}$. Set $\gamma = h_k^{-1} \cdot \hat{\gamma}$, $\alpha = h_k^{-1} \cdot \hat{\alpha}$, and $\beta = h_k^{-1} \cdot \hat{\beta}$. Then it follows

$$h_k^{-1} \cdot \Lambda \otimes I_n - I_s \otimes f_z = \begin{pmatrix} \gamma \cdot I_n - f_z & 0 & 0 \\ 0 & \alpha \cdot I_n - f_z & -\beta \cdot I_n \\ 0 & \beta \cdot I_n & \alpha \cdot I_n - f_z \end{pmatrix}.$$

Thus there are two linear systems of dimension n and $2 \cdot n$, respectively. The second can be transformed into a n-dimensional, complex system

$$((\alpha + i \cdot \beta) \cdot I_n - f_z) \cdot (u + i \cdot v) = a + i \cdot b$$

which can be solved by simple Gaussian elimination (Chapter IV.8, [36]).

4.1.3 Integration of the pulse generator into RADAR5

The model GynCycle does not only consist of pure DDEs since the GnRH pulse generator is modeled stochastically, more precisely the pulse time points and the resulting pulse mass.

It holds (see Eq. (2.24) in Chapter 2) for all $j \in \mathbb{N}$

$$F(T_j - T_{j-1}) = 1 - \exp\left(-\left(\int_{T_{j-1}}^{T_j} \lambda(r)\, dr\right)^{\gamma}\right).$$

In order to calculate the pulse time points T_j, first the random variable $U_j \sim U[0,1]$ must be generated. Then it must be equated with $F(T_j - T_{j-1})$:

$$U_j = 1 - \exp\left(-\left(\int_{T_{j-1}}^{T_j} \lambda(r)\, dr\right)^{\gamma}\right).$$

It follows

$$\Lambda(t_k) - \Lambda(T_{j-1}) = \int_{T_{j-1}}^{T_j} \lambda(r)\, dr = (-\ln(1-U_j))^{\frac{1}{\gamma}}$$

since the function $\lambda(\cdot)$ is positive.

For the integration of the calculation of the pulses into RADAR5, the system of delay differential equations is solved until the inequality

$$g(t_k; T_{j-1}, U_j) := \Lambda(t_k) - \Lambda(T_{j-1}) - (-\ln(1-U_j))^{\frac{1}{\gamma}} \geq 0 \tag{4.7}$$

is satisfied, where $t_k \geq T_{j-1}$ denotes the discrete time point. In [46, 47] for the male case, the next pulse time point is determined by

$$T_j := t_k = \min_{l \in \mathbb{N}_0} \{t_l \geq T_{j-1} | g(t_k; T_{j-1}, U_j) \geq 0\}.$$

More precisely, they calculate

$$T_j := t_k = \min_{l \in \mathbb{N}_0} \{t_l \geq T_{j-1} + \Delta_{min}T | g(t_k; T_{j-1}, U_j) \geq 0\},$$

where $\Delta_{min}T$ denotes the minimum distance between two pulses.

This is only feasible if the step sizes are small compared to the intervals between the pulses: $t_k - t_{k-1} \ll T_j - T_{j-1}$. If the first model part (which consists of only one equation, the pulse intensity of GnRH) is simulated, the step sizes can become quite large compared to the interval length between two pulses. Moreover, since in general a stiff integrator only is efficient if large step sizes are allowed, it is adequate to solve the equation "correctly". This is approximately given, if the equation is solved with the (simplified) Newton method. That means, in order to obtain a more accurate result, it must be proceeded in the case of

$$g(t_k; T_{j-1}, U_j) > 0.$$

The nonlinear equation

$$g(t_k; T_{j-1}, U_j) = 0$$

is solved with aid of the simplified Newton method with starting value

$$t_k^{(0)} = t_k$$

and iterations ($i \in \mathbb{N}_0$)

$$\begin{aligned} t_k^{(i+1)} &= t_k^{(i)} - \frac{1}{g'(t_k^{(0)})} \cdot g(t_k^{(i)}) \\ &= t_k^{(i)} - \frac{1}{\lambda(t_k^{(0)})} \cdot g(t_k^{(i)}) \end{aligned}$$

since it holds

$$g'(t_k^{(0)}) = \frac{d}{dt} \left(\int_{T_{j-1}}^{t_k^{(0)}} \lambda(r)\, dr - (-\ln(1-U_j))^{\frac{1}{\gamma}} \right) = \lambda(t_k^{(0)}) > 0.$$

The term $g(t_k^{(i)})$ can be calculated via the collocation polynomial ($\Lambda(\cdot)$ is provided). The function $\lambda(\cdot)$ is dependent on $\mathrm{E}_2(\cdot)$ and $\mathrm{P}_4(\cdot)$ and can be calculated via the collocation polynomial as well.

There is a zero of $g(\cdot; T_{j-1}, U_j)$ in the interval $[T_{j-1}, t_k]$ since $g(\cdot; T_{j-1}, U_j)$ is continuous and it is $g(T_{j-1}; T_{j-1}, U_j) < 0$ and $g(t_k; T_{j-1}, U_j) > 0$ (intermediate value theorem). Moreover $g(\cdot; T_{j-1}, U_j)$ is arbitrarily often continuously differentiable and it is $g'(t_k^{(0)}) \neq 0$, thus the (simplified) Newton method is convergent in this case. A local method is sufficient, since the distance of the starting value is already close to the solution.

There can be more than one pulse time point between two successive grid points t_{k-1} and t_k. Thus T_j and U_{j+1} must be reset and the condition

$$g(t_k; T_j, U_{j+1}) = \Lambda(t_k) - \Lambda(T_j) - (-\ln(1-U_{j+1}))^{\frac{1}{\gamma}} \geq 0$$

checked again. The algorithm is continued (increment of j) until it holds for the smallest $j' > j$

$$g(t_k; T_{j'-1}, U_{j'}) = \Lambda(t_k) - \Lambda(T_{j'-1}) - (-\ln(1-U_{j'}))^{\frac{1}{\gamma}} < 0.$$

Since $\lambda(\cdot)$ is bounded, there is no problem with the next pulse time point.

Lemma 4.1. *If $U_j \in (0,1)$, it holds for all $j \in \mathbb{N}$*

$$T_j - T_{j-1} \in (0, \infty).$$

Proof. It is

$$\int_{T_{j-1}}^{T_j} \lambda(r)\,dr = (-\ln(1-U_j))^{\frac{1}{\gamma}}$$

and it is assumed that

$$(-\ln(1-U_j))^{\frac{1}{\gamma}} \in (0,\infty).$$

Since furthermore $\lambda(\cdot) < 2 \cdot \lambda_{max}$, it holds

$$\int_{T_{j-1}}^{T_j} \lambda(r)\,dr \leq 2 \cdot \lambda_{max} \cdot (T_j - T_{j-1}).$$

Thus it follows

$$(T_j - T_{j-1}) \cdot 2 \cdot \lambda_{max} \geq (-\ln(1-U_j))^{\frac{1}{\gamma}} > 0$$

and finally

$$T_j - T_{j-1} \geq \frac{(-\ln(1-U_j))^{\frac{1}{\gamma}}}{2 \cdot \lambda_{max}} > 0.$$

Since it holds

$$(-\ln(1-U_i))^{\frac{1}{\gamma}} < \infty$$

it is

$$\int_{T_{j-1}}^{T_j} \lambda(r)\,dr < \infty.$$

Moreover, the pulse intensity function $\lambda(\cdot)$ is bounded and positive which yields $T_j < \infty$ and in particular $T_j - T_{j-1} < \infty$. □

Lemma 4.2. *It holds for all* $j \in \mathbb{N}$

$$\lim_{j\to\infty} T_j = \infty.$$

Proof. It is

$$\lim_{j\to\infty} \int_{T_0}^{T_j} \lambda(r)\,dr \leq \lim_{j\to\infty} (2 \cdot \lambda_{max} \cdot T_j) = 2 \cdot \lambda_{max} \cdot \lim_{j\to\infty} T_j,$$

since $T_0 = 0$. Further it holds

$$\begin{aligned}\lim_{j\to\infty} \int_0^{T_j} \lambda(r)\,dr &= \lim_{j\to\infty} \sum_{i=1}^{j} \int_{T_{i-1}}^{T_i} \lambda(r)\,dr \\ &= \lim_{j\to\infty} \sum_{i=1}^{j} (-\ln(1-U_i))^{\frac{1}{\gamma}} = \lim_{j\to\infty} j \cdot \int_0^1 (-\ln(1-u))^{\frac{1}{\gamma}}\,du = \infty,\end{aligned}$$

i.e. the limit is not existing. It follows that

$$\lim_{j\to\infty} T_j = \infty.$$

□

Lemma 4.3. *There is a $j' > j$ such that*

$$g(t_k; T_{j'-1}, U_{j'}) < 0.$$

Proof. If $T_{j'-1} > t_k$ it follows $\Lambda(T_{j'-1}) > \Lambda(t_k)$ and thus $g(t_k; T_{j'-1}, U_{j'}) < 0$. This occurs in finite steps since $T_j - T_{j-1} < \infty$ and $\lim_{j\to\infty} T_j = \infty$ (see Lemma 4.1 and 4.2).

It is also possible that $T_{j'-1} \leq t_k$ and $g(t_k; T_{j'-1}, U_{j'}) < 0$. This is the case if $\Lambda(T_{j'-1}) > \Lambda(t_k) - (-\ln(1-U_{j'}))^{\frac{1}{\gamma}}$. □

If the "exact" pulse time point is calculated, the "exact" pulse mass must also be calculated. The subroutine which is called in RADAR5 when the solution is updated is given in Algorithm 4.

subroutine event(t_k, T_{j-1}, U_j)
$g(t_k, T_{j-1}, U_j) = \Lambda(t_k) - \Lambda(T_{j-1}) - (-\ln(1-U_j))^{\frac{1}{\gamma}}$;
$t_k^{(0)} = t_k$;
while $g(t_k^{(0)}, T_{j-1}, U_j) \geq 0$ **do**
  $i = 0$;
  while $|g(t_k^{(i)}, T_{j-1}, U_j)| > \varepsilon$ **do**
    $t_k^{(i+1)} = t_k^{(i)} - (\lambda(t_k^{(0)}))^{-1} \cdot g(t_k^{(i)}, T_{j-1}, U_j)$;
    $i = i + 1$;
  end
  % update of pulse time point and pulse mass:
  $T_j = t_k^{(i)}$;
  $M_{GnRH,j} = M_{GnRH}(T_j) - M_{GnRH}(T_{j-1})$;
  % preparation for calculation of new pulse time point:
  $j = j + 1$;
  $U_j \sim [0, 1]$;
  $g(t_k^{(0)}, T_{j-1}, U_j) = \Lambda(t_k) - \Lambda(T_{j-1}) - (-\ln(1-U_j))^{\frac{1}{\gamma}}$;
end
end subroutine event

Algorithm 4: Algorithm for the determination of the GnRH pulse time points and pulse masses.

An update of the remaining equations is done at the next time step. It is assumed that, in the case of several pulse time points between t_{k-1} and t_k, the amount of mass that could be stored is not large which is why a direct update is not necessary.

4.2 Sensitivity analysis

Now that the numerical basis is provided, the parameters that are suitable for the parameter estimation can be determined.

Consider the non-autonomous system of DDEs (see Section 4.1, Eq. (4.1)) of the form

$$\begin{aligned} \frac{d}{dt}y(t;p) &= f(t;y(t;p);y(t-\tau_1;p),\ldots,y(t-\tau_m;p);p), \quad t \geq 0, \\ y(t;p) \quad &= \phi(t;p), \qquad\qquad\qquad\qquad\qquad\qquad\quad t \leq 0, \end{aligned}$$

where the dependency of the parameter vector p is highlighted. It is $m \in \mathbb{N}$, $y(t;p) = (y_1(t;p), y_2(t;p), \ldots, y_n(t;p))^T \in \mathbb{R}^n$, and $p = (p_1, p_2, \ldots, p_{n_p})^T \in \mathbb{R}^{n_p}$.

The *sensitivity* means here the influence of changes in the parameter vector p on the solution vector y [19, 31]. A parameter is called *sensitive* if small changes in its value lead to large changes in the solution [22]. The sensitivities of the elements with respect to the parameters are an important issue when dealing with parameter estimation. The parameters are only simultaneously identifiable if the system's sensitivity with respect to these parameters is high enough compared to the most sensitive one. In order to be able to compare the different sensitivities, the condition, or more precisely the subcondition, is calculated.

The parameters that are not sensitive compared to the remaining parameters do not influence the system significantly at that state, thus their value can be considered to be negligible for the solution. It is only important that their values are not set to zero.

A solution must be found how to handle the stochastic part of the system which is presented in Section 4.2.1. Since the parameters have positive values by definition, they are transformed (Section 4.2.2). For the determinization of the sensitive parameters first the sensitivity matrix is introduced in Section 4.2.3, then the calculation of the sensitivities in the case of DDEs is presented in Section 4.2.4, and finally the analysis of the calculated sensitivities is treated in Section 4.2.5. The results for GynCycle are presented at the end of this section in Section 4.2.6 and in the appendix.

4.2.1 Determinization of the stochastic pulse generator

When performing parameter estimation, the GnRH pulse generator (or more precisely, the calculation of the GnRH pulse frequency) must be considered separately since it is modeled stochastically (see Section 2.2).

When solving the system of delay differential equations, where the pulse time points are determined by a stochastic process, it must be considered that only *one* possible realization is calculated. It is not acceptable to do parameter estimation only for *one* arbitrary realization. In order to work correctly two possibilities for representative simulations are mentioned here:

- In order to assess the simulation, a certain number of realizations must be determined and from these values the mean value. This is associated with high costs.

- Another possibility is to "determinize" the value which is random in order to obtain a deterministic character. In this case only one realization is necessary. If the sequence of GnRH pulse time points is given, then the system is deterministic, a sequence of DDEs.

Here the second possibility is chosen since it is cheaper. The determinization could be proceeded as follows: It holds that U_j is stochastic and therefore $(-\ln(1-U_j))^{\frac{1}{\gamma}}$ is stochastic ($U_j \sim [0,1]$). The expected value of $(-\ln(1-U_j))^{\frac{1}{\gamma}}$, $j \in \mathbb{N}$, is given by

$$E((-\ln(1-U_j))^{\frac{1}{\gamma}}|j \in \mathbb{N}) = \int_0^1 (-\ln(1-u))^{\frac{1}{\gamma}}\, du = 0.8826.$$

Instead of the inequality in Eq. (4.7), the inequality

$$\Lambda(t_k) - \Lambda(T_{j-1}) - E((-\ln(1-U_j))^{\frac{1}{\gamma}}|j \in \mathbb{N}) = \Lambda(t_k) - \Lambda(T_{j-1}) - 0.8826 \geq 0$$

can be used for simplicity.

4.2.2 Transformation of the parameters

Since all parameters in GynCycle are defined with positive values (if not even more restricted), transformation of the parameters is necessary in order to use an unrestricted method.

Thus define $p_0' := \ln(p_0)$ for the initial values p_0 of the parameter vector. The initial values must be chosen positive which ensures that the iteratives of the parameter vector are also positive (if the Gauss-Newton method is used) [60]. After termination of the parameter estimation, the optimal parameter values are obtained by $p^* = \exp(p^{'*})$, where $p^{'*}$ denotes the solution of the iteration.

If the parameter estimation (in the case of Gauss-Newton) conducted with the transformed parameter (p'-iteration) is compared to the parameter estimation with the original parameter (p-iteration), the following can be observed [61]:

- For non-critical examples, the p'-iteration may be slower.
- For critical examples, the p'-iteration may converge but the p-iteration may diverge.
- If the p'-iteration diverged but the p-iteration converged, it follows that the solution p^* contained negative components.

In the following, the sensitivity calculation and analysis refer to the transformed parameter vector.

4.2.3 Definition of the sensitivity

Generally, the (absolute) sensitivity can be defined as follows:

Definition 4.1. The *absolute sensitivity* of the i-th element with respect to the j-th chosen parameter is expressed by

$$s_{ij}^{abs}(t;p) := \frac{\partial y_i(t;p)}{\partial p_j}, \quad i = 1,\dots,n, \quad j = 1,\dots,n_p. \tag{4.8}$$

First these sensitivities are calculated for all elements of the system and for all parameters that should be estimated. The solution is given for all grid points in a defined time interval.

Further definitions of sensitivities are presented in Section 4.2.5 where special sensitivities are calculated in order to determine the subcondition where experimental data for the least-squares method are considered.

Note that the sensitivity holds approximately only in a vicinity of the state determined by y and p.

4.2.4 Calculation of sensitivities in the case of DDEs

In this section it is shown how the sensitivities can be calculated via the variational equation.

Solving the variational equation in RADAR5

Denote by $P^{est} \subseteq P$ the set of parameters that are considered in the sensitivity analysis. Let for simplicity be $|P^{est}| = n_p$. For the calculation of the sensitivities, the variational equation is solved. The variational equation arises by total differentiation of the system with respect to the parameter $p_j \in P^{est}$:

$$\frac{d}{dp_j}\left(\frac{d}{dt}y(t;p) = f(t;y(t;p);y(t-\tau_1;p),\dots,y(t-\tau_m;p);p_1,\dots,p_j,\dots,p_{n_p})\right).$$

There are two cases that must be distinguished when dealing with DDEs (in contrast to ODEs) [3]. If $p_j \neq \tau_l$ for all $l = 1,\dots,m$, i.e. p_j is no delay, then the following variational equation for y_i and p_j is obtained ($i = 1,\dots,n$, $j = 1,\dots,n_p$):

$$\begin{aligned}\frac{d}{dp_j}f_i(t;y(t;p);y(t-\tau_1;p),\dots,y(t-\tau_m;p);p) &= \frac{d}{dp_j}\left(\frac{d}{dt}y_i(t;p)\right)\\ &= \frac{d}{dt}\left(\frac{d}{dp_j}y_i(t;p)\right) = \frac{d}{dt}s_{ij}^{abs}(t;p)\end{aligned}$$

and finally

$$\begin{aligned}\frac{d}{dt}s_{ij}^{abs}(t;p) &= \frac{\partial}{\partial y(t;p)}f_i(t;y(t;p);y(t-\tau_1;p),\dots,y(t-\tau_m;p);p)\cdot\frac{d}{dp_j}y(t;p)\\ &\quad+\sum_{l=1}^{m}\frac{\partial}{\partial y(t-\tau_l;p)}f_i(t;y(t;p);y(t-\tau_1;p),\dots,y(t-\tau_m;p);p)\cdot\frac{d}{dp_j}y(t-\tau_l;p)\\ &\quad+\frac{\partial}{\partial p_j}f_i(t;y(t;p);y(t-\tau_1;p),\dots,y(t-\tau_m;p);p)\\ &= f_{i,y}\cdot s_j^{abs}(t;p)+\sum_{l=1}^{m}f_{i,y_{\tau_l}}\cdot s_j^{abs}(t-\tau_l;p)+f_{i,p_j},\end{aligned}$$

where

$$
\begin{aligned}
f_{i,y} &:= \frac{\partial}{\partial y(t;p)} f_i(t; y(t;p); y(t-\tau_1;p), \ldots, y(t-\tau_m;p); p) \\
f_{i,y_{\tau_l}} &:= \frac{\partial}{\partial y(t;p)} f_i(t; y(t;p); y(t-\tau_1;p), \ldots, y(t-\tau_m;p); p), \quad l = 1, \ldots, m \\
f_{i,p_j} &:= \frac{\partial}{\partial p_j} f_i(t; y(t;p); y(t-\tau_1;p), \ldots, y(t-\tau_m;p); p)
\end{aligned}
$$

and $s_j^{abs}(t;p) := (s_{1j}^{abs}(t;p), \ldots, s_{nj}^{abs}(t;p))^T$. From this it follows that

$$
\frac{d}{dt} S^{abs}(t;p) = f_y \cdot S^{abs}(t;p) + \sum_{l=1}^{m} f_{y_{\tau_l}} \cdot S^{abs}(t-\tau_l;p) + f_p,
$$

where $S^{abs}(t;p) := (s_{ij}^{abs}(t;p))_{i=1,\ldots,n, j=1,\ldots,n_p}$ and

$$
\begin{aligned}
f_y &:= (f_{1,y}, \ldots, f_{n,y})^T \\
f_{y_{\tau_l}} &:= (f_{1,y_{\tau_l}}, \ldots, f_{n,y_{\tau_l}})^T, \quad l = 1, \ldots, m \\
f_p &:= (f_{1,p}, \ldots, f_{n,p})^T.
\end{aligned}
$$

Hence the following system (extension of the original system for sensitivity integration) must be solved (compare [31, 70] for the case of ODEs):

$$
\frac{d}{dt}\hat{y} := \frac{d}{dt}\begin{pmatrix} y \\ s_1^{abs} \\ \vdots \\ s_{n_p}^{abs} \end{pmatrix} = \begin{pmatrix} f \\ f_y \cdot s_1^{abs} + \sum_{l=1}^{m} f_{y_{\tau_l}} \cdot s_{\tau_l,1}^{abs} + f_{p_1} \\ \vdots \\ f_y \cdot s_{n_p}^{abs} + \sum_{l=1}^{m} f_{y_{\tau_l}} \cdot s_{\tau_l,n_p}^{abs} + f_{p_{n_p}} \end{pmatrix} =: \hat{f}(t; \hat{y}; \hat{y}_{\tau_1}, \ldots, \hat{y}_{\tau_m}).
$$

Otherwise if $p_j = \tau_l$ for a $l \in \{1, \ldots, m\}$, i.e. if the parameter p_j is a delay, it is [3] for all $i = 1, \ldots, n$

$$
\begin{aligned}
\frac{d}{dt} s_{ij}^{abs}(t;p) &= \frac{\partial}{\partial y(t;p)} f_i \cdot \frac{d}{d\tau_l} y(t;p) + \sum_{l'=1}^{m} \frac{\partial}{\partial y(t-\tau_{l'};p)} f_i \cdot \frac{d}{d\tau_l} y(t-\tau_{l'};p) \\
&\quad + \frac{\partial}{\partial y(t-\tau_l;p)} f_i \cdot \frac{d}{d(t-\tau_l)} y(t-\tau_l;p) \cdot \frac{d}{d\tau_l}(t-\tau_l) \\
&= \frac{\partial}{\partial y(t;p)} f_i \cdot \frac{d}{d\tau_l} y(t;p) + \sum_{l'=1}^{m} \frac{\partial}{\partial y(t-\tau_{l'};p)} f_i \cdot \frac{d}{d\tau_l} y(t-\tau_{l'};p) \\
&\quad - \frac{\partial}{\partial y(t-\tau_l;p)} f_i \cdot \frac{d}{d(t-\tau_l)} y(t-\tau_l;p) \\
&= f_{i,y} \cdot s_j^{abs}(t;p) + \sum_{l'=1}^{m} f_{i,y_{\tau_{l'}}} \cdot s_j^{abs}(t-\tau_{l'};p) - f_{i,y_{\tau_l}} \cdot \frac{d}{d(t-\tau_l)} y(t-\tau_l;p).
\end{aligned}
$$

4.2.5 Analysis of the special sensitivity matrix

Basically, the following definitions are based on [31] and [61] (for the case of ODEs). By analyzing the sensitivity matrix, important indications concerning the suitability of the chosen parameters for identification by means of a parameter estimation method can be obtained [31].

The sensitivities are calculated for all elements of the system. However, only the elements for which experimental data are available are considered in the subsequent analysis. The sensitivities must then be calculated at the measure time points.

If data are not given for all elements of the system, the sensitivity only for these N elements is relevant. Keep in mind that the set of exp-elements is given by $V^{exp} = \{i_1, \dots, i_N\}$ where $N = |V^{exp}|$ (see Chapter 3).

The measure time points can vary among the exp-elements. Let $(t_j)_{j=0,\dots,k_{max}}$ be the discretization grid on the considered interval $[t_0, t_{end}]$, where $t_{end} = t_{k_{max}}$. Define $T_l = (t_j^l)_{j=1,\dots,n_t^l}$, where $t_j^l < t_{j+1}^l$ for all $j = 1, \dots, n_t^l - 1$ as the set of time points where experimental data are available for the element i_l, $l = 1, \dots, N$. If the measure time points are the same for all exp-elements, set n_t as the number of data $(t_j^0)_{j=1,\dots,n_t}$ for each exp-element.

Definition 4.2. The *special absolute sensitivity* of the i_l-th chosen element and the k-th chosen time-point with respect to the j-th chosen parameter is given by

$$s^{*,abs}_{\sum_{l'=1}^{l-1} n_t^{l'}+k,j} := s^{abs}_{i_l,j}(t_k^l; p), \quad k = 1, \dots, n_t^l, \quad l = 1, \dots, N, \quad j = 1, \dots, n_p. \tag{4.9}$$

If the time points are the same for all considered elements, it is:

$$s^{*,abs}_{(l-1)\cdot n_t+k,j} := s^{abs}_{i_l,j}(t_k^0; p), \quad k = 1, \dots, n_t, \quad l = 1, \dots, N, \quad j = 1, \dots, n_p. \tag{4.10}$$

For simplicity in the following define $n' := \sum_{l=1}^{N} n_t^l$. Thus $S^{abs}(\cdot; p)$ denotes the solution of the variational equation and $S^{*,abs} := (s^{*,abs}_{i,j})_{i=1,\dots,n',j=1,\dots,n_p}$ the values that are relevant for parameter estimation.

Both the model parameters and the solutions have (usually different) physical units. Moreover the values can be of different scales. To attain comparability they must be put in relation to the absolute values of the parameters and the solution values [31].

Definition 4.3. The *special normalized sensitivity* is defined by

$$s^{*,norm}_{\sum_{l'=1}^{l-1} n_t^{l'}+k,j} := s^{abs}_{i_l,j}(t_k^l; p) \cdot \frac{|p_j|}{|y_{i_l}|}, \quad k = 1, \dots, n_t^l, \quad l = 1, \dots, N, \quad j = 1, \dots, n_p.$$

The normalization can be done for $|y_{i_l}|$ by, for example, using the norm over all selected measure time points:

$$|y_{i_l}| := \left\| \{y_{i_l}(t_1), \dots, y_{i_l}(t_{n_t^l})\} \right\|, \quad l = 1, \dots, N.$$

In order to obtain reasonable results by the normalization even if the parameter or solutions have small values, *threshold values* $y_{trsh} \in \mathbb{R}_+$ and $p_{trsh} \in \mathbb{R}_+$ are defined for y and p, respectively [31].

Definition 4.4. The *special relative sensitivity* is defined for $k = 1, \ldots, n_t^l$, $l = 1, \ldots, N$, $j = 1, \ldots, n_p$ as follows:

$$s_{\sum_{l'=1}^{l-1} n_t^{l'}+k,j} := s^{*,rel}_{\sum_{l'=1}^{l-1} n_t^{l'}+k,j} := s^{abs}_{i_l,j}(t_k^l; p) \cdot \frac{\max(|p_j|, p_{trsh})}{\max(|y_{i_l}|, y_{trsh})}. \tag{4.11}$$

The sensitivity vectors $s_j := (s_{1j}, \ldots, s_{\sum_{l=1}^{N} n_t^l, j})^T$, $j = 1, \ldots, n_p$, for the n_p parameters $p_1, \ldots, p_{n_p}$ result in the columns of the sensitivity matrix $S := (s_{ij})_{i=1,\ldots,n', j=1,\ldots,n_p}$ with the dimension $(\sum_{l=1}^{N} n_t^l) \times n_p$ and if the time points are the same for all elements $(n_t \cdot N) \times n_p$. This matrix must be calculated in order to determine which parameters are sensitive. In the following suppose for simplicity that the time points are the same for all elements.

Parameters with little or no sensitivity are not estimatable. In the corresponding column of the sensitivity matrix the values are in this case equal or close to zero. For the calculation of the column-sum norm here the weighted l_2-norm is used. The norm of the j-th column s_j of the sensitivity matrix S is thereby given by

$$||s_j|| := \sqrt{\frac{1}{n'} \sum_{i=1}^{n'} s_{ij}^2}, \quad j = 1, \ldots, n_p.$$

Almost-singularities can be detected by column norms close to zero (non-sensitive parameters) [31].

In the case of linear dependencies, the parameters influence the solution in a comparable manner and lead therefore to linearly dependent columns in the sensitivity matrix. The corresponding parameters cannot be estimated simultaneously. In order to detect linear dependencies, further examinations must be conducted [31].

In both cases the matrix S is singular or from a numerical point of view almost-singular. If it leads to no confusion, in the following n' is denoted by n. The following theorem and definition can be found in [20].

Theorem 4.1. *If S is an arbitrary and real $(n \times n_p)$-matrix, then there is an orthogonal $(n \times n)$-matrix U and an orthogonal $(n_p \times n_p)$-matrix V such that*

$$S = U \cdot \Sigma \cdot V^T, \tag{4.12}$$

where $\Sigma = \mathrm{diag}(\sigma_1, \ldots, \sigma_{\min(n,n_p)})$ is a $(n \times n_p)$-matrix with

$$\sigma_1 \geq \cdots \geq \sigma_{\min(n,n_p)} \geq 0.$$

Definition 4.5. The factorization of S in Theorem 4.1 is called the *singular value decomposition* and σ_i, $i = 1, \ldots, \min(n, n_p)$, are called the *singular values* of S.

Definition 4.6. The *condition number* κ of the matrix S is defined by

$$\kappa(S) := ||S|| \cdot ||S^{-1}||.$$

It holds $\kappa(S) \geq 1$ since $\kappa(S) = ||S|| \cdot ||S^{-1}|| \geq ||S \cdot S^{-1}|| = ||I|| = 1$.

Lemma 4.4. *The condition number κ of the $(n \times n_p)$-matrix S is the ratio of the biggest to the smallest singular value:*

$$\kappa(S) = \frac{\sigma_1}{\sigma_{\min(n,n_p)}}.$$

Proof. It holds

$$\begin{aligned}\kappa(S) &= ||S|| \cdot ||S^{-1}|| = ||U \cdot \Sigma \cdot V^T|| \cdot ||(U \cdot \Sigma \cdot V^T)^{-1}|| \\ &= ||U \cdot \Sigma \cdot V^T|| \cdot ||V \cdot \Sigma^{-1} \cdot U^T|| = ||\Sigma|| \cdot ||\Sigma^{-1}||\end{aligned}$$

since it is $||Q \cdot A|| = ||A||$ for Q orthogonal and A arbitrary. Further it is

$$||\Sigma||_\infty = \max_{i \in \{1,\ldots,\min(n,n_p)\}} \sigma_i = \sigma_1.$$

For Σ^{-1} the row-sum norm yields analogously

$$||\Sigma^{-1}||_\infty = \max_{i \in \{1,\ldots,\min(n,n_p)\}} \sigma_i^{-1} = \frac{1}{\sigma_{\min(n,n_p)}}.$$

Finally it is

$$\kappa(S) = ||\Sigma|| \cdot ||\Sigma^{-1}|| = \frac{\sigma_1}{\sigma_{\min(n,n_p)}}.$$

□

The condition number of the sensitivity matrix S is a measure for the estimability of the parameter vector p. With increasing condition number, the simultaneous estimability of the chosen parameters decreases. A matrix with a very big condition number is almost singular. If the system that is solved in parameter estimation with, e.g. the Gauss-Newton method (see Section 4.3), the system can be become numerically seen singular and the method cannot be successful. As limit for the condition number $\kappa_{max} \approx 10^3$ has proved to be reasonable [31]. In chemical applications typical values of the maximal subcondition range between 10^{-1} and 10^{-3} [61].

The calculation of the condition is theoretically more satisfactory, but computationally more expensive [18] than the method that is presented in the following [31].

The triangularization of a nonsymmetric matrix by means of certain unitary transformations (by Householder, see e.g. [21]), is given by (see e.g. [20]):

Lemma 4.5. *If S is an arbitrary $(n \times n_p)$-matrix, then there is an orthogonal $(n \times n)$-matrix Q (the product of Housholder matrices) and an upper triangular $(n \times n_p)$-matrix R such that*

$$S = Q \cdot R. \tag{4.13}$$

Definition 4.7. The factorization of S in Lemma 4.5 is called *QR decomposition.*

Define the diagonal elements of R by $r_j := r_{jj}$, $j = 1, \ldots, \min(n, n_p)$. By means of a suitable transformation, a column permutation strategy (see e.g. [21]) with the permutation matrix Π, the diagonal elements of the matrix R can be arranged such that $|r_1| \geq \cdots \geq |r_{\min(n,n_p)}|$:

$$S \cdot \Pi = Q \cdot R.$$

By multiplication with Π, a ranking of the corresponding parameters with respect to increasing subcondition is obtained:

$$(p_1, \ldots, p_{n_p}) \cdot \Pi =: (p_{i_1}, \ldots, p_{i_{n_p}}).$$

Definition 4.8. The *subcondition sc* of the matrix S is defined by the ratio of the biggest to the smallest diagonal element:

$$sc(S) := \left| \frac{r_1}{r_{\min(n,n_p)}} \right|.$$

The subcondition *sc* has similar properties as the condition number κ.

Lemma 4.6. *Let S be an arbitrary matrix. Among the condition number $\kappa(S)$ and the subcondition $sc(S)$ the relation*

$$sc(S) \leq \kappa(S)$$

holds [20].

The subcondition depends on the number of parameters that must be estimated and on the number of elements and measure time points. The subcondition of a part matrix of the sensitivity matrix, $S' := (s_{ij})_{i=1,\ldots,n',j=1,\ldots,n'_p}$, for a smaller number of model parameters ($n'_p \leq n_p$) and for a smaller number of elements ($n' \leq n$) is always smaller than the subcondition of the original matrix $S = (s_{ij})_{i=1,\ldots,n,j=1,\ldots,n_p}$.

Lemma 4.7. *Let $S := (s_{ij})_{i=1,\ldots,n,j=1,\ldots,n_p}$ be a $(n \times n_p)$-matrix, $\Pi := (\pi_{ij})_{i,j=1,\ldots,n_p}$ the permutation matrix such that $S \cdot \Pi = Q \cdot R$, where $Q := (q_{ij})_{i,j=1,\ldots,n}$ orthogonal and $R := (r_{ij})_{i=1,\ldots,n,j=1,\ldots,n_p}$ upper triangular with decreasing diagonal elements. Moreover define $S' := (s'_{ij})_{i=1,\ldots,n',j=1,\ldots,n'_p}$, a $(n' \times n'_p)$-matrix with $n'_p \leq n_p$ and $n' \leq n$, by*

$$s'_{ij} := \sum_{k=1}^{n_p} s_{ik} \cdot \pi_{kj}, \quad i = 1, \ldots, n', \quad j = 1, \ldots, n'_p.$$

Then it follows

$$sc(S') \leq sc(S).$$

Proof. It is $S \cdot \Pi = Q \cdot R$ and $S' = Q' \cdot R'$, where $Q' =: (q_{ij})_{i,j=1,\dots,n'}$ and $R =: (r_{ij})_{i=1,\dots,n',j=1,\dots,n'_p}$. It holds

$$sc(S') = \frac{|r_1|}{|r_{\min(n',n'_p)}|} \leq \frac{|r_1|}{|r_{\min(n,n_p)}|} = sc(S \cdot \Pi) = sc(S).$$

□

The sequence of parameters that arises that way can be regarded as classification for their estimability which decreases with increasing subcondition.

4.2.6 Result of the sensitivity analysis for GynCycle

A list of the parameters ordered by model parts can be found in the appendix. The parameters that are sensitive, i.e. if the subcondition is smaller than the maximal subcondition 10^3, are marked. With these parameters, parameter estimation can be started.

The number of sensitive parameters within one model part varies, the percentage of sensitive parameters seems to be higher if the total number of parameters is small. Note that there are always parameters from the direct equations that belong to the most sensitive ones.

4.3 Parameter estimation

In the precedent sections, the numerical solution and the determination of sensitive parameters are presented. In this section, it is shown how the sensitive parameters can be estimated in order to optimize the simulation result. Here the Gauss-Newton method for nonlinear least-squares problems is used. More precisely, parameter estimation is done by means of the software NLSQ_ERR (Deuflhard and Nowak, 2004). This software solves nonlinear least-squares problems with a global unconstrained Gauss-Newton method with error oriented convergence criterion and adaptive trust region strategies (see also [18]). Alternatively, NLSQ_RES (global unconstrained Gauss-Newton method with a convergence criterion based on a projected residuum; by Deuflhard and Nowak, 2004) or NLSCON (older; for global constrained (or unconstrained) Gauss-Newton method with error oriented convergence criterion; by Nowak, Weimann, and Deuflhard, 1993) can be used.

4.3.1 Least-squares formulation

The least-squares formulation for the parameter estimation of GynCycle with the Gauss-Newton method (see e.g. [20]) is presented. The goal is to determine the parameter vector $p \in \mathbb{R}^{n_p}$, which arises within the solution $y(\cdot; p)$ of GynCycle (see Eq. (4.1)) or of a model part, such that it fits given measurements y^{exp} in a least-squares sense.

Data are given for the set of experimental data V^{exp} (see Chapter 3) at the measure time points T_l, $l = 1, \dots, N$ (see Section 4.2). In the following set $n' := N \cdot n_t$.

Since the parameters enter nonlinearly in y, a nonlinear least-squares problem of the general form

$$\min_{p \in D} g(p)$$

is given, where $g(p) := ||F(p)||_2^2$. It is $F : D \to \mathbb{R}^{n'}$, $F =: (F_i)_{i=1,\ldots,N \cdot n_t}$, a twice continuously differentiable function $F \in C^2(D)$ on an open set $D \subset \mathbb{R}^{n_p}$ with

$$F_{(l-1)\cdot n_t+k}(p) := \frac{y_{i_l}(t_k; p) - y_{l,k}^{exp}}{y_{l,k}^{wgt}}, \quad \forall l = 1, \ldots, N, k = 1, \ldots, n_t.$$

Here it is $D := \mathbb{R}_+$ and the weights are defined as follows:

$$y_{l,k}^{wgt} := ||\{y_{l,1}^{exp}, \ldots, y_{l,n_p}^{exp}\}||_2^2, \quad l = 1, \ldots, N, j = 1, \ldots, n_p.$$

4.3.2 Gauss-Newton method

In this section the Gauss-Newton method (see e.g. [20]) is presented.

Sufficient conditions for a local minimum p^* where $g(p^*) = \min_{p \in D} g(p)$ are $g'(p^*) = 0$ and $g''(p^*)$ positive definite. Since it holds $g'(p) = 2 \cdot F'(p)^T \cdot F(p)$, the problem can be formulated as follows

$$G(p) := F'(p)^T \cdot F(p) = 0.$$

This system of n_p nonlinear equations must be solved. Thereby it holds for $l = 1, \ldots, N$ and $j = 1, \ldots, n_p$

$$\begin{aligned} \frac{\partial F_{(l-1)\cdot n_t+k}(p)}{\partial p_j} &= \frac{1}{y_{l,k}^{wgt}} \cdot \frac{\partial y_{i_l}(t_k; p)}{\partial p_j} \\ &= \frac{1}{y_{l,k}^{wgt}} \cdot s_{i_l,j}^{abs}(t_k; p) = \frac{1}{y_{l,k}^{wgt}} \cdot s_{(l-1)\cdot n_t+k,j}^{*,abs}. \end{aligned}$$

Note the connection to the sensitivity analysis. This nonlinear system of equations can now be solved numerically by appliance of the Newton method. The iteration instruction is for $k' \in \mathbb{N}_0$ and initial value $p^{(0)}$

$$G'(p^{(k')}) \cdot \Delta p^{(k')} = -G(p^{(k')}).$$

Differentiation of G with respect to p leads to

$$G'(p) = F'(p)^T \cdot F'(p) + F''(p)^T \cdot F(p).$$

It holds for $l = 1, \ldots, N$ and $j, j' = 1, \ldots, n_p$

$$\begin{aligned} \frac{\partial^2 F_{(l-1)\cdot n_t+k}}{\partial p_j \partial p_{j'}} &= \frac{1}{y_{l,k}^{wgt}} \cdot \frac{\partial^2 y_{i_l}(t_k; p)}{\partial p_j \partial p_{j'}} \\ &= \frac{1}{y_{l,k}^{wgt}} \cdot \frac{\delta s_{i_l,j}^{abs}(t_k; p)}{\delta p_{j'}}. \end{aligned}$$

Under the above assumption, $G'(p)$ is positive definite in a vicinity of p^* and thus invertible. Assume that the model and data are approximately compatible, i.e. $F(p^*) \approx 0$. Moreover it holds in a vicinity of p^*, $p \in U(p^*)$

$$F(p) \approx 0$$

and therefore

$$G'(p) \approx F'(p)^T \cdot F'(p).$$

That way the costly calculation of $F''(p)$ can be avoided. Therefore as simplification for the $(k'+1)$-th step it is obtained

$$F'(p^{(k')})^T \cdot F'(p^{(k')}) \cdot \Delta p^{(k')} = -F'(p^{(k')})^T \cdot F(p^{(k')}).$$

That in turn are the normal equations of the linear least-squares problem

$$\min_{p \in D} ||F'(p) \cdot \Delta p + F(p)||_2^2,$$

where it follows

$$F'(p) \cdot \Delta p + F(p) = 0.$$

The solution for the k'-th step results then in

$$\begin{aligned} \Delta p^{(k')} &= -F' p^{(k')})^+ \cdot F(p^{(k')}), \\ p^{(k'+1)} &= p^{(k')} + \Delta p^{(k')}, \end{aligned}$$

where $F'(p^{(k')})^+$ denotes the pseudo-inverse (in the case of NLSQ_ERR outer inverse) of $F'(p^{(k')})$:

$$F'(p^{(k')})^+ = (F'(p^{(k')})^T \cdot F'(p^{(k')}))^{-1} \cdot F'(p^{(k')})^T.$$

In the global case it would be

$$p^{(k'+1)} = p^{(k')} + \lambda_{k'} \cdot \Delta p^{(k')}, \quad 0 < \lambda_{k'} \leq 1.$$

With aid of the QR decomposition the equation

$$F'(p^{(k')}) \cdot \Delta p^{(k')} = F(p^{(k')})$$

is solved.

The numerical solution of the original nonlinear least-squares problem therefore is reduced to the numerical solution of a sequence of linear least-squares problems.

The main costs consist in the calculation of the Jacobian matrix $F'(p)$. This contains all derivations of F with respect to the parameter vector p and therefore it is identical with the special sensitivity matrix S.

If this is calculated, $\Delta p^{(k')}$ can be determined and the procedure for the determination of the optimal parameter vector can be continued with $p^{(k'+1)}$.

4.3.3 Result of the parameter estimation for GynCycle

The parameter values are given in the appendix.

4.4 Simulation and comparison with experimental data

The parameter estimation for the model parts is conducted. Then the model parts are recomposed and last adaptions are done manually. Then the parameters that are needed for GynCycle are available and simulations of GynCycle are possible.

The simulation results are not shown for all 50 elements, especially comparison with experimental data is only possible for $N = 12$ of them. Additionally, the simulations of the GnRH concentration and of the follicular masses are plotted. The simulations visualize the dynamics over five cycles of length 31 d. The experimental data that are used for comparison with the simulation results can be found in the appendix.

GnRH pulse frequency

The simulation of the GnRH pulse frequency is shown in Fig. 4.2.

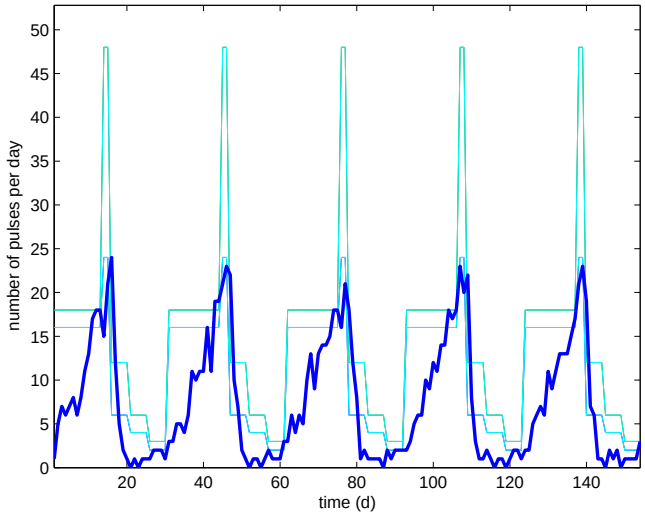

Figure 4.2: Simulation of the GnRH pulse frequency (blue solid: simulation result, light blue solid: interpolation of experimental data).

The increase of the pulse frequency in the first half of the cycle is reproduced by the model as the simulation shows, as well as the decrease in the second half. The constant phase with the typical pulse frequency of one pulse every 90 minutes is not given. Since the frequency is assumed to be relatively low in the end of the cycle and relatively high at the beginning of the cycle, the transition should be similar to the simulations even if the experimental data tell otherwise.

GnRH concentration in the pituitary portal system

The simulations of the GnRH concentration is shown in Fig. 4.3.

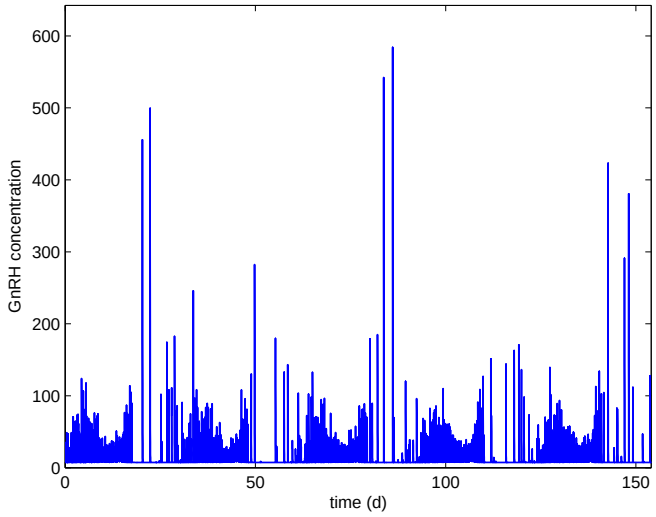

Figure 4.3: Simulation of the GnRH concentration in the pituitary portal system.

The pulsatile character is clearly recognizable.

LH concentration in the blood

The simulation of the LH blood concentration is shown in Fig. 4.4.

The most important characteristic is the peak at mid-cycle. During the remaining cycle, the concentrations is comparatively small and constant. The simulation shows that the model can reproduce these characteristics.

FSH concentration in the blood

The simulation of the FSH blood concentration is shown in Fig. 4.5.

In the first half of the cycle there is first an increase, then a decrease of the concentration. At mid-cycle there is a peak, even though not as distinctive as in the case of LH. In the second half there is first decrease and then increase. The simulation shows that GynCycle is able to reflect the FSH dynamics.

Follicular masses in the ovaries

The simulations of the follicular masses are shown in Fig. 4.6.

One would except that the maxima of the phases should occur consecutively within one cycle:

$$\arg(\max_t(F_s(t))) < \cdots < \arg(\max_t(L_a(t)))$$

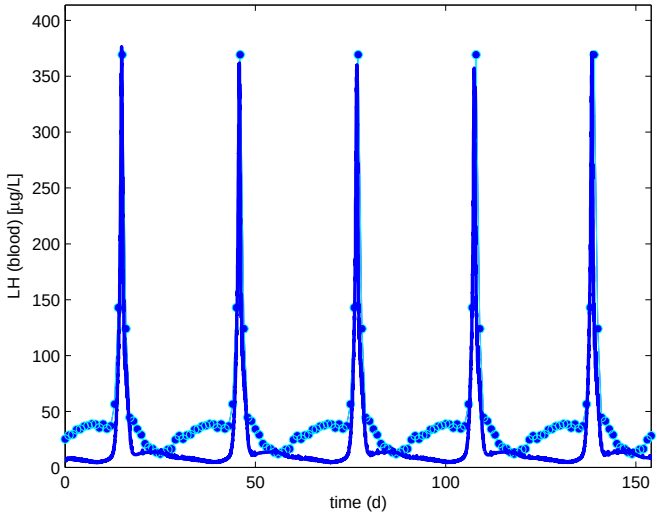

Figure 4.4: Simulation of the LH blood concentration (blue solid: simulation result, blue points: experimental data [37, 58], light blue solid: interpolation of experimental data).

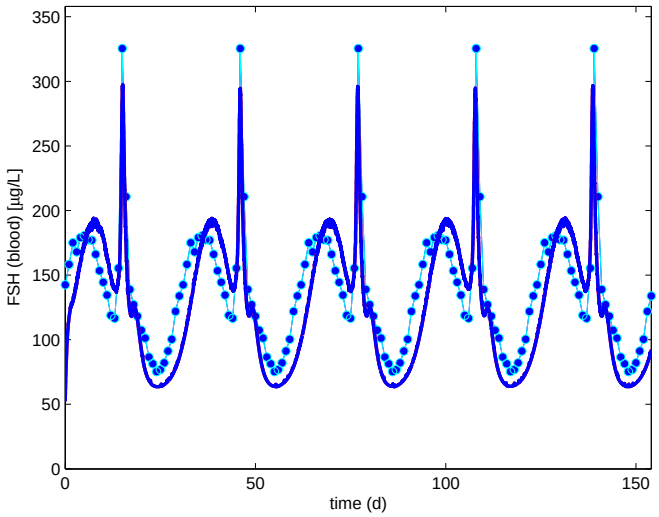

Figure 4.5: Simulation of the FSH blood concentration (blue solid: simulation result, blue points: experimental data [37, 58], light blue solid: interpolation of experimental data).

which is given here. The mass of F_g should be larger and there is growth in the luteal phase which is not reproduced by the simulations. Note that the equations for y_{11}

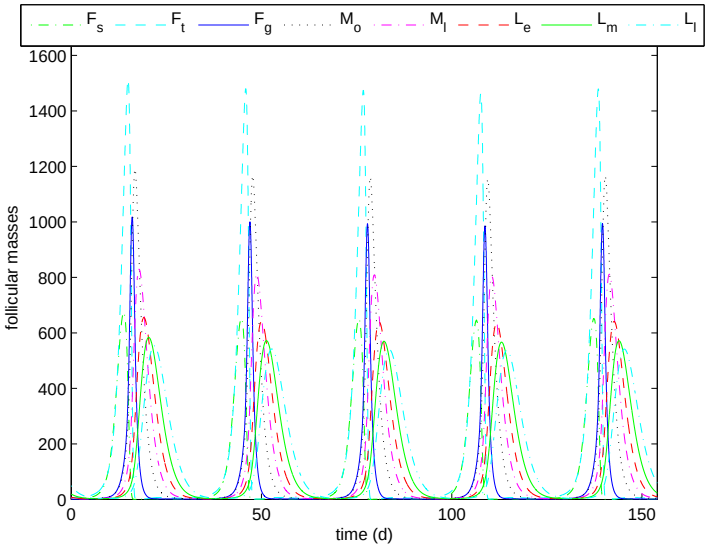

Figure 4.6: Simulation of the follicular masses at the different phases.

and y_{12} has been modified for the benefit of a better simulation result. The term $p_{66} \cdot y_{10}(t - p_{64})^{p_{68}} \cdot y_{11}(t)$ is adapted to the term in the corresponding equations of the basic compartment model:

$$p_{66} \cdot y_8(t - p_{70})^{p_{68}} \cdot y_{11}(t).$$

Progesterone concentration in the blood

The simulation of the progesterone blood concentration is shown in Fig. 4.7.

The concentration is low in the first half of the cycle (follicular phase), then there is a peak in the second half of the cycle, finally the concentration declines. This is well represented by the simulations.

Estradiol concentration in the blood

The simulations of the estradiol blood concentration is shown in Fig. 4.8.

There is an increase in the first half of the cycle, then there is a peak approximately one day before mid-cycle (the peak of LH). There is a second, smaller peak in the second half of the cycle, then the concentration declines. This is well represented by the simulations.

17α-Hydroxypregnenolone concentration in the blood

The simulation of the 17α-hydroxypregnenolone blood concentration is shown in Fig. 4.9.

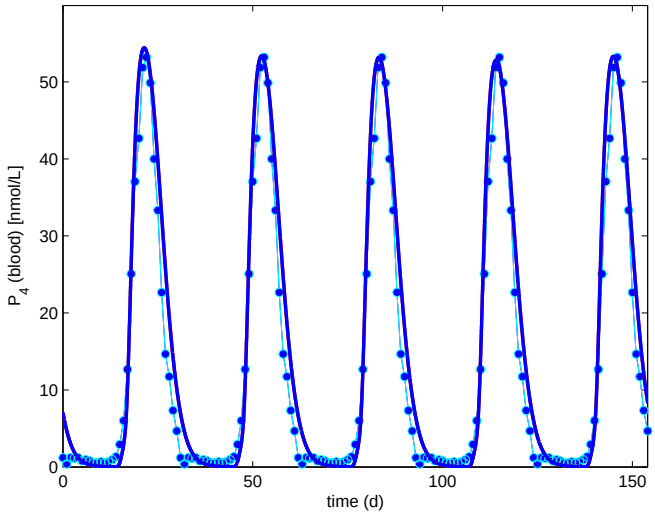

Figure 4.7: Simulation of the progesterone blood concentration (blue solid: simulation result, blue points: experimental data [37, 58], light blue solid: interpolation of experimental data).

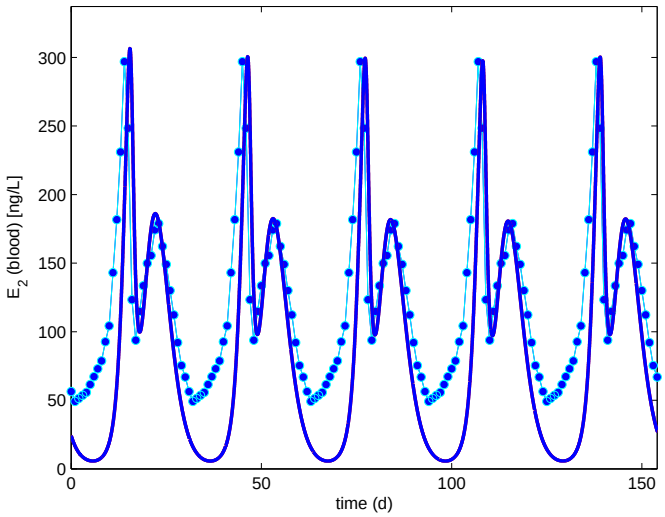

Figure 4.8: Simulation of the estradiol blood concentration (blue solid: simulation result, blue points: experimental data [37, 58], light blue solid: interpolation of experimental data).

The dynamics of 17α-hydroxypregnenolone is not given by experimental data, only a range. Similar dynamics as the one of 17α-hydroxyprogesterone (see Fig. 4.10) are

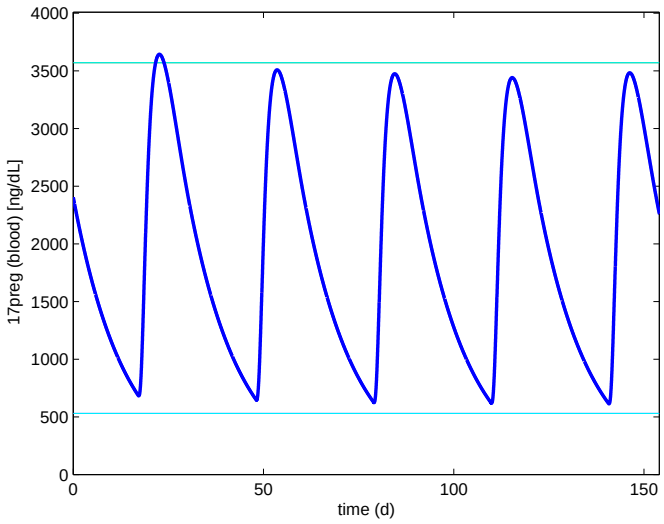

Figure 4.9: Simulation of the 17α-hydroxypregnenolone blood concentration (blue solid: simulation result, light blue solid: interpolation of experimental data).

assumed which is well reproduced by the simulations.

17α-hydroxyprogesterone concentration in the blood

The simulation of the 17α-hydroxyprogesterone blood concentration is shown in Fig. 4.10.

The dynamics of 17α-hydroxyprogesterone are qualitatively comparable to the one of progesterone, there is a peak in the second half of the cycle. The model can reproduce quite well the dynamics of 17α-hydroxyprogesterone given by experimental data.

DHEA, androstenedione, and testosterone concentrations in the blood

The simulation of the DHEA blood concentration is shown in Fig. 4.11, the simulation of the androstenedione blood concentration in Fig. 4.12, and the simulation of the testosterone blood concentrations in Fig. 4.13.

The dynamics of the DHEA, androstenedione, and testosterone blood concentrations are not reproduced. Since no other element is dependent on neither the DHEA nor the androstenedione nor the testosterone blood concentration, this is negligible for the time being. The dynamics of estrone and estradiol are well reproduced which suggests that the simulations for DHEA, androstenedione, and testosterone represent intermediate steps of the biosynthesis of the steroids. The model GynCycle should be improved to describe the dynamics of DHEA, androstenedione, and testosterone adequately.

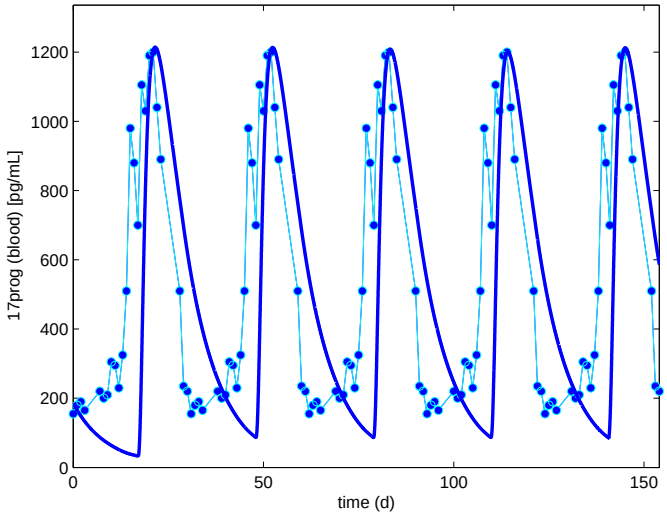

Figure 4.10: Simulation of the 17α-hydroxyprogesterone blood concentration (blue solid: simulation result, blue points: experimental data [48], light blue solid: interpolation of experimental data).

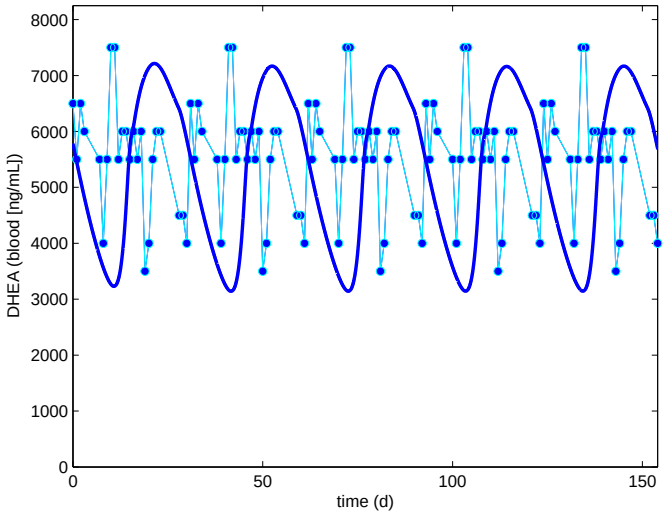

Figure 4.11: Simulation of the DHEA blood concentration (blue solid: simulation result, blue points: experimental data [48], light blue solid: interpolation of experimental data).

Estrone concentration in the blood

The simulation of the estrone blood concentration is shown in Fig. 4.14.

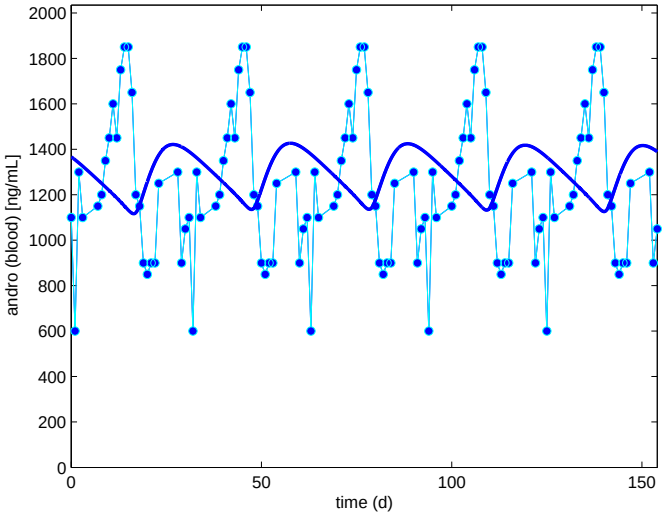

Figure 4.12: Simulation of the androstenedione blood concentration (blue solid: simulation result, blue points: experimental data [48], light blue solid: interpolation of experimental data).

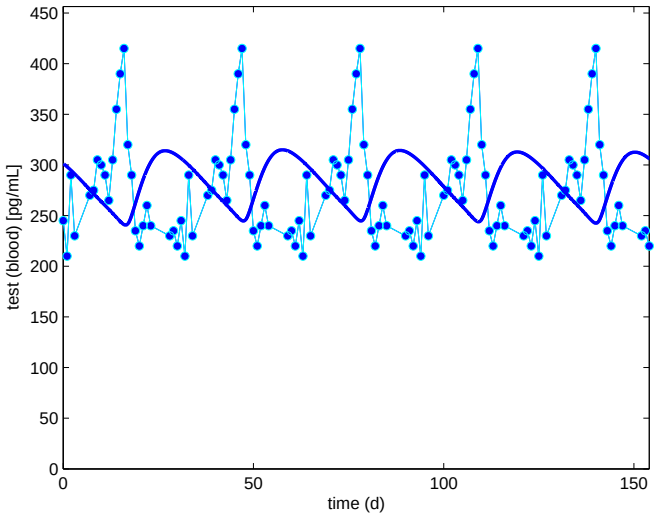

Figure 4.13: Simulation of the testosterone blood concentration (blue solid: simulation result, blue points: experimental data [48], light blue solid: interpolation of experimental data).

There is an increase in the first half of the cycle, then there is a peak approximately one day before mid-cycle (the peak of LH). There is a second, smaller peak in the second

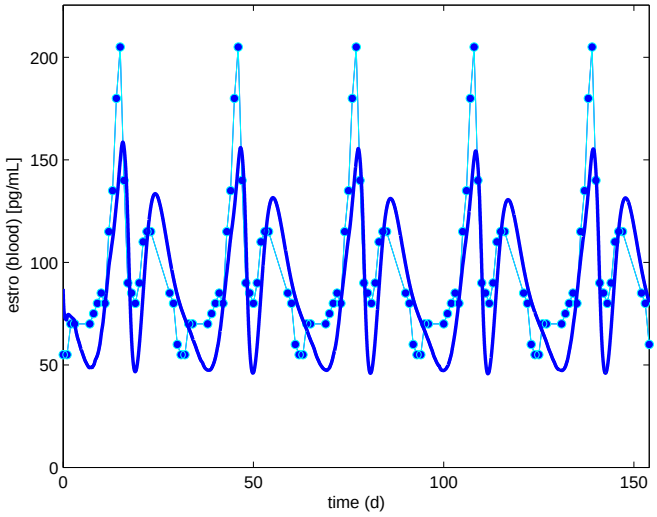

Figure 4.14: Simulation of the estrone blood concentration (blue solid: simulation result,blue points: experimental data [48], light blue solid: interpolation of experimental data).

half, then the concentration declines. This is quite well reproduced by the simulations.

Inhibin concentration in the blood

The simulation of the inhibin blood concentration is shown in Fig. 4.15.

In the case of the inhibin concentration there is first a small peak at mid-cycle and a larger one in the second half of the cycle. Then the concentration decreases. Both characteristics are given even if the first peak is too small in the simulation.

4.5 Summary

A numerical integrator, RADAR5, is chosen for this problem and the sensitive parameters are optimized for each model part. Simulations of the complex model are possible after recomposition of the model parts. The modeling could be proceeded, for example, the modeling of the steps around DHEA, androstenedione, and testosterone could be improved.

The utilization of delays shows another advantage: the length of the cycle can be varied by modifying the delay values (but other parameters have influence on the cycle length as well). This is necessary for a flexible model, especially since individual cases should be simulated.

For now the focus is on the qualitative result in view of first applications. The quantitative result becomes important when considering real, individual data.

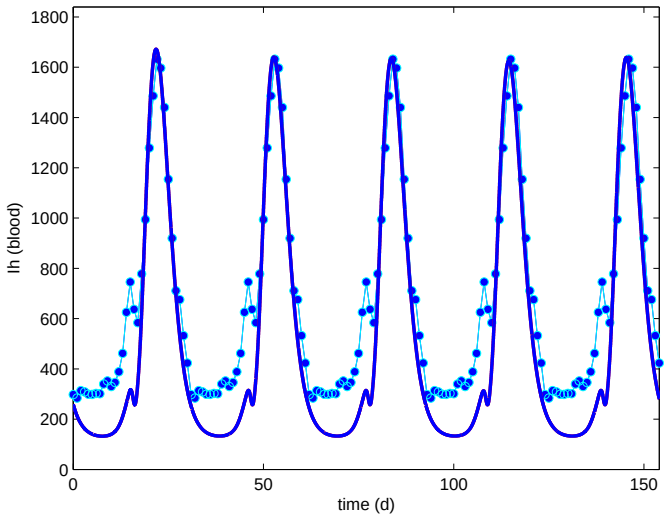

Figure 4.15: Simulation of the inhibin blood concentration (blue solid: simulation result, blue points: experimental data [37, 58], light blue solid: interpolation of experimental data).

Chapter 5

Applications of GynCycle

The premises for the simulation of GynCycle are established in Chapter 4. The simulations show that the model is able to reproduce the dynamics of essential characteristics of the female menstrual cycle. Thus it is appropriate to deal with applications of GynCycle which is done in this chapter.

More precisely, some approaches for the modeling of hormonal manipulations of the cycle are presented. First some models for hormonal contraceptives are introduced and simulations are shown in Section 5.1. Then the case that GnRH is administrated continuously is treated in Section 5.2. The results are summarized in Section 5.3.

5.1 Modeling the effects of hormonal contraceptives

Hormonal contraceptives belong to the most important and effective methods to avoid pregnancy [45]. Worldwide there are over 60 million women taking regularly the birth control pill, an oral hormonal contraceptive [27, 50]. The number of general contraceptive users is even higher (already in 1990 there were about 384 million [28]). Moreover hormonal contraceptives can be used, for example, therapeutically for the regulation of the cycle [45].

There are different types of hormonal contraceptives. Here it is distinguished between the way the intake or the administration takes place. That means that it is examined on the one hand which compartments are affected and on the other hand whether the administration occurs continuously, i.e. at a constant rate, or whether the hormones are administered or taken at certain time points. There are further hormonal methods, which act locally (i.e. at the cervix uteri or the endometrium). However, these are not treated in this context.

As first group of hormonal contraceptives those are counted that are administered non-orally and continuously and which affect mainly the blood compartment (and possibly the skin or muscles):

- Subdermal implants [24]. One or more flexible rods containing a gestagen are implanted under the skin.
- Injections [24]. A gestagen is injected every 12 weeks intramuscular or subcutaneous (under the skin). Others are effective for 2 to 5 years. The follicular

maturation and the LH mid-cycle peak are suppressed. Furthermore there are combined injectables, a monthly injection of a gestagen and an estrogen.

- Contraceptive patch [43]. An adhesive patch containing a gestagen and an estrogen is applied to the skin and worn continuously. It is changed each week for three weeks and removed for one week.

The oral contraceptives ("birth control pill"), hormonal contraceptives that are taken orally, are gathered in a second group. Those are taken usually once a day and affect among other things the compartments stomach, intestine, blood, and liver:

- Combined oral contraceptives [24]. The tablets contain an estrogen component (usually ethinylestradiol) and a gestagen component. Each tablet contains the same amount of the gestagen and of the estrogen. The intake occurs e.g. for 21 days followed by a break of 7 days (there are combined oral contraceptives that are taken without break [25]).

- Bi- or triphasic oral contraceptives [45]. The tablets contain, as the combined oral contraceptives, an estrogen component and a gestagen component, but they are taken in two (three) phases where the doses of gestagen and estrogen differ, e.g. 11 days phase 1, 10 days phase 2, 7 days break.

- Progestogen only pill ("mini pill") [45]. The tablets only contain a gestagen component. They are taken without break. The ovulation is not suppressed since the amount of hormone is low. The mini pill acts at the cervix uteri and the endometrium.

The action of hormonal contraceptives primarily consists in the suppression of ovulation [45]. There are exceptions as e.g. the progestogen only pill which comes in small doses and acts differently. The suppression of the ovulation is mainly due to the gestagen component and is amplified by an estrogen component. Additionally the estrogen results in a significant improvement of the regulation of the cycle.

Furthermore the secretion of FSH and LH is inhibited [45], in particular, the mid-cycle peak of LH is suppressed. The mid-cycle peak of LH is essential for the ovulation but can only result in the release of the ovum if there is a Graafian follicle that can become an ovulatory follicle (see Chapter 2). In GynCycle the suppression of the ovulation can be modeled via the suppression of the follicular mass at ovulation. If the mass of ovulation is low, i.e. below a critical value, it can be said that ovulation does not occur.

Usually ethinylestradiol (EE) is used as estrogen which is a pharmacological variant of E_2 and amplifies the action of E_2 [45]. The gestagens that are orally effective can be divided into three groups due to their structure (derivates of 17α-hydroxyprogesterone, norethisterone, and norgestrel) [45]. They differ in their potency to inhibit ovulation [26].

Drugs are in general not well-mixed in the body. Thus it is adequate to regard the body as a build-up of compartments [44] which is also described in Chapter 1. Here it is assumed that each of these compartments has a well-defined volume and that the drug that is taken or administered is well-mixed within these compartments [44].

First two simple modeling approaches for the effect of extraneous gestagen and estrogen are discussed. Then the representations of the different types of the hormonal contraceptives by model equations and their connection to GynCycle are shown and exemplary simulations are visualized.

5.1.1 Simple approaches

The dynamics of the elements in GynCycle that are dependent on progesterone (P_4) and estradiol (E_2) are influenced by the gestagen and estrogen components as well. Suppose that the concentrations of the gestagen and the estrogen components are constant. Denote the constant gestagen component concentration by d_{GC} where $[d_{GC}] = [P_4]$ and the constant estrogen component concentration by d_{EC} where $[d_{EC}] = [E_2]$. Then it follows for the dynamics in the hypothalamus and pituitary of the elements that are dependent on P_4 and E_2 (i.e. $GnRH_{freq}$, P_{LH}, LH, P_{FSH}, and FSH):

$$\frac{d}{dt}y_i = f_i(P_4 + \theta_{GC} \cdot d_{GC}, E_2 + \theta_{EC} \cdot d_{EC}), \quad i = 1, 7, \ldots, 10,$$

and dependent on only E_2 (i.e. $GnRH_{mass}$):

$$\frac{d}{dt}y_2 = f_2(E_2 + \theta_{EC} \cdot d_{EC}),$$

where $\theta_{GC}, \theta_{EC} \in \mathbb{R}_+$ consider the potency of the gestagen and estrogen component compared to P_4 and E_2, respectively. If the potency of the gestagen component is comparable to the one of P_4, then it is $\theta_{GC} = 1$ (for θ_{EC} analogously).

In this approach the metabolism of the gestagen and estrogen components is not considered. Even if the administration is continuous, the concentrations of the gestagen and estrogen components are not constant until the steady state is reached. Thus this approach is assessed as not suitable since the simplification is too strong.

A better and still simple approach to consider oral contraceptives in GynCycle is the addition of constants in the differential equations for E_2 and P_4 (compare with Eqs. (2.97) and (2.98) in Chapter 2):

$$\begin{aligned}\frac{d}{dt}P_4(t) &= \frac{\theta_{GC} \cdot \nu_{GC} \cdot \beta_{GC} \cdot d_{GC}}{V_B} + \frac{s_{P_4}}{V_B} \cdot prog_0(t - \tau_{prog}) - \alpha_{P_4} \cdot P_4(t) \\ \frac{d}{dt}E_2(t) &= \frac{\theta_{EC} \cdot \nu_{EC} \cdot \beta_{EC} \cdot d_{EC}}{V_B} + \frac{s_{E_2}}{V_B} \cdot estra_0(t - \tau_{estra}) - \alpha_{E_2} \cdot E_2(t),\end{aligned}$$

where d_{GC} (with $[d_{GC}] = [P_4] \cdot \frac{L}{d}$) and d_{EC} (with $[d_{EC}] = [E_2] \cdot \frac{L}{d}$) denote the intake dose per day of the gestagen and estrogen component, respectively, $\nu_{GC}, \nu_{EC} \in (0, 1]$ consider the bioavailability, and $\beta_{GC}, \beta_{EC} \in (0, 1]$ the fraction that is not bounded to plasma proteins for the gestagen and estrogen component, respectively. Both components are distributed in the blood volume V_B. The model equations for the dynamics in the hypothalamus and in the pituitary are not affected since the concentrations of the components are added in the equations for P_4 and E_2:

$$\frac{d}{dt}y_i = f_i(P_4, E_2), \quad i = 1, 7, \ldots, 10.$$

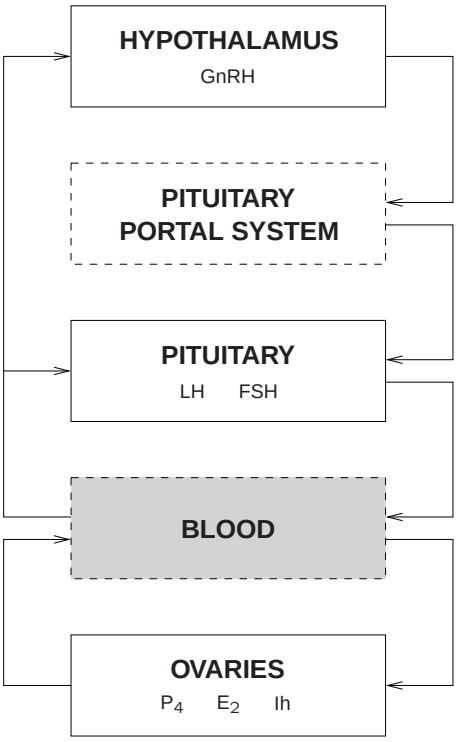

Figure 5.1: Single-compartment model (shaded gray) that is integrated in the compartmental model of GynCycle.

and

$$\frac{d}{dt}y_2 = f_2(E_2).$$

Here it is assumed that the metabolism (in this case simple clearance) of the endogenous hormones is comparable to the one of the extraneous components. Thus it may be more correct to consider the dynamics of the components themselves.

5.1.2 Single-compartment model

In this approach it is assumed that the dose of the hormonal contraceptive has been taken or administered and has reached the blood compartment. That means that only the dynamics in the blood compartment are considered (see Fig. 5.1).

The general model equation for the dynamics of the extraneous hormone concentration $H(\cdot)$ can be written as

$$\frac{d}{dt}H(t) = \frac{\xi_H(t)}{V(t)} - \alpha_H(t; H(t)), \quad H(t_0) = 0,$$

where $\xi_H(\cdot)$ denotes the intake function, $V(\cdot)$ the volume of the blood compartment, and $\alpha_H(\cdot;\cdot)$ the clearance function.

If the hormone is administered at a constant rate d_H, the intake function is given by

$$\xi_H(t) := \nu_H \cdot \beta_H \cdot d_H, \quad \forall t \geq t_0,$$

where ν_H denotes the fraction of bioavailability of the hormone H and β_H the fraction of unbounded molecules.

If the intake occurs at the time point $t_j > t_0$, the intake of the hormone H is better described by

$$\xi_H(t) := \nu_H \cdot \beta_H \cdot d_H \cdot \psi(t - t_j), \quad \forall t \geq t_j, \tag{5.1}$$

where $\psi(\cdot)$ denotes a probability density, e.g. the Gamma density. If the hormone is taken at the time points t_j, $j \in \mathbb{N}_0$ (as e.g. in the case of oral contraceptives), the intake function can be written as

$$\xi_H(t) := \nu_H \cdot \beta_H \cdot d_H \cdot \sum_{i=1}^{j} \psi(t - t_i), \quad t \in [t_j, t_{j+1}).$$

For simplicity only the last pulse time point can be considered (compare Chapter 2).

For the clearance it can be assumed for all $t \geq t_0$ that the hormone is metabolized linearly (see e.g. [44]) at a constant rate:

$$\alpha_H(t; H(t)) := \alpha_{H,B} \cdot H(t),$$

or the enzymatic metabolism can be considered:

$$\alpha_H(t; H(t)) := V_{H,max} \cdot \frac{H(t)}{K_M + H(t)}.$$

Here the volume is assumed to be constant: $V(t) := V_B$ for all $t \geq t_0$. W.l.o.g. set $t_0 := 0$.

First group: continuous administration

For the gestagen and the estrogen components of, for example, a contraceptive patch assume a constant administration rate and a constant clearance in the blood:

$$\begin{aligned}
\frac{d}{dt}GC(t) &= \frac{\nu_{GC} \cdot \beta_{GC} \cdot d_{GC}}{V_B} - \alpha_{GC} \cdot GC(t), \quad GC(0) = 0 \\
\frac{d}{dt}EC(t) &= \frac{\nu_{EC} \cdot \beta_{EC} \cdot d_{EC}}{V_B} - \alpha_{EC} \cdot EC(t), \quad EC(0) = 0,
\end{aligned}$$

where $GC(\cdot)$, $EC(\cdot)$ denote the concentrations of the gestagen component and of the estrogen component, respectively, d_{GC}, d_{EC} the intake dose per day that is distributed in the blood volume V_B, and that is cleared at the rate α_{GC}, α_{EC}, ν_{GC}, ν_{EC} the fraction of bioavailability, and β_{GC}, β_{EC} the fraction of unbounded molecules, respectively.

If, for example, a contraceptive patch is used for three weeks and then a break of one week occurs, the equations for the time of the break are given by

$$\frac{d}{dt}GC(t) = -\alpha_{GC} \cdot GC(t)$$
$$\frac{d}{dt}EC(t) = -\alpha_{EC} \cdot EC(t)$$

i.e. $\xi_{GC}(t) = 0$ and $\xi_{EC}(t) = 0$, the gestagen and estrogen components are cleared from the blood compartment.

If the hormones are administered without break (e.g. injection or subdermal implants for the period where they are effective), a steady state is reached:

$$GC^* = \frac{\nu_{GC} \cdot \beta_{GC} \cdot d_{GC}}{V_B \cdot \alpha_{GC}}$$
$$EC^* = \frac{\nu_{EC} \cdot \beta_{EC} \cdot d_{EC}}{V_B \cdot \alpha_{EC}}.$$

In Fig. 5.2 a simulation is visualized for the case that the hormones are administered for the first 21 days of a cycle of length 28 and in Fig. 5.3 a simulation is visualized for the case that the administration is not interrupted. The parameter values that are used are listed in Table 5.1.

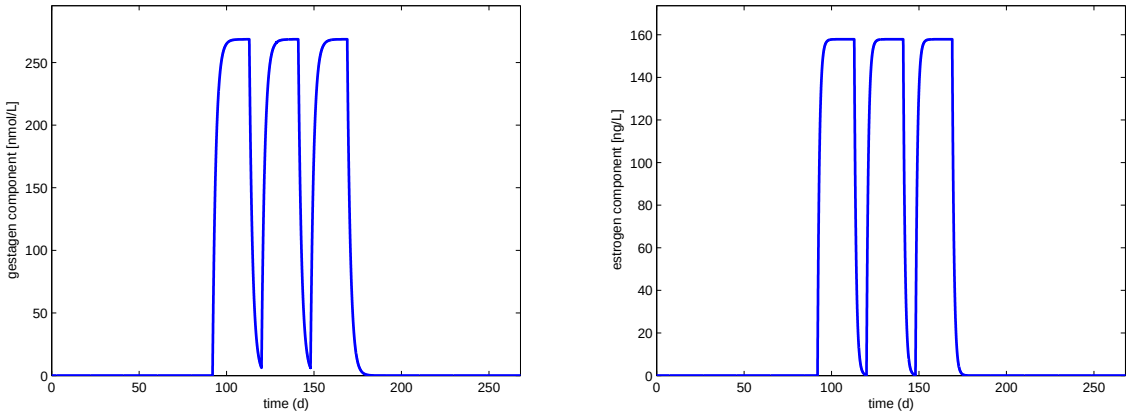

Figure 5.2: Simulations of the gestagen and estrogen component concentrations (for example: contraceptive patch (with both components)). Administration is from day 92 for three cycles with length 28 days on the first 21 days of every cycle.

Second group: oral contraceptives

Suppose that the intake rate is not constant, but that there are intake time points and that the dose is distributed, i.e. a maximum is reached and then the concentration declines. For simplicity it can be said that the intake time points are given by: $t_j = t_0 + j$, $j \in \mathbb{N}$, i.e. every day the dose is taken at the same time (which is recommended). Then the equations are of the form, $t \in [t_j, t_{j+1})$, $j \in \mathbb{N}$,

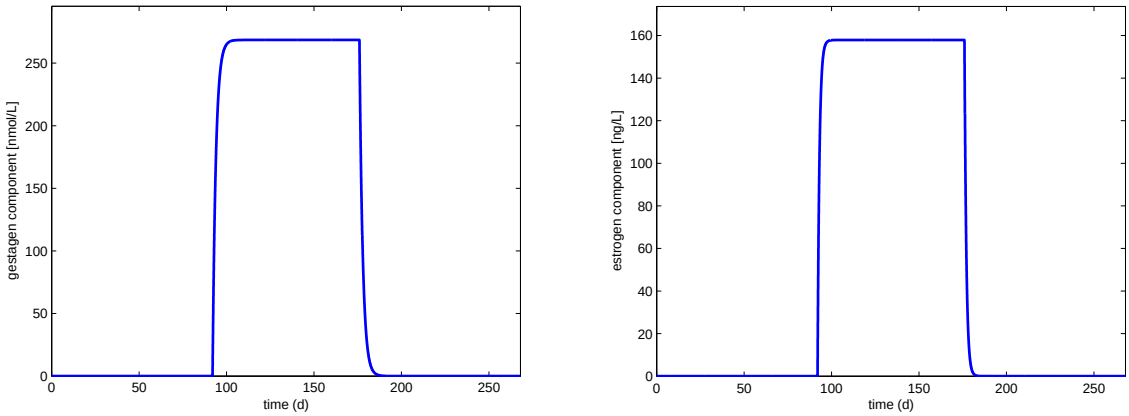

Figure 5.3: Simulations of the gestagen and estrogen component concentrations (for example: implants and injections (if both components; otherwise only gestagen component relevant)). Administration is from day 92 for 84 days.

$$\frac{d}{dt}GC(t) = \frac{\nu_{GC} \cdot \beta_{GC} \cdot d_{GC}}{V_B} \cdot \psi(t - t_j) - \alpha_{GC} \cdot GC(t), \quad GC(0) = 0$$
$$\frac{d}{dt}EC(t) = \frac{\nu_{EC} \cdot \beta_{EC} \cdot d_{EC}}{V_B} \cdot \psi(t - t_j) - \alpha_{EC} \cdot EC(t), \quad EC(0) = 0,$$

where d_{GC}, d_{EC} denote the dose of the gestagen and of the estrogen component, respectively, and $\psi(\cdot)$ denotes the Gamma distribution. Similar to the GnRH pulse generator and the resulting GnRH concentration described in Sections 2.2 and 2.3, it would be more correct to model

$$\frac{d}{dt}GC(t) = \frac{\nu_{GC} \cdot \beta_{GC} \cdot d_{GC}}{V_B} \cdot \sum_{i=1}^{j} \psi(t - t_i) - \alpha_{GC} \cdot GC(t), \quad GC(0) = 0$$
$$\frac{d}{dt}EC(t) = \frac{\nu_{EC} \cdot \beta_{EC} \cdot d_{EC}}{V_B} \cdot \sum_{i=1}^{j} \psi(t - t_i) - \alpha_{EC} \cdot EC(t), \quad EC(0) = 0.$$

Maximum serum concentrations of the gestagen and estrogen components are reached within 1 to 2 hours after oral intake [45, 26]. Within the break, EE is metabolically cleared [45].

In Fig. 5.4 a simulation for the intake for the first 21 days of a 28-days-cycle and in Fig. 5.5 a simulation for the intake without break are visualized.

The continuous administration and the intake at discrete time points are comparable which is justified in the following. Denote the dynamics for continuous administration by $y_1(\cdot)$ with

$$\frac{d}{dt}y_1(t) = p, \quad y_1(0) := 0,$$

Table 5.1: Parameter values for the single-compartment model. On the left: gestagen component; on the right: estrogen component.

Name	Value based on [49]	Name	Value based on [8, 26, 50, 64]
θ_{GC}	0.19	θ_{EC}	1.9
ν_{GC}	0.76	ν_{EC}	0.5
β_{GC}	0.05	β_{EC}	0.025
α_{GC}	0.54 1/d	α_{EC}	0.95 1/d
d_{GC}	3.0 mg $= 3.0 \cdot 3.18 \cdot 10^3$ nmol	d_{EC}	30.0 μg $= 30.0 \cdot 10^3$ ng
a_{GC}	84.1	a_{EC}	87.0
m_{GC}	2	m_{EC}	2

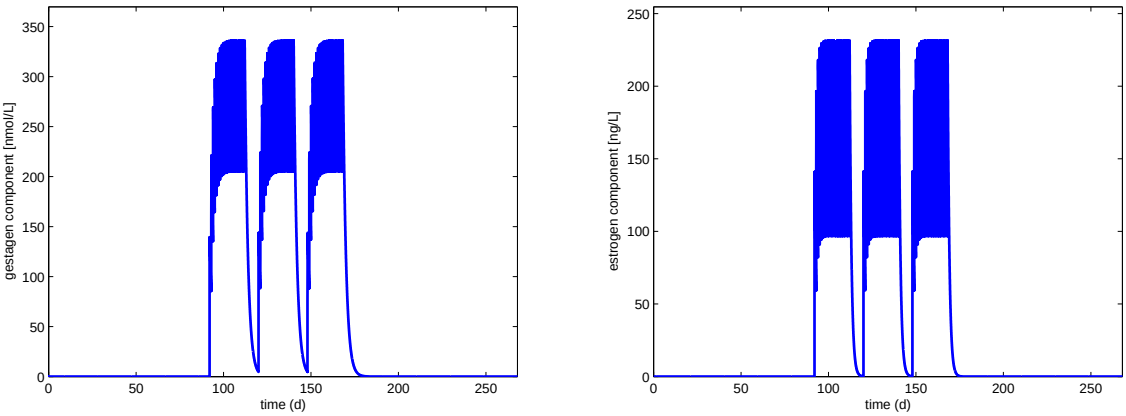

Figure 5.4: Simulations of the gestagen and estrogen component concentrations (for example: combined oral contraceptive (intake with break)). Intake is from day 92 for three cycles with length 28 days on the first 21 days of every cycle.

and the distributed intake by $y_2(\cdot)$ with

$$\frac{d}{dt}y_2(t) = p \cdot \psi(t), \quad y_2(0) := 0,$$

where p denotes the constant rate (amount per day). Calculation of the amount of hormone after one day yields

$$y_1(1) = p$$

and

$$y_2(1) = p \cdot \int_0^1 \psi(s)\, ds \approx p.$$

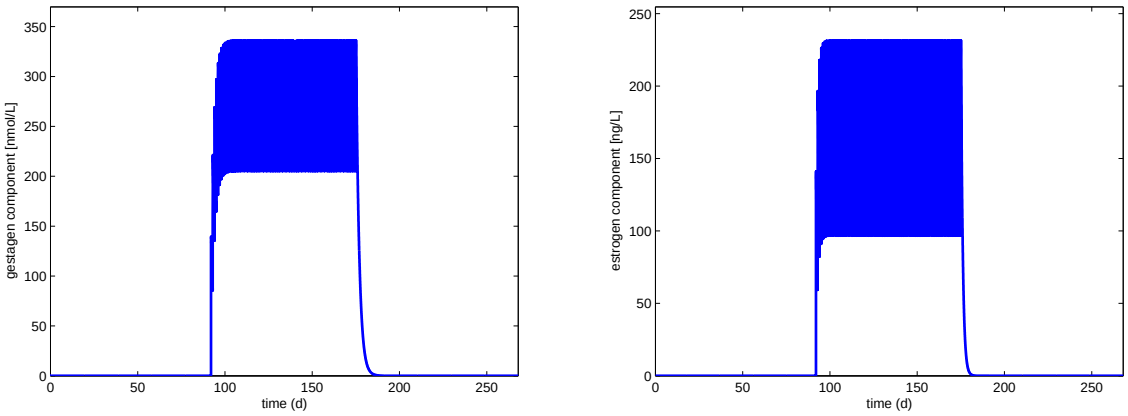

Figure 5.5: Simulations of the gestagen and estrogen component concentrations (for example: combined oral contraceptive (intake without break)). Intake is from day 92 for 84 days.

The amount is smaller in the second case but the difference is negligible if a and m are chosen as done above. Thus the effects are considered to be similar which can be assured by the simulation results. Hence the model equations for the first group can be used as simplification of the model equations for the second group.

Effects on GynCycle

The resulting hormone concentrations that are regulated by oral contraceptives in the hypothalamus and pituitary (the right hand side is dependent on P_4 and E_2) are given by

$$\frac{d}{dt}y_i = f_i(P_4 + \theta_{GC} \cdot GC, E_2 + \theta_{EC} \cdot EC), \quad i = 1, 7, \ldots, 10.$$

and dependent on only E_2:

$$\frac{d}{dt}y_2 = f_2(E_2 + \theta_{EC} \cdot EC),$$

where θ_{GC} and θ_{EC} denote the potency of the gestagen component compared to P_4 and the potency of the estrogen component compared to E_2, respectively.

One example is shown in Figs. 5.6, 5.7, 5.8 (with break), and 5.9, 5.10, 5.11 (without break) where the follicular masses, the follicular mass at ovulation in particular, and the LH concentration are shown.

It can be observed that the follicular mass is suppressed while taking oral contraceptives. The LH (and FSH) concentration is suppressed during intake as well. If there is a break after 21 days, the follicular masses are larger than in the case of intake without break. That is consistent with the fact, the oral contraceptives are indeed safer if the intake is not interrupted. There are other effects that must be considered as well when taking oral contraceptives continuously, which is why not every oral

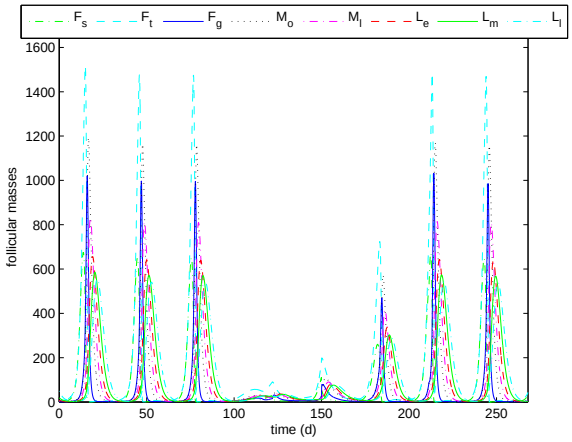

Figure 5.6: Simulation of the follicular masses (intake 21 of 28 days). Administration is from day 92 for three cycles with length 28 days.

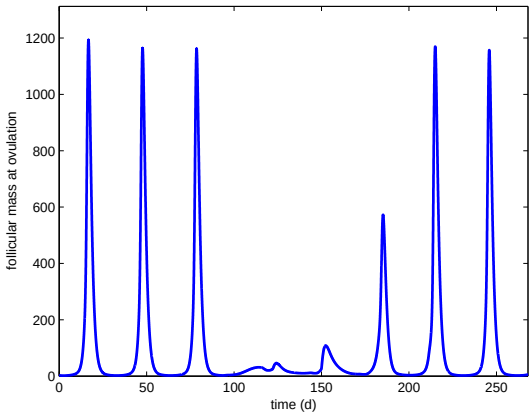

Figure 5.7: Simulation of the ovulatory follicular mass (intake 21 of 28 days). Administration is from day 92 for three cycles with length 28 days.

contraceptive is suitable for the intake without break. Moreover, the total amount of hormone that is taken is higher than in the case of the normal intake which cannot be ignored especially when considering time dependent effects. The difference between intake with and without break is shown in Fig. 5.12. The higher amount of hormone that is obtained for the case without break leads to a shift of the cycle in comparison to the case with break: the “normal” cycle starts later.

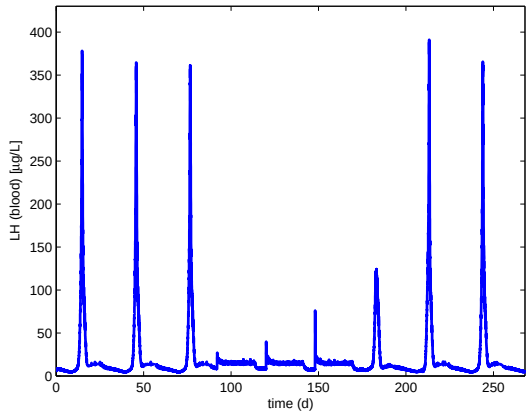

Figure 5.8: Simulation of the LH concentration (intake 21 of 28 days). Administration is from day 92 for three cycles with length 28 days.

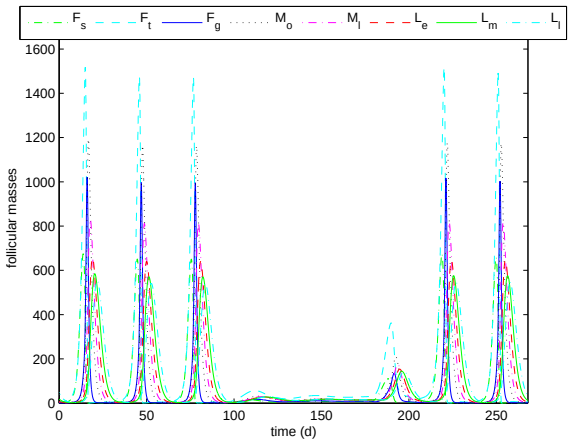

Figure 5.9: Simulation of the follicular masses (intake without break). Administration is from day 92 for three cycles with length 28 days.

Modeling an accidental break of intake

Since oral contraceptives are taken as tablets by the users, the possibility that the intake is missed on one day (or more) of the cycle must be considered. In this case there is no input for that day which decreases the concentrations of the gestagen and estrogen components and increases the follicular masses. It is known that the follicular mass at the ovulatory state can become critical under certain circumstances dependent on the day of the cycle where this additional "break" occurs and the individual conditions

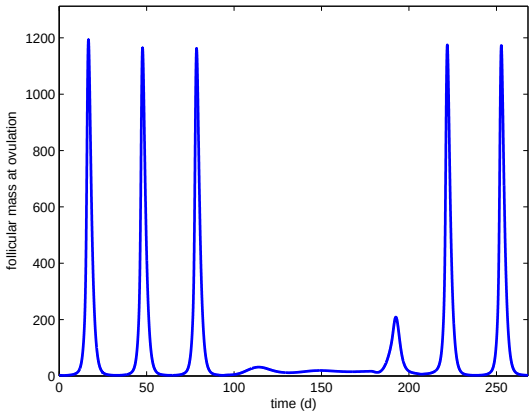

Figure 5.10: Simulation of the ovulatory follicular mass (intake without break). Administration is from day 92 for three cycles with length 28 days.

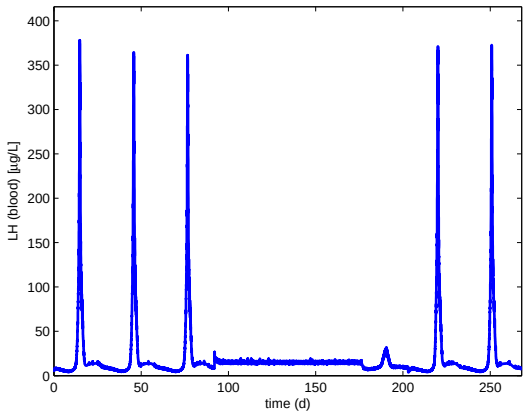

Figure 5.11: Simulation of the LH concentration (intake without break). Administration is from day 92 for three cycles with length 28 days.

[50]. In Fig. 5.13 an example is shown and compared with the dynamics if the intake is regular. Indeed the follicular mass at the ovulatory state can become higher already when one tablet is missed. If the critical value is exceeded, ovulation can occur if the LH concentration is high enough. This is dependent on the day of the cycle. If the tablet is not taken on day 1 of the cycle, the follicular mass is significantly increased.

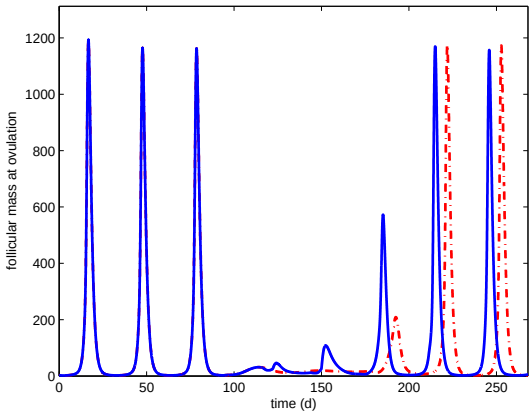

Figure 5.12: Simulation of the ovulatory follicular mass (intake 21 of 28 days: blue solid, intake without break: red dashed). Intake is from day 92 for three cycles with length 28 days.

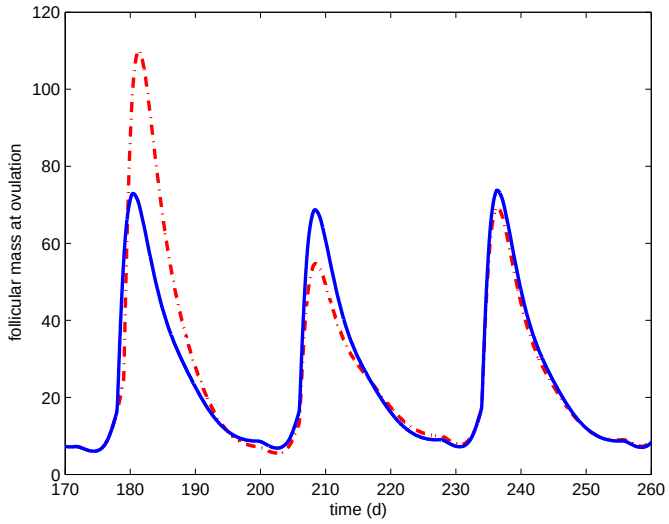

Figure 5.13: Simulation of the ovulatory follicular mass (intake 21 of 28 days). Break of one day during intake in the fourth cycle. Intake is from day 92. blue solid: normal; red dashdot: not on day 1 of cycle 4.

5.1.3 Multi-compartment models for oral contraceptives

In order to model more realistically, more compartments must be taken into consideration, e.g. the stomach, the intestine, and the liver. The consideration of other compartments is especially relevant when examing certain processes in other compartments as, for example, adverse effects. Here only possible modeling approaches are

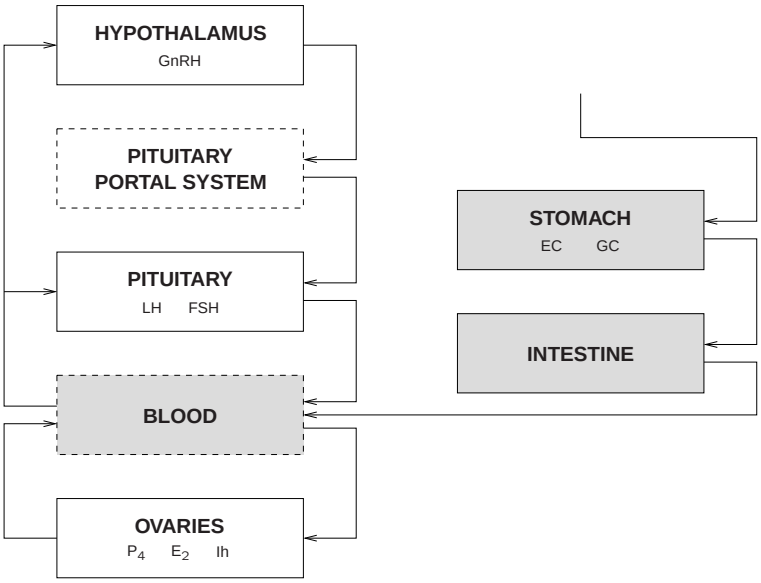

Figure 5.14: Three-compartment model integrated in the compartmental model of GynCycle.

presented.

The oral contraceptive is taken and reaches the stomach. Then it leaves the stomach (assumed at a constant rate) and reaches the intestine where it is distributed in the volume of the intestine. There it is absorbed within the small intestinal wall [26]. The gestagen component arrives the blood circulation (assumed at a constant rate) and the estrogen component gets first to the liver. Finally the gestagen component reaches the liver (assumed at a constant rate) where it is eliminated enzymatically. The estrogen component reaches the blood through the liver and a re-entry from the circulation to the intestine and the enzymatic clearance in the liver is possible (enterohepatic circulation) [26]. Usually the gestagens have a high bioavailability, but not ethinylestradiol since it undergoes enterohepatic circulation [63, 64]. The enzymatic metabolism is modeled by use of the Michaelis-Menten mechanism (see Chapter 1). For the other reactions, simple reaction kinetics are assumed.

For simplicity, first the dynamics are modeled by neglecting the processes in the liver. The three-compartment model is visualized in Fig. 5.14.

The dynamics of the gestagen component in the stomach (if $GC_S(0) = 0$ and if the intake time points are at t_j, $j \in \mathbb{N}_0$, $t_{j+1} = t_j + 1$ with the dose d_{GC}) can be modeled by

$$\begin{aligned}
\frac{d}{dt}GC_{S,0}(t) &= -k_{GC,1} \cdot GC_{S,0}(t), \quad GC_{S,0}(0) = 0, \quad t \in [0, t_1] \\
\frac{d}{dt}GC_{S,j}(t) &= -k_{GC,1} \cdot GC_{S,j}(t), \quad GC_{S,j}(t_j) = GC_{S,j-1}(t_j) + d_{GC}, \quad t \in [t_j, t_{j+1}], \forall j \in \mathbb{N}.
\end{aligned}$$

Define then for all $t \geq 0$

$$GC_S(t) := GC_{S,j}(t), \quad t \in [t_j, t_{j+1}).$$

Thus the dynamics of the gestagen component in the stomach, intestine, and blood can be described for all $t \geq 0$ by

$$\begin{aligned}
\frac{d}{dt}GC_S(t) &= -k_{GC,1} \cdot GC_S(t), & GC_S(0) = 0 \\
\frac{d}{dt}GC_I(t) &= \frac{k_{GC,1}}{V_I} \cdot GC_S(t) - k_{GC,2} \cdot GC_I(t), & GC_I(0) = 0 \\
\frac{d}{dt}GC_B(t) &= \frac{k_{GC,2} \cdot V_I}{V_B} \cdot GC_I(t) - \alpha_{GC}(t; GC_B(t)), & GC_B(0) = 0,
\end{aligned}$$

where $k_{GC,1}, k_{GC,2} \in \mathbb{R}_+$ denote the rate constants. Analogous for the estrogen component the following system is obtained:

$$\begin{aligned}
\frac{d}{dt}EC_S(t) &= -k_{EC,1} \cdot EC_S(t), & EC_S(0) = 0 \\
\frac{d}{dt}EC_I(t) &= \frac{k_{EC,1}}{V_I} \cdot EC_S(t) - k_{EC,2} \cdot EC_I(t), & EC_I(0) = 0 \\
\frac{d}{dt}EC_B(t) &= \frac{k_{EC,2} \cdot V_I}{V_B} \cdot EC_I(t) - \alpha_{EC}(t; EC_B(t)), & EC_B(0) = 0,
\end{aligned}$$

where $k_{EC,1}, k_{EC,2} \in \mathbb{R}_+$ denote the rate constants. Then again the concentrations that are dependent on P_4 and E_2 are influenced analogously to the single-compartment model.

If time delays are considered, then it follows, for example, for the gestagen component:

$$\begin{aligned}
\frac{d}{dt}GC_S(t) &= -k_{GC,1} \cdot GC_S(t) \\
\frac{d}{dt}GC_I(t) &= \frac{k_{GC,1}}{V_I} \cdot GC_S(t - \tau_S) - k_{GC,2} \cdot GC_I(t) \\
\frac{d}{dt}GC_B(t) &= \frac{k_{GC,2} \cdot V_I}{V_B} \cdot GC_I(t - \tau_I) - \alpha_{GC}(t; GC_B(t)).
\end{aligned}$$

In the four-compartment model, additionally the liver is incorporated. Then it is necessary to distinguish between the gestagen and estrogen component. Two possibilities of the four-compartment model are visualized in Figs. 5.15 and 5.16. In the first case, high bioavailability can be expected, which is the case for the gestagens. In the second case, because of this first-pass effect (due to the enterohepatic circulation), the bioavailability is diminished, which is the case for EE. The bioavailability is modeled here directly, thus no additional parameter ν is necessary.

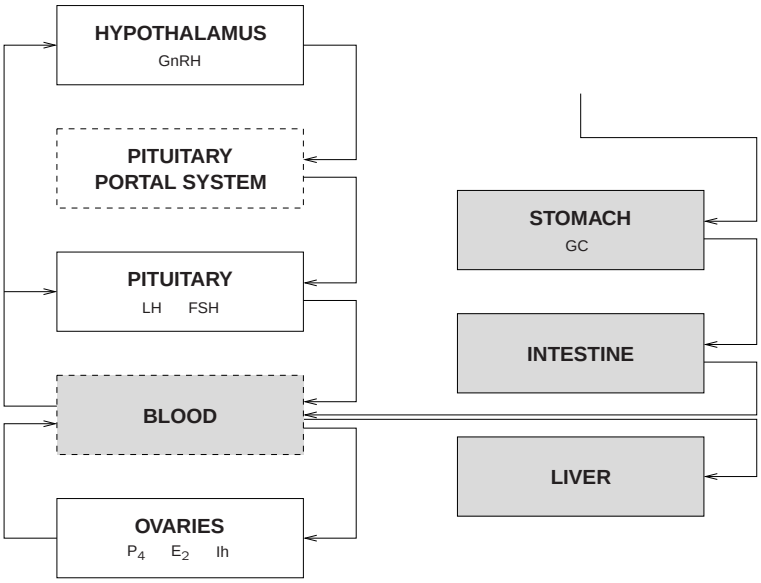

Figure 5.15: Four-compartment model for the gestagen component integrated in the compartmental model of GynCycle.

Then the mathematical model for the gestagen component is given by

$$\begin{aligned}
\frac{d}{dt}GC_S(t) &= -k_{GC,1} \cdot GC_S(t) \\
\frac{d}{dt}GC_I(t) &= \frac{k_{GC,1}}{V_I} \cdot GC_S(t) - k_{GC,2} \cdot GC_I(t) \\
\frac{d}{dt}GC_B(t) &= \frac{k_{GC,2} \cdot V_I}{V_B} \cdot GC_I(t) - k_{GC,3} \cdot GC_B(t) \\
\frac{d}{dt}GC_L(t) &= \frac{k_{GC,3} \cdot V_B}{V_L} \cdot GC_B(t) - \alpha_{GC}(t; GC_L(t)),
\end{aligned}$$

where $GC_S(\cdot)$ is defined as above. Analogously the mathematical model for the estrogen component is given by

$$\begin{aligned}
\frac{d}{dt}EC_S(t) &= -k_{EC,1} \cdot EC_S(t) \\
\frac{d}{dt}EC_I(t) &= \frac{k_{EC,1}}{V_I} \cdot EC_S(t) + \frac{k_{EC,3} \cdot V_L}{V_I} \cdot EC_B(t) - k_{EC,2} \cdot EC_I(t) \\
\frac{d}{dt}EC_B(t) &= \frac{k_{EC,4} \cdot V_L}{V_B} \cdot EC_L(t) - k_{EC,5} \cdot EC_B(t) \\
\frac{d}{dt}EC_L(t) &= \frac{k_{EC,2} \cdot V_I}{V_L} \cdot EC_I(t) + \frac{k_{EC,5} \cdot V_B}{V_L} \cdot EC_B(t) \\
&\quad - (k_{EC,3} + k_{EC,4}) \cdot EC_L(t) - \alpha_{EC}(t; EC_L(t)),
\end{aligned}$$

where $EC_S(\cdot)$ is defined as above.

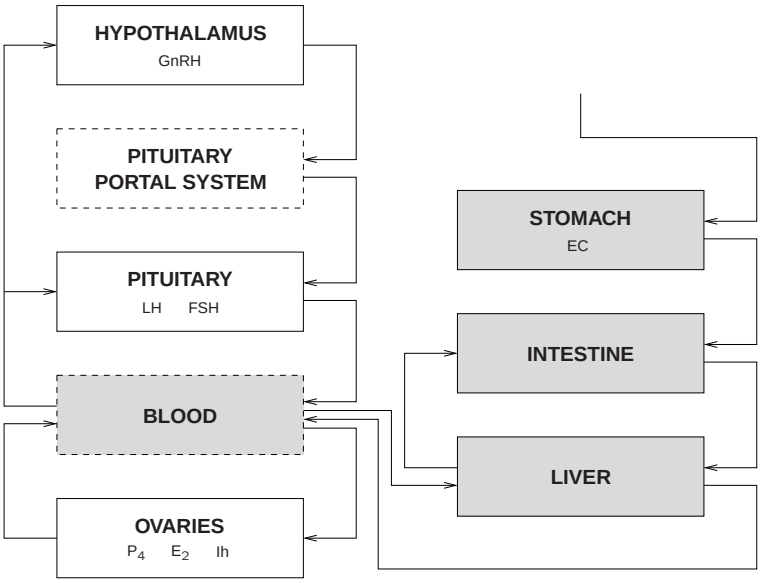

Figure 5.16: Four-compartment model for the estrogen component (with enterohepatic circulation) integrated in the compartmental model of GynCycle.

5.2 Administration of GnRH

The GnRH pulse generator is an essential element in the human menstrual cycle (see Chapter 2). If it fails or if GnRH is administered, the cycle is disturbed.

If GnRH is administrated, it is expected that the GnRH receptors are desensitized. In GynCycle, three states for the GnRH receptors are assumed: free, complex, and desensitized. The total receptor concentration (sum of free, complex, and desensitized) is not constant but depends on the GnRH concentration. As a reminder, the equations (see Chapter 2) that are directly affected by a continuous administration of GnRH are listed:

$$\begin{aligned}
\frac{d}{dt}GnRH(t) &= d_G + \frac{b_{GnRH}}{V_{PPS}} + \frac{M_{GnRH,j}}{V_{PSS}} \cdot \psi(t - T_j) \\
&\quad - \beta_{GnRH} \cdot GnRH(t) \cdot R_{GnRH}(t) - \alpha_{GnRH} \cdot GnRH(t) \\
\frac{d}{dt}R_{GnRH}(t) &= r_4 \cdot \frac{T_{GnRH} - GnRH(t)}{T_{GnRH} + GnRH(t)} + r_3 \cdot R_{GnRH}\text{-}d(t) \\
&\quad - r_1 \cdot GnRH(t) \cdot R_{GnRH}(t) \\
\frac{d}{dt}(GnRH\text{-}R_{GnRH})(t) &= r_1 \cdot GnRH(t) \cdot R_{GnRH}(t) - r_2 \cdot (GnRH\text{-}R_{GnRH})(t) \\
\frac{d}{dt}R_{GnRH}\text{-}d(t) &= r_2 \cdot (GnRH\text{-}R_{GnRH})(t) - r_3 \cdot R_{GnRH}\text{-}d(t),
\end{aligned}$$

where d_G denotes the amount of GnRH that is administered.

In Figs. 5.17 and 5.18 one example for the administration of GnRH and its effect on the percentage of desensitized receptors is shown. In can be clearly seen that

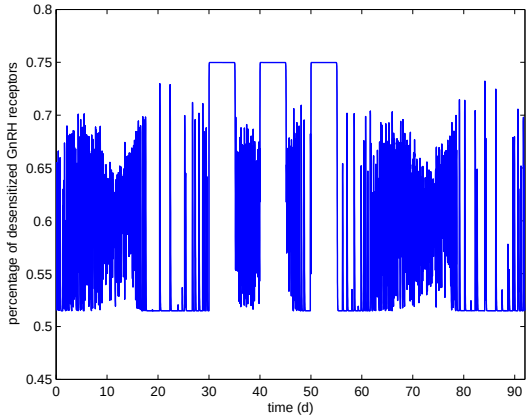

Figure 5.17: The percentage of desensitized GnRH receptors if GnRH is administered (start: on day 30, duration: 30 d, cycle: 5/10).

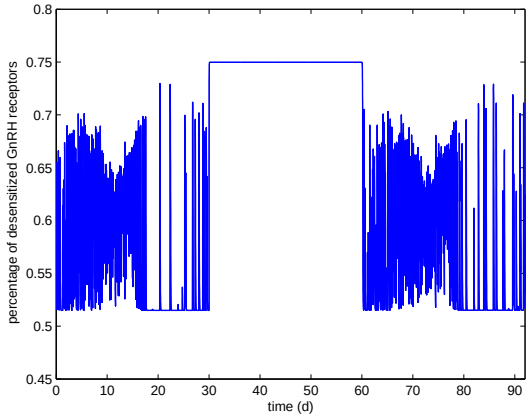

Figure 5.18: The percentage of desensitized GnRH receptors if GnRH is administered (start: on day 30, duration: 30 d, without break).

the percentage of the desensitized GnRH receptors in the periods where GnRH is administered is increased. The calculation of the limit for the percentage of the GnRH receptors (if $GnRH(\cdot)$ is assumed fix) yields

$$\lim_{d_G \to \infty} \lim_{t \to \infty} \frac{R_{GnRH}\text{-}d(t)}{R_{GnRH}(t) + (GnRH\text{-}R_{GnRH})(t) + R_{GnRH}\text{-}d(t)} = \frac{r_2}{r_2 + r_3},$$

i.e., with the values given in the appendix, there is a limit percentage of approximately 75% which is consistent with the simulations.

5.3 Summary

Some approaches to model the effects of hormonal contraceptives are presented and shown for the case of GynCycle. It is advantageous to model the dynamics of the gestagen and estrogen components separately instead of including them into the progesterone and estradiol dynamics. The result of the simulations is the suppression of the follicular mass at ovulation and of the LH (and FSH) concentration. The administration of GnRH results in a higher percentage of desensitized GnRH receptors which is expected.

Conclusion

GynCycle is a complex mathematical model for the female menstrual cycle and describes the dynamics of 49 hormones, enzymes, receptors (partly at different states and in different compartments), follicular masses, and the GnRH pulse generator. The simulation of this model correctly mimics the qualitative dynamics for essential elements in comparison with the given experimental data. Some first applications to medical treatments lead to realistic results confirming the functionality of the model and thus justify its use for medical investigation.

In order to simplify parameter estimation, a method for the decomposition into several model parts has been developed in this thesis. Moreover, the numerical solution of the stochastic pulse generator that is coupled with a system of delay differential equations in GynCycle has been integrated into RADAR5, a solver for stiff delay differential equations.

For special medical questions, it might be inevitable to couple GynCycle with other physiological models, for example, when other factors such as (mal)nutrition or top level competitive sports play an important role. On the other side, the full model should certainly be reduced as soon as it is intended as part of larger packages, e.g. optimization cycles.

Last, but not least, parameter values for GynCycle have been estimated on the basis of averaged data in this thesis. Thus GynCycle represents a "virtual", healthy woman with a "virtual" cycle length. In order to simulate the individual case, which will be the ultimate goal of such a model, individual data will be necessary and parameter values must be adapted individually.

Appendix

Experimental data

First some general remarks are made about experimental data for the human menstrual cycle that are found in the literature. Then the sources that are used for comparison of the different experimental data are defined. If there are several sources for one element, the different sources are compared in a plot. Finally the sources that are chosen for comparison with simulations of GynCycle are listed.

When doing research of experimental data in the literature, two points must to mentioned:

- The quality of the experimental data varies.
- The various sources are partly inconsistent with one another.

In the case of the human menstrual cycle, values of high precision from a clinical study with many subjects can be available as well as ranges of values for different phases of the cycles without reflecting the dynamics for the different days of the cycle. When presenting the experimental data, inconsistencies are remarked.

The following sources are used for comparison of the experimental data:

- **Source 1:**
  Table A.1 in [37] (values estimated from plot in [58])
  33 normal women (serum concentration)
- **Source 2:**
  [48] (estimated from plot)
  5 normal women (serum concentration)
- **Source 3:**
  Fig. 13-7 in [32], p. 442 (values estimated from plot)
  9 normal women (serum concentration)
- **Source 4:**
  [34] (estimated from plot)
  6 normal women (plasma concentration)

The term “normal women” means in general healthy women of age between 18 and 40 with a regular cycle. The values are estimated from a plot. Thus errors in the values

may occur. Since in particular the qualitative result instead of a hundred percent correct solution (which would be left to define since the cycle varies from woman to woman), the values estimated from the plot can be used for comparison. The data from the different cycles might vary in cycle length or the cycle length is not even defined (values around the mid-cycle peak and around the menses might be given). The different sources of experimental data are shown for LH in Fig. 5.19, for FSH in Fig. 5.20, for P_4 in Fig. 5.21, for E_2 in Fig. 5.22, and for 17α-hydroxyprogesterone in Fig. 5.23. Even if the values can vary, qualitative similarities are detectable.

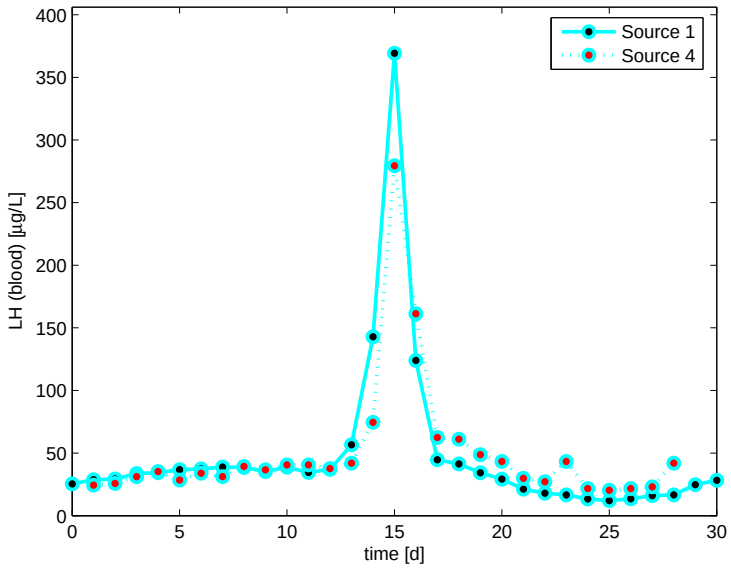

Figure 5.19: Experimental data for the LH concentration (source 4 uses IU/L as unit, thus the conversion factor is adjusted to the data from source 1 since focus is on the qualitative course).

Finally for comparison with the simulations, source 1 (see Table 5.2) is chosen for LH, FSH, P_4, E_2 and source 2 (see Table 5.3) for 17prog, DHEA, andro, test, and estro. For the GnRH pulse frequency see Table 5.4 and Table 5.5. For 17preg no daily values have been found (see Table 5.6). The abbreviations that are used are listed in Table 5.7.

The values from source 1 are used for LH, FSH, Ih, P_4, and E_2 since they are the best available (plots quite accurate, many subjects). The values are given for 31 data points. The data for E_2, P_4, and Ih are decreasing on day 30 but are still larger than the values on day 0. Hence, it is assumed that the period is (at least) 31 days and that the value of day 31 is the same as on day 0 [74].

In source 2, values are given around the menses and the mid-cycle peak of LH, no length of the cycle is defined. Here a length of 31 days is assumed and thus the values matched to this cycle.

Concerning the experimental data, the following is also remarked:

- Since the values in [37] are estimated from the plots in [58], the accuracy of the

Table 5.2: Experimental data for LH, FSH, Progesterone, Estradiol, and Inhibin (source 1).

Day	LH [μg/L]	FSH [μg/L]	P_4 [nmol/L]	E_2 [ng/L]	Ih [U/L]
0	25.34	142.5	1.2	56.387	297.9
1	28.74	158.3	0.4	49.168	284.1
2	29.36	175.1	1.2	51.3653	313.8
3	33.71	168	1.113	53.5627	308.7
4	34.29	179.1	1.2	55.76	299.3
5	36.78	180.6	0.8	61.494	298.7
6	37.35	177.3	0.933	67.228	302.2
7	38.88	177	0.8	72.962	301.5
8	38.52	166.1	0.533	78.696	339.8
9	35.28	153.4	0.533	92.67	352
10	38.71	144.4	0.667	104.3	329.7
11	34.54	134.5	0.533	143.04	346.3
12	37.02	118.9	0.667	181.75	388.8
13	56.62	116.6	0.933	231.05	461.7
14	142.9	155.3	1.33	296.92	625.4
15	369.2	325.4	2.933	248.43	745.8
16	124	210.7	6	123.4	636.9
17	44.63	138.9	12.667	93.76	584.2
18	41.39	127.1	25.067	114.82	778.3
19	34.32	118.2	37.067	133.5	993.9
20	29.18	107.3	42.667	149.85	1279
21	21.18	101.2	51.867	155.57	1486
22	17.95	86.53	53.2	174.28	1632
23	16.64	81.36	49.867	178.83	1597
24	13.38	75.29	40	162.19	1440
25	12.02	76.79	33.3333	149.06	1154
26	13.54	82.1	22.667	130.04	919.5
27	16.02	91.23	14.667	112.23	711.1
28	16.56	100.4	11.733	92.044	675.8
29	24.72	121.9	7.33	75.373	532.2
30	28.2	133.9	4.667	66.983	423.4

Table 5.3: Experimental data for 17α-Hydroxyprogesterone, DHEA, Androstenedione, Testosterone, and Estrone (source 2; adjusted to a 31-days-cycle).

Day	17prog [pg/mL]	DHEA [ng/mL]	andro [ng/mL]	test [pg/mL]	estro [pg/mL]
0	155	$6.45 \cdot 10^3$	$1.10 \cdot 10^3$	245	55
1	180	$5.30 \cdot 10^3$	$0.60 \cdot 10^3$	210	55
2	190	$6.45 \cdot 10^3$	$1.30 \cdot 10^3$	290	70
3	165	$5.90 \cdot 10^3$	$1.10 \cdot 10^3$	230	70
4	–	–	–	–	–
5	–	–	–	–	–
6	–	–	–	–	–
7	220	$5.30 \cdot 10^3$	$1.15 \cdot 10^3$	270	70
8	200	$4.10 \cdot 10^3$	$1.20 \cdot 10^3$	275	75
9	210	$5.30 \cdot 10^3$	$1.35 \cdot 10^3$	305	80
10	305	$7.65 \cdot 10^3$	$1.45 \cdot 10^3$	300	85
11	295	$7.65 \cdot 10^3$	$1.60 \cdot 10^3$	290	80
12	230	$5.30 \cdot 10^3$	$1.45 \cdot 10^3$	265	115
13	325	$5.90 \cdot 10^3$	$1.75 \cdot 10^3$	305	135
14	510	$5.90 \cdot 10^3$	$1.85 \cdot 10^3$	355	180
15	980	$5.30 \cdot 10^3$	$1.85 \cdot 10^3$	390	205
16	880	$5.90 \cdot 10^3$	$1.65 \cdot 10^3$	415	140
17	700	$5.30 \cdot 10^3$	$1.20 \cdot 10^3$	320	90
18	1105	$5.90 \cdot 10^3$	$1.15 \cdot 10^3$	290	85
19	1030	$3.55 \cdot 10^3$	$0.90 \cdot 10^3$	235	80
20	1190	$4.10 \cdot 10^3$	$0.85 \cdot 10^3$	220	90
21	1200	$5.30 \cdot 10^3$	$0.90 \cdot 10^3$	240	110
22	1040	$5.90 \cdot 10^3$	$0.90 \cdot 10^3$	260	115
23	890	$5.90 \cdot 10^3$	$1.25 \cdot 10^3$	240	115
24	–	–	–	–	–
25	–	–	–	–	–
26	–	–	–	–	–
27	–	–	–	–	–
28	510	$4.70 \cdot 10^3$	$1.30 \cdot 10^3$	230	85
29	235	$4.70 \cdot 10^3$	$0.90 \cdot 10^3$	235	80
30	220	$4.10 \cdot 10^3$	$1.05 \cdot 10^3$	220	60

Table 5.4: Experimental data for the GnRH pulse frequency. The frequency is counted between day-1 and day. It is *pulse frequency* $= 1/$*length of intervals between pulses.*

Phase	Days [d]	Frequency [1/d]	Source
F	1 - 14	16 - 18	90 min (F) [9], 90 min (F) [45], 80 min (EF) ([86], Table 7-2)
LF	15 - 16	24 - 48	30 min (O) ([45], Fig. 1.6, LH), $<$ 80 min, 53 min (LF) ([86], p. 197, Table 7-2, LH)
EL	17 - 21	6 - 12	2 - 4 h (EL) [9], 120 min (EL) ([45], Fig. 1.6)
ML	22 - 26	4 - 6	4 - 6 h (ML) [9], 177 - 395 min (ML) ([86], p. 197, Table 7-2, LH), 240 min (L) [45]
LL	27 - 31	2 - 3	8 - 12 h (LL) [9]

Table 5.5: Experimental data for the GnRH pulse frequency.

Day	1	2	3	4	5	6	7	8	9	10	
Lower bound	16	16	16	16	16	16	16	16	16	16	
Upper bound	18	18	18	18	18	18	18	18	18	18	
Day	11	12	13	14	15	16	17	18	19	20	
Lower bound	16	16	16	16	24	24	6	6	6	6	
Upper bound	18	18	18	18	48	48	12	12	12	12	
Day	21	22	23	24	25	26	27	28	29	30	31
Lower bound	6	4	4	4	4	4	2	2	2	2	2
Upper bound	12	6	6	6	6	6	3	3	3	3	3

Table 5.6: Experimental data for 17α-Hydroxypregnenolone.

Source	Phase	Conv. Unit [ng/dL]	SI Unit [nmol/L]	Conv. Factor
[32] (appendix) serum	A	$530 - 3570$	$1.6 - 10.7$	0.0307

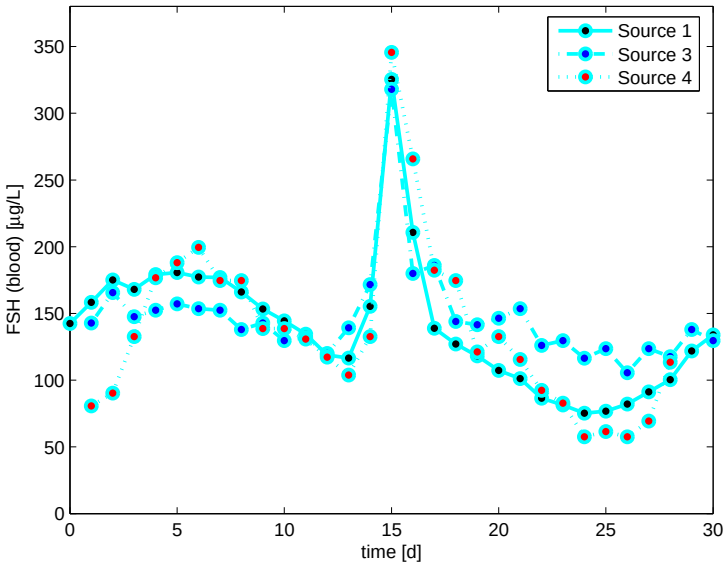

Figure 5.20: Experimental data for the FSH concentration (sources 3 and 4 use IU/L as unit, thus the conversion factor is adjusted to the data from source 1 since focus is on the qualitative course).

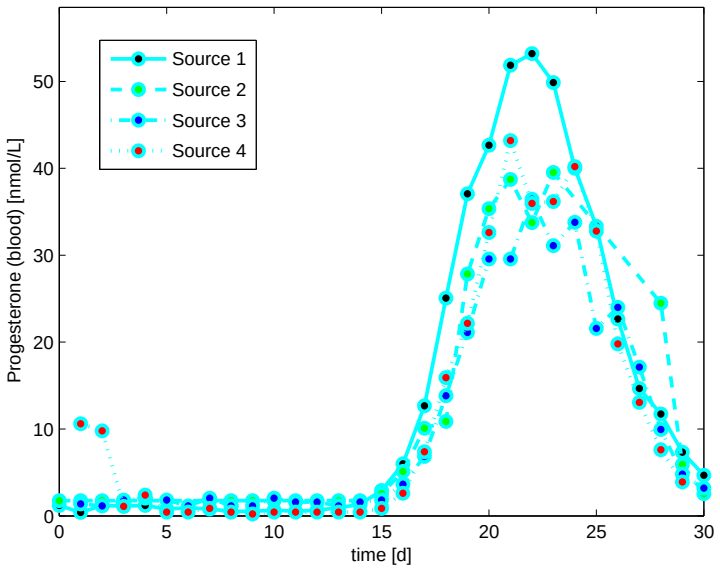

Figure 5.21: Experimental data for the P_4 concentration.

data is possibly not as high as the values may promise.

- The return from low to high (LH) pulse frequency is quite rough, a smoother transition is possible but the rough one as well ([86], p. 194).

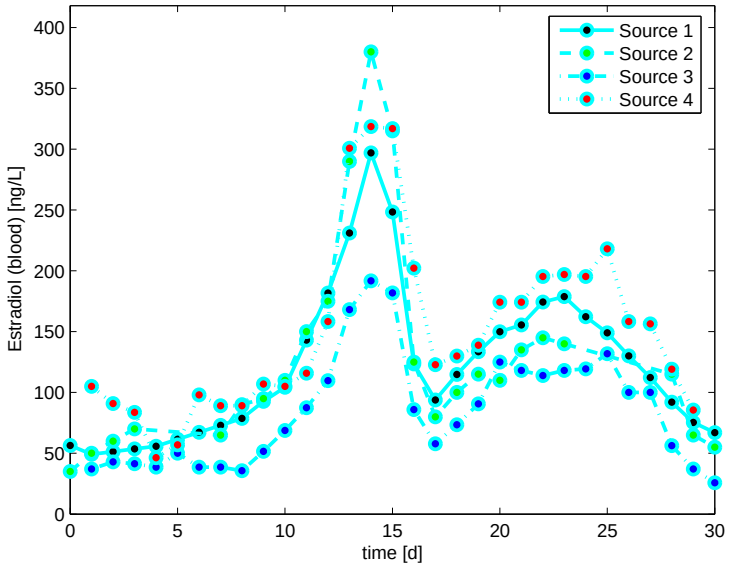

Figure 5.22: Experimental data for the E_2 concentration.

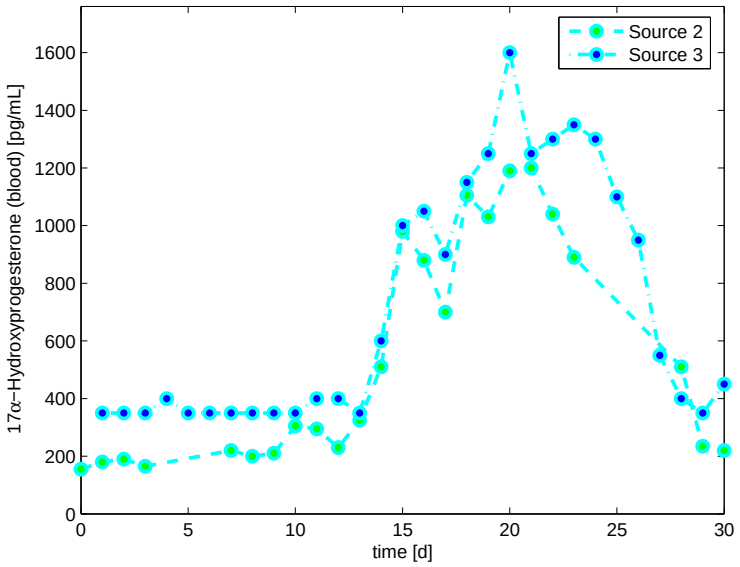

Figure 5.23: Experimental data for the 17α-Hydroxyprogesterone concentration.

- The values for the LH concentration (serum) in [37] and [58] are not consistent with the values in [32] (appendix, plasma or serum): for adults, a range of $[0.5, 2.7]$ μg/L is specified with values at mid-cycle peak in the range of $[4.2, 15.8]$ μg/L.

- The values for the FSH concentration (serum) in [37] and [58] are not consistent

Table 5.7: Legend.

Abbreviation	Meaning
F	follicular
EF	early follicular
LF	late follicular
O	ovulatory
L	luteal
EL	early luteal
ML	mid-luteal
LL	late luteal
A	adult (female)

with the values in [32] (appendix, plasma/serum (heparin)): for premenopausal adults, a range of $[1.1, 5.3]$ μg/L is specified with values at mid-cycle peak in the range of $[2.6, 24]$ μg/L.

- The values for the 17α-hydroxyprogesterone concentration (serum) in [32] (appendix) are not consistent with the values in [45] (appendix, serum): for adults in the follicular phase, in [32] a range of < 1.0 μg/L is specified in contrast to [45] ($[3.3, 10]$ μg/L).

- Only 10 % of DHEA are produced in the ovaries, 90 % are produced in the adrenal cortex.

- The values for the free testosterone concentration (serum) in [32] (appendix) are not consistent with the values in [45] (appendix, serum): For adults, in [32] a range of $[3, 13]$ pg/mL is specified in contrast to [45] ($[0.7, 3.6]$ pg/L). The free testosterone concentration is dependent on the SHBG concentration, approximately 10 % of the total concentration is free.

In order to validate the model, real individual data must be used for comparison. But for the time being, the given data are taken as it is done in [37].

Parameter values of GynCycle

Table 5.8: Model part 1 - GnRH pulse frequency: parameter values.

No. (p)		Name	Value	Unit	Remark[1]
1	f	γ	2.000	-	2 in [47][2]
2	s	λ_{max}	11.26	$[y_1]$/d	[3]
3	s	$T_{P_4}^{freq}$	1.873	nmol/L	mean(P_4) = 13.83 (exp. data) in [37][4]
4		$n_{P_4}^{freq}$	1.000	-	simple approach
5	s	$T_{E_2}^{freq}$	54.95	ng/L	mean(E_2) = 121.2 (exp. data) in [37]
6		$n_{E_2}^{freq}$	1.000	-	simple approach
7	f	τ_{P_4}	0.09000	d	simple approach
8	f	τ_{E_2}	0.09000	d	simple approach

Table 5.9: Model part 2 - LH: parameter values.

No. (p)		Name	Value	Unit	Remark
9		M_{max}	102.4	$[y_2]$/d	simple approach
10		$T_{E_2,1}$	7.829	ng/L	$< T_{E_2,2}$ [5]
11		$n_{E_2,1}$	1.000	-	$n_{E_2,2}$
12		$T_{E_2,2}$	207.8	mol/L	$> T_{E_2,1}$ [6]
13	-	$n_{E_2,2}$	1.000	-	$n_{E_2,1}$
14	s	α_{GnRH}	47.61	1/d	$\ln 2/t_{1/2} = \ln 2/0.0028 = 249.5$ [47]
15		β_{GnRH}	5.104	$1/([y_4]\cdot$ d)	$\leftrightarrow r_1$ [7]
16	s	b_{GnRH}	38.00	$([y_3]\cdot$ L)/d	simple approach
17		V_{PPS}	0.08769	L	$< V_B$
18	f	a	814.3	-	48[8]
19	f	m	2.000	-	simple approach
20		r_1	5.104	$1/([y_3]\cdot$ d)	$\leftrightarrow \beta_{GnRH}$ [9]
21		r_3	22.76	1/d	simple approach
22		r_4	$1.000 \cdot 10^{-3}$	$[y_4]$/d	simple approach
23	s	T_{GnRH}	10.69	$[y_3]$	$\approx$ mean of GnRH conc.
24	s	r_2	68.23	1/d	simple approach
25	s	b_{LH}	344.3	μg/d	comparison with [37]
26	s	$T_{P_4}^{LH,syn,-}$	1.338	nmol/L	mean(P_4) = 13.83 (exp. data) in [37][10]

[1] f: fix value, s: sensitive parameter; all values rounded to four digits
[2] more regularity than the Poisson but still flexible enough [47]
[3] $p_1, p_3, \ldots, p_8$ fix $\Rightarrow \lambda_{max} \in [10.0, 13.7]$
[4] mean(P_4): mean of exp. data in [37] (equidistant time points)
[5] $T_{E_2}^{mass} = (T_{E_2,1} \cdot T_{E_2,2})^{\frac{1}{2}}$ if $n_{E_2,1} = n_{E_2,2}$
[6] $T_{E_2,2} = (T_{E_2}^{mass})^2 / T_{E_2,1}$
[7] $p_{15} \cdot [y_4] = p_{20} \cdot [y_3]$
[8] assumption: maximum is reached after 30 min and $m = 2$
[9] $p_{20} \cdot [y_3] = p_{15} \cdot [y_4] = 5.463$
[10] mean(P_4): mean of exp. data in [37] (equidistant time points)

Table 5.9: Model part 2 - LH: parameter values.

No. (p)		Name	Value	Unit	Remark
27		$n_{P_4}^{LH,syn,-}$	1.000	-	simple approach
28	s	$T_{E_2}^{LH,syn,+}$	119.9	ng/L	mean(E_2) = 121.2 (exp. data) in [37]
29	s	$n_{E_2}^{LH,syn,+}$	5.136	-	simple approach
30	s	$syn_{LH,max}$	8576	μg/d	comparison with [37]
31		$T_{E_2}^{LH,rel,-}$	0.04647	ng/L	$\leftrightarrow T_{E_2,1}$
32		$n_{E_2}^{LH,rel,-}$	1.000	-	$n_{E_2}^{LH,rel,+}$
33	s	$T_{E_2}^{LH,rel,+}$	348.8	ng/L	$\leftrightarrow T_{E_2,2}$[11]
34	-	$n_{E_2}^{LH,rel,+}$	1.000	-	$n_{E_2}^{LH,rel,-}$
35	s	$T_{P_4}^{LH,rel,+}$	1.301	nmol/L	mean(P_4) = 13.83 (exp. data) in [37]
36		$n_{P_4}^{LH,rel,+}$	1.000	-	simple approach
37	s	$rel_{LH,max}$	40.92	1/([y_5]· d)	comparison with [37]
38	f	V_B	2.500	L	[12]
39	f	$\tau_{LH,1}$	0.04333	d	simple approach
40	s	α_{LH}	15.73	1/d	$cl_L = 14$ in [37]

Table 5.10: Model part 3 - FSH: parameter values.

No. (p)		Name	Value	Unit	Remark
41	s	b_{FSH}	227.6	μg/d	comparison with [37]
42		$T_{Ih}^{FSH,syn,-}$	1.424	U/L	[13]
43		$n_{Ih}^{FSH,syn,-}$	1.000	-	simple approach
44	s	$syn_{FSH,max}$	$6.381 \cdot 10^4$	μg/d	simple approach
45	f	τ_{Ih}	1.800	d	$\delta_{Ih} = 2.00$ [37]
46	s	$T_{E_2}^{FSH,rel,-}$	42.09	ng/L	$\leftrightarrow T_{E_2,1}$
47		$n_{E_2}^{FSH,rel,-}$	0.9996	-	$n_{E_2}^{FSH,rel,+}$
48		$T_{E_2}^{FSH,rel,+}$	0.3118	ng/L	$\leftrightarrow T_{E_2,2}$
49	-	$n_{E_2}^{FSH,rel,+}$	1.000	-	$n_{E_2}^{FSH,rel,-}$
50	s	$T_{P_4}^{FSH,rel,+}$	4.159	nmol/L	[14]
51		$n_{P_4}^{FSH,rel,+}$	0.9994	-	simple approach
52	s	$T_{Ih}^{FSH,rel,-}$	638.8	U/L	[15]
53		$n_{Ih}^{FSH,rel,-}$	1.001	-	simple approach
54	s	$rel_{FSH,max}$	41.53	1/([y_5]· d)	comparison with [37]
59	f	$\tau_{FSH,1}$	0.06934	d	simple approach
60		α_{FSH}	1.779	1/d	$cl_F = 8.2$ in [37]

[11] $T_2^+ = (T_{E_2}^{LH})^2/T_2^-$

[12] $0.55 \cdot 4.5L$; v_{dis} in [37]; $> 2.5L$ [78]

[13] mean(Ih) = 672.2 (exp. data) in [37]; mean(Ih): mean of exp. data in [37] (equidistant time points)

[14] mean(P_4) = 13.83 (exp. data) in [37]

[15] mean(Ih) = 672.2 (exp. data) in [37]

Table 5.11: Model part 4 - Progesterone: parameter values.

No. (p)		Name	Value	Unit	Remark
93		k_{-}^{LH}	1.164	1/d	k_{-}^{FSH}
94		k_{r}^{LH}	24.33	1/d	k_{r}^{FSH}
95		k_{+}^{LH}	13.74	L/(μg $\cdot$ d)	k_{+}^{FSH}
96		ρ^{LH}	33.21	1/d	ρ^{FSH}
97		k_{i}^{LH}	656.4	1/d	k_{i}^{FSH}
98	s	a_1	665.4	$[y_{28}]/([y_{25}]\cdot$ d)	simple approach
99		a_2	415.6	1/d	simple approach
100		$e_{1,1}$	0.8740	$1/[y_{12}]$	simple approach
101	s	$e_{1,2}$	56.05	$1/[y_{13}]$	simple approach
102		$e_{1,3}$	0.1751	$1/[y_{14}]$	simple approach
103		$e_{1,4}$	2.131	$1/[y_{15}]$	simple approach
104		$e_{1,5}$	0.6526	$1/[y_{16}]$	simple approach
105		$e_{1,6}$	0.8377	$1/[y_{17}]$	simple approach
106		$e_{1,7}$	1.024	$1/[y_{18}]$	simple approach
117		a_5	15.32	$[y_{30}]/([y_{25}]\cdot$ d)	simple approach
118		a_6	1.105	1/d	simple approach
119		$e_{3,1}$	0.4289	$1/[y_{12}]$	simple approach
120		$e_{3,2}$	1.048	$1/[y_{13}]$	simple approach
121		$e_{3,3}$	0.8771	$1/[y_{14}]$	simple approach
122		$e_{3,4}$	0.1372	$1/[y_{15}]$	simple approach
123		$e_{3,5}$	0.9190	$1/[y_{16}]$	simple approach
124		$e_{3,6}$	0.9577	$1/[y_{17}]$	simple approach
125		$e_{3,7}$	$2.851 \cdot 10^{-4}$	$1/[y_{18}]$	simple approach
126		a_7	188.0	$[y_{31}]/([y_{25}]\cdot$ d)	simple approach
127	s	a_8	2090	1/d	simple approach
128	s	$e_{4,1}$	49.76	$1/[y_{12}]$	simple approach
129	s	$e_{4,2}$	454.9	$1/[y_{13}]$	simple approach
130		$e_{4,3}$	3.366	$1/[y_{14}]$	simple approach
131		$e_{4,4}$	$5.486 \cdot 10^{-4}$	$1/[y_{15}]$	simple approach
132		$e_{4,5}$	24.44	$1/[y_{16}]$	simple approach
133		$e_{4,6}$	0.3695	$1/[y_{17}]$	simple approach
134		$e_{4,7}$	$9.008 \cdot 10^{-5}$	$1/[y_{18}]$	simple approach
145		$c_1 \cdot chol$	0.9014	$[y_{33}]/([y_{30}]\cdot$ d)	simple approach
146		$p_{1,1}$	0.07649	[16]	simple approach
147		$p_{1,2}$	0.7450	[17]	simple approach
148		$p_{1,3}$	0.2185	$[y_{33}]$	simple approach
149		$p_{1,4}$	1.865	$[y_{33}]/[y_{34}]$ = -	simple approach
150		$k_{1,1}$	1.000	[18]	simple approach
151		$k_{1,2}$	510.0	$[y_{33}]$	simple approach
152		c_2	28.34	1/d	simple approach

[16] $[y_{33}]/([y_{28}]\cdot$ d) = $[y_{34}]/([y_{28}]\cdot$ d)
[17] $[y_{33}]/([y_{28}]\cdot$ d) = $[y_{34}]/([y_{28}]\cdot$ d)
[18] $[y_{33}]/([y_{31}]\cdot$ d) = $[y_{35}]/([y_{31}]\cdot$ d)

Table 5.11: Model part 4 - Progesterone: parameter values.

No. (p)		Name	Value	Unit	Remark
153		$k_{2,1}$	0.1071	[19]	simple approach
154		$k_{2,2}$	$4.229 \cdot 10^{-3}$	$[y_{34}]$	simple approach
155		c_3	0.4227	1/d	$\leftrightarrow s_{P_4}$
185	s	s_{P_4}	2.021	nmol/($[y_{34}]\cdot$ d)	$\leftrightarrow c_3$
186	f	τ_{prog}	0.01000	d	simple approach
187		α_{P_4}	0.5494	1/d	simple approach

Table 5.12: Model part 5 - Estrone and Estradiol: parameter values.

No. (p)		Name	Value	Unit	Remark
179	s	$p_{4,1}$	0.5036	[20]	simple approach
180	s	$p_{4,2}$	$5.777 \cdot 10^{-4}$	[21]	simple approach
181	s	$p_{4,3}$	0.08541	$[y_{40}]$	simple approach
182		$p_{4,4}$	$1.000 \cdot 10^{-4}$	$[y_{40}]/[y_{41}]$ = -	simple approach
183	s	c_9	55.59	1/d	simple approach
184	s	c_{10}	64.22	1/d	simple approach
188	s	s_{E_2}	$1.282 \cdot 10^4$	ng/($[y_{41}]\cdot$ d)	simple approach
189	f	τ_{estra}	0.06137	d	simple approach
190		α_{E_2}	1806	1/d	simple approach
206	s	s_{estro}	$1.253 \cdot 10^4$	ng/($[y_{40}]\cdot$ d)	simple approach
207	f	τ_{estro}	0.9968	d	simple approach
208		α_{estro}	5.387	1/d	simple approach

Table 5.13: Model part 6 - 17α-Hydroxypregnenolone and 17α-Hydroxyprogesterone: parameter values.

No. (p)		Name	Value	Unit	Remark
156		$p_{2,1}$	$7.383 \cdot 10^{-4}$	[22]	simple approach
157	s	$p_{2,2}$	0.01870	[23]	simple approach
158		$p_{2,3}$	0.9999	$[y_{35}]$	simple approach
159		$p_{2,4}$	$8.044 \cdot 10^{-3}$	$[y_{35}]/[y_{36}]$ = -	simple approach
160	s	$k_{3,1}$	0.3282	[24]	simple approach
161		$k_{3,2}$	0.05246	$[y_{35}]$	simple approach
162	s	c_4	0.8533	1/d	simple approach

[19] $[y_{34}]/([y_{31}]\cdot$ d) = $[y_{36}]/([y_{31}]\cdot$ d)
[20] $[y_{40}]/([y_{29}]\cdot$ d) = $[y_{41}]/([y_{29}]\cdot$ d)
[21] $[y_{40}]/([y_{29}]\cdot$ d) = $[y_{41}]/([y_{29}]\cdot$ d)
[22] $[y_{35}]/([y_{28}]\cdot$ d) = $[y_{36}]/([y_{28}]\cdot$ d)
[23] $[y_{35}]/([y_{28}]\cdot$ d) = $[y_{36}]/([y_{28}]\cdot$ d)
[24] $[y_{35}]/([y_{31}]\cdot$ d) = $[y_{37}]/([y_{31}]\cdot$ d)

Table 5.13: Model part 6 - 17α-Hydroxypregnenolone and 17α-Hydroxyprogesterone: parameter values.

No. (p)		Name	Value	Unit	Remark
163	s	$k_{4,1}$	0.07914	[25]	simple approach
164		$k_{4,2}$	0.02609	$[y_{36}]$	simple approach
165		c_5	0.9489	1/d	simple approach
191	s	$s_{17\text{-}preg}$	0.6017	10·ng/($[y_{35}]$· d)	simple approach
192	f	$\tau_{17\text{-}preg}$	0.9990	d	simple approach
193	s	$\alpha_{17\text{-}preg}$	0.07352	1/d	simple approach
194	s	$s_{17\text{-}prog}$	2.751	μg/($[y_{36}]$· d)	simple approach
195	f	$\tau_{17\text{-}prog}$	0.9980	d	simple approach
196	s	$\alpha_{17\text{-}prog}$	0.1139	1/d	simple approach

Table 5.14: Model part 7 - DHEA: parameter values.

No. (p)		Name	Value	Unit	Remark
166	s	$k_{5,1}$	0.3302	[26]	simple approach
167	s	$k_{5,2}$	118.5	$[y_{37}]$	simple approach
168	s	c_6	0.04839	1/d	simple approach
197	s	s_{DHEA}	23.79	μg/($[y_{37}]$· d)	simple approach
198	f	τ_{DHEA}	$2.640 \cdot 10^{-3}$	d	simple approach
199	s	α_{DHEA}	0.08372	1/d	simple approach

Table 5.15: Model part 8 - Androstenedione and Testosterone: parameter values.

No. (p)		Name	Value	Unit	Remark
88		k_-^{FSH}	1.164	1/d	$3 \cdot 10^{-4}$ 1/s [14]
89		k_r^{FSH}	48.15	1/d	$5 \cdot 10^{-4}$ 1/s [14]
90		k_+^{FSH}	2.406	L/(μg · d)	$5 \cdot 10^{6}$ 1/(M · s) [14]
91		ρ^{FSH}	19.62	1/d	$3 \cdot 10^{-4}$ 1/s[27] [14]
92		k_i^{FSH}	416.9	1/d	$5 \cdot 10^{-4}$ 1/s [14]
107		a_3	1.598	$[y_{29}]$/($[y_{21}]$· d)	simple approach
108		a_4	20.05	1/d	simple approach
109		$e_{2,1}$	0.01012	1/$[y_{11}]$	simple approach
110		$e_{2,2}$	3.861	1/$[y_{12}]$	simple approach
111		$e_{2,3}$	630.9	1/$[y_{13}]$	simple approach
112		$e_{2,4}$	206.4	1/$[y_{14}]$	simple approach

[25] $[y_{36}]/([y_{31}]\cdot \text{ d}) = [y_{38}]/([y_{31}]\cdot \text{ d})$

[26] $[y_{37}]/([y_{28}]\cdot \text{ d}) = [y_{38}]/([y_{28}]\cdot \text{ d})$

[27] $\rho^{FSH}(cAMP) = \frac{\alpha^{FSH} \cdot cAMP^{\gamma^{FSH}}}{\delta^{FSH,\gamma^{FSH}} + cAMP^{\gamma^{FSH}}}$; $cAMP \approx \delta^{FSH} \Rightarrow \rho^{FSH} \approx \frac{\alpha^{FSH}}{2}$; α^{FSH}: 51.84 1/d = $6 \cdot 10^{-4}$ 1/s; γ^{FSH}: 5.0; δ^{FSH}: $6.5 \cdot 10^4$ molecules/cell [14]

Table 5.15: Model part 8 - Androstenedione and Testosterone: parameter values.

No. (p)		Name	Value	Unit	Remark
113		$e_{2,5}$	4.204	$1/[y_{15}]$	simple approach
114		$e_{2,6}$	7.360	$1/[y_{16}]$	simple approach
115		$e_{2,7}$	17.40	$1/[y_{17}]$	simple approach
116		$e_{2,8}$	218.7	$1/[y_{18}]$	simple approach
135		a_9	0.3743	$[y_{32}]/([y_{21}]\cdot$ d)	simple approach
136		a_{10}	1.000	1/d	simple approach
137		$e_{5,1}$	$1.959 \cdot 10^{-3}$	$1/[y_{11}]$	simple approach
138		$e_{5,2}$	432.3	$1/[y_{12}]$	simple approach
139		$e_{5,3}$	0.08895	$1/[y_{13}]$	simple approach
140		$e_{5,4}$	3.362	$1/[y_{14}]$	simple approach
141		$e_{5,5}$	9.885	$1/[y_{15}]$	simple approach
142		$e_{5,6}$	100.7	$1/[y_{16}]$	simple approach
143		$e_{5,7}$	56.68	$1/[y_{17}]$	simple approach
144		$e_{5,8}$	516.2	$1/[y_{18}]$	simple approach
169		$p_{3,1}$	0.05772	[28]	simple approach
170	s	$p_{3,2}$	25.98	see $p_{3,1}$	simple approach
171		$p_{3,3}$	0.4596	$[y_{38}]$	simple approach
172		$p_{3,4}$	0.1119	$[y_{38}]/[y_{39}]$ = -	simple approach
173	s	$k_{6,1}$	0.01241	[29]	simple approach
174		$k_{6,2}$	$1.920 \cdot 10^{-3}$	$[y_{38}]$	simple approach
175	s	c_7	0.01847	1/d	simple approach
176		$k_{7,1}$	$1.649 \cdot 10^{-6}$	[30]	simple approach
177		$k_{7,2}$	0.07960	$[y_{39}]$	simple approach
178		c_8	0.2819	1/d	simple approach
200	s	s_{andro}	$4.611 \cdot 10^{-3}$	μg/($[y_{38}]\cdot$ d)	simple approach
201	f	τ_{andro}	0.9956	d	simple approach
202	s	α_{andro}	0.02635	1/d	simple approach
203		s_{test}	0.4967	μg/($[y_{39}]\cdot$ d)	simple approach
204	f	τ_{test}	0.9999	d	simple approach
205	s	α_{test}	0.02820	1/d	simple approach

Table 5.16: Model part 9 - Inhibin: parameter values.

No. (p)		Name	Value	Unit	Remark
55		ih_1	119.2	U/L	$h_1 = 274.28$ in [37]
56		ih_2	0.09728	U/(L $\cdot[y_{12}]$)	$h_2 = 0.4064$ in [37]
57		ih_3	$4.878 \cdot 10^{-4}$	U/(L $\cdot[y_{17}]$)	$h_3 = 0.4613$ in [37]
58		ih_4	2.803	U/(L $\cdot[y_{18}]$)	$h_4 = 2.1200$ in [37]
61		d_1	40.44	$[y_{11}]$/d	comparison with [37]

[28] $[y_{38}]/([y_{29}]\cdot$ d) = $[y_{39}]/([y_{29}]\cdot$ d)
[29] $[y_{38}]/([y_{32}]\cdot$ d) = $[y_{40}]/([y_{32}]\cdot$ d)
[30] $[y_{39}]/([y_{32}]\cdot$ d) = $[y_{41}]/([y_{32}]\cdot$ d)

Table 5.16: Model part 9 - Inhibin: parameter values.

No. (p)		Name	Value	Unit	Remark
62	s	T_{FSH}^{foll}	2487	μg/L	mean(FSH) = 139.5 (exp. data) in [37]
63		n_{FSH}^{foll}	1.000	-	simple approach
64	f	$\tau_{FSH,2}$	2.000	d	simple approach
65	s	d_2	$6.983 \cdot 10^{-3}$	1/d	$c_1 = 0.0058$ in [37]
66	s	d_3	0.2014	1/d	comparison with [37], [31]
67		α_1	1.000	-	1 in [37]
68		α_2	0.7753	-	$\alpha = 0.7736$ in [37], [31]
69		d_4	$5.551 \cdot 10^{-3}$	1/d	comparison with [37]
70	f	$\tau_{LH,2}$	2.000	d	simple approach
71	s	d_5	0.02594	1/d	comparison with [37]
72		α_3	$9.942 \cdot 10^{-3}$	-	1 (simple approach)
73		α_4	0.1458	-	$\beta = 0.1566$ in [37]
74		α_5	$8.551 \cdot 10^{-3}$	-	1 (simple approach)
75		α_6	1.000	-	1 (simple approach)
76		d_6	$1.056 \cdot 10^{-3}$	1/d	1 (simple approach)
77		d_7	1.162	1/d	comparison with [37]
78		α_7	0.01294	-	$\gamma = 0.0202$ in [37]
79		α_8	0.02536	-	$\gamma = 0.0202$ in [37]
80		d_8	0.6839	1/d	$d_1 = 0.6715$ 1/d in [37]
81		d_9	0.7192	1/d	$d_2 = 0.7048$ 1/d in [37]
82		d_{10}	0.7119	1/d	comparison with [37]
83		α_9	0.01436	-	0.01 (simple approach)
84		d_{11}	0.7085	1/d	comparison with [37]
85		α_{10}	$8.477 \cdot 10^{-3}$	-	0.01 (simple approach)
86		d_{12}	0.6786	1/d	$k_3 = 0.6891$ 1/d in [37]

Table 5.17: Rest set: parameter values.

No. (p)	Name	Value	Unit	Remark
87	d_{13}	1.000	1/d	$k_4 = 0.7093$ 1/d in [37]

[31] in connection with the modified model equation

Table 5.18: Initial values.

No. (y)	Name	Value	Unit	Remark
1	Λ	0.000	-	0 (simple approach)
2	M_{GnRH}	0.000	$[y_2] = [y_3] \cdot$ L	0 (simple approach)
3	$GnRH$	8.379	$[y_3] = [y_2]$/L	1 (simple approach)
4	R_{GnRH}	1.904	[32]	1 (simple approach)
5	($GnRH$-R_{GnRH})	1.201	see R_{GnRH}	1 (simple approach)
6	R_{GnRH}-d	4.110	see R_{GnRH}	1 (simple approach)
7	P_{LH}	65.08	μg	600 μg in [37]
8	LH	4.465	μg/L	25.34 μg/L (exp. data) in [37]
9	P_{FSH}	15.21	μg	352 μg in [37]
10	FSH	52.35	μg/L	142.5 μg/L (exp. data) in [37]
11	F_s	1.724	[33]	9 in [37]
12	F_t	6.175	see F_s	1 in [37]
13	F_g	1.194	see F_s	1 in [37]
14	M_o	2.579	see F_s	1 in [37]
15	M_l	3.801	see F_s	1 in [37]
16	L_e	7.852	see F_s	1 in [37]
17	L_m	19.58	see F_s	1 in [37]
18	L_l	49.96	see F_s	1 in [37]
19	L_a	1.000	see F_s	1 in [37]
20	R_{FSH}	0.2832	[34]	1 (simple approach)
21	(FSH-R_{FSH})	2.555	see R_{FSH}	1 (simple approach)
22	(FSH-R_{FSH}-p)	0.1203	see R_{FSH}	1 (simple approach)
23	R_i^{FSH}	1.041	see R_{FSH}	1 (simple approach)
24	R_{LH}	0.4245	[35]	1 (simple approach)
25	(LH-R_{LH})	1.480	see R_{LH}	1 (simple approach)
26	(LH-R_{LH}-p)	0.07489	see R_{LH}	1 (simple approach)
27	R_i^{LH}	2.020	see R_{LH}	1 (simple approach)
28	3β-HSD_a	364.0	[36]	1 (simple approach)
29	17β-HSD_a	2624	see 3β-HSD_a	1 (simple approach)
30	$P450scc_a$	1028	see 3β-HSD_a	1 (simple approach)
31	$P450_{17\text{-}OH,a}$	140.9	see 3β-HSD_a	1 (simple approach)
32	$P450arom_a$	$4.446 \cdot 10^4$	see 3β-HSD_a	1 (simple approach)
33	$preg$	32.32		simple approach
34	$prog$	1.397		simple approach
35	17-$preg$	0.01874		simple approach
36	17-$prog$	0.5697		simple approach
37	$DHEA$	15.89		simple approach
38	$andro$	$1.228 \cdot 10^4$		simple approach
39	$test$	26.27		simple approach
40	$estro$	0.07716		simple approach
41	$estra$	8.571		simple approach

[32] $[y_4] = [y_5] = [y_6]$ (1/cell)
[33] $[y_{11}] = [y_{12}] = [y_{13}] = [y_{14}] = [y_{15}] = [y_{16}] = [y_{17}] = [y_{18}] = [y_{19}]$
[34] $[y_{20}] = [y_{21}] = [y_{22}] = [y_{23}]$ (1/cell)
[35] $[y_{24}] = [y_{25}] = [y_{26}] = [y_{27}]$ (1/cell)
[36] $[y_{28}] = [y_{29}] = [y_{30}] = [y_{31}] = [y_{32}]$

Table 5.18: Initial values.

No. (y)	Name	Value	Unit	Remark
42	P_4	7.103	nmol/L	1.2 nmol/L (exp. data) in [37]
43	E_2	24.34	ng/L	56.387 ng/L (exp. data) in [37]
44	17-*preg*	2406	ng/dL	[37]
45	17-*prog*	185.5	ng/mL	155 pg/mL (exp. data) in [48]
46	*DHEA*	5785	ng/mL	6450 ng/mL (exp. data) in [48]
47	*andro*	1368	ng/mL	1100 ng/mL (exp. data) in [48]
48	*test*	301.7	pg/mL	245 pg/mL (exp. data) in [48]
49	*estro*	87.06	pg/mL	55 pg/mL (exp. data) in [48]
50	*Ih*	259.8	U/L	[38]

[37] $(530 + 3570)/2 = 2050$ ng/dL [32] (experimental data)

[38] $p_{55} + p_{56} \cdot y_{12}(0) + p_{57} \cdot y_{17}(0) + p_{58} \cdot y_{18}(0)$

Bibliography

[1] M. E. Andersen. Physiological modelling of organic compounds. *Annals of Occupational Hygiene*, 35(3):309–321, 1991.

[2] L. Anderson. Intracellular mechanisms triggering gonadotrophin secretion. *Reviews of Reproduction*, 1:193–202, 1996.

[3] C. T. H. Baker and F. A. Rihan. Sensitivity analysis of parameters in modelling with delay-differential equations. Technical report, Manchester Centre for Computational Mathematics, The University of Manchester, September 1999.

[4] L. W. Beineke and R. J. Wilson (eds.). *Graph Connections*. Oxford Science Publications, 1997.

[5] J. J. Blum, M. C. Reed, J. A. Janovick, and P. M. Conn. A mathematical model quantifying GnRH-induced LH secretion from gonadotropes. *Am. J. Physiol. Endocrinol. Metab.*, 278:E263–E272, 2000.

[6] R. J. Bogumil, M. Ferin, J. Rootenberg, L. Speroff, and R. L. vande Wiele. Mathematical studies of the human menstrual cycle. I. Formulation of a mathematical model. *J. Clin. Endocrinol. Metab.*, 35(1):126–143, 1972.

[7] R. J. Bogumil, M. Ferin, and R. L. vande Wiele. Mathematical studies of the human menstrual cycle. II. Simulation performance of a model of the human menstrual cycle. *J. Clin. Endocrinol. Metab.*, 35(1):144–156, 1972.

[8] R. A. Boyd, E. A. Zegarac, and M. A. Eldon. The effect of food on the bioavailability of norethindrone and ethinyl estradiol from norethindrone acetate/ethinyl estradiol tablets intended for continuous hormone replacement therapy. *J. Clin. Pharmacol.*, 43:52–58, 2003.

[9] N. Chabbert-Buffet and P. Bouchard. The normal human menstrual cycle. *Reviews in Endocrine and Metabolic Disorders*, 3:173–183, 2002.

[10] R. J. Chang and R. B. Jaffe. Progesterone effects on gonadotropin release in women pretreated with estradiol. *Journal of Clinical Endocrinology and Metabolism*, 47:119–125, 1978.

[11] A. Chávez-Ross, S. Franks, H. D. Mason, K. Hardy, and J. Stark. Modelling the control of ovulation and polycystic ovary syndrome. *Journal of Mathematical Biology*, 36:95–118, 1997.

[12] F. Clément. Optimal control of the cell dynamics in the granulosa of ovulatory follicles. *Mathematical Biosciences*, 152:123–142, 1998.

[13] F. Clément, M. A. Gruet, P. Monget, M. Terqui, E. Jolivet, and D. Monniaux. Growth kinetics of the granulosa cell population in ovarian follicles: An approach by mathematical modelling. *Cell Proliferation*, 30:255–270, 1997.

[14] F. Clément, D. Monniaux, J. Stark, K. Hardy, J. C. Thalabard, S. Franks, and D. Claude. Mathematical model of FSH-induced cAMP production in ovarian follicles. *Am. J. Physiol. Endocrinol. Metab.*, 281:E35–E53, 2001.

[15] A. J. Conley and I. M. Bird. Minireview: The role of cytochrome P450 17α-hydroxylase and 3β-hydroxysteroid dehydrogenase in the integration of gonadal and adrenal steroidogenesis via the δ5 and δ4 pathways of steroidogenesis in mammals. *Biology of Reproduction*, 56:789–799, 1997.

[16] B. A. Cooke, R. J. B. King, and H. J. van der Molen (eds.). *Hormones and their Actions, Part II.* Elsevier Science Publishers BV, 1988.

[17] KEGG PATHWAY Database. http://www.genome.jp/kegg/pathway.html, 2006.

[18] P. Deuflhard. *Newton methods for nonlinear problems. Affine invariance and adaptive algorithms.* Springer Series in Computational Mathematics 35. Springer, Berlin, 2004.

[19] P. Deuflhard and F. Bornemann. *Scientific computing with ordinary differential equations.* Texts in Applied Mathematics 42. Springer, Berlin, 2002.

[20] P. Deuflhard and A. Hohmann. *Numerical Analysis in Modern Scientific Computing. An Introduction.* Second Edition. Springer, New York, 2003.

[21] P. Deuflhard and W. Sautter. On rank-deficient pseudoinverses. *Lin. Alg. Appl.*, 29:91–111, 1980.

[22] R. P. Dickinson and R. J. Gelinas. Sensitivity analysis of ordinary differential equation systems - a direct method. *Journal of Computational Physics*, 21:123–143, 1976.

[23] R. Diestel. *Graph Theory.* 3rd edition. Springer, 2005.

[24] E. A. Drey and P. D. Darney. Recent developments in hormonal contraception. *Reviews in Endocrine & Metabolic Disorders*, 3:257–265, 2002.

[25] A. B. Edelman, S. L. Koontz, M. D. Nichols, and J. T. Jensen. Continuous oral contraceptives. *Obstetrics & Gynecology*, 107(3):657–665, 2006.

[26] K. Elomaa. *The Risk of Escape Ovulation under Treatment with Low-Dose Combined Oral Contraceptives.* PhD thesis, University of Helsinki, 2001.

[27] M. Elstein. Present status of hormonal contraception (COCs). *Advances in Contraception*, 12:155–166, 1996.

[28] M. Elstein and H. Furniss. The fiction of an ideal hormonal contraceptive. *Advances in Contraception*, 12:129–138, 1996.

[29] C. Godsil and G. Royle. *Algebraic Graph Theory*. Springer, 2001.

[30] J. D. Gordan, B. J. Attardi, and D. W. Pfaff. Mathematical exploration of pulsatility in cultured gonadotropin-releasing hormone neurons. *Neuroendocrinology*, 67:2–17, 1998.

[31] A. Grah. *Entwicklung und Anwendung modularer Software zur Simulation und Parameterschätzung in gaskatalytischen Festbettreaktoren*. Dissertation. Martin-Luther-Universität Halle-Wittenberg, 2004.

[32] F. S. Greenspan and G. J. Strewler (ed.). *Basic & Clinical Endocrinology*. 5th edition. Appleton & Lange, 1997.

[33] R. Grigoliene and D. Švitra. The mathematical model of the female menstrual cycle and its modifications. *Informatica*, 11(4):411–420, 2000.

[34] N. P. Groome, P. J. Illingworth, M. O'Brien, R. Pai, F. E. Rodger, J. P. Mather, and A. S. McNeilly. Measurement of dimeric inhibin B throughout the human menstrual cycle. *Journal of Clinical Endocrinology and Metabolism*, 81(4):1401–1405, 1996.

[35] N. Guglielmi and E. Hairer. Implementing Radau IIA methods for stiff delay differential equations. *Computing*, 67:1–12, 2001.

[36] E. Hairer and G. Wanner. *Solving Ordinary Differential Equations II. Stiff and Differential-Algebraic Problems*. 2nd edition. Springer, Berlin Heidelberg, 1996.

[37] L. A. Harris. *Differential Equation Models for the Hormonal Regulation of the Menstrual Cycle*. PhD thesis, North Carolina State University, 2001.

[38] L. Harris Clark, P. M. Schlosser, and J. F. Selgrade. Multiple stable periodic solutions in a model for hormonal control of the menstrual cycle. *Bulletin of Mathematical Biology*, 65:157–173, 2003.

[39] F. Hayes, J. E. Hall, P. A. Boepple, and Jr. W. F. Crowley. Clinical review 96. Differential control of gonadotropin secretion in the human: Endocrine role of inhibin. *Journal of Clinical Endocrinology and Metabolism*, 83:1835–1841, 1998.

[40] T. Hearn, C. Haurie, and M. C. Mackey. Cyclical neutropenia and the peripheral control of white blood cell production. *Journal of Theoretical Biology*, 192:167–181, 1998.

[41] K. Heinze, R. W. Keener, and A. R. Midgley Jr. A mathematical model of luteinizing hormone release from ovine pituitary cells in perifusion. *Am. J. Physiol. Endocrinol. Metab.*, 275:E1061–E1071, 1998.

[42] A. E. Herbison. Noradrenergic regulation of cyclic GnRH secretion. *Reviews of Reproduction*, 2:1–6, 1997.

[43] P. J. Adams Hillard. Overview of contraception. *Adolescent Medicine Clinics*, 16:485–493, 2005.

[44] A. Källén. *Computational Pharmacokinetics*. Biostatistics Series. Chapman & Hall/CRC, Boca Raton, 2008.

[45] C. Keck, J. Neulen, H. M. Behre, and M. Breckwoldt. *Endokrinologie, Reproduktionsmedizin, Andrologie*. 2nd edition. Georg Thieme Verlag, 2002.

[46] D. M. Keenan, W. Sun, and J. D. Veldhuis. A stochastic biomathematical model of the male reproductive hormone system. *Siam J. Appl. Math.*, 61(3):934–965, 2000.

[47] D. M. Keenan and J. D. Veldhuis. A biomathematical model of time-delayed feedback in the human male hypothalamic-pituitary-Leydig cell axis. *Am. J. Physiol. Endocrinol. Metab.*, 275(1):E157–E176, 1998.

[48] O. R. Kling and P. K. Westfahl. Steroid changes during the menstrual cycle of the baboon (papio cynocephalus) and human. *Biology of Reproduction*, 18:392–400, 1978.

[49] R. Krattenmacher. Drospirenone: pharmacology and pharmacokinetics of a unique progestogen. *Contraception*, 62:29–38, 2000.

[50] A. Kubba and J. Guillebaud. Combined oral contraceptives: acceptability and effective use. *British Medical Bulletin*, 49(1):140–157, 1993.

[51] H. M. Lacker and E. Akin. How do the ovaries count? *Mathematical Biosciences*, 90:305–332, 1988.

[52] F. J. López, I. J. Merchenthaler, M. Moretto, and A. Negro-Vilar. Modulating mechanisms of neuroendocrine cell activity: The LHRH pulse generator. *Cellular and Molecular Neurobiology*, 18(1):125–146, 1998.

[53] R. H. Luecke and W. D. Wosilait. Drug elimination interactions: Analysis using a mathematical model. *Journal of Pharmacokinetics and Biopharmaceutics*, 7(6):629–641, 1979.

[54] N. MacDonald. *Time Lags in Biological Models*. Lecture Notes in Biomathematics. Springer, 1978.

[55] D. A. Magoffin and A. J. Jakimiuk. Inhibin A, inhibin B and activin A in the follicular fluid of regularly cycling women. *Human Reproduction*, 12(8):1714–1719, 1997.

[56] Mammakarzinom-Info.de. http://www.mammakarzinom-info.de, 2006.

[57] J. C. Marshall, A. C. Dalkin, D. J. Haisenleder, S. J. Paul, G. A. Ortolano, and R. P. Kelch. Gonadotropin-releasing hormone pulses: Regulators of gonadotropin synthesis and ovulatory cycles. *Recent Progress in Hormone Research*, 47:155–187, 1991.

[58] R. I. McLachlan, N. L. Cohen, K. D. Dahl, W. J. Bremner, and M. R. Soules. Serum inhibin levels during the periovulatory interval in normal women: Relationships with sex steroid and gonadotrophin levels. *Clinical Endocrinology*, 32:39–48, 1990.

[59] S. M. Moenter, R. C. Brand, and F. J. Karsch. Dynamics of gonadotropin-releasing hormone (GnRH) secretion during the GnRH surge: Insights into the mechanism of GnRH surge induction. *Endocrinology*, 130(5):2978–2984, 1992.

[60] U. Nowak and P. Deuflhard. Towards parameter identification for large chemical reaction systems. In P. Deuflhard and E. Hairer, editors, *Numerical Treatment of Inverse Problems in Differential and Integral Equations*, Progress in Scientific Computing 2, pages 13–26. Birkhäuser, Basel, 1983.

[61] U. Nowak and P. Deuflhard. Numerical identification of selected rate constants in large chemical reaction systems. *Applied Numerical Mathematics*, 1:59–75, 1985.

[62] A. Obruca, F. Fischl, and J. Huber. GnRH - Gonadotropin Releasing Hormon: Mechanismen und Therapeutische Anwendung in der Assistierten Reproduktion. *J. Fertil. Reprod.*, 2:28–33, 1998.

[63] M. Orme. Drug absorption in the gut. *Br. J. Anaesth.*, 56:59–67, 1984.

[64] M. Orme and D. J. Back. Oral contraceptive steroids - pharmacological issues of interest to the prescribing physician. *Advances in Contraception*, 7(4):325–331, 1991.

[65] N. L. Rasgon, L. Pumphrey, P. Prolo, S. Elman, A. Negrao, J. Licinio, and A. Garfinkel. Emergent oscillations in mathematical model of the human menstrual cycle. *SNS Spectrums*, 8(11):805–814, 2003.

[66] I. Reinecke and P. Deuflhard. A complex model of the human menstrual cycle. *Journal of Theoretical Biology*, 247(2):303–330, 2007.

[67] I. Reinecke and P. Deuflhard. Model development and decomposition in physiology. In A. Daskalaki, editor, *Handbook of Research on Systems Biology Applications in Medicine*. Medical Information Science Reference, 2008.

[68] E. F. Rissman. Mini-Review. Behavioral regulation of gonadotropin-releasing hormone. *Biology of Reproduction*, 54:413–419, 1996.

[69] J. F. Roche. Control and regulation of folliculogenesis - a symposium in perspective. *Reviews of Reproduction*, 1:19–27, 1996.

[70] M. Schlegel, W. Marquardt, R. Ehrig, and U. Nowak. Sensitivity analysis of linearly-implicit differential-algebraic system by one-step extrapolation. ZIB-Report 02-38, Konrad-Zuse-Zentrum für Informationstechnik Berlin, November 2002.

[71] P. M. Schlosser and J. F. Selgrade. A model of gonadotropin regulation during the menstrual cycle in women: Qualitative features. *Environmental Health Perspectives Supplements*, 108(supp. 5):873–881, 2000.

[72] I. H. Segel. *Enzyme Kinetics. Behavior and Analysis of Rapid Equilibrium and Steady-State Enzyme Systems*. Wiley-Interscience, 1975.

[73] A. Sehested, A. Juul, A. M Andersson, J. H. Petersen, T. K. Jensen, J. Müller, and N. E. Skakkebaek. Serum inhibin A and inhibin B in healthy prepubertal, pubertal, and adolescent girls and adult women: Relation to age, stage of puberty, menstrual cycle, follicle-stimulating hormone, luteinizing hormone, and estradiol levels. *Journal of Clinical Endocrinology and Metabolism*, 85(4):1634–1640, 2000.

[74] J. F. Selgrade. Modeling hormonal control of the menstrual cycle. *Comments on Theoretical Biology*, 6(1):79–101, 2001.

[75] J. F. Selgrade and P. M. Schlosser. A model for the production of ovarian hormones during the menstrual cycle. *Fields Institute Communications*, 21:429–446, 1999.

[76] W. J. Shack, P. Y. Tam, and T. J. Lardner. A mathematical model of the human menstrual cycle. *Biophysical Journal*, 11:835–848, 1971.

[77] D. C. Skinner, N. P. Evans, B. Delaleu, R. L. Goodman, P. Bouchard, and A. Caraty. The negative feedback actions of progesterone on gonadotropin-releasing hormone secretion are transduced by the classical progesterone receptor. *Proc. Natl. Acad. Sci.*, 95:10978–10983, 1998.

[78] L. A. Stephenson and M. A. Kolka. Plasma volume during heat stress and exercise in women. *Proc. Natl. Acad. Sci.*, 95:10978–10983, 1998.

[79] J. F. Strauss III. The synthesis and metabolism of steroid hormones. In S. S. C. Yen, R. B. Jaffe, and R. L. Barbieri, editors, *Reproductive Endocrinology. Physiology, Pathophysiology, and Clinical Management*, pages 125–154. W.B. Saunders Company, 1999.

[80] J. F. Strauss III and C. J. Williams. The ovarian life cycle. In S. S. C. Yen, R. B. Jaffe, and R. L. Barbieri, editors, *Reproductive Endocrinology. Physiology, Pathophysiology, and Clinical Management*, pages 213–253. W.B. Saunders Company, 1999.

[81] D. Švitra, R. Grigoliene, and A. Puidokaite. Regulation of an ovulatory cycle. *Nonlinear Analysis: Modelling and Control*, (2):107–114, 1998.

[82] R. S. Swerdloff, H. S. Jacobs, and W. D. Odell. Synergistic role of progestogens in estrogen induction of LH and FSH surge. *Endo*, 90(6):1529–1536, 1972.

[83] Y. Takeuchi, Y. Iwasa, and K. Sato (Eds.). *Mathematics for Life Science and Medicine*. Springer, 2007.

[84] C. C. Tsai and S. S. Yen. The effect of ethinyl estradiol administration during early follicular phase of the cycle on the gonadotropin levels and ovarian function. *Journal of Clinical Endocrinology and Metabolism*, 33(6):917–923, 1971.

[85] T. M. Washington, J. J. Blum, M. C. Reed, and P. M. Conn. A mathematical model for LH release in response to continuous and pulsatile exposure of gonadotrophs to GnRH. *Theoretical Biology and Medical Modelling*, 1(9):1–17, 2004.

[86] S. S. C. Yen. The human menstrual cycle: Neuroendocrine regulation. In S. S. C. Yen and R. B. Jaffe, editors, *Reproductive Endocrinology. Physiology, Pathophysiology, and Clinical Management*, pages 191–217. W.B. Saunders Company, 1991.

[87] A. J. Zeleznik. The physiology of follicle selection. *Reproductive Biology and Endocrinology*, 2(31), 2004.

Danksagung

Zuallererst möchte ich Peter Deuflhard für dieses inspirierende Thema, seinen Mut, dieses Thema anzugehen, sowie sein Vertrauen in mich danken. Dieser thematische Glückstreffer hat meine Hoffnungen und Erwartungen, in meiner Doktorarbeit Mathematik mit einem medizinischen Thema zu verbinden, übertroffen.

Auch möchte ich Marcus Weber für seine Bemühungen, das Thema nach außen zu tragen, danken. Ebenso danke ich der Kette von Kontakten bei Bayer Schering Pharma über Wolfram Langer, Henrik Seidel, Tim Wintermantel zu Gertrud Ahr, Rolf Burghaus und Hartmut Blode, die letztendlich zu einer fruchtbaren Kooperation geführt haben.

Erwähnen möchte ich auch die Kontakte, die am Anfang dieses Projekts eine Rolle gespielt haben: Horst Lübbert und Julia Bartley (Charité Campus Benjamin Franklin), Bertram Wiedenmann und Ursula Plöckinger (Charité Campus Virchow-Klinikum) sowie auch Wilhelm Huisinga und Andrea Weiße (ehemals Freie Universität Berlin).

Weiterhin möchte ich meiner Mutter und Schwester dafür danken, dass sie immer für mich da waren und sind, und meinem Freund Martin, dass er so verständnisvoll und unterstützend in der ganzen Zeit war und mir sehr viel Kraft gegeben hat.

Zusammenfassung

Die vorliegende Dissertation beschäftigt sich mit der Modellierung und Simulation des weiblichen Hormonzyklus. Unter dem weiblichen Hormonzyklus versteht man die Abläufe des Regelkreises im Körper der Frau, die im gesunden Fall in regelmäßigen Intervallen zur Ovulation führen und damit die Reproduktion ermöglichen. Auch wenn dieses Thema etwa die Hälfte der Bevölkerung betrifft, fand es in der mathematischen Modellierung bislang wenig Aufmerksamkeit.

In der vorliegendenden Arbeit wurde ein mathematisches Modell, GynCycle, hergeleitet, das die Dynamik von 49 Hormonen, Enzymen, Rezeptoren (teilweise in verschiedenen Zuständen und an verschiedenen Orten), Follikelphasen und dem Pulsgenerator beschreibt. GynCycle besteht dabei aus Delaydifferentialgleichungen, wodurch berücksichtigt wird, dass die Prozesse in unterschiedlichen Bereichen im Körper stattfinden und sich zeitverzögert beeinflussen. Eine Besonderheit und ein wichtiger Bestandteil dieses Regelkreises ist der GnRH-Pulsgenerator, der zu der pulsatilen Freisetzung des Hormons GnRH führt. Die Pulszeitpunkte werden dabei durch einen stochastischen Prozess modelliert. Ein solches mathematisches Modell, das die Dynamik des weiblichen Hormonzyklus in diesem Umfang und Komplexität beschreibt, hat es soweit bekannt bislang noch nicht gegeben.

Wenn komplexe physiologische Prozesse und Regelsysteme im menschlichen Körper wie der weibliche Hormonzyklus modelliert werden, treten viele Parameter auf. Zum großen Teil sind ihre Werte nicht bekannt, wodurch Parameterschätzung notwendig wird. Um dieses oft hochdimensionale Problem zu vereinfachen, wurde in der vorliegenden Arbeit eine Methode entwickelt, um das Modell durch Zuhilfenahme von experimentellen Daten in mehrere kleinere Modellteile zu zerlegen. Für die einzelnen Modellteile wurde dann nacheinander und zum Teil auch parallel Parameterschätzung durchgeführt. Es wurden dabei nur die Parameter geschätzt, die sensitiv sind, was eine Sensitivitätsanalyse für Delaydifferentialgleichungen erfordert. Durch anschließende Zusammenführung der einzelnen Modellteile zu dem Gesamtmodell sind dynamische Simulationen des Modells möglich. Für die Simulation wurde ein Integrator für steife Delaydifferentialgleichungen verwendet (RADAR5 von Guglielmi und Hairer (2001)). Um auch den Pulsgenerator zu berücksichtigen, wurde der Integrator erweitert.

Der Vergleich mit experimentellen Daten zeigte, dass das Modell in der Lage ist, die Dynamik wesentlicher Elemente des Zyklus für eine virtuelle Frau, da gemittelte experimentelle Daten vorlagen, wiederzugeben. Die Einnahme von hormonalen Kontrazeptiva wurde modelliert und simuliert und auch diese Ergebnisse zeugen von dem richtigen Ansatz in der Modellierung.